CHAPTER 1

An Invitation to Neurobiology

The brain is a world consisting of a number of unexplored continents and great stretches of unknown territory.

Santiago Ramón y Cajal

How does the nervous system control behavior? How do we sense the environment? How does the brain create a representation of the world out of the sensations? How much of our brain function and behavior is shaped by our genes, and how much reflects the environment in which we grew up? How is the brain wired up during development? What changes occur in the brain when we learn something new? How have nervous systems evolved? What goes wrong in brain disorders?

We are about to embark on a journey to explore these questions, which have fascinated humanity for thousands of years. Our ability to address these questions *experimentally* has greatly expanded in recent years. What we currently know about the answers to these questions comes mostly from findings made in the past 50 years; in the next 50 years, we will likely learn more about the brain and its control of behavior than in all of prior human history. We are at an exciting time as students of neurobiology, and it is my hope that many readers of this book will be at the forefront of groundbreaking discoveries.

PRELUDE: NATURE AND NURTURE IN BRAIN FUNCTION AND BEHAVIOR

As we begin this journey, let's discuss one of the questions we raised regarding the contributions of genes and environment to our brain function and behavior. We know from experience that both genetic inheritance (**nature**) and environmental factors (**nurture**) make important contributions, but how much does each contribute? How do we begin to tackle such a complex question? In scientific research, asking the right questions is often a critical step toward obtaining the right answers. As evolutionary geneticist Theodosius Dobzhansky put it, "The question about the roles of the genotype and the environment in human development must be posed thus: To what extent are the *differences* observed among people conditioned by the differences of their genotypes and by the differences between the environments in which people were born, grew and were brought up?"

1.1 Human twin studies can reveal the contributions of nature and nurture

Francis Galton first coined the phrase *nature versus nurture* in the nineteenth century. He also introduced a powerful method for studying this conundrum: statistical analysis of human twins. Identical twins (**Figure 1-1**), or **monozygotic twins**, share 100% of their genes in almost all cells, as they are products of the same fertilized egg, or **zygote**. One can compare specific traits among thousands of pairs of identical twins to see how correlated they are within each pair. For example, if we compare the intelligence quotients (IQs)—an estimate of general intelligence—of any two random people in the population, the correlation is 0. (Correlation is a statistic of resemblance that ranges from 0, indicating no resemblance, to 1, indicating perfect resemblance.) This correlation is 0.86 for identical twins (**Figure 1-2**), a striking similarity. However, identical twins also usually grow

Figure 1-1 Identical (monozygotic) twins. Identical twins develop from a single fertilized egg and therefore share 100% of their genes in almost all cells (some lymphocytes are an exception due to stochasticity in DNA recombination). Most identical twins also share similar childhood environments. (Courtesy of Christopher J. Potter.)

up in the same environment, so this correlation alone does not help us distinguish between the contributions of genes and the environment.

Fortunately, human populations provide a second group that allows researchers to tease apart the influence of genetic and environmental factors. Nonidentical (fraternal) twins occur more often than identical twins in most human populations. These are called **dizygotic twins** because they originate from two independent eggs fertilized by two independent sperm. As full siblings, dizygotic twins are 50% identical in their genes according to Mendel's laws of inheritance. However, like monozygotic twins, dizygotic twins usually share very similar prenatal and postnatal environments. Thus, the differences between traits exhibited by monozygotic and dizygotic twins should result from the differences in 50% of their genes. In our example, the correlation of IQ scores between dizygotic twins is 0.60 (Figure 1-2).

Behavioral geneticists use the term **heritability** to describe the contribution of genetic differences to trait differences. Heritability is defined as the difference between the correlations of monozygotic and dizygotic twins multiplied by 2 (because the genetic difference is 50% between monozygotic and dizygotic twins). Thus, the heritability of IQ is $(0.86 - 0.60) \times 2 = 0.52$. Roughly speaking, then, genetic differences account for about half of the *variation* in IQ scores within human populations. Traditionally, the non-nature component has been presumed to come from environmental factors. However, "environmental factors" as calculated in twin studies include *all* factors not inherited from the parents' DNA. These include the postnatal environment, which is what we typically think of as nurture, but also prenatal environment, stochasticity in developmental processes, somatic mutations (alterations in DNA sequences in somatic cells after fertilization), and gene expression changes due to **epigenetic modifications**. Epigenetic

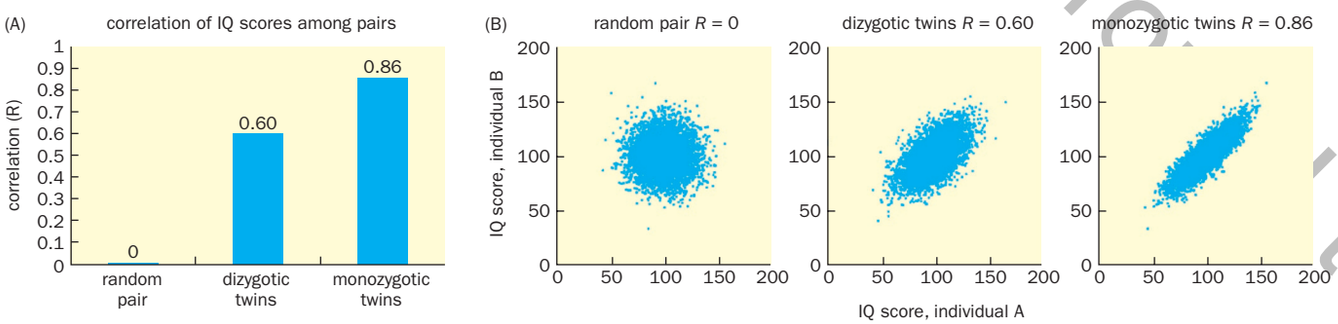

Figure 1-2 Twin studies for determining genetic and environmental contributions to intelligence quotient (IQ). (A) Correlation, or *R* value, of IQ scores for 4672 pairs of monozygotic twins and 5546 pairs of dizygotic twins. The correlation between the IQ scores of randomly selected pairs of individuals is zero. The difference in correlation between monozygotic and dizygotic twins can be used to calculate the heritability of traits. The large sample size makes these estimates highly accurate. **(B)** Simulation of IQ score correlation plots for 5000 pairs of unrelated individuals ($R = 0$), 5000 pairs of dizygotic twins ($R = 0.60$), and 5000 pairs of monozygotic twins ($R = 0.86$). The *x* and *y* axes of a given dot represent the IQ scores of one pair. The simulations assume a normal distribution of IQ scores (mean = 100, standard deviation = 15). (A, based on Bouchard TJ & McGue M [1981] *Science* 212:1055–1059.)

modifications refer to changes made to DNA and chromatin that do not modify DNA sequences but can alter gene expression—these include DNA methylation and various modifications of histones, the protein component of chromatin. As we will learn later, all of these factors contribute to nervous system development, function, and behavior.

Twin studies have been used to estimate the heritability of many human traits, ranging from height (~90%) to the chance of developing schizophrenia (60–80%). An important caveat regarding these estimates is that most human traits result from complex interactions between genes and the environment, and heritability itself can change with the environment. Still, twin studies offer valuable insights into the relative contributions of genes and nongenetic factors to many aspects of brain function and dysfunction in a given environment. The completion of the Human Genome Project and the development of tools permitting detailed examination of the genome sequence data, combined with a long history of medical and psychological studies of human subjects, have made our own species the subject of a growing body of neurobiological research (Section 14.5). However, mechanistic understanding of how genes and the environment influence brain development, function, and behavior requires experimental manipulations that often can be carried out only in animal models. The use of vertebrate and invertebrate model species (Sections 14.1–14.4) has yielded much of what we have learned about the brain and behavior. Many principles of neurobiology revealed by experiments on specific model species have turned out to operate in a wide variety of organisms, including humans.

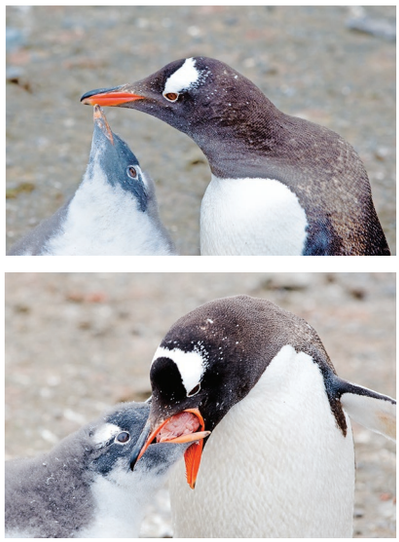

Figure 1-3 Penguin feeding. The instinctive behaviors of an adult penguin and its offspring photographed in Antarctica, 2009. Top, the young penguin asks for food by bumping its beak against its parent's beak. Bottom, the parent releases the food into the young penguin's mouth. (Courtesy of Lubert Stryer.)

1.2 Examples of *nature*: animals exhibit instinctive behaviors

Animals exhibit remarkable instinctive behaviors that help them find food, avoid danger, seek mates, and nurture their progeny. For example, a baby penguin, directed by its food-seeking instinct, bumps its beak against its parent's beak to remind its parent to feed it; in response, the parent instinctively releases the food it has foraged from the sea to feed its baby (**Figure 1-3**).

Instinctive behaviors can be elicited by very specific sensory stimuli. For instance, experimenters have tested the responses of young chicks to an object resembling a bird in flight, with wings placed close to either end of the head–tail axis. When moved in one direction, the object looks like a short-necked, long-tailed hawk; when moved in the other direction, the object looks like a long-necked, short-tailed goose. Seeing the object overhead, a young chick produces different responses depending on the direction in which the object moves, running away when the object resembles a hawk but making no effort to escape when the object resembles a goose (**Figure 1-4**). This escape behavior is **innate**: it is with the chick from birth and is likely genetically programmed. The behavior is also stereotypic: different chicks exhibit the same escape behavior, with similar stimulus specificity. Once the behavior is triggered, it runs to completion without

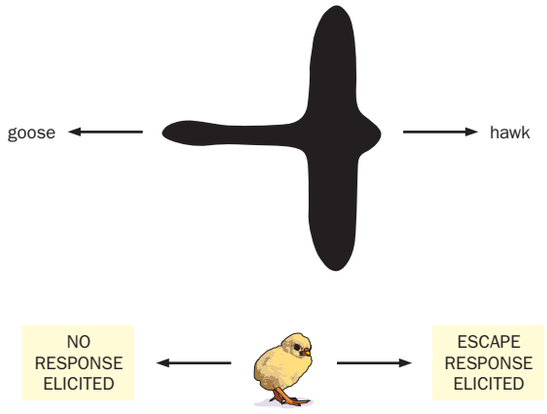

Figure 1-4 Innate escape response of a chick to a hawk. A young chick exhibits instinctive escape behavior in response to an object moving overhead that resembles a short-necked, hawk-like bird; moving the pictured object from left to right triggers this instinctive behavior. Moving the object from right to left so that it resembles a long-necked goose does not elicit the chick's escape behavior. (Adapted from Tinbergen N [1951] The Study of Instinct. Oxford University Press.)

Figure 1-5 Barn owls use their auditory system to locate prey in complete darkness. The photograph was taken in the dark with infrared light flashed periodically while the camera shutter remained open. (Courtesy of Masakazu Konishi.)

further sensory feedback. **Neuroethology**, a field of study that emphasizes observing animal behavior in natural environments, refers to such instinctive behaviors as following **fixed action patterns**. The essential features of the stimulus that activates the fixed action pattern are referred to as **releasers**.

How do genes and developmental programs specify such specific instinctive behaviors? In Chapter 10, we will explore this question using sexual behavior as an example. We will learn about how a single gene in the fruit fly named *fruitless* can exert profound control over many aspects of fruit fly mating behavior.

1.3 An example of *nurture*: barn owls adjust their auditory maps to match altered visual maps

Animals also exhibit a remarkable capacity for learning as they adapt to a changing world. We use the ability of barn owls to adjust their auditory maps to changes in their vision to illustrate this capacity.

Barn owls have superb visual and auditory systems that help them catch prey at night when nocturnal rodents are active. In fact, owls can catch prey even in complete darkness (**Figure 1-5**), relying entirely on their auditory system. They can accurately locate the source of sounds made by prey, based on the small difference in the time it takes for a sound to reach their left and right ears. The owl's brain creates a map of space using these time differences, such that activation of individual nerve cells at specific positions in this brain map informs the owl of the physical position of its prey.

Experiments in which prisms were attached over a juvenile barn owl's eyes (**Figure 1-6**A) revealed how the owl responds when its auditory and visual maps provide conflicting information. Normally, the owl's auditory map matches its visual map, such that perceptions of sight and sound direct the owl to the same location (Figure 1-6B). The prisms shift the owl's visual map 23° to the right. The owl rapidly learns to adjust its motor responses to restore its reaching accuracy on visual targets. However, a mismatch occurs between the owl's visual and auditory maps on the first day after the prisms are placed (Figure 1-6C): sight and sound indicate different locations to the owl, causing confusion about the prey's location. The juvenile owl copes with this situation by adjusting its auditory map to

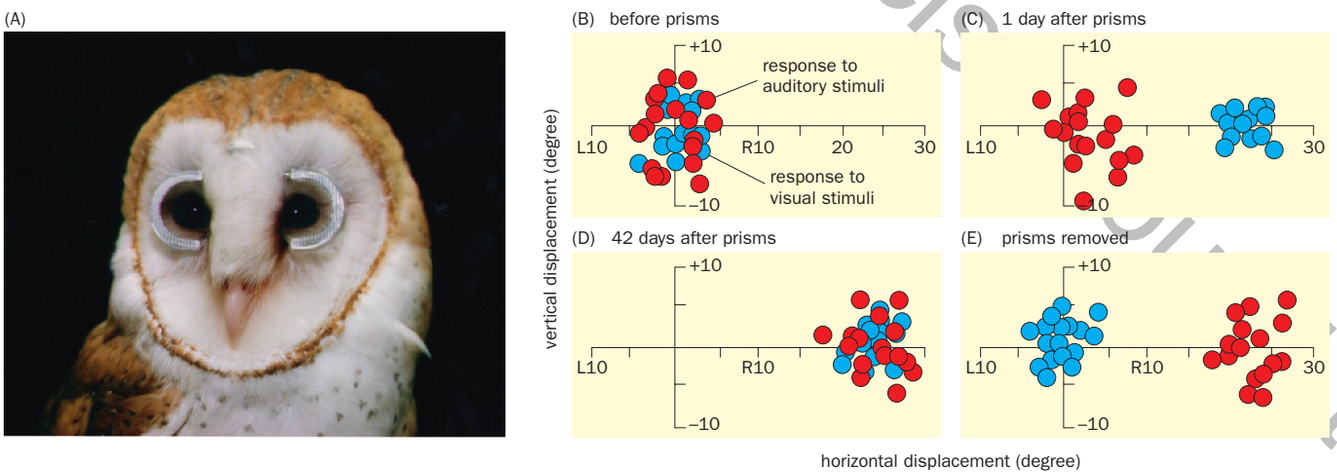

Figure 1-6 Juvenile barn owls adjust their auditory map to match a displaced visual map after wearing prisms. (A) A barn owl fitted with prisms that shift its visual map. **(B)** Before the prisms are attached, the owl's visual map (blue dots) and auditory map (red dots) are matched near 0°. Each dot represents an experimental measurement of an owl's head orientation in response to an auditory or visual stimulus presented in the dark. **(C)** One day after the prisms were fitted, the visual map is displaced 23° to the right of the auditory map. **(D)** After a juvenile owl has worn the prisms for 42 days, its auditory map has adjusted to match its shifted visual map. **(E)** The visual map shifts back immediately after the prisms are removed, causing a temporary mismatch. This mismatch is corrected as the auditory map shifts back soon after (not shown). (A, courtesy of Eric Knudsen. B–E, from Knudsen EI [2002] *Nature* 417:322–328. With permission from Springer Nature.)

match its altered visual map within 42 days after starting to wear the prisms (Figure 1-6D), eliminating the positional conflict between sight and sound. The owl adjusts its strike behavior to accurately target a single location. When the prisms are removed, a mismatch recurs (Figure 1-6E), but the owl adjusts its auditory map and strike behavior back to their native states shortly afterward.

The story of the barn owl is an example of how the nervous system learns to cope with a changing world. Neurobiologists use the term **neural plasticity** to refer to changes in the nervous system in response to experience and learning. But the story does not end here. Studies have shown that plasticity declines with age: juvenile owls have the plasticity required to adjust their auditory map to match a visual map displaced by 23°, but owls will have lost this ability by the time they reach sexual maturity (**Figure 1-7**A). Some human learning capabilities, such as the ability to learn foreign languages, likewise decline with age. Thus, experiments targeted toward improving the plasticity of adult owls may reveal strategies for improving the learning abilities of adult humans as well.

Several ways have been found for adult owls to overcome their limited plasticity in shifting their auditory maps. If an owl experiences adjusting to a 23°-prism shift as a juvenile, it can readily readjust to the same prisms as an adult (Figure 1-7B). Alternatively, even adult owls that cannot adjust to a 23° shift all at once can learn to shift their auditory maps if the visual field displacement is applied in small increments. Thus, by taking baby steps, adult owls can eventually reach nearly the same shift magnitude as young owls. Once they have learned to shift via gradual increments, adult owls can subsequently shift in a single, large step when tested several months after returning to normal conditions (Figure 1-7C).

What are the neurobiological mechanisms underlying these fascinating plasticity phenomena? In Chapters 4 and 6, we will explore the nature of the visual and auditory maps. In Chapters 5 and 7, we will study how neural maps are formed during development and modified by experience. And in Section 11.25, we will address the mechanism of owls' map adjustment in the context of memory and learning. Before studying these topics, however, we need to learn more basics about the brain and its building blocks. We devote the rest of this chapter to providing an overview of the nervous system and introducing how key historical discoveries helped build the conceptual framework of modern neuroscience.

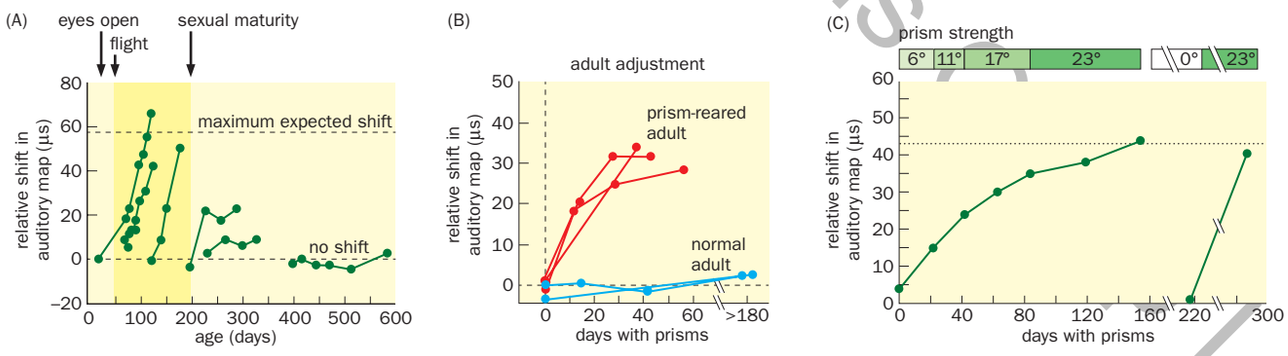

Figure 1-7 Ways to improve the ability of adult barn owls to adjust their auditory maps. (A) Owls' ability to adjust their auditory maps to match displaced visual maps declines with age. The *y* axis quantifies this ability to shift the auditory map, measured by the difference in time (μs, or microseconds) it takes for sounds to reach the left and right ears, which the owl uses to locate objects. Each trace represents a single owl, and each dot represents the average of auditory map shift measured at a specific time after the prisms were applied. The shaded zone indicates a sensitive period, during which owls can easily adjust their auditory maps in response to visual map displacement. Owls older than 200 days have a limited ability to shift their auditory maps. **(B)** Three owls that had learned to adjust their auditory maps in response to prism attachment as juveniles also shifted their auditory maps as adults (red traces). Two owls with no juvenile experience could not shift their maps as adults (blue traces). **(C)** Adult owls could learn to shift their auditory maps if given small prisms in incremental steps, as shown on the left side of the graph. This incremental training enabled adult owls to accommodate a sudden shift to the maximal visual displacement of 23° after a period without prisms, as shown on the right side of the graph. The dotted line at $y = 43$ μs represents the median shift in juvenile owls in response to a single 23°-prism step. (A & B, after Knudsen EI [2002] *Nature* 417:322–328. With permission from Springer Nature. C, after Linkenhoker BA & Knudsen EI [2002] *Nature* 419:293–296. With permission from Springer Nature.)

HOW IS THE NERVOUS SYSTEM ORGANIZED?

For all vertebrate and many invertebrate animals, the nervous system can be divided into the **central nervous system** (**CNS**) and **peripheral nervous system** (**PNS**). The vertebrate CNS consists of the **brain** and the **spinal cord** (**Figure 1-8**A,B). Both structures are bilaterally symmetric; the two sides of the brain are referred as **hemispheres**. The mammalian brain consists of morphologically and

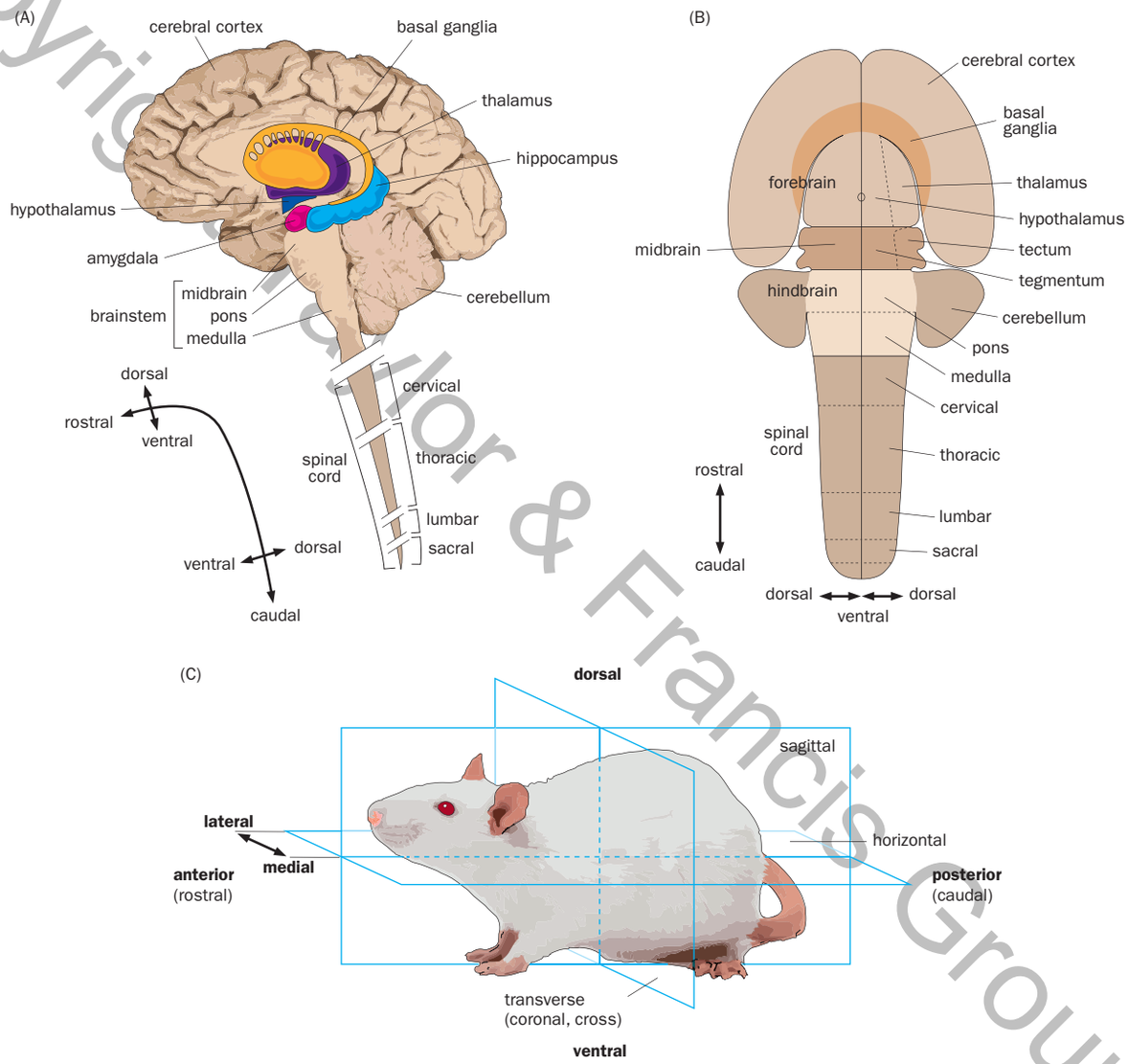

Figure 1–8 The organization of the mammalian central nervous system (CNS). (A) A sagittal (side) view of the human CNS. The basal ganglia (orange), thalamus (purple), hypothalamus (dark blue), hippocampus (light blue), and amygdala (red) from the left hemisphere are superimposed onto a midsagittal section of the CNS (tan background), the left half of which has been cut away to reveal right hemisphere structures (see Panel C for more explanation of the section plane). Major brain structures are indicated and will be studied in greater detail later in the book. From rostral to caudal, the brainstem is divided into midbrain, pons, and medulla. Spinal cord segments are divided into cervical, thoracic, lumbar, and sacral groups. Bottom left, illustration of the rostral–caudal neuraxis (CNS axis). At any given position along the neuraxis in a sagittal plane, the dorsal–ventral axis is perpendicular to the rostral–caudal axis. **(B)** A flatmap of the rat CNS reveals the internal divisions of major brain structures. The flatmap is a two-dimensional representation based on a developmental stage when progenitor cells of the nervous system are arranged as a two-dimensional sheet. It can be approximated by cutting the CNS along the midsagittal plane from the dorsal side and opening the cut surface using the ventral midline as the axis; the ventral-most structures are at the center and the dorsal-most structures are at the sides. (Imagine a book opened to display its pages; the spine of the book—the ventral midline—lays face down.) The left half of the flatmap indicates the major CNS divisions; the right side indicates major subdivisions. **(C)** Schematic illustration of the three principal section planes defined by the body axes. Transverse sections are perpendicular to the rostral–caudal axis, sagittal sections are perpendicular to the medial–lateral axis, and horizontal sections are perpendicular to the dorsal–ventral axis. (B, adapted from Swanson LW [2012] Brain Architecture. 2nd ed. Oxford University Press.)

functionally distinct structures, including the **cerebral cortex**, **basal ganglia**, **hippocampus**, **amygdala**, **thalamus**, **hypothalamus**, **cerebellum**, **midbrain**, **pons**, and **medulla**; the last three structures are collectively called the **brainstem**. The brain can also be divided into **forebrain**, **midbrain**, and **hindbrain**, according to the developmental origins of each region (Figure 7-3A). The spinal cord consists of repeated structures called segments, which are divided into cervical, thoracic, lumbar, and sacral groups. Each segment gives off a pair of spinal nerves. The PNS is made up of **nerves** (discrete bundles of axons) connecting the brainstem and spinal cord with the body and internal organs as well as isolated **ganglia** (clusters of cell bodies of nerve cells) outside the brain and spinal cord. We will study the organization and function of all of these neural structures in subsequent chapters.

The internal structure of the nervous system has traditionally been examined in histological sections. Three types of sections are commonly used and are named following the conventions of histology. In **transverse sections**, also called cross or **coronal sections**, section planes are perpendicular to the long, **anterior–posterior** axis of the animal (also termed the **rostral–caudal** axis, meaning snout to tail). In **sagittal sections**, section planes are perpendicular to the **medial–lateral** axis (midline to side) of the animal. In **horizontal sections**, section planes are perpendicular to the **dorsal–ventral** (back to belly) axis (Figure 1-8C). Note that in humans and other primates, which have a curved CNS, some of the anatomical terms may differ from these definitions. For uniformity, the definition of the rostral–caudal axis in this book always follows the **neuraxis** (axis of the CNS; bottom left of Figure 1-8A) rather than the body axis. Transverse or coronal sections are perpendicular to the neuraxis while horizontal sections are in parallel with the neuraxis. The neuraxis is defined by the curvature of the embryonic **neural tube**, from which the vertebrate nervous system derives, as we will learn in Chapter 7.

1.4 The nervous system consists of neurons and glia

The nervous system is made up two major categories of cells: **neurons** (nerve cells) and **glia**. A typical neuron has two kinds of **neuronal processes** (cytoplasmic extensions): a long, thin process called the **axon**, which often extends far beyond the cell body (**soma**), and thick, bushy processes called **dendrites**, which are usually close to the soma (**Figure 1-9**A). At the ends of the axons are **presynaptic terminals**, specialized structures that participate in the transfer of information between neurons. Dendrites of many vertebrate neurons are decorated with

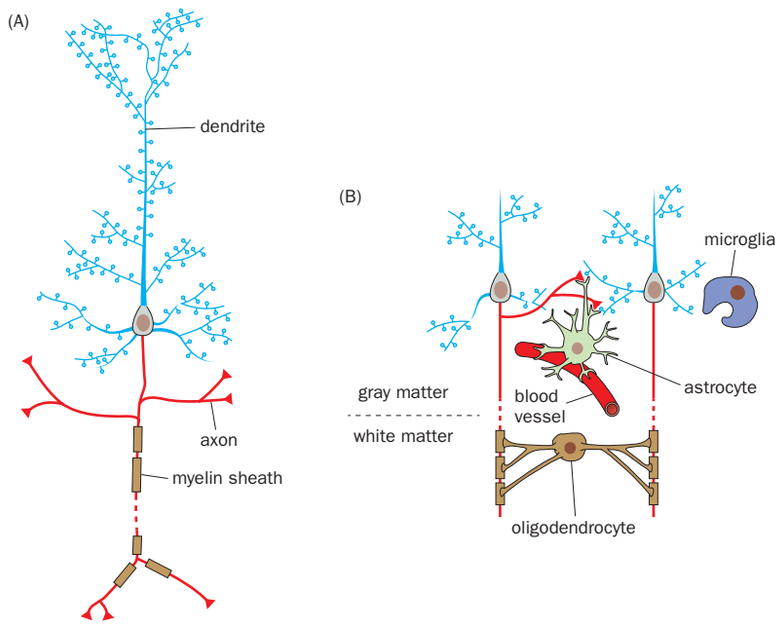

Figure 1-9 Neurons and glia. **(A)** Schematic drawing of a typical neuron in the mammalian CNS. Dendrites are in blue; the axon is in red. The dashed break in the axon indicates that it can extend a long distance from the cell body. The brown structures surrounding the axon are myelin sheaths made by glia. The triangles at the ends of the axonal branches represent presynaptic terminals and the protrusions along the dendritic tree are dendritic spines. **(B)** Schematic drawing of glia in the CNS. Oligodendrocytes form myelin sheaths to wrap the axons of CNS neurons. (Schwann cells, not shown here, play a similar role in the PNS.) Astrocyte end feet wrap around connections between neurons (or synapses, which will be introduced later) in addition to blood vessels. Microglia are immune cells that engulf damaged cells and debris upon activation by injury and during developmental remodeling. (B, based on Allen NJ & Barres BA [2009] *Nature* 457:675–677.)

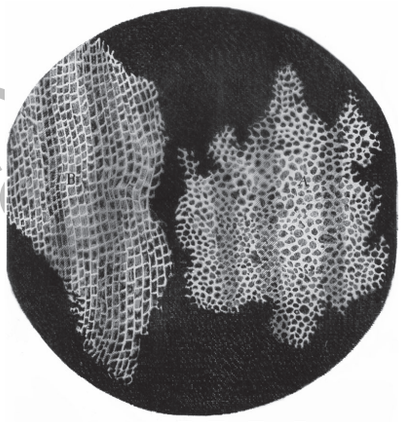

Figure 1-10 The first image of cells. A drawing by Robert Hooke illustrates the repeating units visible in thin sections of cork under a primitive microscope. Hooke thought the units resembled small rooms and coined the term *cells* to describe them. (From Hooke R [1665] Micrographia. J. Martyn and J. Allestry.)

small protrusions called **dendritic spines**, which likewise function in intercellular information transfer. Over the course of this book, we will encounter many neuronal types with distinct morphologies. Most of them have well-differentiated axons and dendrites serving distinct functions, as will be discussed in Section 1.7.

There are four major types of glia in vertebrate nervous systems: **oligodendrocytes**, **Schwann cells**, **astrocytes**, and **microglia** (Figure 1-9B). Oligodendrocytes and Schwann cells play analogous functions in the CNS and PNS, respectively: they wrap axons with their cytoplasmic extensions, called **myelin sheath**, which increases the speed at which information propagates along axons. Oligodendrocytes and myelinated axons constitute **white matter** in the CNS because myelin is rich in lipids and thus appears white. Astrocytes play many roles in neural development and regulation of neuronal communication; they are present in the **gray matter** of the CNS, which is enriched in neuronal cell bodies, dendrites, axon terminals, and connections between neurons. Microglia are the resident immune cells of the nervous system: they engulf damaged cells and debris and help reorganize neuronal connections during development and in response to experience. Invertebrate nervous systems have a similar division of labor for different glial types.

1.5 Individual neurons were first visualized by the Golgi stain in the late nineteenth century

Contemporary students of neurobiology may be surprised to learn that the cellular organization of the nervous system was not uniformly accepted at the beginning of the twentieth century, well after biologists in other fields had embraced the cell as the fundamental unit of life. Robert Hooke first used the term *cell* in 1665 to describe the repeating units he observed in thin slices of cork (**Figure 1-10**) when using a newly invented piece of equipment—the microscope. Scientists subsequently used microscopes to observe many biological samples and found cells to be ubiquitous structures. In 1839, Matthias Schleiden and Theodor Schwann formally proposed the **cell theory**: all living organisms are composed of cells as their basic units. The cell theory was widely accepted in almost every discipline of biology by the second half of the nineteenth century, except among researchers studying the nervous system. Although cell bodies had been observed in nervous tissues, many histologists of that era believed that nerve cells were linked together by their elaborate processes to form a giant net, or reticulum, of nerves. Proponents of this **reticular theory** believed that the reticulum as a whole, rather than its individual cells, constituted the unit of the nervous system.

Among the histologists who supported the reticular theory of the nervous system was Camillo Golgi, who made many important contributions to science, including the discovery of the Golgi apparatus, an intracellular organelle responsible for processing proteins in the secretory pathway (Figure 2-1). Golgi's greatest contribution, however, was the invention of the **Golgi stain**. When a piece of neural tissue is soaked in a solution of silver nitrate and potassium dichromate in the dark for several weeks, black precipitates (microcrystals of silver chromate) stochastically form in a small fraction of nerve cells, rendering these cells visible against an unstained background. Importantly, once black precipitates form within a cell, an autocatalytic reaction occurs such that the entire cell, including most or all of the elaborate extensions, can be visualized in its native tissue (**Figure 1-11**). Golgi stain thus enabled visualization of the entire morphology of individual neurons for the first time. Despite inventing this key method for neuronal visualization, however, Golgi remained a believer in the reticular theory (**Box 1-1**).

It took another great histologist, Santiago Ramón y Cajal, to effectively refute the reticular theory. The work of Ramón y Cajal and several contemporaries instead supported the **neuron doctrine**, which postulated that neuronal processes do not fuse to form a continuous reticulum. Instead, neurons intimately contact each other, with communication between distinct neurons occurring at these contact sites (Box 1-1). The term **synapse** was later coined by Charles

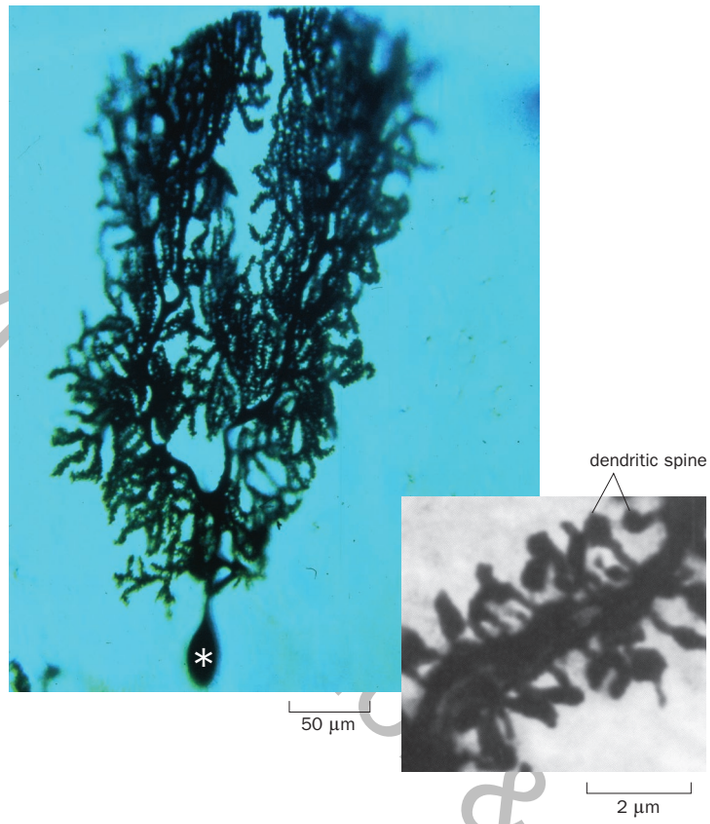

Figure 1-11 Golgi stain. An individual Purkinje cell in the mouse cerebellum is stained black by the formation of silver chromate precipitate, allowing visualization of its complex dendritic tree. The axon, which is not included in this image, projects downward from the cell body indicated by an asterisk. The inset shows a higher magnification of a dendritic segment, highlighting protruding structures called dendritic spines. (Adapted from Luo L, Hensch TK, Ackerman L, et al. [1996] *Nature* 379:837–840. With permission from Springer Nature.)

Sherrington to describe these sites, at which signals flow from one neuron to another. After systematically applying the Golgi stain to study tissues in many parts of the nervous systems of many organisms, ranging from insects to humans, and at many developmental stages, Ramón y Cajal concluded that individual neurons are embryologically, structurally, and functionally independent units of the nervous system.

Box 1-1: The debate between Ramón y Cajal and Golgi: why do scientists make mistakes?

Camillo Golgi and Santiago Ramón y Cajal were the most influential neurobiologists of their time. They shared the 1906 Nobel Prize for Physiology or Medicine, the first to be awarded for findings in the nervous system. However, their debates on how nerve cells constitute the nervous system—via a reticular network or as individual neurons communicating with each other through synaptic contacts—continued during their Nobel lectures (**Figure 1-12**A,B). We now know that Ramón y Cajal's view was correct and Golgi's view was largely incorrect. For example, utilizing the brainbow method (Section 14.18), individual neurons, their dendritic trees, and even their axon terminals can be visualized in and distinguished by distinct colors (Figure 1-12C). Interestingly, Ramón y Cajal used the Golgi stain to refute Golgi's theory. Why didn't Golgi reach the correct conclusion using his own method? Was he not a careful observer? After all, he made many great discoveries, including those describing the Golgi apparatus. According to Ramón y Cajal's analysis, "Golgi arrived at this conclusion by an unusual blend of accurate observations and preconceived ideas. . . . Golgi's work actually consists of two separate parts. On the one hand, there is his method, which has generated a prodigious number of observations that have been enthusiastically confirmed. But on the other, there are his interpretations, which have been questioned and rejected."

Before the invention of the Golgi stain, histologists could not resolve processes of individual nerve cells and therefore believed that nerve processes were fused together in a giant net. Golgi was trained in a scientific environment in which this reticular theory was the dominant interpretation of nervous system organization and so tried to fit his observations into existing theory. For example, even though Golgi was the first to discover, using his staining method, that dendritic

(*Continued*)

Box 1-1: continued

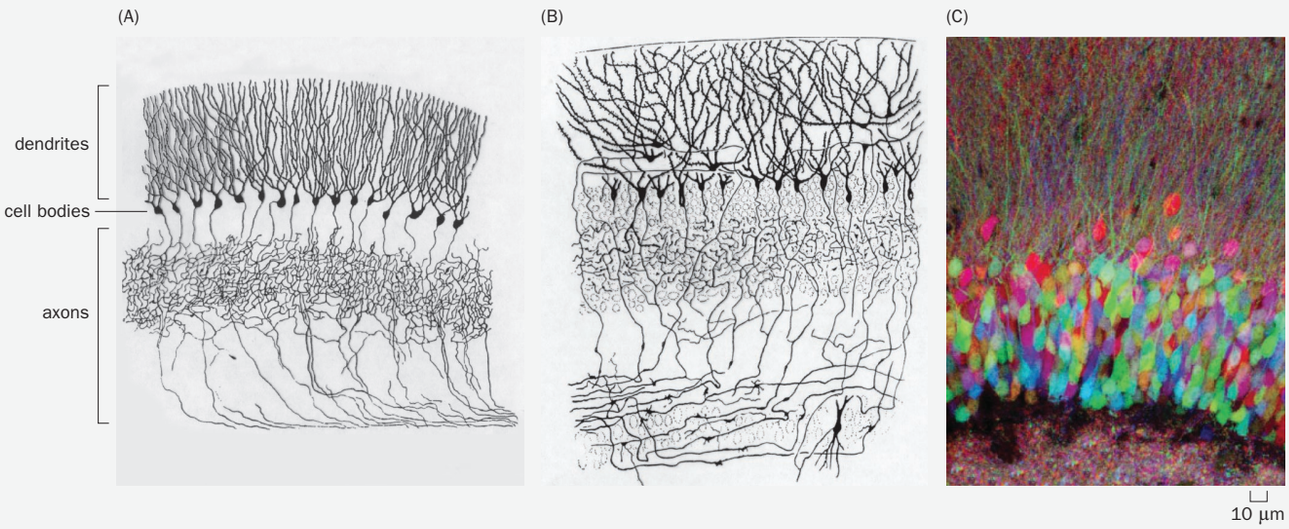

Figure 1-12 Three different views of hippocampal granule cells. **(A)** Golgi's drawing of granule cells of the hippocampus. The dendritic, cell body, and axonal layers are indicated on the left. In Golgi's drawing, all axons are fused together to form a giant reticulum. **(B)** Ramón y Cajal's depiction of the same hippocampal granule cells. Note that axons below the cell bodies have definitive endings. **(C)** Hippocampal granule cells labeled by the brainbow technique, which allows the spectral separation of individual neurons expressing different mixtures of cyan, yellow, and red fluorescent proteins. Not only cell bodies but also some dendrites above and axon terminals below can be resolved by different colors. (A, after Golgi C [1906] Nobel Lecture. B, after Ramón y Cajal S [1911] Histology of the Nervous System of Man and Vertebrates. Oxford University Press. C, after Livet J, Weissman TA, Kang H, et al. [2007] *Nature* 450:56–62. With permission from Springer Nature.)

trees have free endings (Figure 1-12A, top), he thought that dendrites were used to collect nutrients for nerve cells. He believed that it was their axons, which formed an inseparable giant net as he viewed them (Figure 1-12A, bottom), that performed all the special functions of the nervous system. This story teaches an important lesson: scientists need to be observant, but they also need to be as *objective and unbiased* as possible when interpreting their own observations.

1.6 Twentieth-century technology confirmed the neuron doctrine

Ramón y Cajal could not convince Golgi to abandon the reticular theory, but many lines of evidence since the Golgi–Ramón y Cajal debate (Box 1-1) have provided strong support for the neuron doctrine. For example, during development, neurons begin with only cell bodies. Axons then grow out from the cell bodies toward their final destinations. This was demonstrated by observing axon growth *in vitro* via experiments made possible by tissue culture techniques, which were initially developed for the purpose of visualizing neuronal process growth (**Figure 1-13**). Axons are led by a structure called the **growth cone**, which changes its shape dynamically as axons extend. We will learn more about the function of the growth cone in axon guidance in Chapter 5.

The final pieces of evidence that neuronal processes are not fused with each other came from observations made possible by the development of **electron microscopy**, a technique allowing visualization of structures at nanometer (nm) resolution. (Conventional **light microscopy**, which scientists since Hooke have used to observe biological samples, cannot resolve structures less than 200 nm apart because of the physical properties of light.) The use of electron microscopy to examine **chemical synapses** (so named because communication between cells is mediated by release of chemicals called **neurotransmitters**) revealed that the **synaptic cleft**, a 20–100 nm gap, separates a neuron from its target, which can be another neuron or a muscle cell (**Figure 1-14**A). Synaptic partners are not symmetric: presynaptic terminals of neurons contain small **synaptic vesicles** filled

with neurotransmitters, which, upon stimulation, fuse with the plasma membrane and release neurotransmitters into the synaptic cleft. Postsynaptic target cells have **postsynaptic specializations** (also called **postsynaptic densities**) enriched in neurotransmitter receptors on their plasma membrane surfaces. Chemical synapses are the predominant type of synapse allowing neurons to communicate with each other and with muscle cells. We will study them in greater detail in Chapter 3.

Neurons can also communicate with each other by **electrical synapses** mediated by **gap junctions** (Figure 1-14B). Here, each partner neuron contributes protein subunits to form gap junction channels that directly link the cytoplasms of two adjacent neurons, allowing ions and small molecules to travel between them. These gap junctions come closest to what the reticular theory would imagine as a fusion between different neurons. However, macromolecules cannot pass between gap junctions, and the neurons remain distinct cells with highly regulated communication. The existence of gap junctions, therefore, does not violate the premise that *individual neurons are the building blocks of the nervous system*.

1.7 In vertebrate neurons, information generally flows from dendrites to cell bodies to axons

As introduced in Section 1.4, neurons have two kinds of processes: dendrites and axons. The dendritic morphologies and axonal projection patterns of specific types of neurons are characteristic and are often used for classification. For example, the most frequently encountered type of neuron in the mammalian cerebral cortex and hippocampus, the **pyramidal neuron**, has a pyramid-shaped cell body with an apical dendrite and several basal dendrites that branch extensively (**Figure 1-15**A). Much of the dendritic tree sprouts dendritic spines (Figure 1-11 inset), which contain postsynaptic specializations in close contact with presynaptic terminals of partner neurons. Another widely encountered neuronal type, **basket cells** (Figure 1-15B), wrap their axon terminals around the cell bodies of pyramidal cells in the cerebral cortex or **Purkinje cells** (Figure 1-11) in the cerebellum.

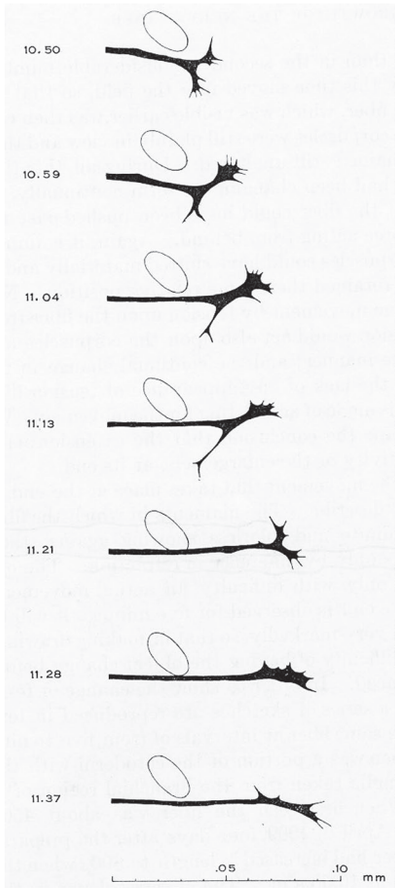

Figure 1-13 The first time-lapse depiction of a growing axon. Frog embryonic spinal cord tissue was cultured *in vitro*. Growth of an individual axon was sketched with the aid of a camera lucida at the time indicated on the left (hour.minute). The stationary blood vessel (oval) provided a landmark for the growing tips of the axon, called growth cones, which undergo dynamic changes in shape, including both extensions and retractions. A distance scale is at the bottom of the figure. (From Harrison RG [1910] *J Exp Zool* 9:787–846.)

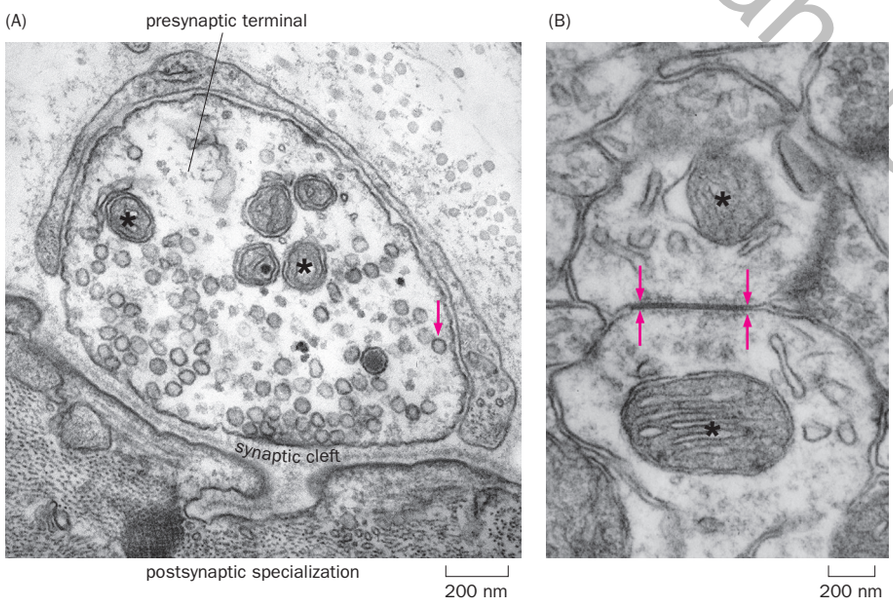

Figure 1-14 Chemical and electrical synapses. (A) Electron micrograph of a chemical synapse between the presynaptic terminal of a motor neuron and the postsynaptic specialization of its target muscle cell. A synaptic cleft separates the two cells. The arrow points to a synaptic vesicle. **(B)** Electron micrograph of an electrical synapse (gap junction) between two dendrites of mouse cerebral cortical neurons. Two opposing pairs of arrows mark the border of the electrical synapse. Asterisks indicate mitochondria in both micrographs. (A, courtesy of Jack McMahan. B, courtesy of Josef Spacek & Kristen M. Harris, SynapseWeb.)

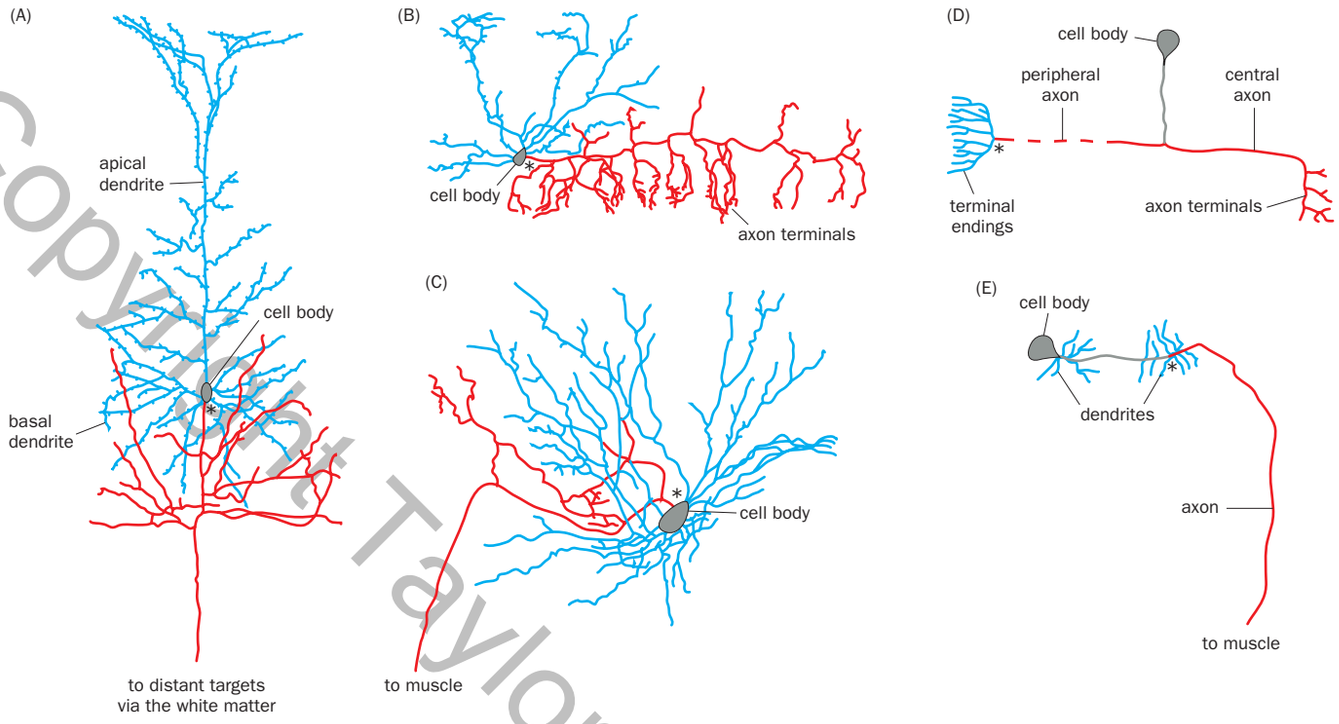

Figure 1-15 Morphological diversity of neurons. (A) A pyramidal cell from rabbit cerebral cortex. A typical pyramidal cell has an apical dendrite (blue) that gives off branches as it ascends, several basal dendrites (blue) that emerge from the cell body, and an axon (red) that branches locally and projects to distant targets. **(B)** A basket cell from mouse cerebellum. The basket cell axon (red) forms a series of "basket" terminals that wrap around Purkinje cell bodies (not drawn). **(C)** A motor neuron from cat spinal cord. Its bushy dendrites (blue) receive input within the spinal cord, and its axon (red) projects outside the spinal cord to muscle, while also leaving behind local branches. **(D)** A mammalian sensory neuron from a dorsal root ganglion. A single process from the cell body bifurcates into a peripheral axon (dashed to indicate the long distance) with terminal endings in the skin (equivalent of dendrites for collecting sensory information) and a central axon that projects into the spinal cord. **(E)** A motor neuron from the fruit fly ventral nerve cord (equivalent to the vertebrate spinal cord). Most invertebrate central neurons are unipolar: a single process extends out of the cell body, giving rise to dendritic branches (blue) and an axon (red). In all panels, asterisks denote axon initiation segments; as will be discussed in Section 1.8, action potentials are usually initiated at these sites. (A–D, adapted from Ramón y Cajal S [1911] Histology of the Nervous System of Man and Vertebrates. Oxford University Press. E, based on Lee T & Luo L [1999] *Neuron* 22:451–461.)

The spinal cord **motor neuron** extends bushy dendrites within the spinal cord (Figure 1-15C) and projects its axon out of the spinal cord and into muscle. Located in the **dorsal root ganglion** just outside the spinal cord, a **sensory neuron** of the **somatosensory system** (which processes bodily sensation) extends a single process that bifurcates, forming a peripheral axon that gives rise to branched terminal endings and a central axon that projects into the spinal cord (Figure 1-15D). Most vertebrate neurons have both dendrites and an axon leaving the cell body, and hence are called **multipolar** (or **bipolar** if there is only a single dendrite); somatosensory neurons are *pseudounipolar* because, although there is just one process leaving the cell body, it gives rise to both peripheral and central branches.

What is the direction of information flow within individual neurons? After systematically observing different types of neurons in various parts of the nervous system, Ramón y Cajal proposed the **theory of dynamic polarization**: transmission of neuronal signals proceeds from dendrites and cell bodies to axons. Therefore, every neuron has (1) a receptive component, the cell body and dendrites; (2) a transmission component, the axon; and (3) an effector component, the axon terminals. With few exceptions (the somatosensory neuron being one), this important principle has been validated by numerous observations and experiments since it was proposed a century ago and has been used extensively to deduce the direction of information flow in the vertebrate CNS. We will study the cell biological basis of neuronal polarization in Chapter 2.

How did observing the morphologies of individual neurons lead to the discovery of this rule? Ramón y Cajal took advantage of the fact that, in sensory systems,

information must generally flow from sensory organs to the brain. By examining different neurons along the visual pathway (**Figure 1-16**), for example, one can see that at each connection, dendrites are at the receiving end, facing the external world, while axons are oriented so as to deliver such information to more central targets, sometimes at a great distance from the cell body where the axon originates. This applies to neurons in other sensory systems as well. Conversely, in motor systems, information must generally flow from the CNS to the periphery. The morphology of the motor neuron indeed supports the notion that its bushy dendrites receive input within the spinal cord, and its long axon, projecting to muscle, provides output (Figure 1-15C).

Neuronal processes in invertebrates can also be defined as dendrites and axons according to their *functions*, with dendrites positioned to receive information and axons to send it. However, the morphological differentiation of most invertebrate axons and dendrites, especially in the CNS, is not as clear-cut as it is for vertebrate neurons. Most often, invertebrate neurons are **unipolar**, extending a single process giving rise to both dendritic and axonal branches (Figure 1-15E). Dendritic branches are often, but not always, closer to the cell body. In many cases, the same branches can both receive and send information; this occurs in some vertebrate neurons as well, as we will learn in Chapters 4 and 6. Thus, in the "simpler" invertebrate nervous systems, it is more difficult to deduce the direction of information flow by examining the morphology of individual neurons.

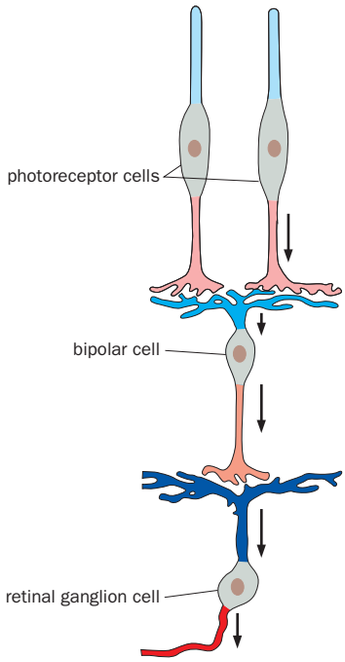

Figure 1–16 Neurons and information flow in the vertebrate retina. Visual information is collected by photoreceptor cells in the retina, communicated to the bipolar cell, and then to the retinal ganglion cell, which projects a long-distance axon into the brain. Note that for both the bipolar cell and the retinal ganglion cell, information is received by their dendrites (blue) and sent via their axons (red). The photoreceptor processes can also be divided into a dendrite equivalent that detects light (blue) and an axon that sends output to the bipolar cell. Arrows indicate the direction of information flow. We will learn more about these cells and connections in Chapter 4. (Adapted from Ramón y Cajal S [1911] Histology of the Nervous System of Man and Vertebrates. Oxford University Press.)

1.8 Neurons use changes in membrane potential and neurotransmitter release to transmit information

What is the physical basis of information flow *within* neurons? We now know that the nervous system uses electrical signals to propagate information. The first evidence of this came from Luigi Galvani's discovery, in the late eighteenth century, that application of an electric current could generate muscle twitches in frogs. It was known by the beginning of the twentieth century that electrical signals were spread in neurons via transient changes in **membrane potential**, the electrical potential difference across the neuronal membrane. As we will learn in more detail in Chapter 2, neurons at the resting state are more negatively charged inside the cells compared to outside the cells. When neurons are excited, their membrane potentials change transiently, creating **nerve impulses** that propagate along their axons. But how is information relayed through nerve impulses? Quantitative studies of how sensory stimuli of different magnitudes induce nerve impulses provided important clues.

Studies of muscle contraction in response to electrical stimulation of motor nerves suggested that an elementary nerve impulse underlies different stimulus strengths. An all-or-none conduction principle became evident when amplifiers for electrical signals built in the 1920s made it possible to record nerve impulses from single axon fibers in response to sensory stimulation. Edgar Adrian and co-workers systematically measured nerve impulses from somatosensory neurons (Figure 1-15D) that convey information about touch, pressure, and pain to the spinal cord. They found that individual nerve impulses were of a uniform size and shape, whether they were elicited by weak or strong sensory stimuli; stronger stimuli increased the frequency of such impulses but not the properties of each impulse (**Figure 1-17**).

These experiments led to two important concepts in modern neuroscience. The first concept is the presence of an elementary unit of nerve impulses that axons use to convey information across long distances; we now call this elementary unit an **action potential**. In Chapter 2, we will study in greater detail the molecular basis of action potentials, including why they exhibit the all-or-none property. The second concept is that neurons use the frequency of action potentials to convey the intensity of signals. Whereas the frequency of action potentials is the most widely used means to convey signal intensity throughout the nervous system, the timing of action potentials can also convey important information.

In addition to action potentials, another important form of communication within neurons are **graded potentials**—membrane potentials that vary continuously

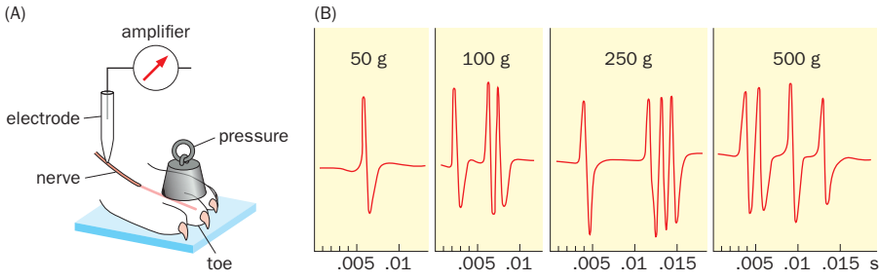

Figure 1-17 Stimulus strength is encoded by the frequency of uniformly sized nerve impulses. **(A)** Experimental setup for applying a specified amount of pressure to the toe of a cat, while recording nerve impulses (action potentials) from an associated sensory nerve. **(B)** With increasing pressure applied to a cat's toe, the frequency of action potentials measured at the sensory nerve also increases, but the size and shape of each action potential remain mostly the same. The *x* axis shows the time scale in units of seconds (s). (Adapted from Adrian ED & Zotterman Y [1926] *J Physiol* 61:465–483.)

in magnitude. One type of graded potential, called **synaptic potentials**, is produced at postsynaptic sites in response to neurotransmitter release from presynaptic partners. Graded potentials can also be induced at peripheral endings of sensory neurons by sensory stimuli, such as the pressure on the toe in Adrian's experiment mentioned earlier; these are called **receptor potentials**. Unlike action potentials, the sizes of graded potentials vary depending on the strength of the input stimuli and the sensitivity of postsynaptic or sensory neurons to those stimuli. Some neurons, including most neurons in the vertebrate retina, do not fire action potentials at all. These **non-spiking neurons** use graded potentials to transmit information, even in their axons.

Synaptic potentials are usually produced at dendritic spines, along the dendrite tree, and at the soma of a neuron. A typical mammalian neuron contains thousands of postsynaptic sites on its dendritic tree, allowing it to collect input from many individual presynaptic partners (**Figure 1-18**). As we will learn later, there are two kinds of inputs: excitatory inputs facilitate action potential production in the postsynaptic neuron, whereas inhibitory inputs impede action potential production. In most neurons, the purpose of these synaptic potentials is to determine whether, when, and how frequently the neuron should fire action potentials so that information can propagate along its axon to its own postsynaptic target neurons. The site of action potential initiation is typically the **axon initial segment** (or the **axon hillock**) adjacent to the soma (Figure 1-15A–C). Thus, synaptic potentials generated in dendrites must travel through the soma to the axon initial segment to contribute to action potential generation.

The rule of action potential initiation near the soma has notable exceptions. For example, in the sensory neuron in Figure 1-15D, action potentials are initiated at the junction between terminal endings and the peripheral axon of the sensory neuron such that sensory information can be transmitted by the peripheral and central axon to the spinal cord across a long distance. In invertebrate neurons, which are mostly unipolar, action potential initiation likely occurs at the junction between the dendritic and axonal compartments (Figure 1-15E).

How is information transmitted *between* neurons? At electrical synapses, membrane potential changes are directly transmitted from one neuron to the next by ion flow across gap junctions (Figure 1-14B). At chemical synapses, the arrival of action potentials (or graded potentials in non-spiking neurons) at presynaptic terminals triggers neurotransmitter release. Neurotransmitters diffuse across the synaptic cleft and bind to their receptors on postsynaptic neurons to produce synaptic potentials (Figure 1-18; Figure 1-14A). The process of neurotransmitter release from the presynaptic neuron and neurotransmitter reception by the postsynaptic neuron is collectively referred to as **synaptic transmission**. Thus, whereas *intraneuronal* communication is achieved by membrane potential changes in the form of graded potentials and action potentials, *interneuronal* communication at chemical synapses relies on neurotransmitter release and reception. We will

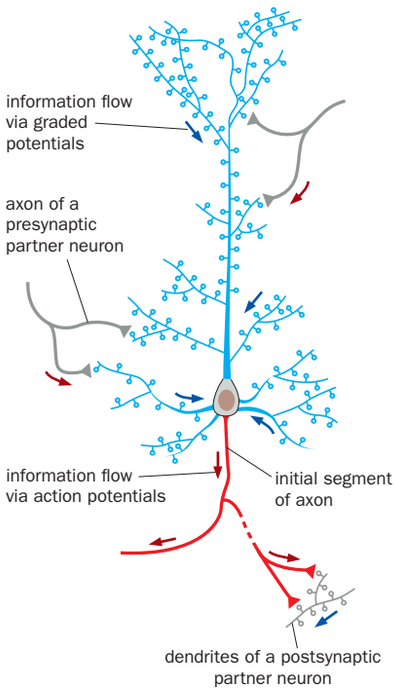

Figure 1-18 The fundamental steps of neuronal communication. A typical neuron in the mammalian CNS receives thousands of inputs at dendritic spines (blue) distributed along its dendritic tree. Inputs are collected in the form of synaptic potentials, which travel toward the cell body (blue arrows) and are integrated at the axon initial segment (red) to produce action potentials. Action potentials propagate to axon terminals (red arrows) and trigger neurotransmitter release, thus conveying information to postsynaptic partner neurons.

study these fundamental steps of neuronal communication in greater detail in Chapters 2 and 3.

1.9 Neurons function in the context of specialized neural circuits

Neurons perform their functions in the context of **neural circuits**—ensembles of interconnected neurons that act together to perform specific functions. The simplest circuits in vertebrates, those that mediate the spinal reflexes, comprise as few as two interconnected neurons: a sensory neuron that receives external stimuli and a motor neuron that controls muscle contraction. Many fundamental neurobiological principles have been derived from studying these simple circuits.

When a neurologist's hammer hits the knee of a subject during a neurological exam, the lower leg kicks forward involuntarily (**Figure 1-19**). The underlying circuit mechanism for this **knee-jerk reflex** has been identified: sensory neurons embed their endings in specialized apparatus called **muscle spindles** in an extensor muscle whose contraction extends the knee joint. These sensory neurons detect stretching of the muscle spindles caused by the physical impact of the hammer and convert this stimulus into electrical signals—namely, receptor potentials—at the sensory endings. Next, the peripheral and central axons of the sensory neurons propagate these electrical signals to the spinal cord as action potentials. There, central axon terminals of the sensory neurons release neurotransmitters directly onto the dendrites of their partner motor neurons. These motor neurons extend their own axons outward from the spinal cord and terminate in the same extensor muscle in which the sensory neurons embed their endings. Sensory axons are also called **afferents**, referring to axons projecting from peripheral tissues to the CNS, whereas motor axons are called **efferents**, referring to axons that project from the CNS to peripheral targets. Both the sensory and motor neurons in this circuit are **excitatory neurons**. When excitatory neurons are activated—that is, when they fire action potentials and release neurotransmitters—they make their postsynaptic target cells more likely to fire action potentials. Therefore, mechanical stimulation activates sensory neurons. This in turn activates the postsynaptic motor neurons. Neurotransmitter release at motor axon terminals leads to contraction of the extensor muscle.

The knee-jerk reflex involves coordination of more than one muscle. The flexor muscle, which is antagonistic to the extensor muscle, must *not* contract at the same time in order for the knee-jerk reflex to occur. (As we will learn in Chapter 8, contraction of extensor muscles increases the angle of a joint, while contraction of flexor muscles decreases the angle of a joint.) Therefore, the sensory axons must *inhibit* contraction of the corresponding flexor muscle in addition to causing contraction of the extensor muscle. This inhibition is mediated by **inhibitory interneurons** in the spinal cord, a second type of postsynaptic neuron targeted by the sensory axons. Note that neurobiologists use the term *interneuron* in two different contexts. In a broad context, all neurons that are not sensory or motor neurons are interneurons. But in most contexts, the term *interneuron* refers to neurons that confine their axons within a specific region, in contrast to **projection neurons**, whose axons link different regions of the nervous system. The spinal inhibitory interneurons fit both criteria.

In this reflex circuit, activation of sensory neurons causes excitation of these inhibitory interneurons, which in turn inhibit the motor neurons innervating the flexor muscle. This inhibition makes it more difficult for the flexor motor neurons to fire action potentials, causing the flexor muscle to relax. Thus, coordinated contraction of the extensor muscle and relaxation of the flexor muscle brings the lower leg forward. First analyzed in studies of spinal reflexes by Charles Sherrington in the 1890s, the role of inhibition is crucial in coordinating neuronal function throughout the nervous system.

In summary, the knee-jerk reflex involves one of the simplest neural circuits: coordinated excitation and inhibition is executed by *monosynaptic* connections between sensory neurons and motor neurons and *disynaptic* connections between sensory neurons and a different group of motor neurons via inhibitory interneuron intermediates. Nervous system functions rely on establishing proper connections

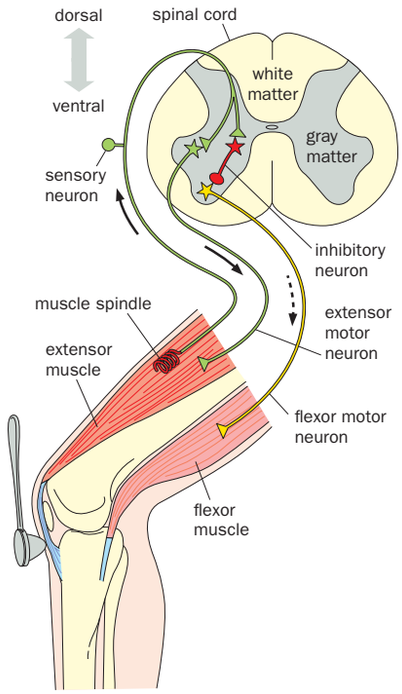

Figure 1-19 The neural circuit underlying the knee-jerk reflex. A simple neural circuit is responsible for the involuntary jerk that results when the front of the knee is hit with a hammer. In this simplified scheme, a single neuron represents a population of neurons performing the same function. The sensory neuron extends its peripheral axon to the muscle spindle of the extensor muscle and its central axon to the spinal cord. In the spinal cord, the sensory neuron has two postsynaptic targets: the green motor neuron that innervates the extensor muscle, and the red inhibitory interneuron that synapses with the yellow motor neuron innervating the flexor muscle. When the knee is hit, mechanical force activates the sensory neuron, resulting in excitation of the extensor motor neuron, which causes contraction of the extensor muscle (following solid arrows). At the same time, sensory neuron activation causes inhibition of the flexor motor neuron, which relaxes the flexor muscle (dashed arrow). The spinal cord is drawn as a cross section. The gray matter at the center contains cell bodies, dendrites, and the synaptic connections of spinal cord neurons; the white matter at the periphery consists of axons of projection neurons. The sensory neuron cell body is located in a dorsal root ganglion adjacent to the spinal cord.

between neurons in numerous neural circuits like the knee-jerk reflex circuit; we will study how the nervous system wires up precisely during development in Chapters 5 and 7.

Most neural circuits are much more complex than the spinal cord reflex circuit. **Box 1-2** discusses commonly used circuit motifs we will encounter in this

Box 1-2: Common neural circuit motifs

The simplest circuit consists of two synaptically connected neurons, such as the sensory neuron–extensor motor neuron circuit in the knee-jerk reflex. In circuits containing more than two neurons, individual neurons can receive input from and send output to more than one partner. Further complexity arises when some neurons in a circuit are excitatory and others are inhibitory. The nervous system employs many **circuit motifs**—common configurations of neural circuits that allow the connection patterns of individual neurons to execute specific functions. Here, we introduce the most common circuit motifs (**Figure 1-20**).

Let's first consider circuits containing only excitatory neurons. **Convergent excitation** (Figure 1-20A) refers to a circuit motif wherein several neurons synapse onto the same postsynaptic neuron. Conversely, **divergent excitation** (Figure 1-20B) refers to a motif wherein a single neuron synapses onto multiple postsynaptic targets via branched axons (axonal branches are also called **collaterals**). Convergent and divergent connections allow individual neurons to integrate input from multiple presynaptic neurons and to send output to multiple postsynaptic targets, respectively. Serially connected excitatory neurons constitute a **feedforward excitation** motif (Figure 1-20C) for propagating information across multiple brain regions, as in the relay of somatosensory stimuli to the primary somatosensory cortex (Figure 1-21). When a postsynaptic neuron synapses onto its own presynaptic partner, this motif is called **feedback excitation** (Figure 1-20D). Neurons that transmit parallel streams of information can also excite each other, forming a **recurrent (lateral) excitation** motif (Figure 1-20E).

When excitatory and inhibitory neurons interact in the same circuit, as is most often the case, many interesting circuit motifs with diverse functionalities can be constructed. The names of motifs involving inhibitory neurons usually emphasize the nature of the inhibition. In **feedforward inhibition** (Figure 1-20F), an excitatory neuron synapses onto both an excitatory neuron and an inhibitory neuron, and the inhibitory neuron further synapses onto the excitatory postsynaptic neuron. In **feedback inhibition** (Figure 1-20G), the postsynaptic excitatory neuron synapses onto an inhibitory neuron, which synapses back onto the postsynaptic excitatory neuron. In both cases, inhibition can control the duration and magnitude of the excitation of the target neuron. In **recurrent (cross) inhibition** (Figure 1-20H), two parallel excitatory pathways cross-inhibit each other via inhibitory neuron intermediates; the inhibition of the flexor motor neuron in the knee-jerk reflex discussed in Section 1.9 is an example of recurrent inhibition. In **lateral inhibition** (Figure 1-20I), an inhibitory neuron receives excitatory input from one or several parallel streams of excitatory neurons and sends inhibitory output to many postsynaptic targets of these excitatory neurons. Lateral inhibition is widely used in processing sensory information, as we will study in greater detail in Chapters 4 and 6. Finally, when an inhibitory neuron synapses onto another inhibitory neuron, the excitation of the first inhibitory neuron reduces the inhibitory output of the second inhibitory neuron, causing **disinhibition** of the final target neuron (Figure 1-20J).

The circuit motifs discussed here are often used in combinations, giving rise to many different ways of processing information. In Chapter 3, we will encounter another group of neurons, the **modulatory neurons**, which can act on both excitatory and inhibitory neurons to up- or downregulate their excitability or synaptic transmission, adding further richness to the information processing functions of neural circuits. In Chapter 14, we will examine circuit architecture from theoretical and computational perspectives. We will see that excitatory and inhibitory neurons can be connected in specific ways to produce logic gates for computation; these logic gates are also the bases of all operations in modern computers (Section 14.32).

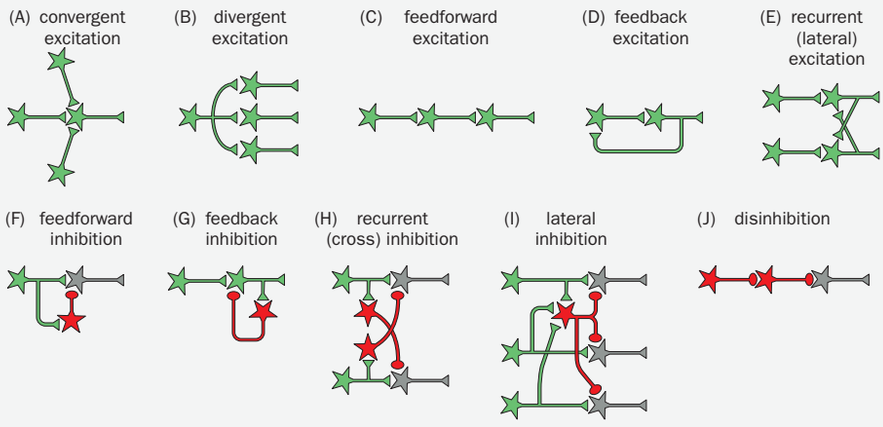

Figure 1-20 Common circuit motifs. In all panels, the general information flow is from left to right. Green, excitatory neuron; red, inhibitory neuron; gray, any neuron. **(A–E)** Circuit motifs consisting of only excitatory neurons. **(F–J)** Circuit motifs that include inhibitory neurons. See text for more details. For recurrent inhibition (H) and lateral inhibition (I), only the feedforward modes are depicted; the feedback modes of these motifs may also be used (not shown), in which case the inhibitory neuron(s) receive input(s) from postsynaptic excitatory neurons, as in Panel G.

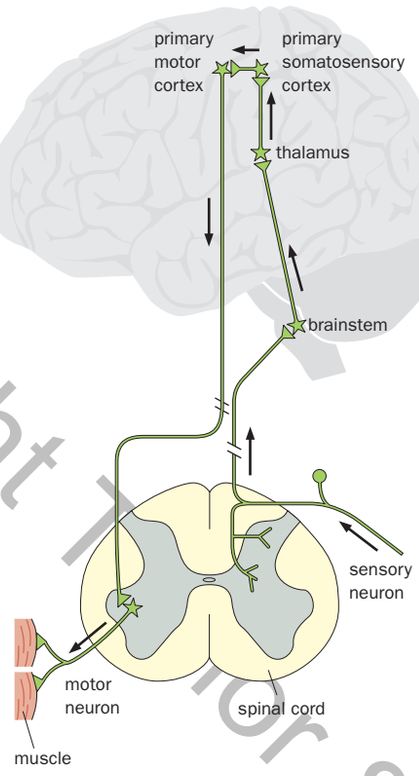

Figure 1-21 Sensory and motor pathways between the spinal cord and cerebral cortex. Some sensory neurons, in addition to participating in the spinal cord reflex circuit, send an ascending branch that connects with relay neurons in the brainstem, which deliver information to neurons in the primary somatosensory cortex via intermediate neurons in the thalamus. Through intercortical connections, information is delivered to neurons in the primary motor cortex, which send descending output directly and indirectly to spinal cord motor neurons for voluntary control of muscles. Shown here are the most direct routes for these ascending and descending pathways. The spinal cord is represented in cross section. The brain is shown from a sagittal view (not at the same scale as the spinal cord). Arrows indicate the direction of information flow.

book. For example, a subject becomes aware that a hammer has hit her knee because sensory neurons also send axonal branches that ascend along the spinal cord. After passing through relay neurons in the brainstem and thalamus, sensory information eventually reaches the **primary somatosensory cortex**, the part of the cerebral cortex that first receives somatosensory input from the body (**Figure 1-21**). Cortical processing of such sensory input generates the perception that her knee has been hit. Such information also propagates to other cortical areas, including the **primary motor cortex**. The primary motor cortex sends descending output directly and indirectly to spinal cord motor neurons to control muscle contraction (Figure 1-21), in case we want to move our leg voluntarily (in contrast to the knee-jerk reflex, which is involuntary). We will study these sensory and motor pathways in greater detail in Chapters 6 and 8, but in general we know far less about the underlying mechanisms of these ascending, cortical, and descending circuits than we do about the spinal cord reflex circuit. Elucidating the principles of information processing in complex neural circuits that mediate sensory perception and motor action is one of the most exciting and challenging goals of modern neuroscience.

1.10 Specific brain regions perform specialized functions

It is well established today that specialized functions of the nervous system are mostly performed by specific parts of the brain. However, throughout prior centuries, philosophers argued about whether brain functions underlie mind, let alone whether specific brain regions are responsible for specific mental activities. Even in the early twentieth century, a prevalent view was that any specific mental function is carried out by neurons across many areas of the cerebral cortex.

Franz Joseph Gall developed a discipline called **phrenology** in the early nineteenth century. Gall supposed that all behavior emanates from the brain, with specific brain regions controlling specific functions. The centers for each mental function, he reasoned, grow with use, creating bumps and ridges on the skull. Based on this reasoning, Gall and his followers attempted to map human mental function to specific parts of the cortex, correlating the size and shape of the bumps

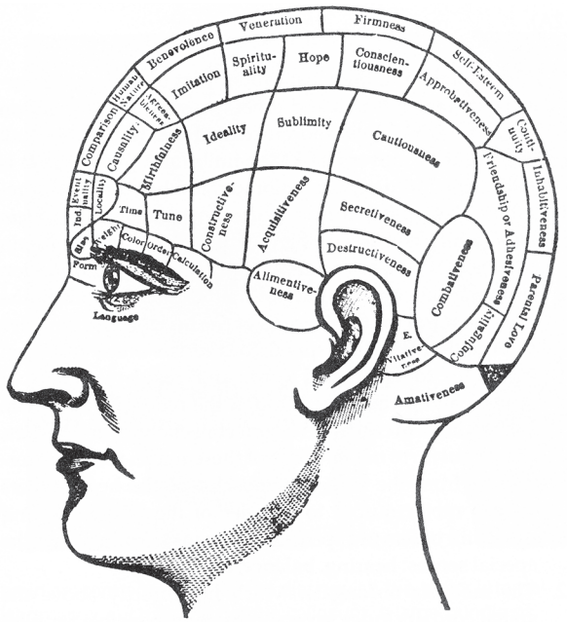

Figure 1-22 Phrenologists' depiction of the brain's functional organization. According to phrenology, the brain is divided into individual areas specialized for defined mental functions. The size of each area is modified by use. For example, a cautious person would have an enlarged area corresponding to cautiousness.

and ridges on individuals' skulls with their talents and character traits (**Figure 1-22**). While we now know that these maps are false, Gall's thinking about brain specialization was actually quite advanced for his time.

Brain lesions provided the first instances of scientific evidence that specialized regions of the human cerebral cortex perform specific functions. Each hemisphere of the cerebral cortex is divided into four lobes, the **frontal**, **parietal**, **temporal**, and **occipital lobes**, based on the major folds (called **fissures**) separating the lobes (**Figure 1-23**A). In the 1860s, Paul Broca discovered lesions in a specific area of the human left frontal lobe (Figure 1-23B) in patients who could not speak. This area was subsequently named **Broca's area** (Figure 1-23A). Carl Wernicke subsequently found that lesions in a distinct area in the left temporal lobe, now named **Wernicke's area** (Figure 1-23A), were also associated with defects in language. Interestingly, lesions in Broca's area and Wernicke's area give distinct symptoms. Patients with lesions in Broca's area have great difficulty producing language, whether in speech or writing, but their understanding of language is largely intact. By contrast, patients with lesions in Wernicke's area have great difficulty understanding language, but they can speak fluently, although often unintelligibly and incoherently. These findings led to the proposal that Broca's and Wernicke's areas are responsible for language production and comprehension,

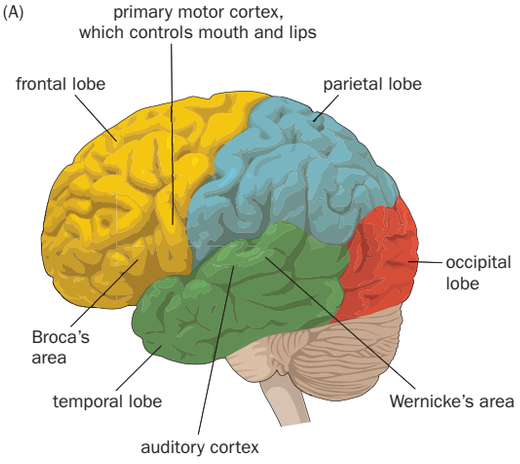

Figure 1-23 Language centers in the human brain were originally defined by lesions. (A) Major fissures divide each cerebral cortex hemisphere into frontal, parietal, temporal, and occipital lobes. Broca's area is located in the left frontal lobe adjacent to the part of the primary motor cortex that controls movement of the mouth and lips (Figure 1-25). Wernicke's area is located in the left temporal lobe adjacent to the auditory cortex. **(B)** Photograph of the brain of one of Broca's patients, Leborgne, who could speak only a single syllable, "tan." The lesion site is circled. Observation of similar lesions in language-deficient patients led Broca to propose that the area is essential for language production. (B, from Rorden C & Karnath H [2004] *Nat Rev Neurosci* 5:813–819. With permission from Springer Nature.)

respectively. These distinct functions are consistent with the locations of Broca's and Wernicke's areas being close to the motor cortex and the **auditory cortex** (the part of the cortex that analyzes auditory signals), respectively (Figure 1-23A).

In the twentieth century, two important techniques—brain stimulation and brain imaging—confirmed and extended findings from lesion studies, revealing in greater detail specific brain regions that perform distinct functions. Brain stimulation is a standard procedure for mapping specific brain regions to guide brain surgeries, such as severing axonal pathways to treat intractable **epilepsy**. (Epilepsy is a medical condition characterized by recurrent seizures—strong surges of abnormal electrical activity that affect part or all of the brain; Box 12-4.) Such surgeries are often performed without general anesthesia (the brain does not contain pain receptors) so that patients' responses to brain stimulation can be observed. Stimulation of Broca's area, for instance, causes a transient arrest of speech in patients. These brain stimulation studies have identified additional areas involved in language production.

One of the most remarkable methods developed in the late twentieth century is the noninvasive functional brain imaging of healthy human subjects as they perform specific tasks. The most widely used technique is **functional magnetic resonance imaging** (**fMRI**), which monitors signals originating from changes in blood flow that results from local neuronal activity. By allowing researchers to observe whole-brain activity without bias while subjects perform specific tasks, fMRI has revolutionized our understanding of brain regions implicated in specific functions. Such studies have confirmed that Broca's and Wernicke's areas are involved in language production and comprehension, respectively.

Because fMRI offers higher spatial resolution than do lesion studies, it has enabled researchers to ask more specific questions. For example, do bilingual speakers use the same cortical areas for their native and second languages? The answer depends on the cortical area in question and the age at which an individual acquires the second language. In late bilinguals who were first exposed to the second language after 10 years of age, representations of the native and second languages in Broca's area map to adjacent but distinct loci (**Figure 1-24**A). In early bilinguals who learned both languages as infants, the two languages map to the same locus in Broca's area (Figure 1-24B). Thus, the age of language acquisition appears to determine how the language is represented in Broca's area. It is possible that after a critical period during development (we will study this important concept in Chapter 5), native language has consolidated a space in Broca's area, such that a second language acquired later must utilize other (adjacent) cortical areas. By contrast, the loci in Wernicke's area that represent the two languages are inseparable by fMRI even in late bilinguals (Figure 1-24C).

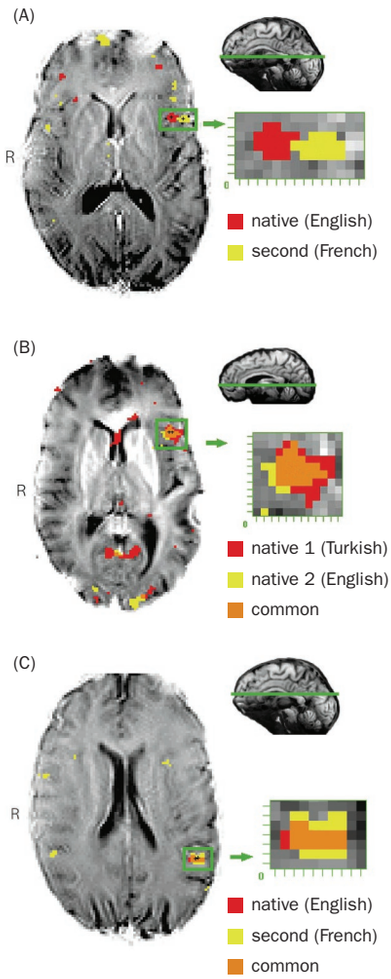

Figure 1-24 Representations of native and second languages as revealed by functional magnetic resonance imaging (fMRI). The detection of blood-flow signals associated with brain activity by fMRI provides a means for imaging the brain loci where native and second languages are processed. In the brain scans on the left side of the figure, green rectangles highlight language-processing areas in the left hemisphere; the highlighted areas are magnified on the right. In the miniature brain profiles located at top right of each panel, the green lines represent the section plane visualized in the scanned images. R, right hemisphere. **(A)** In a late bilingual, the two languages are represented in separate, adjacent loci within Broca's area. **(B)** In an early bilingual who learned both languages from infancy, the language representations in Broca's area overlap. **(C)** In Wernicke's area, the representations of native and second languages overlap regardless of when the second language was acquired; Panels A and C came from the same late bilingual subject. (From Kim KH, Relkin NR, Lee KM, et al. [1997] *Nature* 388:171–174. With permission from Springer Nature.)

1.11 The brain uses maps to organize information

Thanks to a combination of anatomical, physiological, functional, and pathological studies on human subjects, we now have a detailed understanding of the gross organization of the human nervous system (Figure 1-8A). Experimental studies of mammalian model organisms, which share this gross organization (Figure 1-8B), complement our understanding. We will study the organization and function of many nervous system regions in detail in subsequent chapters.

An important organizational principle worth emphasizing now is that the nervous system uses maps to represent information. We have already seen this phenomenon in our earlier discussion of the auditory and visual maps that barn owls use to target their prey. Two striking examples of maps in the human brain are the **motor homunculus** and the **sensory homunculus** (**Figure 1-25**). These homunculi ("little men") were discovered through the use of electrical stimulation during brain surgeries to treat epilepsy, as discussed in Section 1.10. For example, stimulation of cortical neurons in specific parts of the primary motor cortex elicits movement of specific body parts on the contralateral side. (Movement of the left side of the body is controlled by the right side of the brain and vice versa.) Systematic studies revealed a cortical **topographic map** corresponding to movement of specific body parts: nearby neurons in the motor homunculus control the

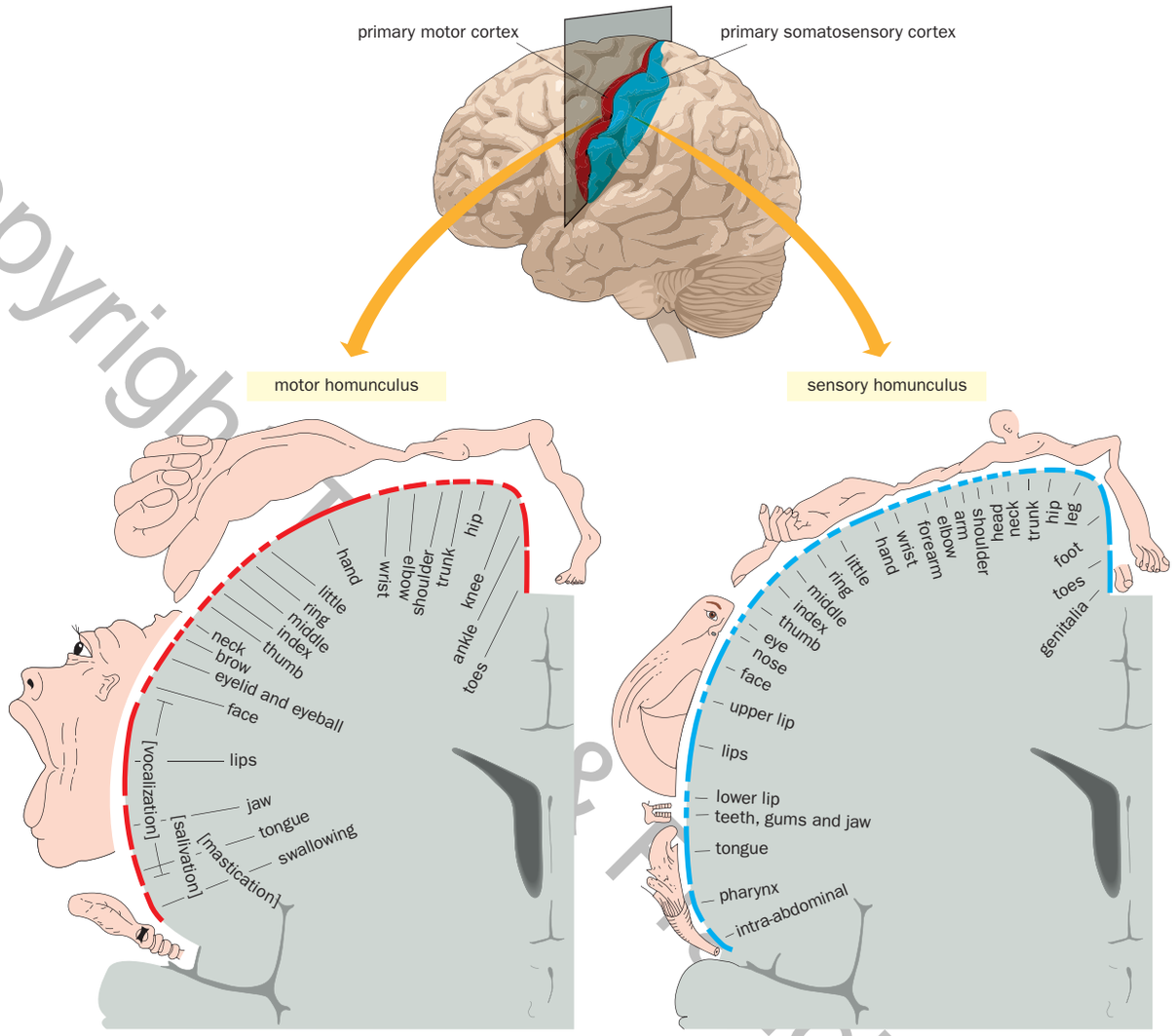

Figure 1-25 Sensory and motor homunculi. Top, the locations in the brain of the primary motor and primary somatosensory cortices. Arrows indicate that sections along the plane with a 90° turn would produce the homunculi in the bottom panels. Bottom left, cortical neurons in the primary motor cortex control movement of specific body parts according to a topographic map. For example, neurons that control movement of the lips and jaw are close together but are distant from neurons that control finger movement. Bottom right, cortical neurons in the primary somatosensory cortex represent a topographic map of the body. For example, neurons that represent touch stimuli on the lips, jaw, and tongue are in adjacent areas but are distant from neurons that represent touch stimuli on the fingers. (From Penfield W & Rasmussen T [1950] The Cerebral Cortex of Man. Macmillan.)

movements of nearby body parts. This map is distorted in its proportions: the hand, and in particular, the thumb, is highly overrepresented, as are the muscles surrounding the mouth that enable us to eat and speak (Figure 1-25, bottom left). These distortions reflect disproportional use of different muscles. As we will learn in Chapter 8, the motor homunculus is a simplified representation of a more complex organization of the motor cortex for movement control.

In the adjacent primary somatosensory cortex, there is a corresponding sensory homunculus. Stimulation of specific areas in the primary somatosensory cortex elicits sensations in specific body parts on the contralateral side (Figure 1-25, bottom right). Again, cortical neurons in adjacent areas represent adjacent body parts, forming a topographic map in the primary somatosensory cortex. This preservation of spatial information is all the more striking, considering that these cortical neurons are at least three synaptic connections away from the sensory world they represent (Figure 1-21). Obvious distortions are also evident: some body parts (for example, the hand and especially the thumb) are overrepresented

compared to others (for example, the trunk). These distortions reflect differential sensitivities of different body parts to sensory stimuli such as touch. Interestingly, cortical neurons in the sensory and motor homunculi that represent the same body part are physically near each other, reflecting a close link between the two cortical areas in coordinating sensation and movement.

Neural maps are widespread throughout the brain. We will learn more about maps in the visual system (Chapter 4); the olfactory, taste, auditory, and somatosensory systems (Chapter 6); the motor system (Chapter 8); and the hippocampus and **entorhinal cortex** (part of the temporal cortex overlying the hippocampus), where maps represent spatial information of the outside world (Chapter 11). We will also study in detail how neural maps are established during development (Chapters 5 and 7).

1.12 The brain is a massively parallel computational device

The brain is often compared to the computer, another complex system with enormous problem-solving power. Both the brain and the computer contain a large number of elementary units—neurons and transistors, respectively—wired into complex circuits to process information conveyed by electrical signals. At a global level, the architectures of the brain and the computer resemble each other, consisting of input, output, central processing, and memory (**Figure 1-26**). Indeed, the comparison between the brain and the computer has been instructive to both neuroscientists and computer engineers.

The computer has huge advantages over the brain in speed and precision of basic operations (**Table 1-1**). Personal computers nowadays can perform elementary arithmetic operations such as addition at a rate of 10^{10} operations per second. However, the rate of elementary operations in the brain, whether measured by action potential frequency or by the speed of synaptic transmission across a chemical synapse, is at best 10^3 per second. Furthermore, the computer can represent quantities (numbers) with any desired precision according to the *bits* (binary digits, or 0s and 1s) assigned to each number. For instance, a 32-bit number has a precision of 1 in 2^{32} or ~4.3×10^9. Empirical evidence suggests that most quantities in the nervous system have variability of at least a few percent due to biological noise, or a precision of 1 in 10^2 at best. However, calculations performed by the brain are neither slow nor imprecise. For example, a professional tennis player can follow the trajectory of a tennis ball after it is served at a speed of 150 miles per hour, move to the optimal spot on the court, position her arm, and swing the racket to return the ball to the opponent's court—and all of this within a few hundred milliseconds. Moreover, the brain can accomplish all of these tasks (with the help of the body it controls) with a power consumption about 10-fold less than a personal computer. How does the brain achieve that?

A notable difference between the brain and the computer is the methods by which information is processed within each system. Computer tasks are largely performed in **serial processing** steps; this can be seen in the way engineers program computers by creating a sequential flow of instructions and by the fact that the operation of each basic unit, the transistor, has only three nodes for input and output altogether. For this sequential cascade of operations, high precision

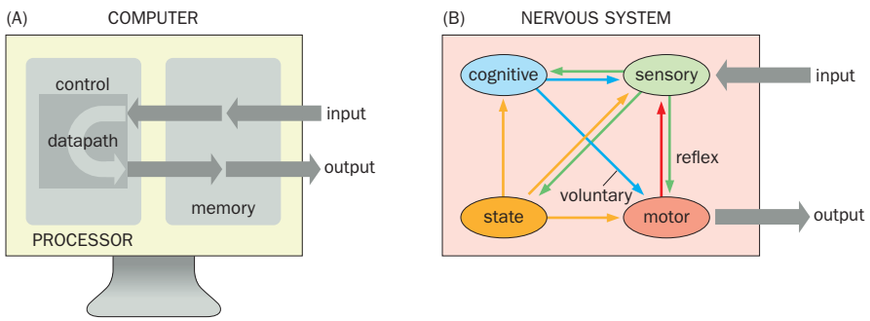

Figure 1-26 Architectures of the computer and the nervous system. **(A)** Schematic of the five classic components of a computer: input (such as a keyboard or a mouse), output (such as a screen or a printer), memory (where data and programs are kept when programs are running), datapath (which performs arithmetic operations), and control (which tells datapath, memory, and input/output devices what to do according to the instructions of the program). Control and datapath together are also called the processor. **(B)** The nervous system can be partitioned in several different ways, one of which is shown here. In this four-system model, the motor system controls the output of the nervous system (behavior). It is in turn controlled by three other systems: the sensory system, which receives input from external environment and the body; the cognitive system, which mediates voluntary behavior; and the behavioral state system (such as wake/sleep), which influences the performance of all other systems. Arrows indicate extensive and often bidirectional connections between the four systems. As we will learn in Chapter 11, memory is primarily stored in the form of synaptic connection strengths in neural circuits in all of these systems. (A, after Patterson DA & Hennessy JL [2012] Computer Organization and Design. 4th ed. Elsevier. B, after Swanson LW [2012] Brain Architecture. 2nd ed. Oxford University Press.)

Table 1-1: Comparing the computer and the brain

Properties	Computer[a]	Human brain
Number of basic units	~10^9 transistors[b]	~10^{11} neurons; >10^{14} synapses
Speed of basic operation	10^{10}/s	<10^3/s
Precision	1 in 4 × 10^9 for a 32-bit number	~1 in 10^2
Power consumption	10^2 watts	~10 watts
Processing method	Mostly serial	Serial and massively parallel
Input/output for each unit	1–3	~10^3
Signaling mode	Digital	Digital and analog

[a] Based on personal computers in 2008.

[b] The number of transistors per integrative circuit has doubled every 18–24 months in the past few decades; in recent years the performance gains from this transistor growth have slowed, limited by energy consumption and heat dissipation.

(Data from von Neumann [1958] The Computer & the Brain. Yale University Press; Patterson & Hennessy [2012] Computer Organization and Design. 4th ed. Elsevier.)

is necessary at each step because errors accumulate and amplify in successive steps. The brain also uses serial steps for information processing; in the tennis return example, information flows from the eye to the brain and then to the spinal cord to control contraction of leg, trunk, arm, and wrist muscles. However, the nervous system also employs **massively parallel processing**, taking advantage of the large number of neurons and large number of connections each neuron makes. For instance, the moving tennis ball activates many retinal photoreceptors, which transmit information to different kinds of bipolar and retinal ganglion cells (Figure 1-16) that we will learn about in Chapter 4. Information regarding the location, direction, and speed of the ball is extracted by parallel circuits within two to three synaptic connections and transmitted in parallel by different kinds of retinal ganglion cells to the brain. Likewise, the motor cortex sends commands in parallel to control contraction of leg, trunk, arm, and wrist muscles, such that the body and arms are simultaneously well positioned to return the incoming ball.

This massively parallel strategy is possible because each neuron collects inputs from and sends outputs to many other neurons—an average of 10^3 for both inputs and outputs for a mammalian neuron. Using the divergent projection motif (Figure 1-20B), information from one neural center can be delivered to many parallel downstream pathways. The convergent projection motif (Figure 1-20A) allows many neurons that process the same information to send their inputs to the same postsynaptic neuron. While information represented by individual neurons may be noisy, by pooling inputs from many presynaptic neurons, a postsynaptic neuron can represent the same information with much higher precision.

The brain and the computer also have similarities and differences in the signaling modes of their elementary units. Transistors employ **digital** signaling, which uses discrete values (0 or 1) to represent information. Action potentials in neuronal axons are also all-or-none digital signals, enabling reliable long-distance information propagation. However, neurons also utilize **analog** signaling, which uses continuous values to represent information. In non-spiking neurons, output is transmitted by graded potentials that can transmit more information than can action potentials (we will discuss this in more detail in Chapter 4). Neuronal dendrites also use analog signaling to integrate up to thousands of inputs. Finally, signals for interneuronal communication are mostly analog, as synaptic strength is a continuous variable.

Another salient property of the brain clearly at play in the tennis return example is that the connection strengths between neurons can be modified by experience, as we will see in greater detail in Chapter 11. Repetitive training enables the circuits to become better configured for the tasks being performed, resulting in greatly improved speed and precision.

Over the past decades, engineers have taken inspiration from the brain to improve computer design. The principles of parallel processing and use-dependent

modification of circuits have both been incorporated into modern computers. For example, increased parallelism, such as the use of multiple processors (cores) in a single computer, is a current trend in computer design. As another example, "deep learning" (a branch of machine learning and artificial intelligence) has enjoyed great success in recent years and accounts for rapid advances in object and speech recognition by computers and mobile devices (Box 14-6); these advances were inspired by findings from the mammalian visual system. At the same time, neurobiologists can enhance their understanding of the nervous system and the potential strategies it employs to solve complex problems by looking at the brain from an engineering and computational perspective, a subject we will expand on in the final part of Chapter 14.

GENERAL METHODOLOGY

The development and utilization of scientific methodology is essential to advancing our knowledge of neurobiology. We devote the last chapter of this book (Chapter 14) to discussing important methods for exploring the brain. *The relevant sections of Chapter 14 should be frequently consulted when these methods are introduced in Chapters 1–13*. We conclude this chapter by highlighting a few general methodological principles that will be encountered throughout the book.

1.13 Observation and measurement are the foundations of discovery

At the beginning of this chapter, we noted that asking the right question is often a crucial first step in making important discoveries. A good question is usually specific enough to be answered with clarity in the framework of existing knowledge. At the same time, the question's answer should have broad significance.

Careful observation is usually the first step in answering questions. Observations can be made with increasing resolution by using improving technology. Our discussion in this chapter about the organization of the nervous system provides good examples. Cells were discovered because of the invention of the light microscope. The elaborate shapes of neurons were first observed because of the invention of the Golgi staining method. The debate between the neuron doctrine and the reticular theory was finally settled with electron microscopy. Inventing new ways of observing can revolutionize our understanding of the nervous system.

While observations can give us a qualitative impression, some questions can be answered only with quantitative measurements. For instance, to find out how sensory stimuli are encoded by nerve signals, researchers needed to measure the size, shape, and frequency of action potentials induced by stimuli of varying strengths. This led to the discovery that stimulus strength is encoded by the frequency of action potentials, but not by their size or duration. The development of new measurement tools often precedes great discoveries.

Observation and measurement go hand in hand. Observations can be quantitative and often form the basis of a measurement. For example, electron microscopy first enabled visualization of the synaptic cleft. At the same time, it also permitted researchers to measure the approximate distance a neurotransmitter must travel across a chemical synapse and to estimate the physical size of the membrane proteins needed to bridge the two sides of a chemical synapse.

1.14 Perturbation experiments establish causes and mechanisms

While observation and measurement can lead to discovery of interesting phenomena, they are often inadequate for investigating the underlying mechanisms. Further insight can be obtained by altering key parameters in a biological system and studying the consequences. We call such studies **perturbation experiments**. Putting prisms on a barn owl is an example of a perturbation experiment. Artificial displacement of the visual map allowed researchers to measure the owl's ability to adjust its auditory map to match an altered visual map. We will encounter numerous perturbation experiments throughout this textbook.

Most perturbation experiments can be categorized as loss-of-function or gain-of-function. In **loss-of-function experiments**, a specific component is removed from the system. This type of experiment tests whether the missing component is *necessary* for the system to function. As an example, specific brain lesions in Broca's patients caused loss of speech, suggesting that Broca's area is *necessary* for speech production. In **gain-of-function experiments**, a specific component is added to the system. Gain-of-function experiments can test whether a component is *sufficient* for the system to function in a specific context. As an example, electrical stimulation (in epileptic patients) indicated that activation of specific motor cortical neurons is *sufficient* to produce twitches of specific muscles. Both loss- and gain-of-function experiments can be used to deduce causal relationships between specific components in a given biological process.

Originating from genetics, the terms *loss-of-function* and *gain-of-function* refer to the deletion and misexpression, respectively, of a gene—a unit of operation for many biological processes. These perturbations allow researchers to test the function of a gene in a biological process. Powerful genetic perturbations can be performed with high precision in many model organisms (Sections 14.6–14.11). Indeed, we will encounter many examples of gene perturbation experiments that have revealed the mechanisms underlying myriad neurobiological processes.

As the lesion and electrical stimulation exemplify, loss- and gain-of-function perturbations do not refer only to experiments that manipulate genes. In contemporary neuroscience, a central issue is the analysis of neural circuit function in perception and behavior, and here single neurons or populations of neurons of a particular type have been conceptualized as the organizational and operational units. To assess the function of specific neurons or neuronal populations in the operation of a circuit, tools have been developed to conditionally silence their activity (loss-of-function) or artificially activate them (gain-of-function) with high spatiotemporal precision (Sections 14.11 and 14.23–14.25). Given that neurons participate in neural circuits in many different ways (Box 1-2), precise perturbation experiments are crucial in revealing the mechanisms by which neural circuits control neurobiological processes. These experiments also help establish causal relationships between the activity of specific neurons and the processes they control.

With these basic concepts and general methodological frameworks in hand, let us begin our journey!

SUMMARY

In this chapter, we introduced the general organization of the nervous system and some fundamental concepts in neurobiology, framing these topics from a historical perspective. Neurons are the basic building blocks of the nervous system. Within most vertebrate neurons, information, in the form of membrane potential changes, flows from dendrites to cell bodies to axons. Graded potentials in dendrites are summed at the junction between the cell body and the axon to produce all-or-none action potentials that propagate to axon terminals. Neurons communicate with each other through synapses. At chemical synapses, presynaptic neurons release neurotransmitters in response to the arrival of action potentials, and postsynaptic neurons change their membrane potential in response to neurotransmitters binding to their receptors. At electrical synapses, ions directly flow from one neuron to another through gap junctions to propagate membrane potential changes. Neurons act in the context of neural circuits and form precise connections with their synaptic partners to process and propagate information within circuits. Neural circuits in different parts of the brain perform distinct functions, ranging from sensory perception to motor control. The nervous system employs a massively parallel computational strategy to enhance the speed and precision of information processing. In the rest of this book, we will expand our studies of these fundamental concepts in the organization and operation of the nervous system.

FURTHER READING

Books and reviews

Adrian ED (1947) Physical Background of Perception. Clarendon.

Allen NJ & Lyons DA (2018) Glia as architects of central nervous system formation and function. *Science* 362:181–185.

Knudsen EI (2002) Instructed learning in the auditory localization pathway of the barn owl. *Nature* 417:322–328.

Ramón y Cajal S (1995) Histology of the Nervous System of Man and Vertebrates. Oxford University Press. (Original French version 1911)

Swanson LW (2012) Brain Architecture: Understanding the Basic Plan, 2nd ed. Oxford University Press.

Tinbergen N (1951) The Study of Instinct. Oxford University Press.

von Neumann J (1958) The Computer & the Brain. Yale University Press.

CHAPTER 2

Signaling within Neurons

The zoologist is delighted by the differences between animals, whereas the physiologist would like all animals to work in fundamentally the same way.

Alan Hodgkin (1992), *Chance and Design: Reminiscences of Science in Peace and War*

Nervous systems can react rapidly to sensory stimuli. For example, a 5-day-old zebrafish larva begins responding to a pulse of water representing a potential threat within 3 milliseconds, and completely changes its direction of movement within 12 milliseconds, propelling itself away from a potential threat (**Figure 2-1**). This escape behavior relies on detection of mechanical force by sensory neurons, transmission of this sensory information through interneurons to motor neurons, and coordinated contraction or relaxation of appropriate muscles, all of which happens within several milliseconds. Because these escape behaviors, such as avoiding a predator (**Movie 2-1**), are crucial for animal survival, the speed at which neurons communicate has been subject to strong evolutionary selection.

As introduced in Chapter 1, the nervous system uses electrical signals to transmit information within a neuron. Individual neurons are the basic units of the nervous system, receiving, integrating, propagating, and transmitting signals based on changes in the membrane potential (Figure 1-18). A typical vertebrate neuron receives inputs from its presynaptic partners in the form of synaptic potentials at its dendrites and cell body. The neuron integrates these synaptic potentials along their paths toward the axon initial segment, where action potentials are generated. Action potentials propagate along the axon to the neuron's presynaptic terminals, where they cause neurotransmitter release. Neurotransmitters then bind to receptors on the postsynaptic target neurons, producing synaptic potentials and thus completing a full round of neuronal communication.

In this chapter and in Chapter 3, we will discuss the fundamental mechanisms of neuronal communication, focusing on three key steps: (1) the generation and propagation of action potentials, (2) the release of neurotransmitters by presynaptic neurons, and (3) the reception of neurotransmitters by postsynaptic neurons. Before we delve into these key steps, we will first study the special cellular properties of neurons as large cells with elaborate cytoplasmic extensions and as conductors of electrical signals. Understanding these properties is essential for our study of neuronal communication. The first four sections of this chapter also serve as an introduction to or a refresher of basic concepts and terms in molecular and cell biology used throughout this textbook.

Figure 2-1 Rapid escape response of a zebrafish larva. Time-lapse images of the escape behavior of a zebrafish larva in response to a water pulse from the tube at bottom left. The asterisk (*) indicates the first detectable response at 3 milliseconds (ms) after stimulus onset, which is difficult to see in the frames shown here but is evident when observed in video clips. (From Liu KS & Fetcho JR [1999] *Neuron* 23:325–335. With permission from Elsevier Inc.)

CELL BIOLOGICAL AND ELECTRICAL PROPERTIES OF NEURONS

Neurons are the largest cells in animals. For instance, the cell body of a sensory neuron that innervates the toe is located in a dorsal root ganglion at about the level of the waist, but its peripheral branch extends down to the toe, and its central axon extends up to the brainstem (Figure 1-21); thus this sensory neuron spans about 2 m for a tall person and 5 m for a giraffe. Many neurons have complex dendritic trees. For example, the dendritic tree of the cerebellar Purkinje cell (Figure 1-11) has hundreds of branches and receives synaptic inputs from up to 200,000 presynaptic partners. The surface area and volume of axons or dendrites usually exceed those of the cell bodies by several orders of magnitude. This unique architecture, along with signaling molecules that decorate this architecture in specific patterns, enables rapid electrical signaling across long distances and allows individual neurons to integrate information from many cells.

In order for neurons to initiate, integrate, propagate, and transmit electrical signals, they must continuously synthesize proteins and deliver them to the appropriate subcellular compartments. Thus, there are two ways in which communication happens within the neuron: by the transport of RNA, proteins, and organelles along their long processes to get those components to the right part of the cell and by electrical signals moving along those processes. These two might, respectively, be compared to sending a package through the mail, whereby a physical object is delivered, and to sending a text or email, whereby only information is conveyed. Each is critical to nervous system function but relies on very different mechanisms. In the following sections, we will study these mechanisms, beginning with the basic molecular and cell biology of the neuron.

2.1 Neurons obey the central dogma of molecular biology and rules of intracellular vesicle trafficking

Macromolecule synthesis in neurons obeys the **central dogma** of molecular biology, which states that information flows from DNA → RNA → protein (**Figure 2-2**, left). **Genes**, the genetic substrates that carry instructions for how and when to make specific RNAs and proteins, are located in the nucleus on **DNA** molecules. DNAs are long double-stranded chains of nucleotides containing the sugar deoxyribose, a phosphate group, and one of four nitrogenous bases: adenine (A), cytosine (C), guanine (G), or thymidine (T). **Transcription** is the process by which RNA polymerase uses DNA as a template to synthesize single-stranded **RNA** (a chain of ribose-containing nucleotides, in which uracil [U] replaces T); the part of the gene that serves as a template for RNA synthesis is called the gene's **transcription unit**. The premessenger RNAs (pre-mRNAs) produced during gene transcription carry information in their specific ribonucleotide sequence that corresponds to the deoxyribonucleotide sequence of the transcription unit. Pre-mRNAs undergo a series of RNA processing steps. These include capping (adding a modified guanosine nucleotide to the 5′ end of the RNA), **RNA splicing** (removing RNA sequences that don't code for protein, called **introns**, and joining together the remaining sequences, called **exons**), polyadenylation (adding a long sequence of adenosine nucleotides to the RNA's 3′ end), and occasionally **RNA editing** (a regulated event that changes specific RNA sequences). The resulting mature **messenger RNAs** (**mRNAs**) are exported from the nucleus to the cytoplasm, where they are decoded by ribosomes during protein synthesis (**translation**). The information in the mRNA sequence dictates the amino acid sequence of the newly synthesized polypeptide (**protein**).

In addition to mRNAs, cells also transcribe a variety of RNAs that do not encode proteins. These include ribosome RNAs (rRNAs) and transfer RNAs (tRNAs) essential for the translation process as well as a variety of other RNAs collectively called noncoding RNAs. One class of noncoding RNAs that function in the cytoplasm is the **microRNAs**; these short (21–26 nucleotides) RNAs regulate protein production by triggering the degradation and inhibiting the translation of mRNAs

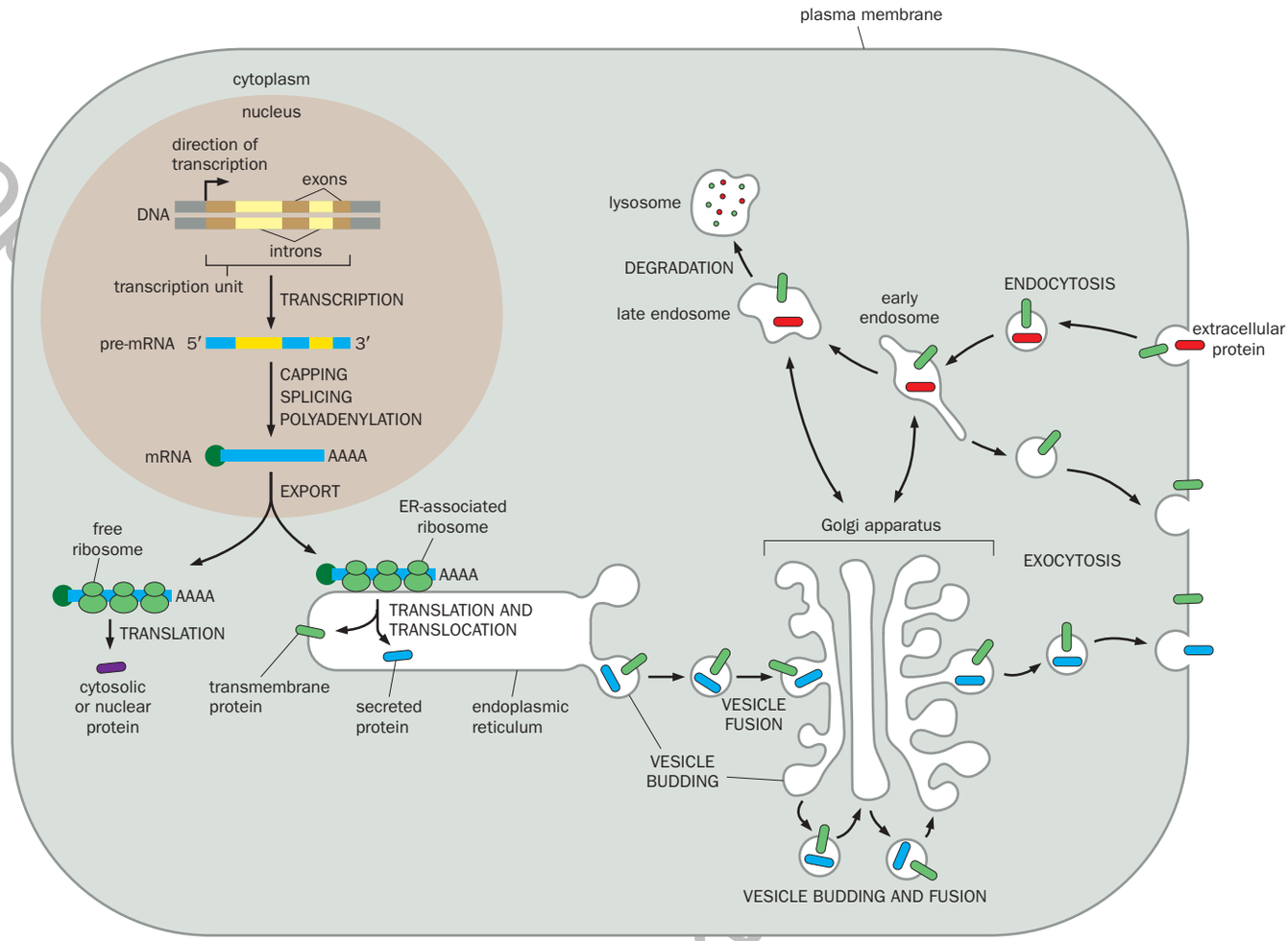

Figure 2-2 Schematic summary of the central dogma of molecular biology and intracellular vesicle trafficking. Left, in the nucleus, double-stranded DNA serves as a template for transcription to produce a pre-mRNA, which grows longer as nucleotides are added to the 3′ end. Pre-mRNA is processed by capping the 5′ end, splicing to remove introns and join exons, and polyadenylation at the 3′ end to produce mature mRNA, which is exported to the cytoplasm. mRNAs encoding cytosolic and nuclear proteins (purple) are translated on free ribosomes in the cytosol (left branch). mRNAs encoding secreted (blue) or transmembrane (green) proteins are translated on ribosomes associated with the endoplasmic reticulum (ER). Bottom right, after synthesis and translocation across the ER membrane, transmembrane and secreted proteins exit the ER through vesicle budding, pass through the Golgi apparatus via a series of vesicle fusion and budding steps, and are transported to the plasma membrane. Fusion of a vesicle with the plasma membrane (exocytosis) leads to the release of secreted proteins into the extracellular space and delivery of the transmembrane proteins to the plasma membrane. Top right, extracellular proteins (red) or transmembrane proteins on the plasma membrane can be internalized through vesicle budding from the plasma membrane (endocytosis) into early endosomes. The content can be recycled back to the plasma membrane through exocytosis or can be delivered to late endosomes and lysosomes for degradation. There is also bidirectional trafficking between the endosomes and the Golgi apparatus. Much of the intracellular vesicle transport is along the microtubule cytoskeleton using molecular motors; we will discuss these in Section 2.3.

with complementary sequences. Other noncoding RNAs play a variety of roles in the nucleus to regulate gene expression.

Translation occurs in one of two distinct locations, depending on the destination of the protein products in eukaryotic cells. Proteins localized in the cytosol and nucleus are synthesized on free ribosomes in the cytoplasm, whereas proteins destined for export from the cell (**secreted proteins**) or that span the lipid bilayer of a membrane (**transmembrane proteins**) are synthesized on ribosomes associated with the **endoplasmic reticulum** (**ER**), a network of membrane-enclosed compartments (Figure 2-2, left).

For most secreted proteins and transmembrane proteins destined for the plasma membrane, all or part of their sequence is translocated across the ER membrane as they undergo translation. Fully translated proteins then undergo a

series of trafficking steps via **intracellular vesicles**, which are small, membrane-enclosed organelles in the cytoplasm. Secreted and transmembrane proteins exit the ER via budding of vesicles from the ER membrane and transit through the Golgi apparatus via a series of vesicle fusion and budding events. Eventually, vesicles that carry these proteins fuse with the plasma membrane in a step called **exocytosis**, so that secreted proteins are released into the extracellular space and transmembrane proteins are delivered to the plasma membrane (Figure 2-2, bottom right).

In addition to exocytosis, neurons (like many other cells) employ a process called **endocytosis**, which allows cells to retrieve fluid and proteins from the extracellular space or transmembrane proteins from the cell's plasma membrane. Endocytosis products are first delivered to early **endosomes**, which are membrane-enclosed organelles that carry newly ingested materials and newly internalized transmembrane proteins. Proteins from early endosomes can either cycle back to the plasma membrane through exocytosis or be transported to late endosomes and **lysosomes**, which contain enzymes for protein degradation (Figure 2-2, top right). In Chapter 3, we will study specific examples of exocytosis and endocytosis in the context of presynaptic neurotransmitter release and postsynaptic neurotransmitter receptor regulation.

While obeying the central dogma and rules of intracellular vesicle trafficking, neurons also have special properties to accommodate their large size and the great distance between the tip of their axonal or dendritic extensions and the cell body (soma). We can ask a simple question: how does a specific protein, such as a neurotransmitter receptor or a protein associated with the presynaptic membrane, get to the dendritic tip or axon terminal? The answer to this "simple" question is quite complex, and we are far from having complete answers for it. In principle, the corresponding mRNAs can be transported to the final destination before directing protein synthesis there. Alternatively, the protein can be synthesized at the soma and can either diffuse passively or be actively delivered to its final destination. For a transmembrane protein, delivery can take one of the following routes: (1) the intracellular vesicle that carries the protein can fuse with the plasma membrane at the soma, and the transmembrane protein can then diffuse over the plasma membrane to its destination; (2) the vesicle can be transported within dendrites or axons and can then fuse with the plasma membrane at its final destination; or (3) the protein can first be targeted to the plasma membrane of one compartment (axon or dendrite) and then endocytosed and trafficked to the final destination, a process called **transcytosis**. Each synthesis and transport mechanism has been observed. Their relative prevalence depends both on the type of protein and the type of neuronal compartment to which that protein is targeted. We will study some of these mechanisms in the next two sections.

2.2 While some dendritic and axonal proteins are synthesized from mRNAs locally, most are actively transported from the soma

Substantial evidence has demonstrated that mRNAs encoding a subset of proteins are targeted to dendritic processes, where they direct **local protein synthesis**. Electron microscopic studies revealed the presence of polyribosomes (clusters of ribosomes) in the dendrites, suggesting the translation of mRNA (**Figure 2-3**A). ***In situ* hybridization** studies, which can determine mRNA distribution in native tissues (Section 14.12), have identified specific mRNAs present in dendrites (Figure 2-3B). These dendritically localized mRNAs encode a variety of proteins known to function in dendrites and postsynaptic sites, such as the α subunit of the Ca^{2+}/calmodulin-dependent protein kinase II (CaMKII; Figure 2-3B, left panel), cytoskeletal elements such as actin and microtubule-associated protein 2 (MAP2), and neurotransmitter receptors. We will revisit many of these proteins later in this chapter and in Chapter 3. The list of dendritically localized mRNA has greatly expanded in recent years, thanks to high-throughput methods such as isolating mRNA from dendritic compartments for RNA sequencing (Section 14.12). In

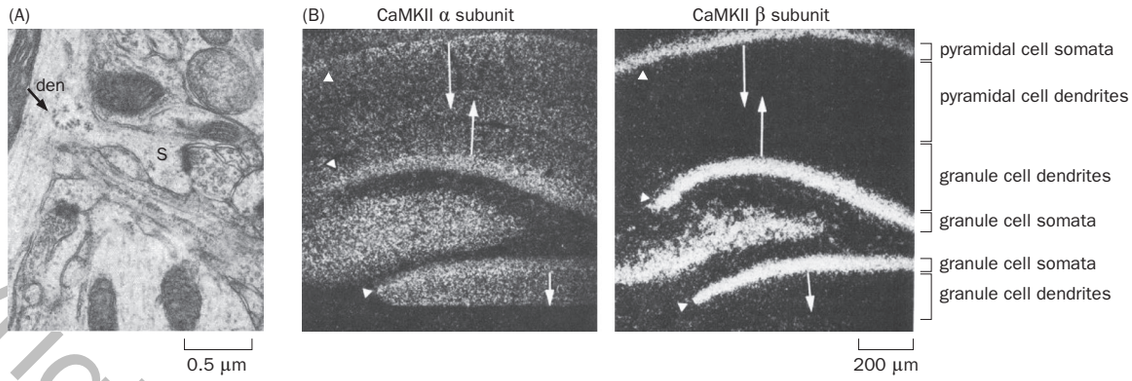

Figure 2-3 Dendritic protein synthesis. (A) Electron micrograph of part of a rat hippocampal granule cell (Figure 1-12). At the left of the micrograph is a segment of a dendrite (den), with a dendritic spine (S) branching to the right. A cluster of ribosomes (arrow) is seen at the junction between the dendritic trunk and the spine. **(B)** Localization of mRNA encoding the α and β subunits of the Ca^{2+}/calmodulin-dependent protein kinase II (CaMKII) in sections of rat hippocampus, detected by *in situ* hybridization using probes specific to each gene. mRNAs for the CaMKII α subunit localize to cell bodies (somata; arrowheads) as well as dendrites of these cells (indicated by the arrows leaving the cell body layers), whereas mRNAs for the CaMKII β subunit are restricted to layers containing somata of both granule cells and pyramidal cells. See Figure 11-5 for a schematic of the hippocampus. (A, from Steward O & Levy WB [1982] *J Neurosci* 2:284–291. Copyright ©1982 Society for Neuroscience. B, from Burgin KE, Waxham MN, Rickling S, et al. [1990] *J Neurosci* 10: 1788–1798. Copyright ©1990 Society for Neuroscience.)

addition to polyribosomes and mRNAs, ER and Golgi apparatus–like membrane organelles have also been observed in distal dendrites, enabling locally synthesized transmembrane and secreted proteins to go through the secretory pathway just as in the soma (Figure 2-2). Finally, local translation in dendrites has been directly demonstrated using a number of *in vitro* preparations.

Local protein synthesis in dendrites solves several problems: it ameliorates the costs of long-distance transport, spatially focuses production of specific proteins where they are needed, and, perhaps most interestingly, allows protein production to be regulated in a specific compartment of the dendritic tree. As discussed in later chapters, such local protein synthesis in dendrites enables rapid changes of protein translation in response to synaptic signaling; these locally synthesized proteins in turn help modify synaptic signals, which may result in regional remodeling of dendrites and synapses in response to synaptic activity. Although much less studied compared to dendritic protein synthesis, local protein synthesis has also been observed in developing and mature axons. The products of local protein synthesis in developing axons may play important roles in axon guidance, a process we will study in detail in Chapters 5 and 7.

Even for proteins known to be synthesized in dendrites, the mRNA is usually more abundant in the soma (Figure 2-3B, left panel), suggesting that they are also synthesized in the soma. For most proteins, mRNAs appear predominantly in the soma (Figure 2-3B, right panel). How do these proteins get to their final destinations in dendrites and axons? This question has been explored primarily in axons because of the relative experimental ease of isolating distal axons from cell bodies. For example, radioactively labeled amino acids can be injected into regions that house cell bodies of sensory or motor neurons, which extend long axons to distant sites. Newly synthesized proteins that incorporate these radioactively labeled amino acids can be isolated from their axons at different times after injection and at different distances from the cell bodies, and analyzed by biochemical methods such as gel electrophoresis to determine their identities (**Figure 2-4**). These studies have identified two major groups of proteins based on the speeds of their appearances in axons. The fast component travels at 50–400 mm per day (0.6–5 μm/s); this includes mostly transmembrane and secreted proteins. The slow component travels at 0.2–8 mm per day; this includes mostly cytosolic proteins and cytoskeletal components. These two modes are termed **fast axonal transport** and **slow axonal transport**, respectively. In addition to **anterograde** transport from the cell body to the axon terminal, some proteins, such as those taken up via endocytosis, travel in the **retrograde** direction from axon terminals back to the cell body;

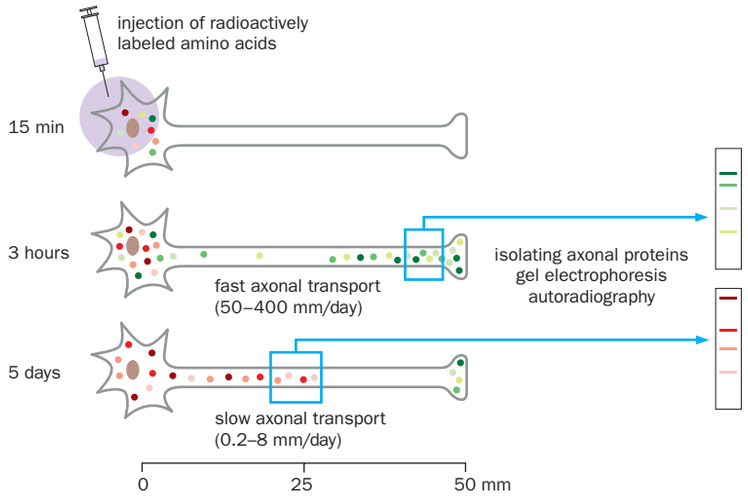

Figure 2-4 Studying axonal transport by isolating radioactively labeled proteins. Top, radioactively labeled amino acids are injected near the neuronal cell body and are either incorporated into newly synthesized proteins shortly after injection or metabolized. Middle and Bottom, at two time periods after the initial injection, proteins are isolated at specific segments of the axons (blue boxes), analyzed by gel electrophoresis, and visualized by autoradiography. (Adapted from Roy S [2014] *Neuroscientist* 20:71–81. With permission from SAGE.)

the speed of retrograde transport is similar to that of the fast anterograde axonal transport.

What mechanisms account for different modes of axonal transport? Theoretical studies indicate that passive diffusion within axons is too slow to account for even slow axonal transport, suggesting that all of these transport modes are active processes. Although less well studied, protein and mRNA transport into dendrites likely utilizes similar active processes. To understand the mechanisms underlying active transport and to appreciate why some proteins are transported to dendrites and others to axons, we need to examine the cytoskeletal organization of neurons.

2.3 The cytoskeleton forms the basis of neuronal polarity and directs intracellular trafficking

Like all eukaryotic cells, neurons rely on two major cytoskeletal elements for structural integrity and motility—**filamentous actin** (**F-actin**, also called microfilaments) and **microtubules**. F-actin is composed of two parallel helical strands of actin polymers, whereas microtubules are hollow cylinders consisting of 13 parallel protofilaments made of α- and β-tubulin subunits (**Figure 2-5**). Most cells also have intermediate filaments, cytoskeletal polymers with diameters between those of F-actin (~7 nm) and microtubules (~25 nm). The most prominent intermediate filaments in vertebrate neurons are the **neurofilaments**, which are concentrated in axons where they promote cytoskeletal stability.

F-actin and microtubules are both polar filaments that have *plus* and *minus* ends with distinct properties. As in all cells, F-actin is mostly concentrated near the plasma membrane. These include the plasma membrane along axonal and dendritic processes, at presynaptic terminals and postsynaptic dendritic spines in mature neurons, and at growth cones of axons and dendrites in developing neurons. Actin subunits are added to the plus ends of F-actin, which localizes close to the plasma membrane, such that actin polymerization can cause membrane protrusions responsible for morphological dynamics and motility of cells. F-actin does not mediate long-distance transport along dendritic or axonal processes, however. Microtubules occupy the center of axonal and dendritic processes, and are thus the cytoskeletal element along which long-distance transport in neuronal processes occurs. In most nonneuronal cells, the more dynamic plus ends of microtubules point toward the periphery, whereas the more stable minus ends are at the centers of cells, anchored in microtubule organizing centers. Microtubule orientation is more complicated in neurons and contributes to the distinction between dendrites and axons.

As introduced in Chapter 1, information generally flows from dendrites to axons. More than a century after Ramón y Cajal's original proposal, there is now a

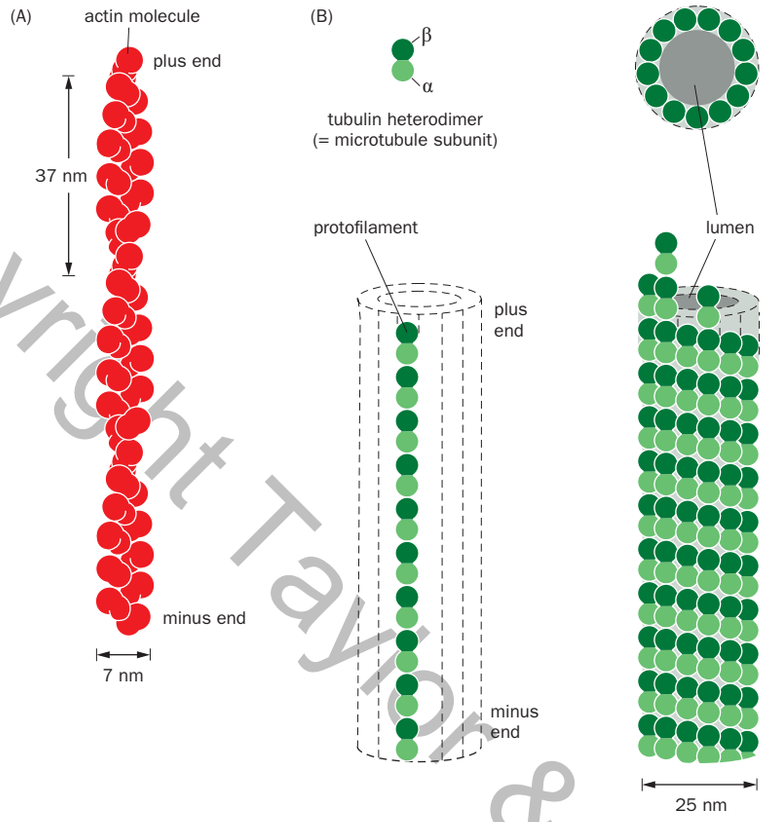

Figure 2-5 Filamentous actin (F-actin) and microtubules are two major cytoskeletal elements. (A) Schematic of F-actin, composed of two helical strands with a repeating unit of 37 nm. **(B)** Schematic of the microtubules. Left, α- and β-tubulin heterodimers assemble into longitudinal protofilaments. Right, the microtubule is made of 13 parallel protofilaments that form a tube with a hollow lumen (cross section is shown above). (Adapted from Alberts B, Johnson A, Lewis J, et al. [2015] Molecular Biology of the Cell, 6th ed. Garland Science.)

good understanding of the cell biological basis of **neuronal polarity**—the distinction between axons and dendrites. Subcellular structures and proteins related to reception of information, such as neurotransmitter receptors, are generally targeted to dendrites. Conversely, structures and proteins related to transmission of information, such as synaptic vesicles, are targeted to axons. These are largely achieved by the asymmetric cytoskeletal organization of the neuron, which enables **motor proteins**—which convert energy from ATP hydrolysis into movement along the cytoskeletal polymers—to transport specific cargos to specific destinations.

The orientation of microtubules differs in axons and dendrites. In axons, parallel arrays of microtubules are oriented with their plus ends pointing away from the cell body and toward the axon terminal, following the plus-end-out rule. However, dendrites have a mixed population of microtubules: plus-end-out and minus-end-out populations are about equally prevalent in proximal dendrites (**Figure 2-6A**). To date, this rule has applied to all vertebrate neurons examined in culture and *in vivo*. As discussed in Section 1.7, most invertebrate neurons have a single neurite that exits the cell body, which then gives rise to both dendritic and axonal branches. Some sensory neurons in the nematode *C. elegans* and the fruit fly *Drosophila* have distinct axonal and dendritic processes (similar to bipolar neurons in vertebrates). In invertebrate bipolar neurons thus far examined, dendrites appear to have mostly minus-end-out microtubules, whereas axons have plus-end-out microtubules. Thus, although details may differ, both vertebrate and invertebrate neurons share the principle that dendrites and axons differ in their microtubule orientations.

Two types of motor proteins move cargos along microtubules: (1) the cytoplasmic **dynein** and (2) a large family of proteins called **kinesins**. Dynein is a minus-end-directed motor; as such, it transports cargos from axon terminals back to the cell body. Most kinesins are plus-end-directed motors and therefore transport cargos from the cell body to axon terminals (Figure 2-6B). In vertebrate dendrites, both dyneins and kinesins can mediate bidirectional transport because of

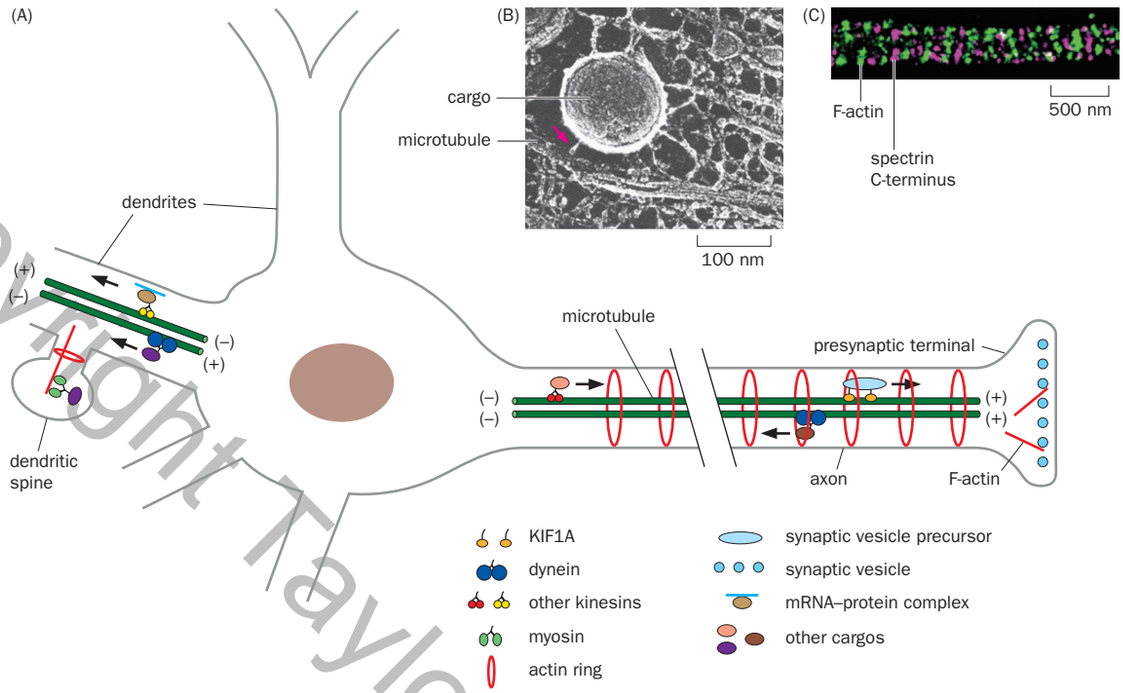

Figure 2-6 Cytoskeletal organization and motor proteins in axons and dendrites. (A) In the axon of a typical vertebrate neuron, microtubules (green) are oriented with the plus end (+) pointing toward the axon terminal, or plus end out. By contrast, dendrites contain microtubules with both plus- and minus-end-out orientations. Cargos destined for axon terminals, such as synaptic vesicle precursors (cyan), are preferentially transported toward axon terminals by plus-end-directed kinesins such as KIF1A (orange). Other cargos are transported by dynein (which moves toward the minus end of microtubules) or other kinesins in the axon and dendrites. For example, an mRNA (cyan line) with an associated protein complex (light brown) is transported by a kinesin into dendrites. Dynein and most kinesins are dimers with two heads (motor domains), whereas KIF1A acts as a monomer. F-actins (red) are distributed near the plasma membrane within axons (where they form rings) and dendrites (not shown) and are particularly enriched in dendritic spines and presynaptic terminals. After leaving microtubules, cargos may be further transported to their local destination by myosin-based movement along F-actin. **(B)** Quick-freeze deep-etch electron microscopy reveals the structure of the axonal cytoskeleton. The arrow points to a structure consistent with kinesin protein moving a cargo along the microtubule. **(C)** Super-resolution fluorescence microscopy image of an axon segment of a cultured rat hippocampal neuron stained with phalloidin (green), which labels F-actin, and an antibody against the C-terminus of βII-spectrin (magenta). Note the periodic distribution of both proteins, with the period being ~190 nm. (B, from Hirokawa N, Niwa S, & Tanaka Y [2010] *Neuron* 68:610–638. With permission from Elsevier Inc. C, from Xu K, Zhing G, & Zhuang X [2013] *Science* 339:452–456.)

mixed polarity microtubules. mRNAs used in dendrites for local protein synthesis are transported by dynein and several kinesins on microtubules in the form of mRNA–protein complexes (Figure 2-6A).

Dynein and kinesins have specific proteins that link them to specific cargos, and some kinesins may bind directly to cargos. For example, synaptic vesicle precursors are transported from the cell body to axon terminals by binding directly to a specific kinesin called KIF1A (Figure 2-6A). Certain types of kinesins are highly enriched in axons whereas others can transport cargoes into both axons and dendrites, increasing the specificity with which cargo is delivered to defined neuronal compartments. The asymmetric organization of the microtubule cytoskeleton and specific motor–cargo interactions together establish and maintain neuronal polarity. Other factors contributing to neuronal polarity include diffusion barriers at the axon initial segment for both cytosolic and membrane proteins. In Chapter 7, we will explore how polarity is initiated in developing neurons.

In vitro motility studies indicate that kinesins and the cytoplasmic dynein mediate fast axonal transport. Kinesins can move along microtubules at about 2 μm/s (**Box 2-1**; **Movie 2-2**), in the same range as fast anterograde axonal transport (Figure 2-4). Recent studies indicate that kinesins also mediate slow anterograde axonal transport. However, slow transport is characterized by much longer pauses between runs (periods when cargos are being transported), whereas fast axonal transport features longer runs and shorter pauses. During its brief runs, slow transport achieves speeds comparable to runs of fast axonal transport.

Box 2-1: How were kinesins discovered?

Breakthroughs in biology often result from utilization of new techniques and appropriate experimental preparations to address important, unsolved questions. The identification of kinesins illustrates how the combination of these ingredients drives new discoveries. In the early 1980s, the invention of video-enhanced differential interference contrast (VE-DIC) microscopy enabled visualization of subcellular organelles in unstained live tissues. When applied to the squid giant axon, a specialized axon whose diameter can reach 1 mm (we will encounter this axon again in our studies of the action potential later in this chapter), VE-DIC microscopy revealed that organelles move along filament-like structures running along the axon's length inside the plasma membrane (**Figure 2-7**A). Furthermore, following extrusion of the axonal cytoplasm (axoplasm), organelle movement along filaments in the axoplasm, free of axonal membrane, was similarly observed.

The ability of the extruded axoplasm to support organelle movement opened the door to many experimental manipulations. For example, researchers could dilute the axoplasm to track organelle movement along a single filament over time and measure its speed (Movie 2-2). The speed was found to be around 2 μm/s for transportation of small

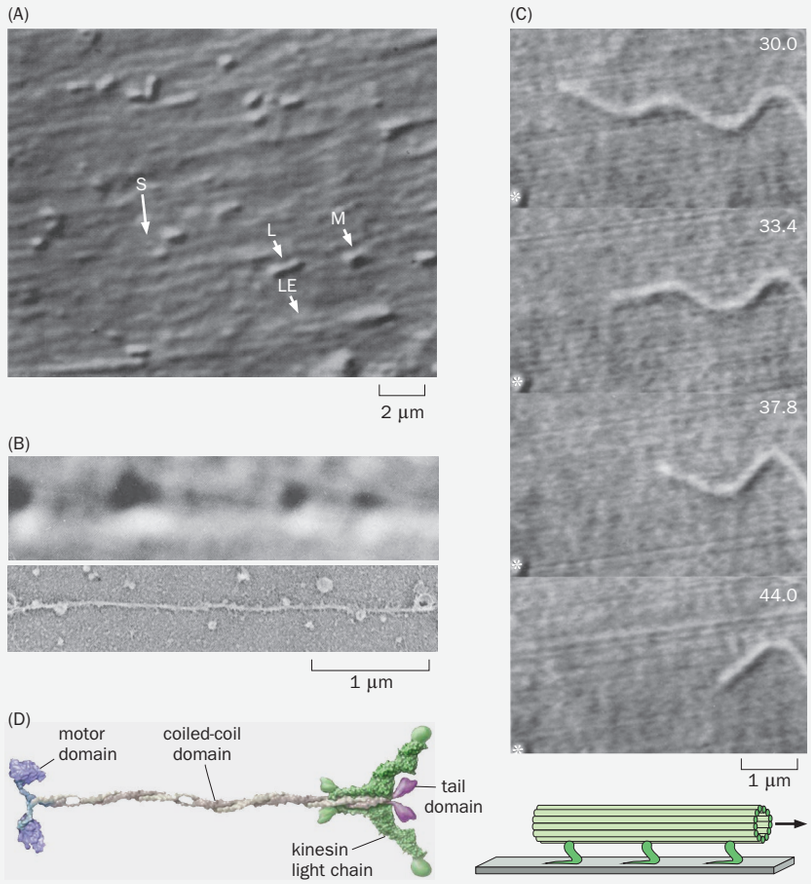

Figure 2-7 Discovery of the first kinesin. (A) An image of a segment from an intact squid giant axon, taken using video-enhanced differential interference contrast (VE-DIC) microscopy, shows horizontal linear elements (LE, which are microtubules) running in parallel with the axon. In video records, many small (S), medium (M), and large (L) organelles can be seen moving along the linear elements. **(B)** Top, VE-DIC image of organelles moving horizontally along what appears to be a single transport filament from extruded squid axoplasm; bottom, the same field of view in electron microscopy, taken after VE-DIC study, confirming the presence of a single microtubule. The apparent diameter of the transport filament in the light microscope is inflated by diffraction to about 10 times its true diameter (25 nm). **(C)** Top, time-lapse movie (time at upper right indicates seconds) of a single microtubule moving rightward on a glass slide to which a soluble fraction purified from squid axoplasm had been immobilized, in the presence of ATP. The object marked with an asterisk at the bottom left serves as a stationary marker. Bottom, a schematic of putative motor proteins from the squid axoplasm attached to the glass and to the microtubule. ATP hydrolysis by multiple motor proteins oriented in the same direction causes microtubule movement relative to the glass. **(D)** Molecular structure the kinesin from the squid giant axon. (A, from Allen RD, Metuzals J, Tasaki I, et al. [1982] *Science* 218:1127–1129. With permission from AAAS. B, adapted from Schnapp BJ, Vale RD, Sheetz MP, et al. [1985] *Cell* 40:455–462. With permission from Elsevier Inc. C, adapted from Vale RD, Schnapp BJ, Reese TS, et al. [1985] *Cell* 40:559–569. With permission from Elsevier Inc. D, from Vale RD [2003] *Cell* 112: 467–480. With permission from Elsevier Inc.)

(*Continued*)

Box 2-1: continued

organelles, in the same range as the fast axonal transport speed determined by tracking radioactively labeled proteins in vertebrate neurons *in vivo* (Figure 2-4). Chemicals or drugs could be added to the axoplasm to study their effects on organelle motility. It was already known then that the actin-based motor myosin utilized ATP hydrolysis to power movement along F-actin, so researchers tested whether ATP hydrolysis is also required for axonal transport. They found that motility was blocked when ATP was depleted from the axoplasm or when a nonhydrolyzable ATP analog was added, indicating that organelle movement along axoplasmic filaments indeed depends on ATP hydrolysis. Finally, following motility studies along a single transport filament using VE-DIC microscopy, electron microscopic analysis of the same filament (Figure 2-7B) provided unequivocal evidence that the individual filaments supporting organelle movement are individual microtubules.

These studies suggested the presence of motor proteins that utilize energy from ATP hydrolysis to move organelles in the squid axoplasm. Indeed, just as microtubules can support organelle movement, a soluble fraction of axoplasm from the squid giant axon containing the putative motor proteins, when immobilized on glass, could also cause individual microtubules to move in the presence of ATP (Figure 2-7C). Using this functional assay, biochemical purification of squid axoplasm led to the identification of a protein complex that could support microtubule movement on glass. Similar protein complexes purified from bovine and chick brains exhibit similar capabilities. Members of this protein family were named kinesins (from the Greek *kinein,* "to move").

We now know that kinesins are evolutionarily conserved molecular motors found in all eukaryotes. The kinesin complex originally purified from the squid axoplasm belongs to a specific kinesin subfamily, consisting of two heavy chains and two light chains. Each heavy chain has an N-terminal globular domain that contains the microtubule-binding site and an ATPase, a long coiled-coil domain that mediates the dimerization of two heavy chains, and a C-terminal domain that binds to the light chain and to cargo (Figure 2-7D). Biochemical and biophysical studies have revealed detailed mechanisms of how kinesins move along microtubules (**Movie 2-3**). Each mammalian genome has about 45 genes encoding different kinesins, many of which are expressed in neurons and are responsible for carrying different cargos to specific subcellular compartments of neurons (Figure 2-6). Mutations in kinesins and proteins associated with kinesins (and dynein) in humans underlie a variety of neurological disorders, highlighting their importance to human health.

Microtubules are integral structural components of dendritic trunks and axons and can be considered the highways that mediate long-distance transport in neurons. However, microtubules are usually absent from dendritic spines and presynaptic terminals. After cargos get off the microtubule highway at their approximate destinations, such as distal segments of dendrites, F-actins direct local traffic utilizing a large family of **myosin** proteins as molecular motors (Figure 2-6). We will study the mechanism by which myosin–actin interactions produce motility in the context of muscle contraction in Section 8.1.

Examination of the actin cytoskeleton at the axonal membrane using super-resolution fluorescence microscopy (see Section 14.17 for details) revealed that F-actin is distributed in periodic rings associated with a network of spectrin, a plasma membrane-associated cytoskeletal element (Figure 2-6C). The period of these actin rings, at ~190 nm, is just below the resolution of conventional diffraction-limited light microscopy, preventing its discovery until recently. Actin rings are also found in dendrites and at the necks of dendritic spines, although less commonly than in axons. These actin rings and their associated spectrin networks may provide stability to long axons and regulate axonal diameters.

In summary, membrane proteins (associated with intracellular vesicles) and cytosolic proteins destined for dendrites or axons are delivered to their destinations via interactions with specific motor proteins, which enable their transport along microtubules for long distances and sometimes along actin filaments for local movements. Although we have an outline of the trafficking rules, we still lack complete answers to many questions: How is motor–cargo selection achieved? How is cargo loading and unloading regulated? What regulates the transition between pauses and runs? Why do certain motors prefer axons? Answers to these questions will reveal how each neuronal compartment acquires a unique assortment of specialized proteins to carry out its functions, thus enriching our understanding not only of neuronal cell biology but also of neuronal physiology and function.

2.4 Channels and transporters move solutes passively or actively across neuronal membranes

The mechanisms we have studied thus far are concerned with how proteins and organelles inside the cell move around, but haven't addressed how extracellular molecules or ions enter the cell via the plasma membrane. This requires a different type of transport: across the lipid bilayer. The lipid bilayer of the plasma membrane and membranes of intracellular vesicles is impermeable to most ions and polar molecules that are soluble in aqueous environments such as the cytosol or extracellular milieu. The lipid bilayers serve as essential compartmental boundaries, delineating cells and intracellular organelles, such as the ER, Golgi apparatus, and synaptic vesicles. Inorganic ions and water-soluble molecules—including nutrients, metabolites, and neurotransmitters, collectively referred to as **solutes**—cannot easily diffuse across the lipid bilayer and thus require specific transport mechanisms to move across. Transport across the lipid bilayer is essential for many neuronal functions, such as electrical signaling.

Specialized transmembrane proteins transport solutes across the membranes of neurons and other cells. These membrane transport proteins can be divided into two broad classes: **channels** and **transporters**. Channels have an aqueous pore that allows specific solutes to pass directly through when they are open. In later sections of this chapter we will study **ion channels**, each of which allows selective passage of one or more specific ions. Transporters have two separate gates that open and close alternately, allowing movement of solutes from one side of the membrane to the other side (**Figure 2-8**A). In general, solutes move through open channels much more rapidly than they do through transporters.

Channels and transporters usually support *net movement* of solutes in one direction across the membrane under a given condition. Uncharged solutes move from the side with higher concentration to the side with lower concentration, or down their **chemical gradient**. Movement across the membrane of charged solutes, such as ions, creates an **electrical gradient**, a difference in the electrical potential across the membrane. The **electrochemical gradient**, which combines the chemical and electrical gradients, determines the direction and magnitude of net solute movement (**Figure 2-9**). When the electrical and chemical gradients are in the same direction, they enhance each other in driving solute movement (Figure 2-9, middle). When these gradients are in opposing directions, they partially (Figure 2-9, right) or sometimes fully cancel out each other's effects. Transport of solutes down their electrochemical gradients does not require external energy and is called **passive transport** (Figure 2-8A).

Some transporters can move a solute across the membrane against its electrochemical gradient (from low to high) using external energy; this process is called **active transport** (Figure 2-8B). Energy for active transport can come from the following sources. (1) Chemical reactions: the most frequent form is ATP hydrolysis, in which the transporter is an ATPase, and chemical energy from ATP hydrolysis

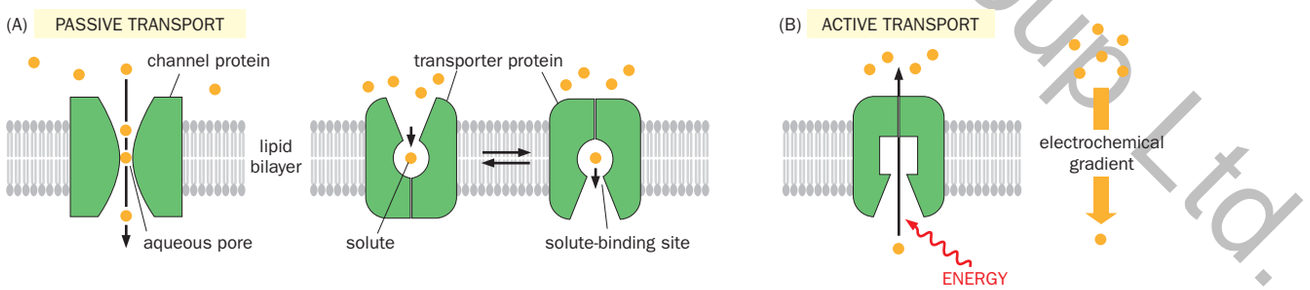

Figure 2-8 Channels and transporters mediate passive and active transport. (A) A channel protein has an aqueous pore that allows solutes to pass through directly when the channel is open, whereas a transporter protein moves the solute across the membrane through sequential opening and closing of at least two gates. In the absence of energy input, solutes move down their electrochemical gradients (Figure 2-9) through channels and transporters; this is called passive transport. **(B)** Transporter proteins can also utilize energy to mediate active transport to move solutes up their electrochemical gradients. (Adapted from Alberts B, Johnson A, Lewis J, et al. [2015] Molecular Biology of the Cell, 6th ed. Garland Science.)

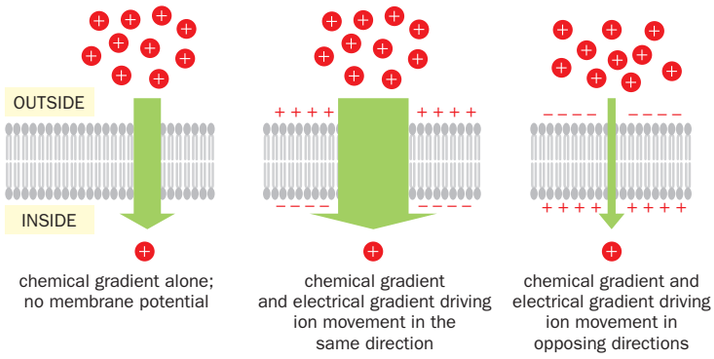

Figure 2-9 Electrochemical gradients of charged solutes such as ions. When there is no electrical potential difference across a membrane, the chemical gradient alone determines the direction of ion movement, from high to low concentrations (left). When there is an electrical potential difference across a membrane, the chemical and electrical gradients act together to determine the direction and magnitude of the force governing ion movement. These two components of the electrochemical gradient may work in the same direction (middle) or in opposing directions (right). The thickness of the arrows symbolizes the magnitude of the force driving ion movement. (Adapted from Alberts B, Johnson A, Lewis J, et al. [2015] Molecular Biology of the Cell, 6th ed. Garland Science.)

is used to drive conformational change of the protein. (2) Light: energy is derived from photon absorption. Transporters driven by chemical reactions or by light are also called **pumps**. We will discuss light-driven pumps in the context of the evolution of vision in Chapter 13. (3) Coupled transport: when a transporter moves multiple solute species together, energy gained from transporting some species down a gradient can be used to transport other species up another gradient. Coupled transporters (also called cotransporters) can be divided into two types: those that move solutes in the same direction are called **symporters**, and those that move solutes in opposite directions are called **antiporters** or **exchangers** (**Figure 2-10**; **Movie 2-4**). (In analogy to cotransporters, transporters that transport a single species of cargo are also called uniporters.) In the next section, we will encounter specific examples of an ATP-driven pump and cotransporters that play crucial roles in establishing electrochemical gradients of different ions across the plasma membrane, which forms the basis of electrical signaling in neurons.

2.5 Neurons are electrically polarized at rest because of ion gradients across the plasma membrane and differential ion permeability

Electrical signals in neurons, as well as in other **excitable cells** (cells that produce action potentials, such as muscle cells), rely on a difference in electrical potential across the plasma membrane. This electrical potential difference between the inside of the cell and the extracellular environment is called the **membrane potential** of the cell. We can measure the membrane potential directly by inserting a microelectrode into the cell, a procedure called **intracellular recording**. A microelectrode for intracellular recording is usually made of glass with a very fine tip filled with a conducting salt solution, so that it makes electrical contact with the inside of a cell; at the other end, the electrode is connected via a wire to an amplifier and an oscilloscope (see Figure 14-34 and Sections 14.20–14.21 for different

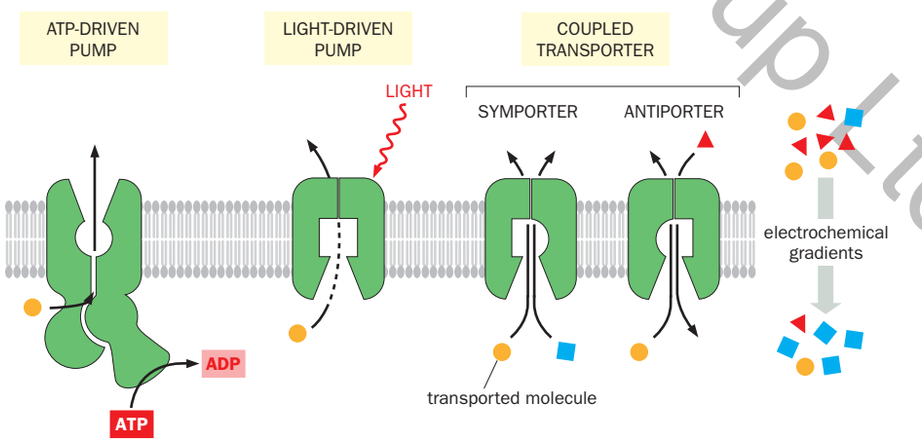

Figure 2-10 Three types of active transport. An active transporter can be an ATP-driven pump, which utilizes energy from ATP hydrolysis to move solutes against their electrochemical gradients (left); a light-driven pump, which derives its energy from photon absorption (middle); or a coupled transporter, which derives its energy from transporting a second species of solute down its electrochemical gradient. Coupled transporters can be symporters or antiporters, depending on whether the two solutes move in the same direction or in opposite directions. The schematic at the far right summarizes the electrochemical gradients of different solutes, with the larger number of a given symbol indicating the high end of an electrochemical gradient. The downward gray arrow shows the electrochemical gradient of the solute represented by yellow circles. (Adapted from Alberts B, Johnson A, Lewis J, et al. [2015] Molecular Biology of the Cell, 6th ed. Garland Science.)

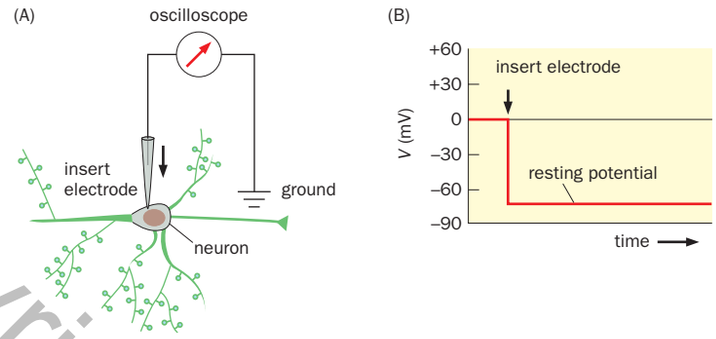

Figure 2-11 Measuring the resting potential of a neuron. (A) Schematic of recording the membrane potential of a neuron at rest. The oscilloscope measures the voltage difference (*V*, in millivolts) between the ground (the electrical potential in the extracellular environment) and the tip of the electrode. **(B)** Before the insertion of the electrode tip into the cell, *V* is zero. After insertion, *V* drops to –75 mV, the resting potential of our model neuron.

methods for recording neuronal activity). The membrane potential of a neuron at rest (the **resting potential**) is typically between –50 and –80 millivolts (mV), depending on the cell type (**Figure 2-11**). Thus, neuronal membranes are electrically polarized. A change in the electrical potential inside the cell toward a less negative value is termed **depolarization**. A change in the electrical potential inside the cell toward a more negative value is called **hyperpolarization**.

Neurons are electrically polarized because (1) ion concentrations differ between the intracellular and extracellular environments; (2) the **permeability** of the plasma membrane to each of the three major ions is different (as we will learn later, permeability is determined by the number of open ion channels that conduct specific ions; when an ion channel is open, it becomes permeable to one or more ions; ions can flow in either direction, with the net flux determined by the ion's electrochemical gradient). For a typical neuron, the concentrations of sodium ions (Na^+) and chloride ions (Cl^-) are 10- to 20-fold higher in the extracellular space than in the cytosol, whereas the intracellular potassium ion (K^+) concentration is 30-fold higher than in the extracellular environment (**Figure 2-12**A), although these values vary with types of neurons and animals. At a neuron's resting state, the plasma membrane is not very permeable to Na^+ and Cl^- but is relatively permeable to K^+. (That is, K^+ crosses the neuronal membrane more readily than Na^+ or Cl^-.) In addition to these two **cations** (positively charged ions such as K^+ and Na^+) and one **anion** (a negatively charged ion such as Cl^-), some organic

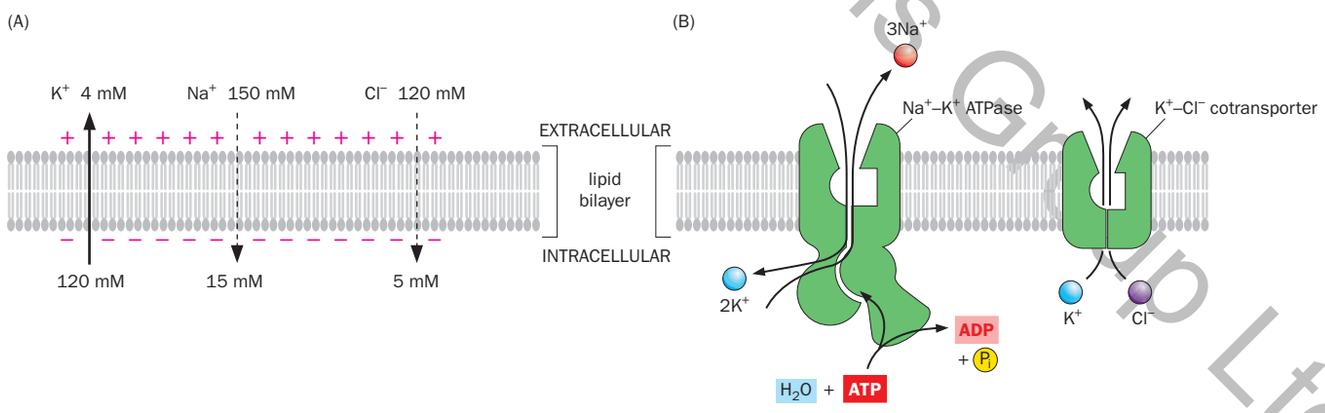

Figure 2-12 Ionic basis of the resting potential. (A) Numbers indicate typical concentrations of K^+, Na^+, and Cl^- inside and outside of a mammalian neuron, in millimoles per liter (mM). At the resting state, the membrane is permeable to K^+ (arrow indicating the direction down the electrochemical gradient) but less permeable to Na^+ and Cl^- (dashed arrows). The resting membrane potential is largely determined by the balance between the chemical gradient that drives K^+ outward, and the electrical gradient that drives K^+ inward. The + and – signs on opposite sides of the membrane indicate that the intracellular electrical potential is more negative than that of the extracellular environment. **(B)** Left, the Na^+–K^+ ATPase uses energy from ATP hydrolysis to transport three Na^+ ions outward and two K^+ inward, against their electrochemical gradients, each cycle. The activity of the Na^+–K^+ ATPase maintains the intracellular concentrations of Na^+ and K^+ and thus the resting potential by counteracting the leak of Na^+ and K^+ across the resting membrane. Right, the K^+–Cl^- cotransporter utilizes energy released as K^+ moves down its electrochemical gradient to move Cl^- up its electrochemical gradient, helping maintain a concentration gradient of Cl^- across the membrane.

anions are enriched intracellularly, but neuronal membranes are usually not permeable to these organic anions.

The ionic concentrations across the neuronal membrane are maintained by active transport, principally by a transporter called the **Na^+–K^+ ATPases**. This ion pump uses energy derived from ATP hydrolysis to pump Na^+ outward and K^+ inward, against their respective electrochemical gradients (Figure 2-12B; **Movie 2-5**), thus maintaining the concentration differences of these two important ions across the resting membrane. It has been estimated that one third or more of neurons' energy is used by the Na^+–K^+ ATPase, highlighting both the importance of this particular pump and the importance of maintaining Na^+ and K^+ concentration gradients. The Cl^- gradient is maintained by several cotransporters, such as the K^+–Cl^- symporter that couples K^+ and Cl^- export (Figure 2-12B).

To understand how chemical gradients and membrane potentials influence ion movement, let's first consider a hypothetical situation in which the membrane is permeable only to K^+. (This situation applies to glia quite well.) The concentration difference across the membrane causes K^+ to diffuse outward down its chemical gradient. As K^+ flows outward, however, the intracellular compartment becomes more negatively charged, thus increasing the electrical potential difference across the membrane. This deters further outward K^+ diffusion, because K^+ is positively charged. Eventually, the chemical and electrical forces will reach the **equilibrium potential** of K^+, E_K, the membrane potential at which the electrical and chemical forces balance each other out, such that there is no net K^+ flow. E_K follows the **Nernst equation**:

$$E_K = \frac{RT}{zF} \ln \frac{[K^+]_o}{[K^+]_i}$$

where $[K^+]_o$ and $[K^+]_i$ are the extracellular and intracellular K^+ concentrations, R and F are the gas and Faraday constants, respectively, T is the absolute temperature (in Kelvin), z is the valence of the ion (+1 for K^+), and ln is the natural logarithm function. At room temperature, the expression RT/F is about 25 mV. Using the K^+ concentration difference of our model neuron (Figure 2-12A), we can calculate the E_K to be about –85 mV, which is slightly hyperpolarized relative to the resting potential.

The Nernst equation can also be used to determine the equilibrium potentials of Cl^- and Na^+. Using the concentration differences across our model neurons (Figure 2-12A), we can determine that E_{Cl} = –79 mV and E_{Na} = +58 mV. Note that despite having a chemical gradient opposite to that of K^+, Cl^- has a similar equilibrium potential to K^+ because it has a negative charge (z = –1). A positive equilibrium potential for Na^+ means that if the membrane were permeable only to Na^+, the intracellular membrane potential would be positive relative to the extracellular environment. We will see the significance of this when we study the ionic basis of the action potential later in this chapter.

In reality, the resting potentials of most neurons are slightly less negative than the K^+ equilibrium potential, because the membrane is also somewhat permeable to Na^+ and Cl^-. When the membrane is simultaneously permeable to multiple ions, the resting membrane potential V_m at equilibrium (that is, when there is no net ion flow) can be calculated using the **Goldman–Hodgkin–Katz (GHK) equation**:

$$V_m = \frac{RT}{F} \ln \frac{P_K[K^+]_o + P_{Na}[Na^+]_o + P_{Cl}[Cl^-]_i}{P_K[K^+]_i + P_{Na}[Na^+]_i + P_{Cl}[Cl^-]_o}$$

where P_K, P_{Na}, and P_{Cl} are the permeabilities for K^+, Na^+, and Cl^-, respectively. In essence, the GHK equation states that each ion makes an independent contribution to the resting potential that is weighted according to the permeability of the resting membrane to that ion.

Because the membrane potential is generally not identical to the equilibrium potential for any single ion, there is a force tending to push each ion into or out of the cell. This is called the **driving force** for that ion, and it is equal to the difference between the membrane potential and the equilibrium potential for that ion. If the

membrane were permeable only to K^+ (that is, $P_{Na} = 0$, $P_{Cl} = 0$), then $V_m = E_K$ according to the GHK equation; the driving force for K^+ would be 0, and the net current would be zero, despite a high permeability for K^+. However, neither P_{Na} nor P_{Cl} is actually 0. As the equilibrium potential of Cl^- is generally very close to the resting potential, Cl^- flow is small at rest because of the small driving force. On the other hand, the driving force for Na^+ is very large as both the chemical and electrical gradients favor its entry into the cell. Na^+ will leak inward, down its electrochemical gradient, despite a small P_{Na}. This will raise the membrane potential slightly above E_K, creating a driving force and causing K^+ to leak outward. If unopposed, these leak currents would steadily decrease the intracellular K^+ concentration and increase the intracellular Na^+ concentration; however, they are counterbalanced by active transport via the Na^+–K^+ ATPase, which pumps Na^+ out and K^+ in (Figure 2-12B). The Na^+–K^+ ATPase thus maintains the intracellular K^+ and Na^+ concentrations, thereby stabilizing the resting potentials of neurons.

2.6 The neuronal plasma membrane can be described in terms of electrical circuits

While ions cannot cross the lipid bilayer of the neuronal plasma membrane by themselves, the intracellular and extracellular environments are both aqueous solutions that support ion movement. We can model how a neuron functions using terminology developed to describe **electrical circuits**—interconnections of electrical elements containing at least one closed current path. In this section, we introduce the basic components and rules of electrical circuits, which will be instrumental to our discussion of neuronal signaling in subsequent sections.

The simplest electrical circuit consists of two electrical elements: a battery and a resistor. The **battery** maintains a constant voltage (electrical potential difference) across its two terminals, thus providing an energy source. The **resistor** implements electrical resistance (that is, opposes the passage of electric current) and produces a voltage across its two terminals when current flows through it (**Figure 2-13**A, left). The electric current (I, the flow of electric charge per unit time) that passes through the resistor follows **Ohm's law**:

$$I = \frac{V}{R}$$

in which V is the voltage across the resistor and R is the **resistance** of the resistor. As the electrical wires connecting the battery and the resistor are assumed to have zero resistance, the voltage across the resistor is the same as the voltage across the battery. The units of I, V, and R are the ampere (A), volt (V), and ohm (Ω), respectively.

When two resistors are connected in series (Figure 2-13A, middle), the current passing through each resistor is the same; the voltage across both resistors is the sum of voltages across each resistor, or $V = V_1 + V_2$; and the combined resistance is $R = R_1 + R_2$. An equivalent but more widely used measure of a resistor in electrophysiology is **conductance** (g), which is the inverse of resistance: $g = 1/R$.

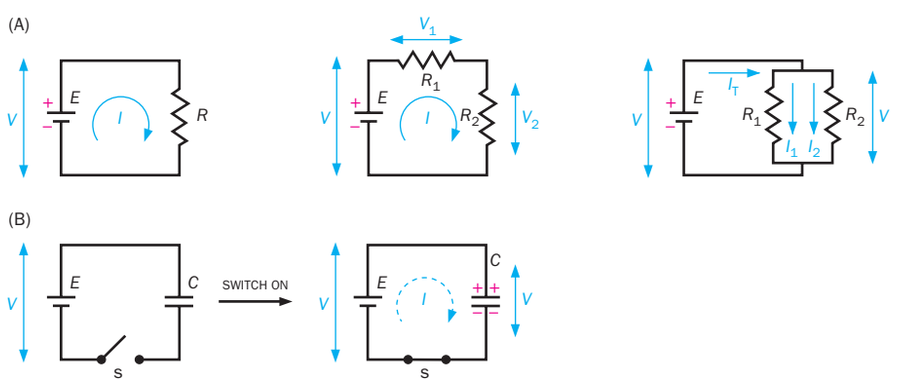

Figure 2-13 Electrical circuits with only resistors or capacitors. (A) Left, an electrical circuit consisting of two elements, a battery (E) with a voltage V across its two terminals and a resistor with a resistance R. The current (I, arrow) flows outside the battery from the positive terminal (+, represented by the longer line of the battery) to the negative (–) terminal. Middle, two resistors (with resistance R_1 and R_2) connected in series. The current flowing through them is the same. The sum of voltages across each resistor ($V_1 + V_2$) equals the voltage across the battery. Right, two resistors connected in parallel. The voltage across each is the same as the voltage across the battery. The total current (I_T) equals the sum of the currents passing through each path ($I_1 + I_2$). **(B)** A circuit consisting of a battery (E), a capacitor (with a capacitance C), and a switch (s). When the switch is turned on, a transient current (dashed arrow) charges the capacitor until the voltage across it equals the voltage across the battery.

Thus, when two resistors are connected in series, $1/g = 1/g_1 + 1/g_2$; in other words, the conductance *decreases*. When the two resistors are connected in parallel (Figure 2-13A, right), the voltages across each resistor are the same; the total current is the sum of the currents passing through each resistor, or $I = I_1 + I_2$; the combined resistance follows the formula $1/R = 1/R_1 + 1/R_2$, and the combined conductance can be calculated as $g = g_1 + g_2$. In other words, the conductance *increases* for resistors in parallel. The unit of conductance is the siemens (S). It follows from the definition of conductance that Ohm's law can also be expressed as:

$$I = gV$$

Note that a resistor is at the same time a **conductor** of electric current, and these two terms are used interchangeably, depending on the context; a resistor with high resistance is a poor conductor, and a resistor with low resistance is a good conductor.

We can now relate these simple electrical circuits to what we have learned so far about the neuron. The lipid bilayer is an **insulator**, a resistor with infinite resistance, as it does not allow electric current to pass through. As noted in Section 2.5, the plasma membrane is not a perfect insulator—even at the resting state, ions can leak through the membrane via specific channels. These ion channels can be modeled as parallel current paths, each consisting of a resistor with a specific resistance and a battery with a specific voltage equivalent to the equilibrium potential of the ion, interposed between the electric potential across the membrane. We will discuss this model in detail in Section 2.7. We will also encounter resistors connected in series when we study propagation of electrical signals along neuronal fibers (dendrites and axons) in Section 2.8.

Another important electrical element is a **capacitor**, consisting of two parallel conductors separated by an insulator. A capacitor is a charge-storing device, as it does not allow current to pass through the insulator. The lipid bilayer of the plasma membrane, along with the extracellular and intracellular milieu, is an excellent example of a capacitor. In a simple circuit consisting of a battery and a capacitor (Figure 2-13B), when the switch is turned on, current flows from the battery to the capacitor until the capacitor is charged to a voltage equal to that of the battery. Positive charge accumulates on one conductor, while negative charge accumulates on the other; this is how charge is stored. The **capacitance** (C), the ability of a capacitor to store charge, is defined as $C = Q/V$, where Q is the electric charge stored when the voltage across the capacitor is V. The unit of capacitance is the farad (F), and the unit of charge is the coulomb (C). When two capacitors are connected in series, the combined capacitor (C) follows the formula $1/C = 1/C_1 + 1/C_2$. When two capacitors are connected in parallel, $C = C_1 + C_2$.

In theory, when a circuit has no resistance (Figure 2-13B), the capacitor is charged instantaneously when the switch is turned on. In practice, circuits always have some resistance. In a circuit containing both resistors and capacitors (an ***R*-*C* circuit**), the current flowing through the resistor and the capacitor changes over time after the switch is turned on. The product of resistance and capacitance has the unit of *time* and is called the **time constant** (designated as τ). The time constant defines how quickly capacitors (such as the plasma membrane) charge or discharge over time in response to external signals, such as a sudden change of current flow (as would result from the opening of channels). The larger the time constant, the longer it takes to charge a capacitor and the more an electrical signal is spread out over time.

Let's examine a parallel *R*-*C* circuit to help clarify the important concept of a time constant (see **Box 2-2** for a quantitative treatment of this subject). In this circuit, a resistor and a capacitor are connected in parallel to a constant current source (**Figure 2-14**, left). Once the switch is turned on, while the sum of the currents (I_T) remains constant, the current flowing through the resistor (I_R) and the voltage across the resistor ($V = I_R R$) increases over time (Figure 2-14, middle), while the current flowing across the capacitor (I_C) decreases over time (Figure 2-14, right). Intuitively, this is because the role of the capacitor is to store charge and the voltage across it cannot change until charge builds up, which takes time, and

Box 2-2: A deeper look at the parallel *R-C* circuit

In Section 2.6 we encountered a parallel *R-C* circuit (Figure 2-14). For students with a background in differential equations, we discuss here how the temporal dynamics of these circuits are derived.

When the parallel *R-C* circuit is connected to a constant current source (after the switch is turned on in Figure 2-14, left), there is a redistribution of current over time from the capacitor path (I_C) to the resistor path (I_R), but their sum (I_T) is constant. Also, the voltage (V) across the resistor and the capacitor both equal $I_R R$. Thus, we have $I_R(t) = I_T - I_C(t) = I_T - dQ/dt = I_T - C\,dV/dt = I_T - RC\,dI_R(t)/dt$. Solving this differential equation gives:

$$I_R(t) = I_T\left(1 - e^{-\frac{t}{RC}}\right)$$

$$V(t) = I_T R\left(1 - e^{-\frac{t}{RC}}\right)$$

$$I_C(t) = I_T e^{-\frac{t}{RC}}$$

The first and third functions are graphically represented in the middle and right panels of Figure 2-14. For example, $I_R(t)$ increases to 63% ($1 - e^{-1}$), 86% ($1 - e^{-2}$), and 95% ($1 - e^{-3}$) of I_T at times equivalent to one, two, and three time constants.

Note that we connect the parallel *R-C* circuit to a constant current source rather than a battery because this is a better model of what happens to neuronal membrane during electrical signaling: inputs can be modeled as a transient supply of a constant current source (opening and closing of ion channels), whereas the membrane potential *continuously* changes with the opening and closing of ion channels. If we were to connect a parallel *R-C* circuit to a battery with a constant voltage, the capacitor would be charged instantaneously, reducing the circuit to one with only a resistor, as in Figure 2-13A.

the voltage across *R* and *C* must be the same in the parallel paths. The time constant τ serves as the unit on the time (x) axis and defines how rapidly electrical signals change over time. The voltage reaches 63%, 86%, and 95% of the peak value at times equal to one, two, or three time constants (Figure 2-14, middle; see Box 2-2 for how these values are derived).

The parallel *R-C* circuit is widely used in neurobiology, as it is an excellent description of the neuronal plasma membrane. The ion channels function as resistors, and the lipid bilayer together with the extracellular and intracellular environments act as a capacitor, storing electrical charge in the form of ions accumulating near the surface of the membrane. Whereas the membrane capacitance per unit area is mostly constant (~1 μF/cm^2), the membrane resistance can change substantially with membrane potential and time. We will now apply these concepts to examine ion flow across the neuronal plasma membrane.

2.7 Electrical circuit models can be used to analyze ion flow across the glial and neuronal plasma membranes

Having introduced the basics of electrical circuits, we discuss two examples to illustrate how these electrical circuit models can help us understand current flow across the plasma membrane.

Let's first suppose that the membrane is permeable only to K^+, a good approximation for glia. This is equivalent to a circuit consisting of two parallel paths, a K^+ conducting path and a membrane capacitance path (**Figure 2-15**A). The membrane capacitance path is symbolized by a capacitor (C_m). The K^+ conducting path

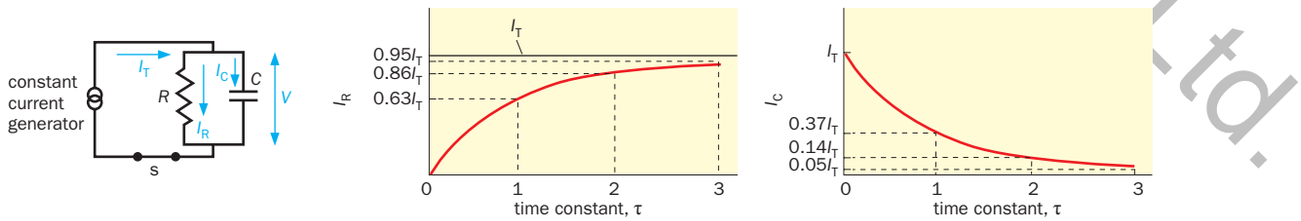

Figure 2-14 Temporal dynamics of a parallel *R-C* circuit. Left, a circuit with a resistor and a capacitor connected in parallel, supplied with a constant current source (with a constant total current I_T). Middle and Right, after the switch (s) is connected, I_R gradually increases to approach its maximal value of I_T (middle), whereas I_C exhibits exponential decay, with a time constant τ equal to the product *RC* (right). I_R and I_C values are indicated at $t = \tau$, 2τ, and 3τ. V changes similarly to I_R (not shown).

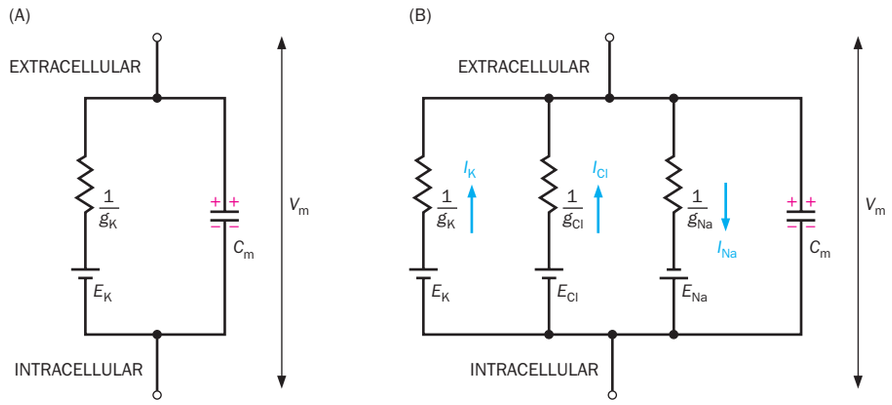

Figure 2-15 Electrical circuit models of the neuronal plasma membrane. (A) In a simplified model in which the membrane is permeable only to K^+, the plasma membrane consists of two parallel paths, a membrane capacitance (C_m) path and a K^+ path. The resistance of the resistor is indicated by the inverse of the conductance, $1/g_K$. The K^+ path also has a battery corresponding to the equilibrium potential of K^+ (E_K). The battery is positive on the extracellular side because the equilibrium potential of K^+ is negative intracellularly. V_m is the membrane potential. At rest, since there is no net current flow, $V_m = E_K$. **(B)** In a more realistic model for neurons, the plasma membrane can be modeled as four parallel paths: one path for membrane capacitance plus one path each for K^+, Cl^-, and Na^+. Arrows indicate the directions of currents within each path according to the equilibrium potential of each ion and the resting potential of our model neuron in Figure 2-12. Note that while Cl^- ions flow inward (as the resting potential is less negative than the equilibrium potential of Cl^- in our model neuron), the current carried by Cl^- is shown flowing outward; this is because electrical circuit diagrams conventionally indicate current as the flow of positive charge. As a result, current carried by negatively charged ion (like Cl^-) is indicated as occurring in the direction opposite to the actual direction of ion movement. (B, adapted from Hodgkin AL & Huxley AF [1952] *J Physiol* 117:500–544.)

has two electrical elements, a resistor and a battery representing the equilibrium potential of K^+. Since resistance is the inverse of conductance, the resistor is symbolized by $1/g_K$, where g_K is the conductance of the K^+ path. The battery in series with the membrane potential symbolizes the electrochemical gradient driving K^+ movement along this path. We can determine the membrane potential, V_m, from the K^+ path as the sum of the voltage across the resistor (I_K/g_K according to Ohm's law) and E_K. At the resting state, the influx and efflux of K^+ balances out, or $I_K = 0$. Thus, $V_m = E_K$; that is, the resting membrane potential is the same as the equilibrium potential of K^+.

Now let's consider a more realistic situation for neurons, in which the membrane is permeable to Cl^- and Na^+, in addition to K^+. We can add two parallel paths to Figure 2-15A, one for Cl^- and one for Na^+ (Figure 2-15B). In what follows, we demonstrate how V_m can be determined based on the conductance and equilibrium potentials for each ion. In this parallel circuit, the voltage across each path is V_m, so we have three equations:

$$V_m = \frac{I_K}{g_K} + E_K \tag{1}$$

$$V_m = \frac{I_{Cl}}{g_{Cl}} + E_{Cl} \tag{2}$$

$$V_m = \frac{I_{Na}}{g_{Na}} + E_{Na} \tag{3}$$

From the three equations, we have $V_m(g_K + g_{Cl} + g_{Na}) = E_K g_K + E_{Cl} g_{Cl} + E_{Na} g_{Na} + I_K + I_{Cl} + I_{Na}$. At rest, the net current that flows across the membrane should be zero. As the membrane potential is constant, the current flow in the capacitance branch is also zero. Thus,

$$I_K + I_{Cl} + I_{Na} = 0 \tag{4}$$

Accordingly, V_m can be derived as

$$V_m = \frac{E_K g_K + E_{Cl} g_{Cl} + E_{Na} g_{Na}}{g_K + g_{Cl} + g_{Na}}$$

where g and E are the conductance and the equilibrium potential for each ion, respectively. This is in fact the circuit model equivalent of the Goldman–Hodgkin–Katz equation introduced in Section 2.5. This, however, is a more useful formula because conductance and equilibrium potential are easier to determine experimentally than permeability and the absolute ionic concentrations used in the formula in Section 2.5. Note that conductance and permeability are both used to describe how easy it is for an ion to flow across the plasma membrane and are often used interchangeably. But there is a subtle difference. Permeability is an intrinsic property of the membrane reflecting the number of opened channels, as we will learn later, and does not vary whether the ions to be conducted are present

or not, whereas conductance depends not only on the permeability but also on the presence of ions.

Once we have determined V_m, we can also determine the currents within each parallel path:

$$I_K = g_K(V_m - E_K)$$
$$I_{Cl} = g_{Cl}(V_m - E_{Cl})$$
$$I_{Na} = g_{Na}(V_m - E_{Na})$$

Note that the values in parentheses represent the driving force for each ion as defined in Section 2.5. Thus, *the current each ion carries is the product of the conductance and the driving force for that ion*. As we will learn later in this chapter, g_{Na} and g_K change as a function of membrane potential, and this voltage dependence underlies the production of action potentials. We will also learn in Chapter 3 that synaptic transmission is mediated by a change in the postsynaptic membrane conductance in response to neurotransmitter release from the presynaptic terminal.

2.8 Passive electrical properties of neurons: electrical signals evolve over time and decay over distance

Having introduced the ionic basis of resting potentials and the electrical circuit model of the neuronal plasma membrane, we are now ready to address two key topics in electrical signaling: how neurons respond to electrical stimulation and how electrical signals propagate within neurons. We start with observations from an idealized experiment on a neuronal fiber (a dendrite or an axon), which summarizes results from real experiments across different preparations and approximates the properties of neuronal dendrites. In this experiment, an electrode connected to a current source is inserted into the neuronal fiber, such that it can "inject" electric current into the neuronal fiber at the command of the experimenter. We call this electrode a **stimulating electrode**. Inserted into the membrane right next to the stimulating electrode is a **recording electrode** (*a*), which is connected to an amplifier and oscilloscope so it can record the membrane potential change in response to the current injection from the stimulating electrode. Two additional recording electrodes (*b* and *c*) are inserted at different distances along the fiber from the stimulating electrode to record membrane potentials at distant sites (**Figure 2-16**A; **Movie 2-6**).

We start by injecting a small depolarizing current (that is, injecting positive charge into the neuron) in the form of a rectangular pulse (Figure 2-16B, left). The injected current will flow through the electrode across the membrane and along the inside of the fiber. We observe that the membrane potential at recording electrode *a* becomes *gradually* depolarized at the beginning of the current pulse (t_1) and returns *gradually* to the resting potential at the end of the current pulse (t_2). At the more distant sites, membrane potentials recorded by electrodes *b* and *c* exhibit similar gradual changes. However, the magnitudes of the membrane potential changes are much diminished (Figure 2-16B, middle and right).

We use an electrical circuit model of the fiber (Figure 2-16C) to explain these results. Each segment of the membrane can be modeled as a parallel *R*-*C* circuit (Figure 2-15B), with membrane conductances of all ions in Figure 2-15 combined as R_m, the resting membrane potential as a battery E_r, and the membrane capacitance as C_m. Different segments of the process can be modeled as parallel *R*-*C* circuits, linked by internal (or axial) resistances (R_i) of ion movement along the longitudinal axis in the fiber interior. Ions flow more freely in the large extracellular environment; therefore, the extracellular resistance is often approximated as zero.

Let's consider our first observation: membrane potentials change gradually in response to a step current pulse, already evident from the recording at the current injection site. In addition to causing ion flow across the membrane, represented by I_R in the circuit diagram, part of the injected current flows across the capacitance path to charge the membrane capacitor (I_C). As discussed in Section 2.6,

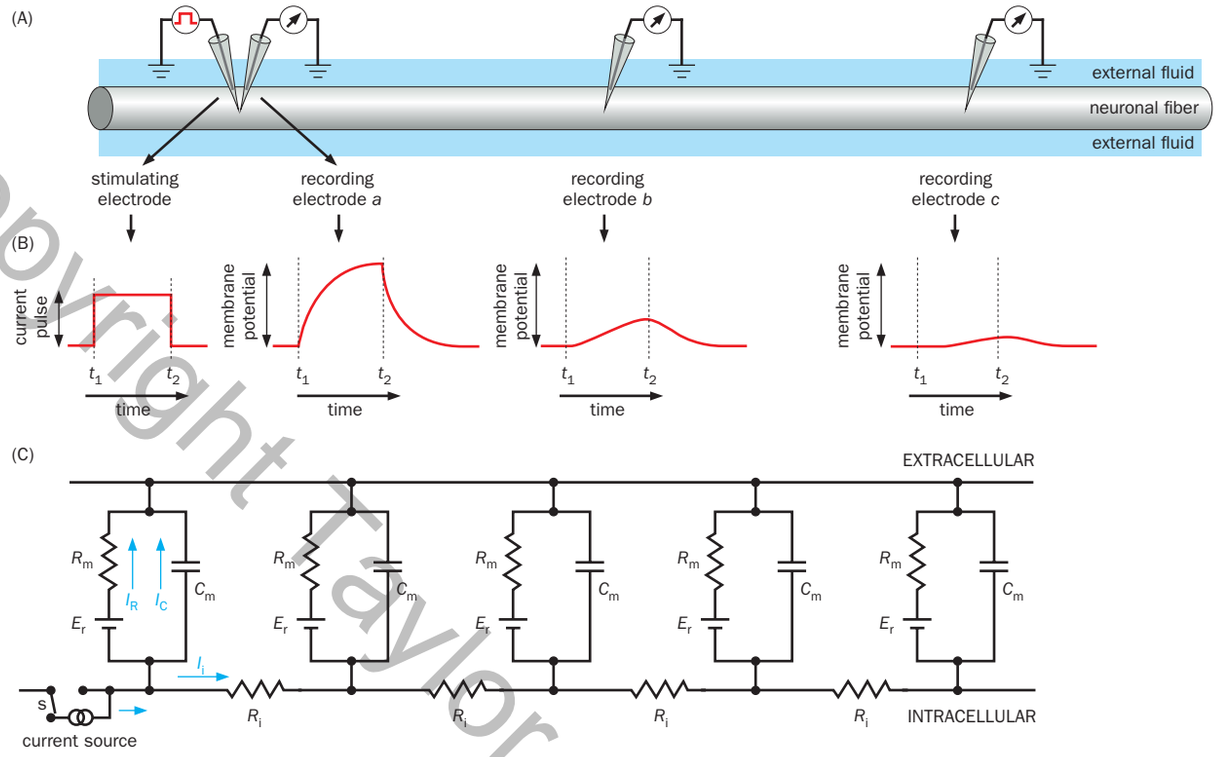

Figure 2-16 Passive electrical properties of neurons observed in an idealized experiment. (A) Illustration of the experimental preparation. A stimulating electrode provides a source of electrical signal in the form of a rectangular current pulse. Three recording electrodes are inserted into the neuronal fiber at different distances from the stimulating electrode. **(B)** When the stimulating electrode delivers a rectangular depolarizing pulse (left), the membrane potential changes at the sites of the three recording electrodes as illustrated (right). Dashed lines represent times (t_1 and t_2) aligned to the onset and offset of the current pulse. The *y* axes of the three membrane potential plots have the same scale. Two properties are evident: (1) membrane potential changes are gradual in response to the square current pulse, and (2) the magnitudes and speeds of the membrane potential changes decay across distance. **(C)** An electrical circuit model of the neuronal fiber. Each membrane segment is approximated as a parallel *R-C* circuit, with a membrane capacitance (C_m); a membrane resistance (R_m) that integrates K^+, Cl^-, and Na^+ conductances; and a battery representing the resting membrane potential (E_r). These segments are joined internally by resistors (with resistance R_i), reflecting internal or axial resistance within the neuronal fiber; the resistance of the external fluid is approximated as 0. Current injection is modeled by transiently connecting the intracellular side with a constant current source through the switch (s). Arrows indicate the direction of current flow caused by injecting positive charges from the current source, including current into the resistor branch (I_R) and capacitance branch (I_C) across the membrane, as well as current that flows within the neuronal fiber (I_i). (Adapted from Katz B [1966] Nerve, Muscle, and Synapse. McGraw Hill.)

I_R follows an exponential curve with the product $R_m C_m$ as the time constant (Figure 2-14), as does the change in membrane potential. The smaller the time constant, the faster the membrane potential changes in response to current injection. This experiment reveals a general property of electrical signaling in neurons. Because of the membrane capacitance, electrical signals evolve over time even when current injection is constant, with the product $R_m C_m$ as a key parameter of these temporal dynamics. This property limits the temporal resolution of electrical signals but also provides opportunities for temporal integration: when two individual signals are delivered within a small time interval, they may not be resolved as individual signals, but rather detected as an integrated signal. We will discuss this further in Chapter 3 in the context of dendritic integration of synaptic inputs.

Let's now turn to our second observation: the magnitude of the change in membrane potential decreases as the distance from the site of current injection increases. Suppose the greatest change in membrane potential at electrode *a* in response to the current injection is V_0. The spread of this change in membrane potential along the fiber is carried by the axial current, which diminishes due to the continual leak of current via membrane conductance along the way. An easy way to visualize this is to simplify the circuit in Figure 2-16C further by considering only the conductance path (**Figure 2-17**A). (This simplification is equivalent

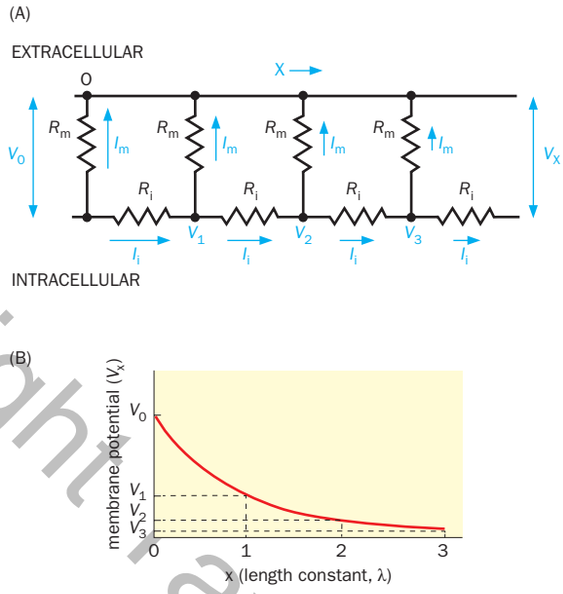

Figure 2-17 A circuit model illustrating electrical signal decay along a neuronal fiber. (A) In this simplified model of Figure 2-16C, batteries symbolizing the resting potential are omitted because only the *change* in the membrane potential from the resting potential is considered here; capacitors are also omitted because only the *peak changes* in membrane potential are considered. The current injection at position 0 causes a peak membrane potential change of V_0. In addition to passing through the membrane (I_m), part of the injected current also spreads in both directions along the interior of the neuronal fiber as an internal current (I_i) (only the rightward spread is shown here). Along the way, the magnitude of I_i diminishes because of leaky transmembrane current (I_m), symbolized by the decreasing lengths of the arrows. **(B)** The changes in membrane potential decay across the fiber, following an exponential decay curve. The *x* axis unit is the length constant of the neuronal fiber. The values for membrane potentials at 1×, 2×, and 3× the length constant equal 0.37 V_0, 0.14 V_0, and 0.05 V_0, respectively. (Adapted from Katz B [1966] Nerve, Muscle, and Synapse. McGraw Hill.)

to considering the peak magnitude of changes in membrane potential after the membrane capacitance is charged.) The axial current (I_i) gradually diminishes in magnitude because part of the current leaks away to the outside due to membrane conductance. The membrane potential change $V(x)$ at distance x from electrode a is given by the following formula:

$$V(x) = V_0 e^{-\frac{x}{\sqrt{dR_m/4R_i}}}$$

where R_m is the membrane resistance per unit area of membrane surface, R_i is the internal (axial) resistance per unit volume of the neuronal cytoplasm, and d is the diameter of the fiber. This equation represents an exponential decay of electrical signal across distance (Figure 2-17B), in analogy to the exponential decay of current over time in an *R-C* circuit we discussed in Section 2.6 and Box 2-2.

The term $\sqrt{dR_m/4R_i}$ is called the **length constant** or **space constant** (designated as λ). It is expressed in units of length; one length constant corresponds to the distance at which the peak magnitude of the membrane potential change has attenuated to $1/e$, or about 37%, of the original peak magnitude. As specific examples, the positions of the electrodes *b* and *c* in our idealized experiment (Figure 2-16A) were chosen to be 1.5 and 3 length constants away from electrode *a*. The longer the length constant, the further electrical signals can be transmitted before they decay to a given fraction of their original value. As indicated by the formula, the length constant increases with increasing membrane resistance or neuronal fiber diameter. This is because if R_m increases, then more current will flow down the axial path (as current is inversely proportional to resistance) and λ will increase; similarly if R_i is reduced by increasing fiber diameter (essentially adding more resistance in parallel, which decreases the total resistance), then more current will flow down R_i, thus increasing λ. Indeed, animals have evolved various strategies to increase the distance across which electrical signals spread, such as enlarging fiber diameter, as in the squid giant axon, or increasing unitary membrane resistance, as in myelination; we will discuss these strategies in more detail in Section 2.13.

The temporal spread of electrical signals and their attenuation across distance are often referred to as **passive electrical properties** of neurons (as opposed to active properties, which we will begin to study in the next section). They are also called the **cable properties** of neuronal fibers, in analogy to the transocean cables that transmit electrical signals using insulators to separate the interior conductor from the exterior conducting seawater. The time constant, which characterizes the

Table 2-1: Time and length constants of axons, dendrites, and muscle cells

Fiber	Diameter (μm)	Length constant (mm)	Time constant (ms)
Squid giant axon[a]	500	5	0.7
Lobster nerve[a]	75	2.5	2
Frog muscle[a]	75	2	24
Apical dendrite of mammalian cortical pyramidal neuron[b]	3	1	~20

[a] Data from Katz B (1966) Nerve, Muscle, and Synapse. McGraw-Hill. Length constants were measured in large extracellular volume.

[b] Data from Stuart G, Spruston N, & Häusser M (1999) Dendrites. Oxford University Press.

temporal spread of electrical signals, and length constant, which characterizes the attenuation across distance, are the two key passive electrical properties of neurons. **Table 2-1** lists experimentally determined time and length constants of neurons and muscles in various experimental preparations that have played important roles in the history of neurophysiology. We will learn about these specific preparations in later sections and chapters.

2.9 Active electrical properties of neurons: depolarization above a threshold produces action potentials

As is evident from Table 2-1, electrical signals would decay considerably across distance if neurons had only passive properties. Even in fibers with very large diameters, length constants are at most a few millimeters. This means that signals would decay to 37% of their original magnitude across just a few millimeters. How do electrical signals propagate faithfully over much greater distances? To state the problem concretely, how do signals propagate reliably through human motor neurons across distances of approximately a meter in order to control muscles in the toe?

To answer this question, let's continue our idealized experiment using the setup in Figure 2-16A. Through the stimulating electrode, we inject step current pulses with varying magnitudes and directions into a neuronal fiber, this time an axon (**Figure 2-18**, top). We begin by injecting negative current, which hyperpolarizes the membrane potential. The magnitude of changes in membrane potential, as measured by electrode *a* (Figure 2-18, bottom), is proportional to the magnitude of injected negative current. If we reverse the sign and inject positive current into the axon, we see that the membrane potential is depolarized rather than hyperpolarized. The magnitude of depolarization is also proportional to the magnitude of injected positive current, provided that only a small amount of positive current is injected. However, when the injected current exceeds a certain magnitude, a much larger and transient elevation of the membrane potential is

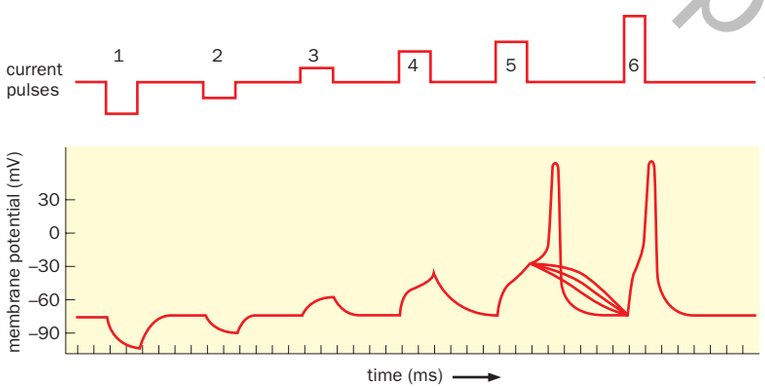

Figure 2-18 Depolarization exceeding a threshold results in action potentials. Using the experimental preparation diagrammed in Figure 2-16A, a series of rectangular current pulses were applied through the stimulating electrode (top). The corresponding changes in membrane potential recorded by electrode *a* are shown at the bottom. The unit of the *x* axis is 1 ms. For both hyperpolarization pulses and the first two depolarization pulses (current pulses 1–4), the membrane potential changes follow the sign of the current pulses, and their magnitudes are proportional to the magnitudes of the current pulses. In response to the fifth current pulse, the membrane potential change becomes unstable and varies across different trials (as illustrated by multiple curves). Occasionally the stimulation results in a very large depolarization—the action potential. Action potentials of the same magnitude are always produced in response to the sixth current pulse. (Adapted from Katz B [1966] Nerve, Muscle, and Synapse. McGraw Hill.)

produced in some fraction of trials. Above that magnitude of current injection, each current pulse invariably produces a large and transient elevation of the membrane potential. This is called an **action potential** or a **spike**. It is caused by depolarization of the membrane potential above a specific level, the **threshold**, in response to an injection of positive current of a certain magnitude (Movie 2-6). A stimulus that can cause the neuron to generate an action potential is called a **suprathreshold stimulus**, and a stimulus that cannot is called a **subthreshold stimulus**.

Note that the size of the action potential does not change with the magnitude of depolarization once the threshold is reached. Furthermore, if an action potential is recorded by electrode *a*, an action potential of similar magnitude and waveform will also be recorded by electrodes *b* and *c* in Figure 2-16A. In other words, action potentials propagate with little or no decay. As opposed to the passive spread of electrical signals discussed in Section 2.8, action potentials are an **active electrical property** of neurons. As we will learn later in this chapter, active electrical properties of neurons are a result of voltage-dependent changes in ion conductance.

Not all neurons fire action potentials: some neurons use only graded potentials to transmit electrical signals even in their axons. From the earlier discussion of length constants, these must necessarily be neurons with short axons; we will see examples of such neurons in the vertebrate retina in Chapter 4. It should also be noted that active electrical properties are not exclusive to axons: some neurons exhibit active properties in dendrites as well; we will discuss these properties in Chapter 3.

How are action potentials produced? How do they propagate along the axon? We devote the next part of this chapter to addressing these fundamental questions in neuronal signaling.

HOW DO ELECTRICAL SIGNALS PROPAGATE FROM THE NEURONAL CELL BODY TO ITS AXON TERMINALS?

In this part of the chapter, we follow the discovery path that has led to our current understanding of mechanisms by which action potentials are produced and propagate. In addition to answering a key question in neuronal communication—how electrical signals propagate from the neuronal cell body to its axon terminals—these studies also established the concept of ion channels and highlighted the mechanisms by which ion channels function.

2.10 Action potentials are initiated by depolarization-induced inward flow of Na^+

The discovery of the ionic basis of the action potential is an excellent example of how scientific breakthroughs can result from the introduction of new methods, model organisms, and analytic tools. Squid of the genus *Loligo* have a giant axon whose diameter reaches up to 1 mm, many times larger than nearby axons (**Figure 2-19**A) or the axons of typical mammalian neurons. The giant axon conducts action potentials very rapidly and controls the squid's jet propulsion system, allowing it to quickly escape danger. The giant axon's large diameter also enabled researchers to insert electrodes and measure action potentials more accurately than before (Figure 2-19B). During such measurements, it was discovered that the membrane potential during the rising phase of the action potential far exceeded zero (Figure 2-19C), indicating that the action potential is not caused by a transient breakdown of the membrane that allows the membrane potential to become zero, a prevalent view held before these measurements.

At the peak of the action potential, the membrane potential was observed to approach the Na^+ equilibrium potential. (Recall that E_{Na} = +58 mV in our model neuron in Figure 2-12.) This finding suggested that the membrane is preferentially

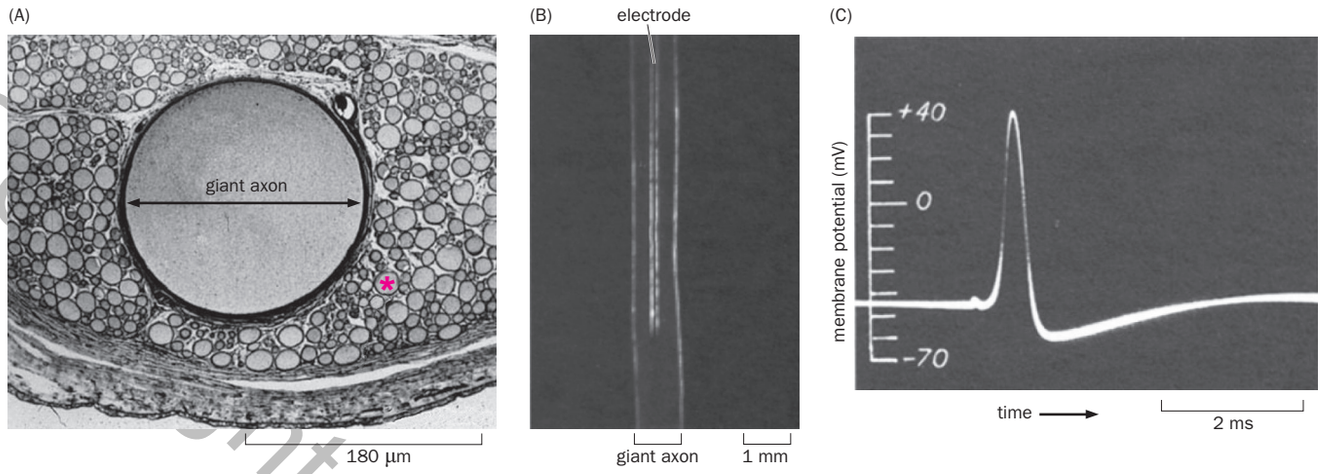

Figure 2-19 Studying action potentials using the squid giant axon. **(A)** Electron micrograph of a cross section of a squid giant axon showcasing its large diameter (~180 µm for this sample), in contrast to neighboring axons (for example, the axon indicated by *). **(B)** Photograph of an electrode inserted into a squid giant axon with a diameter close to 1 mm. **(C)** An action potential recorded from the squid giant axon by an intracellular electrode. (A, courtesy of Kay Cooper and Roger Hanlon; B, from Hodgkin AL & Keyes RD [1956] *J Physiol* 131:592–616. C, from Hodgkin AL & Huxley AF [1939] *Nature* 144:710–711. With permission from Springer Nature.)

permeable to Na^+ at the peak of the action potential and that the inward Na^+ flow is responsible for the rising phase of the action potential. To test this hypothesis, the extracellular Na^+ concentration was systematically reduced. If Na^+ were responsible for the rising phase of the action potential, one would predict from the Nernst equation that the magnitude of the action potential would decrease with lower concentrations of extracellular Na^+. This was indeed the case (**Figure 2-20**).

But how does the membrane become permeable to Na^+? An important conceptual breakthrough was the realization that depolarization could induce an increase in membrane permeability to Na^+, with the influx of Na^+ resulting in further depolarization. Such a self-reinforcing process (positive feedback loop) could account for the rapid change in membrane potential observed during the rising phase of the action potential.

2.11 Sequential, voltage-dependent changes in Na^+ and K^+ conductances account for action potentials

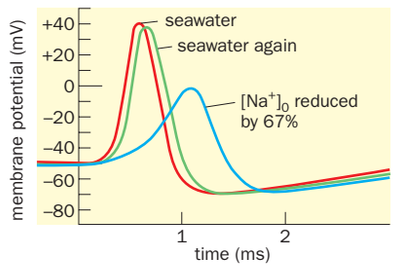

Figure 2-20 Testing the hypothesis that the rising phase of the action potential is caused by Na^+ influx. The magnitude and speed of the action potential are diminished when the normal extracellular solution (seawater, red trace) was replaced by a solution of 33% seawater and 67% isotonic dextrose (hence the extracellular Na^+ concentration, or $[Na^+]_o$, was reduced by 67%; blue trace). Reapplication of seawater (green trace) restored the magnitude and speed of the action potential. (Adapted from Hodgkin AL & Katz B [1949] *J Physiol* 108:37–77.)

To test whether depolarization could render axonal membranes more permeable to Na^+, it was important to quantitatively measure ion flow across the membrane under conditions mimicking the action potential. However, ion flow across the membrane changes the membrane potential, which in turn can affect the permeability of ions, thus complicating the measurement of ion flow. A new method called the **voltage clamp** was introduced to simplify the measurements of ion flow in response to voltage changes (**Figure 2-21**). The voltage clamp compares the intracellular membrane potential with a command voltage set by the experimenter. Differences between the two voltages automatically produce a feedback current that is injected back into the cell, which rapidly changes the intracellular membrane potential to the value of the command voltage. After the initial stimulation, which is usually in the form of a step change in the command voltage, ion flow across the membrane as a consequence of the membrane potential change can be measured by recording how much current must be injected into the cell in order to maintain the membrane potential at a specified value.

Using the voltage clamp technique, Alan Hodgkin and Andrew Huxley carried out a series of classic experiments around 1950 to determine the ionic basis of the action potential. By subjecting the squid giant axon to depolarizing voltages, they were able to dissect the composition of ionic flows that underlie an action potential. Importantly, holding the membrane potential at a constant value eliminated the capacitive current (current that charges the membrane in response to

voltage change, equivalent to I_C in Figure 2-16C) so that they could measure ionic currents across the membrane (equivalent to I_R in Figure 2-16C) and observe how they changed over time. For example, a 56 mV depolarizing step produced an initial inward current, followed by an outward current (**Figure 2-22**, green trace). (According to electrophysiology convention, inward current is net flow of cations into the cell or anions out of the cell; vice versa for outward current.) The inward current was abolished when extracellular Na^+ was replaced by choline, an organic ion that carries a +1 charge similar to Na^+ but is unable to permeate the membrane (Figure 2-22, blue trace). This finding indicated that the initial inward current is indeed caused by Na^+ influx. Thus, the Na^+ current could be calculated by comparing the difference between the two conditions (Figure 2-22, red trace). Other evidence suggested that in the case of choline replacement, the remaining current is caused by outward K^+ flux.

Voltage clamps also allowed systematic measurement of Na^+ and K^+ conductances over a series of different voltages. As introduced in Section 2.7, conductance is the ratio of the current that passes through the membrane and the driving force, which is the difference between the membrane potential and the equilibrium potential. Thus, the conductances for Na^+ and K^+ are given by

$$g_{Na} = \frac{I_{Na}}{V_m - E_{Na}}$$

$$g_K = \frac{I_K}{V_m - E_K}$$

where I_{Na} and I_K are the Na^+ and K^+ currents as measured in Figure 2-22, V_m is the membrane potential, and E_{Na} and E_K are the equilibrium potentials of Na^+ and K^+. By changing V_m (which equals V_{CMD}) and measuring the currents in the voltage clamp experiments, Hodgkin and Huxley could experimentally determine g_{Na} and g_K at different membrane potentials. They found that both Na^+ and K^+ conductances increased when the intracellular membrane potential became more depolarized and that these conductance changes evolve over time (**Figure 2-23**).

Hodgkin and Huxley made several key discoveries from these experiments. First, they confirmed that the rising phase of the action potential results from an influx of Na^+ and determined that the Na^+ influx is caused by a rapid increase in Na^+ conductance as a consequence of membrane depolarization. Second, after the initial depolarization-induced increase, Na^+ conductance would invariably decrease despite continued depolarization (Figure 2-23A), accounting for the falling phase of the Na^+ current (Figure 2-22, red trace). This was termed **inactivation** of the Na^+ conductance. Third, depolarization also caused an increase in K^+ conductance, resulting in K^+ efflux. Importantly, the change in K^+ conductance lagged behind the change in Na^+ conductance (Figure 2-23B). Fourth, the Na^+ and K^+ conductances appeared to be independent of each other, but both depended on the membrane potential. Well before the molecular mechanisms of membrane transport became known, these findings paved the way for the modern concept of ion channels as transmembrane proteins selectively permeable to specific ions (Section 2.4). In particular, in the squid giant axon, channels selectively permeable

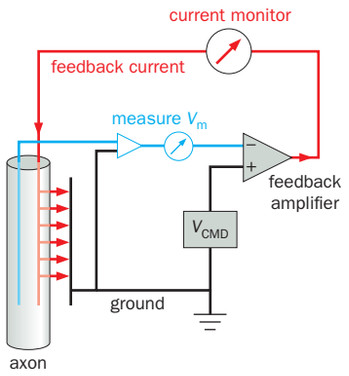

Figure 2-21 Illustration of the voltage clamp technique. The membrane potential (V_m) is measured by the blue wire inserted into the squid giant axon with respect to the ground wire outside the axon. It is then compared to a command voltage set by the experimenter (V_{CMD}) as two different inputs to the voltage clamp feedback amplifier (large triangle). The difference between the two voltages ($V_{CMD} - V_m$) produces a feedback current as the output of the amplifier, which is injected by a second inserted wire (red) into the axon. When $V_{CMD} = V_m$, there is no feedback current. Upon a step change of V_{CMD}, the feedback current rapidly changes V_m to the new V_{CMD} (within microseconds). Thus, the voltage clamp enables experimenters to control V_m of the axon being studied and, at the same time, to measure the amount of feedback current needed to hold V_m to the value of V_{CMD}; this quantity of feedback current equals the current flowing across the axon membrane (parallel red arrows). The feedback current can flow in either direction (that is, the red arrows can reverse) depending on the relative values of V_m and V_{CMD}.

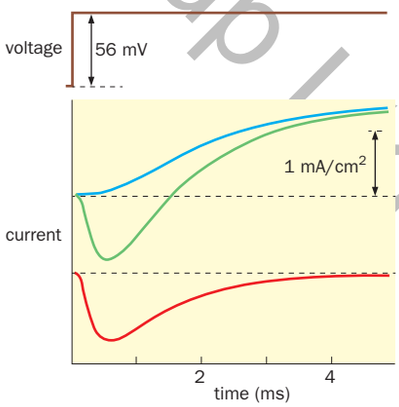

Figure 2-22 Dissociation of Na^+ and K^+ currents via voltage clamp experiments. Top, a voltage step increase of 56 mV was applied to the squid giant axon. Middle, ion flow across a unit area of the axonal membrane in response to the depolarizing voltage step was measured by determining how much current was injected into the axon in order to maintain the axon's membrane potential at the command voltage established by the experimenter (the +56 mV step). The green trace shows the current flow under physiological conditions; an initial inward current (the downward portion of the trace) is followed by an outward current (the upward portion). The dashed line demarcates zero net current. The blue trace shows the current flow under conditions in which the external Na^+ was mostly replaced by choline$^+$, which cannot cross the membrane; this trace illustrates the K^+ current only. Bottom, the red trace represents the deduced Na^+ current, which is the difference between the green and blue traces. (Adapted from Hodgkin AL & Huxley AF [1952] *J Physiol* 116:449–472.)

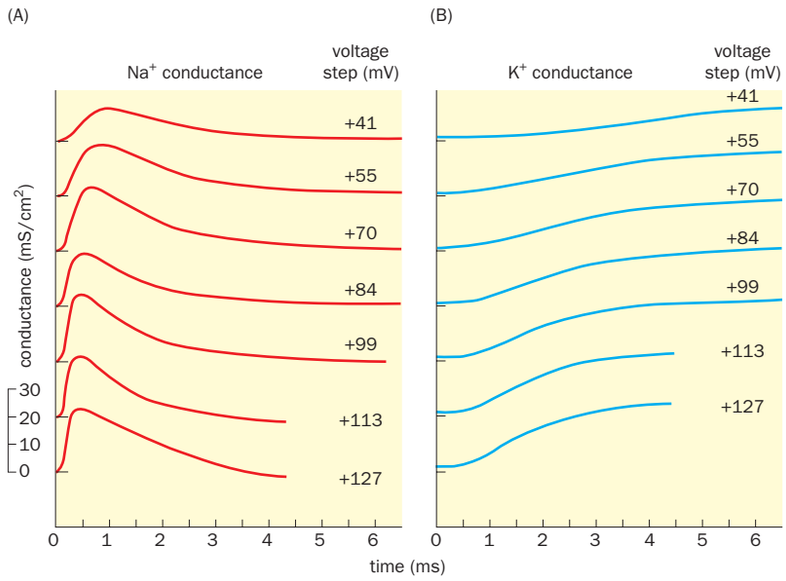

Figure 2-23 Voltage-dependent changes in Na^+ and K^+ conductances. Na^+ **(A)** and K^+ **(B)** conductances (*y* axis, in millisiemens per square centimeter) change over time following a depolarizing voltage step from the resting potential. A series of measurements were performed, each after a voltage step of a different magnitude (indicated on each trace). Over time, the Na^+ conductance first increases then decreases, whereas the K^+ conductance only increases, but more slowly than the initial rise of the Na^+ conductance. Larger voltage steps cause more rapid rises in both conductances. (Adapted from Hodgkin AL & Huxley AF [1952] *J Physiol* 116:449–472.)

to Na^+ or K^+ allow these ions to flow through the membrane. The conductance of these ion channels increases when the axon is depolarized. These channels are now called **voltage-gated ion channels** because their conductances change as a function of the membrane potential.

In summary, the action potential can be accounted for by sequential changes in the Na^+ and K^+ conductances (**Figure 2-24**; **Movie 2-7**), which we now know are caused by the opening and closing of voltage-gated Na^+ and K^+ channels. At the resting state, voltage-gated Na^+ and K^+ channels are both closed. (A different set of K^+ channels accounts for K^+ permeability at rest.) During the rising phase of the action potential, when the membrane is depolarized, opening of voltage-gated Na^+ channels allows Na^+ to flow into the cell down its electrochemical gradient. Depolarization also causes an increase in K^+ efflux (via resting K^+ channels) because the force produced by the new, smaller electrical gradient is less effective in countering the force produced by the chemical gradient. When the Na^+ influx exceeds the K^+ efflux, the neuron passes the threshold for firing an action potential. (For most excitable cells the threshold is 10–20 mV above the resting potential.) More depolarization causes opening of more voltage-gated Na^+ channels, which causes further depolarization. This positive feedback loop generates the rapid rising phase of the action potential.

During the falling phase, Na^+ channels are inactivated after the initial opening, preventing further Na^+ influx. At the same time, voltage-gated K^+ channels open, allowing more K^+ efflux. These two events together account for the falling phase of the action potential, allowing neurons to repolarize to the resting potential and prepare for the next action potential (Figure 2-24). Indeed, based on the

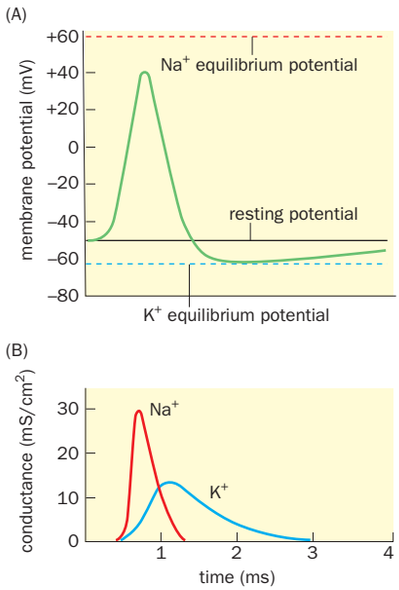

Figure 2-24 A summary of the ionic basis of the action potential. (A) Schematic of an action potential, with reference to the resting potential and the equilibrium potentials of Na^+ and K^+. (The K^+ equilibrium potential and the resting potential of the squid giant axon are more depolarized than for our model neuron in Figure 2-12.) **(B)** Sequential changes in Na^+ and K^+ conductance (calculated according to data in Figure 2-23) during the action potential. Both graphs share the same *x* axis. The rising phase is caused by an increase in Na^+ conductance, leading to Na^+ influx. The falling phase is accounted for by both the inactivation of the Na^+ conductance, which stops the Na^+ influx, and an increase in the K^+ conductance, leading to K^+ efflux. The transition between the rising and falling phase occurs before the rising phase reaches the Na^+ equilibrium potential. The falling phase overshoots the resting potential and approaches the K^+ equilibrium potential, before the membrane potential gradually returns to the resting potential, which is slightly above the K^+ equilibrium potential (Section 2.5). (Adapted from Hodgkin AL & Huxley AF [1952] *J Physiol* 117:500–544.)

measurements in voltage clamp experiments, Hodgkin and Huxley established a model that *quantitatively recapitulates* the dynamics of action potentials and many of their properties (see Section 14.30 for details). Importantly, the ionic basis of the action potential, originally discovered in the squid giant axon, applies to neurons and other excitable cells across most of the animal kingdom, including humans.

2.12 Action potentials are all or none, are regenerative, and propagate unidirectionally along the axon

The Hodgkin–Huxley model satisfactorily explains several properties of the action potential that ensure faithful transmission of information from the cell body to axon terminals.

First, action potentials are **all or none**. When a stimulus-induced neuronal membrane depolarization is below the threshold, the action potential does not occur. When depolarization exceeds the threshold, the waveform of the action potential is determined by the timing of Na^+ and K^+ conductance changes and the relative concentrations of Na^+ and K^+ inside and outside the cell, which remain mostly constant for any given neuron. (The Na^+ influx and K^+ efflux during an action potential cause very small changes in intracellular, and even smaller changes in extracellular, Na^+ and K^+ concentrations.) To a first approximation, action potentials assume the same form in response to any suprathreshold stimulus.

Second, action potentials are **regenerative**—they propagate without attenuation in amplitude. Suppose that an action potential occurs at a particular site on the axon. The rising phase creates a substantial membrane depolarization, which spreads down the axon and brings an adjacent region to threshold, which in turn does so for its adjacent downstream region, and so on (**Figure 2-25**). In this way, the action potential propagates in a similar form continuously and faithfully down the axon toward its terminals.

Third, action potentials propagate *unidirectionally* in the axon, from the cell body to the axon terminals. When an action potential occurs at a given site on the axon (for example, site A in Figure 2-25), in principle depolarization should also spread up the axon toward the cell body (site Z) in addition to spreading down the axon toward the axon terminals (site B). However, the delayed activation of the K^+ channels and the inactivation of the Na^+ channels combine to create a **refractory period** after an action potential has just occurred, during which time another action potential cannot be reinitiated. Because the action potential normally initiates at the axon initial segment and passes through Z before reaching A, another action potential cannot immediately back-propagate from A to Z. This refractory period ensures that the action potential normally propagates only from the cell body down the axon to its terminals, not in the reverse direction.

In most projection neurons, whose axons form synapses on distant target neurons, the action potential first arises at the axon initial segment, where voltage-gated Na^+ channel density per unit membrane area is the highest; this high channel density lowers the threshold for action potential initiation. The axon initial segment is a critical site for the integration of depolarizing and hyperpolarizing

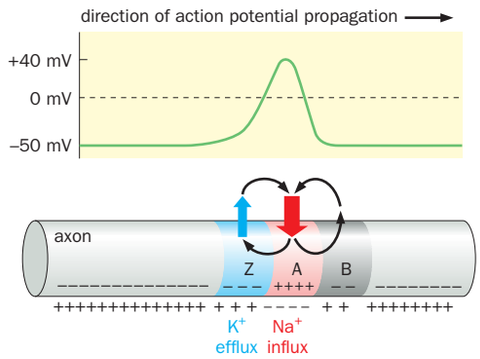

Figure 2-25 Action potential propagation. This schematic of an action potential as it sweeps across an axon provides a snapshot of electrical signaling events in the axon. The wave front is at site A, where voltage-gated Na^+ channels open and depolarize the membrane. Positive charges at site A within the axon spread to site B, where they will cause depolarization above the threshold. Thus, at the next moment, the wave front will reach site B. Site Z, where the wave front has just passed, is experiencing a refractory period during which the delayed activation of K^+ channels and the inactivation of Na^+ channels prevent the action potential from propagating backward from A to Z. Red and blue arrows indicate Na^+ influx and K^+ efflux, respectively. Curved arrows represent current flow completing the left and right circuits as a result of Na^+ influx. The charges below represent the membrane potentials at different segments of the axon.

synaptic potentials from the dendrites and the cell body; this integrative process is discussed further in Section 3.24. After initiation, action potentials travel unidirectionally along the axon toward its terminals. At the initiation site, however, action potentials can in principle travel in both directions; indeed, in some mammalian neurons, action potentials can back-propagate to dendrites, which, like axons, contain voltage-gated Na^+ and K^+ channels. In artificial situations where experimenters electrically stimulate the axon or its terminals, action potentials can propagate in a retrograde direction from axon terminals to the cell body, producing so-called **antidromic spikes**, which can be recorded from the cell body. However, antidromic spikes have not been found to occur under physiological conditions *in vivo*.

Altogether, these three properties make the action potential an ideal means to transmit information faithfully from neuronal cell bodies across long distances to their axon terminals. But since action potentials are all or none, the size of action potentials cannot encode information about the stimulus. Rather, the information is usually encoded by the rate (number of action potentials per unit time) or the timing of action potentials in response to a stimulus (Section 1.8). The spike rate is limited by the refractory period. Some neurons, such as fast-spiking inhibitory neurons in the mammalian cortex, can fire up to 1000 Hz, or one action potential per millisecond; the interval between these action potentials is shorter than the refractory period of many neurons. This requires specializing the ion channels so the action potential is repolarized quickly and the refractory period is complete in time for the next action potential. Thus, ion channel properties (such as Na^+ channel inactivation and the delayed opening of K^+ channels) have been selected during evolution to ensure unidirectional propagation of action potentials, and neurons with high spike rates use specialized ion channels with fast kinetics. The broad range of possible spike rates expands the information-coding capacity of individual neurons.

2.13 Action potentials propagate more rapidly in axons with larger diameters and in myelinated axons

The speed at which action potentials propagate is not the same for all neuronal types but instead depends on axonal properties. This is because the speed at which depolarization spreads down the axon is determined by the cable properties of the axon. Returning to our circuit model of neuronal membranes (Figures 2-16C and 2-17A), we see that this speed is determined by how quickly a change in membrane potential charges the membrane capacitor as well as the relative distribution of current flowing forward versus leaking out into the extracellular environment. If all other properties are equal, these values would be a function of axon diameter: the larger the axon diameter, the lower the axial resistance of the axon and the larger the proportion of current flowing forward. You can deduce this from the equation for the length constant (λ), which is equal to $\sqrt{dR_m/4R_i}$ (Section 2.8). Hence, the larger the diameter (d), the larger the length constant and the further depolarization can spread at a suprathreshold value to produce the next action potential at more distant sites. This is why the squid and some other animals have evolved giant axons with very large diameters, which implement rapid escape behaviors.

In principle, increasing R_m (the membrane resistance per unit area) can also increase the length constant. However, increasing R_m also increases the time constant (which is equal to $R_m C_m$; Section 2.8) required to charge the membrane along the way, which slows down the propagation of action potentials. One way to compensate for this is to also reduce C_m, the membrane capacitance. Indeed, this is how **axon myelination** works. Many vertebrate axons are wrapped in a **myelin sheath**, formed by layers of cytoplasmic extensions of glia—Schwann cells in the PNS and oligodendrocytes in the CNS. Some axons in large invertebrates are also myelinated (Section 13.7). The cytoplasmic extensions of glial cells wrap around the axon many times, with most of the cytoplasm compressed out of the extensions toward the soma to form **compact myelin** consisting of closely packed glial plasma

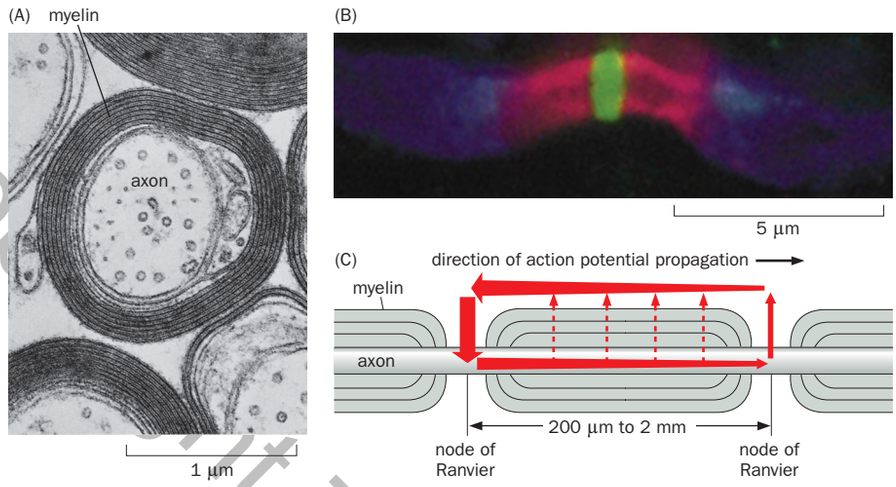

Figure 2-26 Axon myelination increases the speed of action potential propagation. (A) An electron micrograph of a cross section of spinal cord axons wrapped by oligodendrocyte membranes. At the center is a single axon wrapped in myelin sheath. **(B)** A fluorescence microscopic image of the rat optic nerve immunostained to visualize three proteins (see Section 14.12 for more details of the immunostaining method). Na^+ channels (green) are highly clustered at the center of the node of Ranvier. K^+ channels (blue) are distributed peripherally at the node. In between are transmembrane proteins named Caspr (red) that help organize channel distribution at the node. **(C)** Schematic of an action potential hopping between nodes of Ranvier. After an action potential occurs at the left node of Ranvier, positive charges rapidly flow to the next node to the right. This is because, as a consequence of myelin wrapping, the internodal membranes have low capacitance, which requires less charging, and high resistance, which allows only a small amount of current to leak through (dashed arrows). The arrival of positive charges at the right node causes rapid depolarization above threshold to regenerate the action potential there. Red arrows indicate the direction of current flow that completes the circuit as a result of Na^+ influx at the left node. For simplicity, the circuit resulting from depolarization spreading leftward from the left node is omitted. (A, courtesy of Cedric Raine. B, adapted from Rasband MN & Shrager P [2000] *J Physiol* 525:63–73.)

membranes (**Figure 2-26**A). From an electrical circuit perspective, compact myelin is equivalent to having many resistors connected in series, such that the total membrane resistance R_T is equivalent to nR_m, where n is the number of layers of glial membrane. However, in serial connections, the total capacitance C_T is equivalent to C_m/n (recall from Section 2.6 that the total capacitance of two capacitors connecting in series follows $1/C_T = 1/C_1 + 1/C_2$; the combined capacitance of n identical capacitors connected in series follows $1/C_T = n/C$, or $C_T = C/n$). Thus, myelination greatly increases membrane resistance, and hence the length constant, without increasing the time constant (as the product R_TC_T remains unchanged compared to the original R_mC_m); this means that once an action potential is produced at a specific site on the axon, depolarization spreads across a large distance to cause distant regeneration of the action potential.

Despite the increased membrane resistance, small amounts of current still leak out of myelinated axons. Therefore, it is important to have **nodes of Ranvier**, occurring at regular intervals (usually 200 µm to 2 mm apart), where the axon surfaces are exposed to the extracellular ionic environment with highly concentrated voltage-gated Na^+ and K^+ channels (Figure 2-26B). As a result of these channel activities, depolarizing current spreads rapidly in between the nodes, and action potentials are "renewed" only at the nodes of Ranvier (Figure 2-26C). Thus, action potentials in a myelinated axon hop from node to node. This is termed **saltatory conduction** (from the Latin *saltare*, "to jump"), as opposed to continuous propagation in unmyelinated axons (Figure 2-25).

Myelination greatly increases the conduction speed of action potentials and the capacity for high-frequency firing. Action potentials can travel at speeds of up to 120 m/s in myelinated axons, as compared to <2 m/s in unmyelinated axons. Although unmyelinated axons usually have smaller diameters than myelinated axons (**Box 2-3**), the diameter difference alone does not account for the large difference in propagation speeds. Saltatory conduction also saves energy; there is a reduced demand for the Na^+–K^+ ATPase to pump Na^+ outward and K^+ inward, as there is little transmembrane current except at the nodes of Ranvier. Because myelin is so important for proper conduction in the axons of vertebrates, including humans, improper myelination is responsible for several major neurological disorders, including multiple sclerosis and Charcot–Marie–Tooth disease (Box 2-3).

2.14 Patch clamp recording enables the study of current flow through individual ion channels

Studies of the action potential in the squid giant axon suggested the existence of dedicated ion channels for Na^+ and K^+. This idea was later supported by the characterization of toxins that specifically block Na^+ or K^+ channels. The most famous

Box 2-3: Axon-glia interactions in health and disease

Axon myelination provides a striking example of the intimate interactions between glia and neurons. In the white matter of the central nervous system, each oligodendrocyte typically extends several processes that myelinate multiple axons (Figure 1-9). In the peripheral nervous system, each Schwann cell is usually dedicated to wrapping a segment of a single axon. During development and remyelination in adults, oligodendrocyte and Schwann cell extensions wrap the axon many times like a spiral and compress the cytoplasm in between layers of the extensions to form the myelin sheath (**Figure 2-27**A).

Axons and glia interact in diverse ways. For example, as will be discussed in Chapter 6, the somatosensory system contains distinct types of sensory neurons with characteristic axon diameter, degree of myelination, and action potential conduction speed. The thickness of myelin matches the size of the axon. Sensory neurons that innervate muscle and provide rapid feedback regulation of movement have large-diameter axons, thicker myelin sheaths, and conduct action potentials more rapidly. Sensory neurons that sense touch have intermediate axon diameters and conduction speeds. Many sensory neurons that sense temperature and pain are unmyelinated and conduct action potentials more slowly. These unmyelinated axons are nevertheless associated with **Remak Schwann cells**, whose cytoplasm extends in between individual axons to form a Remak bundle (Figure 2-27B). Here the glia's role is simply to segregate individual axons rather than to support saltatory conduction.

What determines whether an axon should be myelinated or not, and if so, to what degree? These questions have been answered in the PNS. An axonal cell-surface protein called **type III neuregulin-1** (**Nrg1-III**) plays a key role: axons expressing high levels of Nrg1-III are associated with thick myelin sheaths, axons expressing intermediate levels of Nrg1-III are thinly myelinated, and axons expressing low levels of Nrg1-III are associated with a Remak bundle (Figure 2-27B). Nrg1-III acts on the erbB receptor complex on Schwann cells to direct their differentiation, including the expression of myelin-associated proteins and the spiral wrapping of axons. Nrg1/erbB signaling is not required for myelination by oligodendrocytes, suggesting alternative axon-glia signals in the CNS. Schwann cells and oligodendrocytes also signal back to axons to provide long-term support to their health and integrity.

The importance of myelination to human health is highlighted by the plethora of **demyelinating diseases**, in which damage to the myelin sheath decreases the resistance between nodes of Ranvier and disrupts the organization of ion channels in the nodal region (Figure 2-26). This slows down or even stops action potential conduction, causing deficits in sensation, movement, and cognition. Demyelinating diseases can be caused by several factors, including autoimmune responses that attack glial cells and mutations in proteins necessary for myelin function.

The most common CNS demyelinating disease is **multiple sclerosis** (**MS**), an adult-onset inflammation-mediated disease that affects 1 in every 3000 people globally. The hallmarks of MS include the formation of inflammatory plaques in white matter caused by destruction of myelin by immune cells. Most MS patients begin with a phase of relapsing-remitting MS, during which patients cycle between inflammatory demyelination with neurological symptoms, and

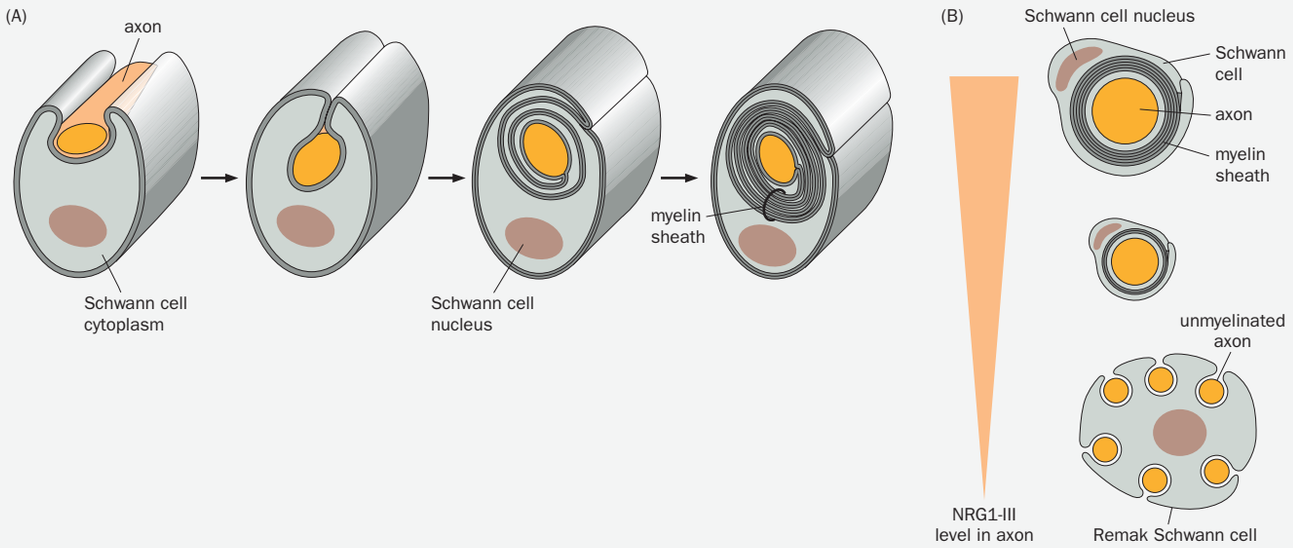

Figure 2-27 Schwann cell wrapping of axons and its regulation by neuregulin signaling. (A) Schematic of sequential steps illustrating a Schwann cell wrapping an axon, forming spiral extensions, and compressing its cytoplasm between the layers of plasma membrane to form myelin sheath. **(B)** Top, large-diameter axons express the highest levels of type III neuregulin-1 (NRG1-III), which direct thicker myelination. Middle, intermediate-diameter axons express intermediate levels of NRG1-III, which direct thinner myelination. Bottom, small-diameter unmyelinated axons express the lowest levels of NRG1-III, which direct their interaction with Remak Schwann cells, forming a Remak bundle. (Adapted from Nave KA & Salzer JL [2006] *Curr Opin Neurobiol* 16:492–500. With permission from Elsevier Inc.)

Box 2-3: continued

remyelination and recovery. The next phase is characterized by continual neurological symptoms and progressive deterioration, which is often irreversible. Although abnormal immune responses clearly play a major role, the causes of MS remain mostly unknown. Variants of certain genes such as the major histocompatibility loci confer risks, but environmental factors appear to play a major role. Thanks to the recent development of drugs that inhibit immune destruction of CNS myelin, the life prognosis for a first diagnosis of MS today is far better than it was several decades ago.

Compared to MS, much more is known about the mechanisms of demyelinating diseases in the PNS because many are caused by inherited mutations in specific genes. **Charcot–Marie–Tooth** (**CMT**) **disease** (first described by J. M. Charcot, P. Marie, and H. H. Tooth in 1886) is the most common inherited disorder of the PNS, affecting 1 in 2500 individuals. CMT patients exhibit age-progressive deficits in sensation and/or movement in a length-dependent manner (that is, distal limbs exhibit the most severe deficits). Genetic alterations in several dozen different genes underlie various forms of the CMT disease that display similar symptoms. Some CMT genes act in Schwann cells. For example, the most common cause of CMT (CMT1A) results from a duplication of a chromosome segment, causing overexpression of the peripheral myelin protein 22 (PMP22). CMT1B is caused by mutations in a gene encoding myelin protein zero (MPZ). Both PMP22 and MPZ are transmembrane proteins expressed abundantly in Schwann cells and involved in the formation of compact myelin. CMT1X is caused by mutations in a gene encoding a gap junction channel (Box 3-5) expressed in Schwann cells, which can facilitate transport of molecules from the area around the nucleus to inner layers of the myelin sheath by introducing shortcuts across the myelin membranes. Some CMT genes act in axons and encode a variety of proteins, such as neurofilaments and those involved in mitochondria fusion and protein translation. Studies of these CMT genes can help us understand both the normal biology of myelination and the pathogenesis of demyelination diseases.

Fundamental studies in neurobiology and research on disorders of the nervous system can greatly benefit each other. We will encounter examples of this synergy throughout the book and will address many in Chapter 12, which focuses on brain disorders.

toxin is puffer fish **tetrodotoxin (TTX)** (**Figure 2-28**), which potently blocks voltage-gated Na^+ channels of many animal species and is widely used to experimentally silence neuronal firing. In recordings from the squid giant axon, for example, TTX application mimics the replacement of Na^+ with choline$^+$ in the original Hodgkin–Huxley experiment (Figure 2-22). Other drugs, such as **tetraethylammonium** (**TEA**), selectively block voltage-gated K^+ channels. Experiments using these drugs provided evidence for the existence of ion channels selectively permeable to specific ions.

Direct support for the existence of ion channels and characterization of individual channel properties came as a result of an important technical innovation in the late 1970s called **patch clamp recording** (see Section 14.21 and Box 14-3 for more details). In its original form, now called a **cell-attached patch**, a **patch pipette** (also called a patch electrode, a glass electrode with a small opening at its tip) forms a high-resistance seal with a small patch of the plasma membrane of an intact cell. This high-resistance seal is called a giga seal because the resistance exceeds 10^9 ohms (giga = 10^9), thus preventing ion flow between the pipette and extracellular solutions. When performing a patch clamp recording, the experimenter can "clamp" the voltage in the patch pipette, which corresponds to the extracellular potential for the small patch of the membrane under the pipette. Ion flow through the small membrane patch, which sometimes contains only a single ion channel, can be resolved and studied in isolation (**Figure 2-29**A).

When a cell-attached patch clamp was applied to cultured rat muscle cells, for example, the opening and closing of a single channel could be detected as discrete events. When a single channel opened in response to a depolarization of the patch, it produced a unitary inward current of ~1.6 picoamperes (circled in Figure 2-29B). When hundreds of these single channel recording traces were summed and averaged over time, a "macroscopic" Na^+ current ensemble much like the Hodgkin–Huxley voltage clamp recording was reconstituted, with characteristic voltage-dependent opening and subsequent inactivation (Figure 2-30B, bottom; compare with the bottom trace of Figure 2-22). This experiment thus revealed the biophysical basis of voltage-dependent changes in Na^+ conductance at the level of single molecules: each voltage-gated Na^+ channel exists in discrete states, open or closed, with stochastic transitions; the proportion of time an individual channel

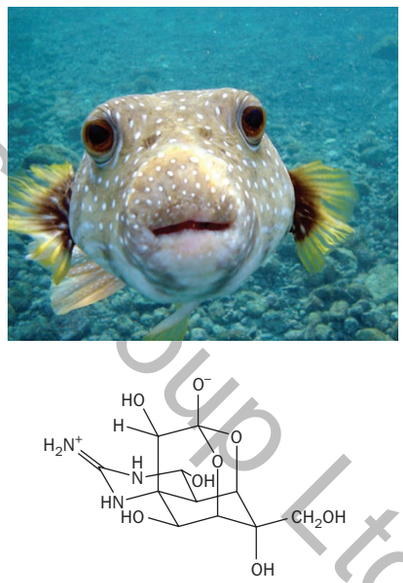

Figure 2-28 Tetrodotoxin (TTX) from the puffer fish. Puffer fish (above), whose resident symbiotic bacteria produce tetrodotoxin (TTX, below), is a delicacy in Japanese cuisine that must be carefully prepared. TTX is a potent blocker of voltage-gated Na^+ channels in many species. (Image courtesy of Brocken Inaglory/Wikipedia.)

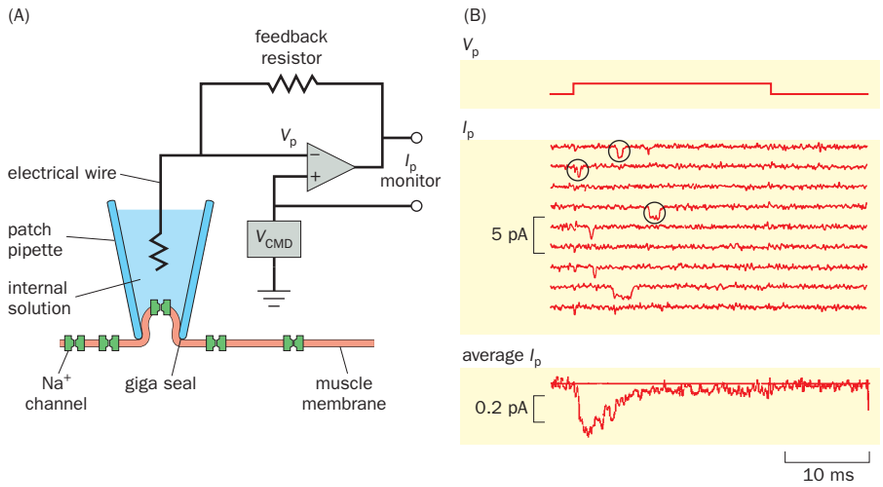

Figure 2-29 Studying ion flow across individual Na^+ channels using patch clamp. (A) A cell-attached patch pipette can record ion flow within a small patch of muscle membrane. The configuration is analogous to that of the voltage clamp schematic shown in Figure 2-21. The patch pipette serves two functions: to measure the voltage of the pipette V_p, and to inject current through a feedback circuit such that V_p matches that of the command voltage (V_{CMD}). The current that needs to be injected in order for V_p to match V_{CMD}, which can be measured with the current monitor, is equivalent to the current that flows through the ion channel(s) under the patch pipette (I_p). **(B)** In response to a depolarization step (V_p) applied to the patch pipette (top), current flows across the patch (I_p, middle). Traces are shown for nine individual current measurements. Na^+ channel openings can be seen as downward, rectangular steps (for example, circles on the first, second, and fourth traces), as positively charged Na^+ ions leave the recording pipette and flow into the cell. The average of 300 I_p traces (bottom) resembles the macroscopic Na^+ current measured by conventional voltage clamp, including voltage-dependent activation and inactivation. In these recordings, a K^+ channel blocker was included in the pipette solution to block ion flow through possible K^+ channel(s) in the membrane patch. (Adapted from Sigworth FJ & Neher E [1980] *Nature* 287:447–449. With permission from Springer Nature.)

is open and able to conduct current—that is, the channel's **open probability**—is temporarily increased by depolarization.

Note that in the experiment each channel opening takes a square-like form, which means that the channel typically transitions between a state that is non-conducting (closed) to one that is conducting (open) without sliding through intermediates. Also note that even though an individual channel makes the closed-to-open transition abruptly, channels do not all open immediately after the membrane potential changes, and they close soon thereafter through an apparent inactivation process. Indeed, a difference in the delay in depolarization-induced open probability between Na^+ and K^+ channels accounts for the temporal difference in Na^+ and K^+ conductance rises during the action potential (Figure 2-24B).

In general, the current (I) carried by a particular ion species across a piece of neuronal membrane can be determined from single channel properties by the following formula:

$$I = NP_o\gamma(V_m - E)$$

where N is the total number of channels present, P_o is the open probability of an individual channel, V_m is the membrane potential, E is the equilibrium potential of that ion (hence $V_m - E$ is the driving force), and γ is the **single channel conductance**. Compared to the relationship between current and driving force we learned in Section 2.7, we see that the product $NP_o\gamma$ is equivalent to the macroscopic conductance, g. Thus, the ion conductance across a neuronal membrane is the product of (1) the number of channels present on the membrane, (2) the open probability of each channel, and (3) the single channel conductance. As discussed earlier, the open probability P_o is a function of both membrane potential and time, whereas the single channel conductance γ is a physical property of the channel protein that can vary with changes in its ionic milieu.

2.15 Cloning of genes encoding ion channels allows studies of their structure–function relationship

The molecular structures of ion channels as individual proteins were determined after the cloning of genes encoding specific ion channels, as the revolution in molecular biology spread to neuroscience in the 1980s. Being able to clone a gene requires one or more of the following approaches: (1) purifying the corresponding protein and using its amino acid sequence to deduce its nucleotide sequence and design a probe to screen a **cDNA library** (consisting of cloned cDNAs, or complementary DNAs, synthesized from mRNA templates derived from a specific tissue), (2) identifying a mutant defective in the gene product and using molecular genetic techniques to trace the causal gene, or (3) expressing the candidate gene product (by partitioning of a cDNA library) in a host cell and using a functional assay to identify the presence of the gene product. If there is a rich source of the protein

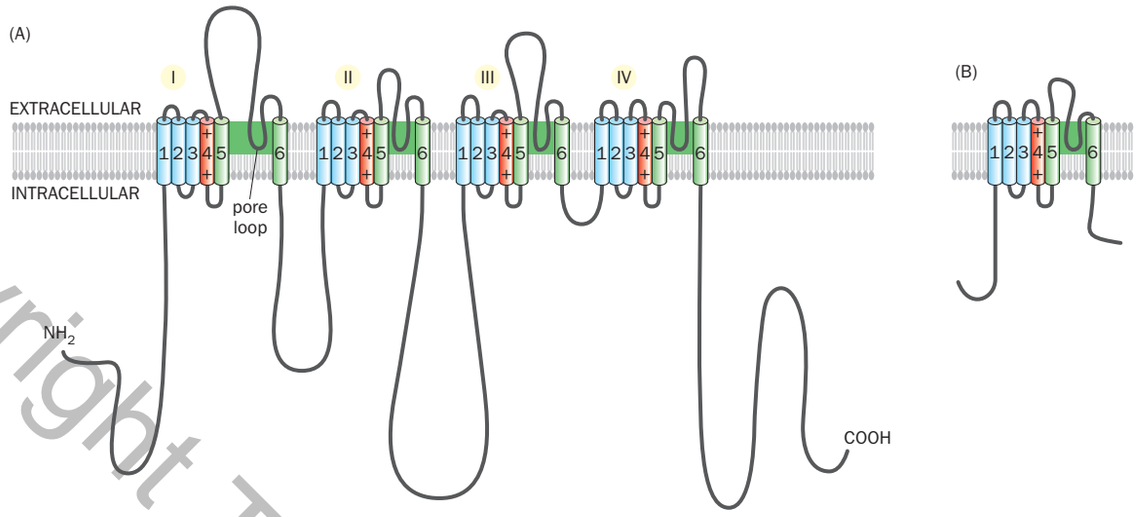

Figure 2-30 Primary structure of voltage-gated Na^+ and K^+ channels. **(A)** A voltage-gated Na^+ channel comprises four repeating modules. Each module consists of six helical transmembrane segments (TMs), with the fourth TM (red) containing positively charged amino acids that play a key role in voltage sensing. The pore loop and the adjacent fifth and sixth TMs together constitute the ion conduction pore (green). This structure was originally derived from the voltage-gated Na^+ channel from electric eel (see Noda M, Shimizu S, Tanabe T et al. [1984] *Nature* 312:121–127). **(B)** A voltage-gated K^+ channel protein resembles one of the four repeating modules of a voltage-gated Na^+ channel; note the positively charged amino acids in the fourth TM and the pore loop between the fifth and sixth TMs. Four such subunits constitute a functional channel. The structure was originally derived from a K^+ channel identified in *Drosophila* after the positional cloning of the *Shaker* gene (see Papazian DM, Schwarz TL, Tempel BL et al. [1987] *Science* 237:749–753 and Tempel BL, Papazian DM, Schwarz TL et al. [1987] *Science* 237:770–775). (From Yu FH & Catterall WA [2004] *Science STKE* 253:re15. With permission from AAAS; adapted from Sato et al. [2001] *Nature* 409:1047.)

and a functional assay (such as a high-affinity ligand) with which to look for the presence of the protein in biochemical fractions, the protein purification route is available; indeed, this route led to the cloning of the first Na^+ channels.

Voltage-gated Na^+ channel proteins were first purified from the electric eel *Electrophorus electricus,* whose electric organ is densely packed with Na^+ channels. (Electric eels use their electric organ to shock their prey with large currents.) Peptide sequences from purified electric eel Na^+ channel proteins were used to identify cDNAs encoding these proteins, and the electric eel cDNAs were then used to identify homologous genes in other organisms, including mammals, leading to the determination of their complete amino acid sequences. These studies revealed a highly conserved primary structure (**Figure 2-30**A): Animals from invertebrates to mammals have voltage-gated Na^+ channels consisting of four repeating modules, each containing six transmembrane segments. This structural conservation explains why toxins such as TTX block Na^+ channels across the animal kingdom. The fourth transmembrane segment, termed S4, contains many positively charged amino acids and was hypothesized to be the sensor that detects voltage changes for channel gating. A hydrophobic stretch of amino acids between the fifth and sixth transmembrane segments (S5 and S6) forms an extra pore loop within the membrane. As we will learn in more detail in Section 2.16, the pore loop, S5, and S6 together form the central pore for ion conduction.

While studies on voltage-gated Na^+ channels benefited from the electric organ, the lack of a similarly enriched source of K^+ channels and the overall heterogeneity of K^+ channels made them resistant to similar biochemical approaches. Fortunately, genetic studies in the fruit fly *Drosophila melanogaster* provided an alternative strategy for cloning genes encoding K^+ channels. A *Drosophila* mutant named ***Shaker,*** so-called because the mutant flies shake their legs under ether anesthesia, exhibited defects in a fast and transient K^+ current in muscles and neurons, as well as defects in action potential repolarization. These findings led to the hypothesis that a K^+ channel was disrupted in *Shaker* mutant flies. **Positional cloning** of the DNA corresponding to the *Shaker* locus (see Section 14.6 for details) identified the first voltage-gated K^+ channel (Figure 2-30B). Interestingly, this K^+ channel protein resembles one of the four repeating modules of the Na^+ channel; like each

of these modules, it has six transmembrane segments, including the positively charged S4 and the pore loop. Subsequent work showed that four such polypeptides (subunits) constitute one functional K^+ channel.

Cloning of ion channels enabled structure–function studies investigating the molecular mechanisms underlying channel properties. One such property is the inactivation of voltage-gated Na^+ channels, which contributes to the repolarization phase of the action potential. This enables action potentials to travel unidirectionally by enforcing a refractory period (Sections 2.10 and 2.11). Biophysical studies in the 1970s led to a **ball-and-chain** inactivation model positing that a cytoplasmic portion of the channel protein (the ball), connected to the rest of the channel by a polypeptide chain, blocks the channel pore after the ion channel opens. It was further hypothesized that depolarization not only opens the channel but also causes movement of charged amino acids to create a negatively charged inner channel pore, which would facilitate binding of a positively charged ball (**Figure 2-31**A).

This ball-and-chain model was elegantly validated in the voltage-gated Shaker K^+ channel, which undergoes inactivation similarly to the voltage-gated Na^+ channel. By using a molecular biology technique called *in vitro* mutagenesis to alter the DNA sequence of the cloned *Shaker* gene, researchers could express Shaker proteins in which selected stretches of amino acids were deleted, inserted, or replaced. This work revealed that the cytoplasmic N-terminal domain of the Shaker K^+ channel is necessary for fast inactivation. Deleting a stretch of amino acids in this domain generated a mutant K^+ channel that could not undergo fast inactivation after depolarization-induced channel opening. Supplying a peptide containing the first 20 amino acids of the cytoplasmic domain was sufficient to

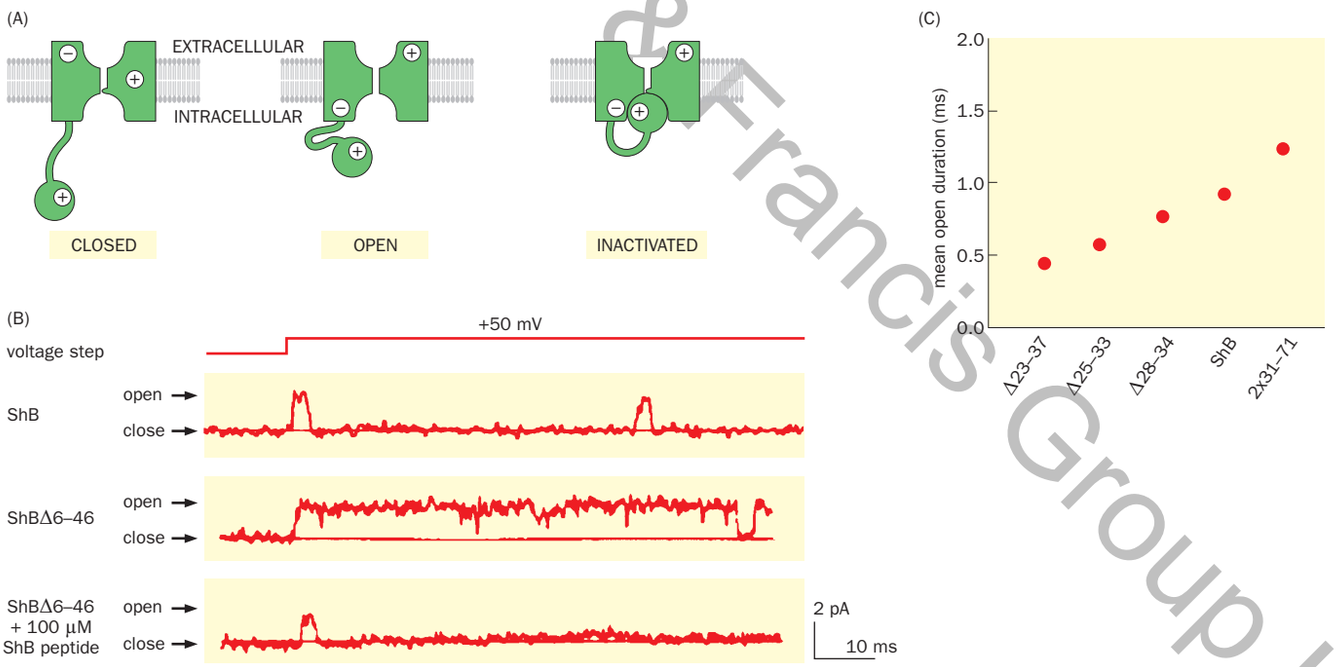

Figure 2-31 Molecular mechanisms of voltage-gated ion channel inactivation. (A) The ball-and-chain model of voltage-gated Na^+ channel inactivation. Depolarization causes the channel to open and, at the same time, moves charged amino acids such that the inner pore of the channel becomes more negatively charged, creating a binding site for a portion of the channel's cytoplasmic domain (the ball), which is positively charged. The binding of the ball to the inner pore inactivates the channel. **(B)** Mutagenesis studies of the Shaker K^+ channel (the ShB isoform) support the ball-and-chain model. In patch clamp experiments, the wild-type ShB channel (top) inactivates after initial depolarization-induced opening, and remains closed despite continued depolarization at +50 mV. When amino acids 6–46 are deleted from ShB (middle), the channel exhibits defective inactivation, as the channel remains open after depolarization. The inactivation defect of the mutant channel is corrected by supplying a soluble ball peptide made up of the first 20 amino acids of the cytoplasmic domain (bottom). **(C)** Compared to the wild-type channel (fourth column), the mean channel open duration is shortened by deleting 15, 9, and 7 amino acids from the chain connecting the ball to the rest of the channel (first three columns, respectively). The mean channel open duration is lengthened by adding 41 amino acids to the chain (fifth column, duplicating amino acids 31–71). (A, adapted from Armstrong CM & Bezanilla F [1977] *J Gen Physiol* 70:567–590. B & C, adapted from Hoshi T, Zagotta WN, & Aldrich RW [1990] *Science* 250:533–538 and Zagotta WN, Hoshi T, & Aldrich RW [1990] *Science* 250:568–571.)

restore the inactivation of this mutant K^+ channel (Figure 2-31B). Thus, the first 20 amino acids correspond to the ball. As predicted by the ball-and-chain model, several positively charged amino acids within the first 20 amino acids were found to be crucial for inactivation. Furthermore, decreasing the length of the chain—the intervening polypeptide between the first 20 amino acids and the rest of the channel—yielded a channel open for shorter periods before inactivation, whereas lengthening the chain increased the duration that the channel remained open (Figure 2-31C). These data suggest that the length of the chain dictates the "search" time for the ball to find the open channel. This example illustrates the power of combining molecular biology and electrophysiology to understand the mechanisms of ion channel function.

2.16 Structural studies reveal the atomic bases of ion channel properties

Ion channels are remarkable molecular machines. A voltage-gated K^+ channel can conduct up to 10^8 K^+ ions per second, which is near the diffusion rate of K^+, while also maintaining a high selectivity for K^+: the channel conducts ~10,000 times fewer Na^+ ions than K^+ ions. Central to the channel's conduction and ion selectivity is the pore loop (Figure 2-31B). *In vitro* mutagenesis studies have shown that mutations in the pore loop alter ion selectivity. Subsequent structural studies at atomic resolution using X-ray crystallography have provided detailed mechanisms of ion conduction and selectivity.

The amino acid residues of the K^+ channel pore loop are highly conserved from bacteria to humans. Thus, the crystal structure of the bacterial K^+ channel KcsA, the first ion channel whose structure was determined at atomic resolution, revealed mechanisms of K^+ conduction and selectivity that are likely universal. The KcsA channel is not voltage gated but nevertheless resembles part of the voltage-gated K^+ channel: each of the four KcsA subunits contains only two transmembrane helices (equivalent to transmembrane segments S5 and S6 of a voltage-gated K^+ channel subunit) and a pore loop in between, part of which forms a pore helix (**Figure 2-32**A). From the side, the channel looks like a conical

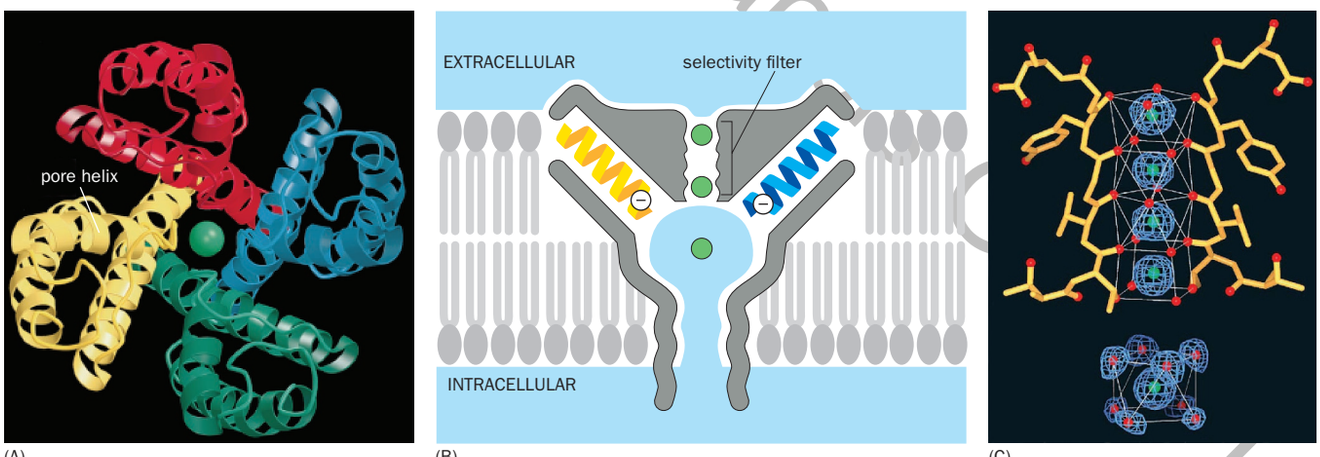

Figure 2-32 Atomic structure of KcsA, a bacterial K^+ channel. **(A)** The KcsA channel viewed from the extracellular side. Each of the four subunits (differently colored) consists of two transmembrane helices and a shorter pore helix (indicated for the yellow subunit). A green K^+ ion is passing through the central pore. **(B)** From a side view, the KcsA channel resembles a conical funnel. An aqueous passage extends from the intracellular side to a central cavity in the middle of the lipid bilayer. Three K^+ ions are shown, one in the cavity and two in the selectivity filter above. The gray shading represents the channel protein viewed from the side. Two of the four pore helices are shown in this side view, with their electronegative carboxyl ends facing the cavity to stabilize the positively charged K^+ ion in the cavity. **(C)** Atomic structure of the selectivity filter. Oxygen atoms from carbonyl groups of the main polypeptide chain (red dots) create four K^+ binding sites within the selectivity filter. At each binding site, the K^+ ion is surrounded by eight oxygen atoms, just as the hydrated K^+ ion is surrounded by eight oxygen atoms from water in the cavity shown at the bottom. This mimicry renders conduction of K^+ (but not the smaller Na^+) more energetically favorable, providing a mechanism for ion selectivity. (A & B, from Doyle DA, Cabral JM, Pfuetzner RA, et al. [1998] *Science* 280:69–77. With permission from AAAS. C, adapted from Zhou Y, Morais-Cabral JH, Kaufman A, et al. [2001] *Nature* 414:43–48. With permission from Springer Nature.)

funnel (Figure 2-32B), with a cavity at the center of the channel to accommodate a hydrated K^+ ion. (Ions in solution, including K^+ and Na^+, are normally present in hydrated form.) Electronegative carboxyl ends of the four pore helices face the cavity and stabilize the K^+ ion as it travels through. When the channel is open, intracellular hydrated K^+ has free access to the cavity. Between the cavity and the extracellular side is the **selectivity filter**, through which K^+ ions pass in dehydrated form. This is accomplished via the interaction of K^+ with the electronegative carbonyl groups from the main polypeptide backbone corresponding to the most highly conserved amino acids of K^+ channels. These close carbonyl interactions, which mimic and replace the water molecules surrounding the K^+ ion in solution, perfectly match the size of the K^+ ion but not the smaller Na^+ ion. This accounts for the K^+ channel's high degree of ion selectivity and the favorable energetics of K^+ conduction through an open channel (Figure 2-32C; **Movie 2-8**). There are four possible positions for K^+ at the selectivity filter, which is usually occupied by two K^+ ions at alternate positions. The repulsion between the two K^+ ions forces K^+ to flow rapidly through the selectivity filter when the channel is open and when there is a driving force (an electrochemical gradient).

Following the pioneering studies on the KcsA K^+ channel, the structures of many ion channels (**Box 2-4**), including eukaryotic voltage-gated K^+ and Na^+ channels (**Figure 2-33**) have been solved by X-ray crystallography and, more recently, cryogenic electron microscopy (**cryo-EM**). The overall architectures of voltage-gated K^+ and Na^+ channels resemble each other, reflecting the similarities in their primary structures (Figure 2-30). Each of the four subunits of the K^+ channel and the repeating units of the Na^+ channel has a voltage-sensing domain (consisting of the transmembrane segments S1–S4) at its periphery and a pore domain (consisting of S5, the pore loop, and S6) at the center of the channel. In both cases, the voltage-sensing domain of one unit latches onto the pore domain of an adjacent unit (Figure 2-33A, B). Depolarization sensed by the S4 segments, which are enriched in positively charged amino acids (Figure 2-30), moves the voltage-sensing domain within the lipid bilayer. This causes conformational

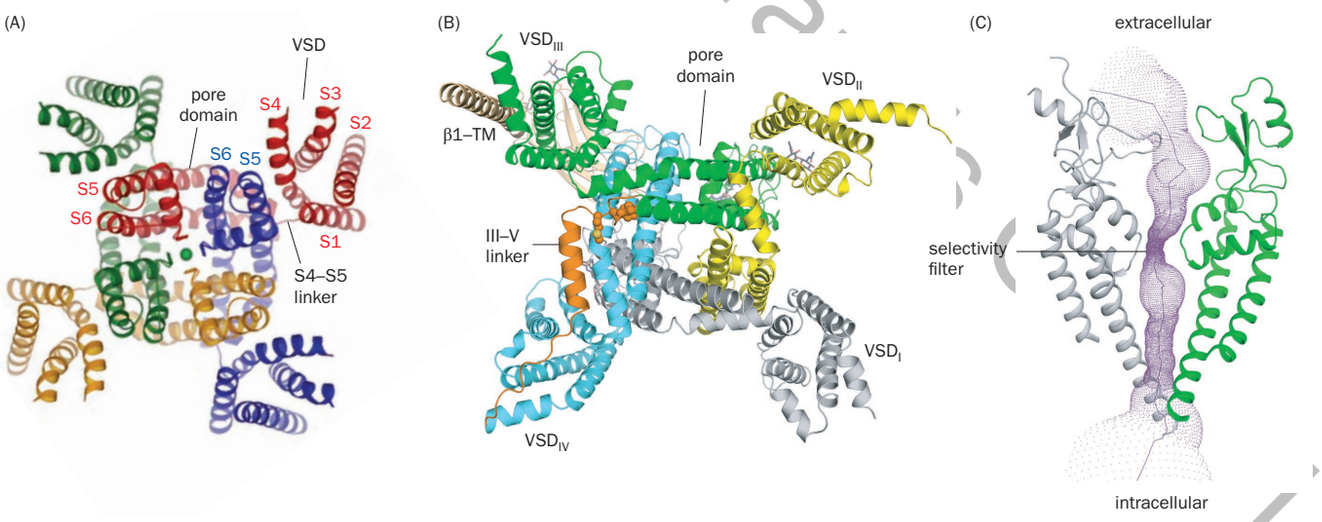

Figure 2-33 Structures of voltage-gated K^+ and Na^+ channels. **(A)** Organization of transmembrane segments of a rat voltage-gated K^+ channel determined by X-ray crystallography, viewed from the extracellular side. There is a fourfold symmetry reflecting the four identical subunits constituting the channel. Each subunit (with a unique color) has six transmembrane segments. The S1–S4 segments constitute the voltage-sensing domain (VSD), whereas the S5, pore loop, and S6 segments constitute the pore domain. These two domains are connected by the S4-S5 linker. Note that the VSD of one subunit latches onto the pore domain of an adjacent subunit—for example, S4 of the red subunit is closest to S5 of the blue subunit. **(B)** Structure of a human skeletal muscle-specific voltage-gated Na^+ channel in complex with the auxiliary subunit β1 determined by cryo-EM. The four repeating units from the N- to C-terminus are colored in gray, yellow, green, and cyan, respectively, with the transmembrane segment of β1 in gold and the linker between the third and fourth repeats in orange. The organization of transmembrane segments resembles that of the voltage-gated K^+ channel. **(C)** Side view of the same structure as in Panel B, showing only the pore segments (S5, pore loop, S6) of two repeating units. The asymmetrical permeation path is illustrated by purple dots. (A, from Long SB, Campbell EB, & MacKinnon R (2005) *Science* 309:903–908. With permission from AAAS. B & C, from Pan X, Li Z, Zhou Q, et al. (2018) *Science* 362:eaau2486. With permission from AAAS.)

changes of the pore domain, leading to the opening of the ion conduction pore. The close interactions between the voltage-sensing domains and the pore domains of different units contribute to the coordinated conformational changes of the pore domains in response to membrane potential changes.

Unlike the fourfold symmetry of the voltage-gated K^+ channels consisting of four identical subunits, the arrangement of the voltage-sensing domains and the ion permeation path in the voltage-gated Na^+ channel are asymmetric (Figure 2-33B, C), reflecting the fact that the channel is made of four homologous but nonidentical repeating units. Furthermore, while K^+ ions pass through the selectivity filter in dehydrated form in K^+ channels, in Na^+ channels (as well as structurally similar Ca^{2+} channels; Box 2-4), ions pass through the selectivity filter in hydrated form. Ion selectivity is determined by specific amino acid side chains in the selectivity filters of the Na^+ and Ca^{2+} channels in addition to the carbonyl groups of the backbone, rather than entirely by the latter as in K^+ channels.

Since the ionic basis of the action potential was discovered in the 1950s, researchers have come a long way in elucidating the mechanisms underlying this most fundamental form of neuronal communication.

Box 2-4: Diverse ion channels with diverse functions

The voltage-gated Na^+ and K^+ channels we discussed in the context of the action potential are just two of many kinds of ion channels. In the human genome, more than 230 genes encode ion channels (**Table 2-2**). Ion channels are usually classified by the ions they conduct and the mechanisms by which they are gated. Many ion channels share sequence similarities, reflecting their shared evolutionary history (see Section 13.6 for details). **Figure 2-34** depicts a phylogenetic tree for 143 structurally related ion channels in the same superfamily to which voltage-gated Na^+ and K^+ channels belong. All 143 channels share a common pore structure with two transmembrane helices (2TMs) and a pore loop. All except two subfamilies of K^+ channels use a 6TM-unit similar to voltage-gated Na^+ and K^+ channels (Figure 2-30).

Table 2-2: Number of genes encoding ion channels in the human genome

Channel type	Gene number	
K^+ channels		78
Voltage-gated K^+ channels	40	
Inward-rectifier K^+ channels	15	
Two-pore domain K^+ channels	15	
Ca^{2+}/Na^+-activated K^+ channels	8	
Na^+/Ca^{2+} channels		29
Voltage-gated Na^+ channels	9	
Voltage-gated Ca^{2+} channels	10	
Other Ca^{2+} and Na^+ channels	10	
TRP channels		28
Cyclic-nucleotide-gated and HCN channels		10
Cl^- channels		10+
Neurotransmitter-gated channels		70
Other ligand-gated channels		11
Piezos		2

Summarized from the Guide to Pharmacology database (www.guidetopharmacology.org). See Figure 2-34 for a phylogenetic tree of channels listed above the row of Cl^- channels. The human genome also encodes 11 channels that conduct water (aquaporins) and 24 channels that form gap junctions between adjacent cells (Box 3-5), which are not included here. Abbreviations: TRP, transient receptor potential; HCN, hyperpolarization-activated cyclic-nucleotide-gated.

K^+ channels make up the most diverse channel family and are encoded by at least 78 genes, many of which have alternatively spliced isoforms. The mix and match of different channel subunits to form heteromeric channels also contributes to channel diversity. K^+ channels play important roles in diverse functions of excitable cells, establishing properties such as the resting potential, the kinetics of repolarization after action potential initiation, and the spontaneous rhythmic firing of **pacemaker cells** (**Figure 2-35**A). Some K^+ channels are activated by depolarization, with diverse activation and inactivation kinetics adapted to neuron types with different firing frequencies. Some K^+ channels are activated by a rise in intracellular Ca^{2+} or a drop in ATP concentration, allowing cells to alter membrane potentials in response to changes in $[Ca^{2+}]_i$ or energy levels. Members of the **inward-rectifier K^+ channel** subfamily preferentially pass inward current at membrane potentials more hyperpolarized than E_K, and allow minimal outward current at membrane potentials more depolarized than E_K. This is because under depolarizing conditions, the inward-rectifier K^+ channels are blocked from the intracellular side by positively charged polyamines and Mg^{2+}. Among other functions, inward-rectifier K^+ channels help maintain the resting potential near E_K and are a major substrate for modulation by metabotropic neurotransmitter receptors (discussed in detail in Chapter 3). K^+ channels are also present in many nonexcitable cells. For example, K^+ channels are the predominant ion channels in glia.

Like K^+ channels, **Cl^- channels** generally stabilize the resting membrane potential, as E_K and E_{Cl} are both near the resting potential. Cl^- channels also play diverse roles in different cell types, often involving intracellular vesicles. Cl^-

(*Continued*)

Box 2-4: continued

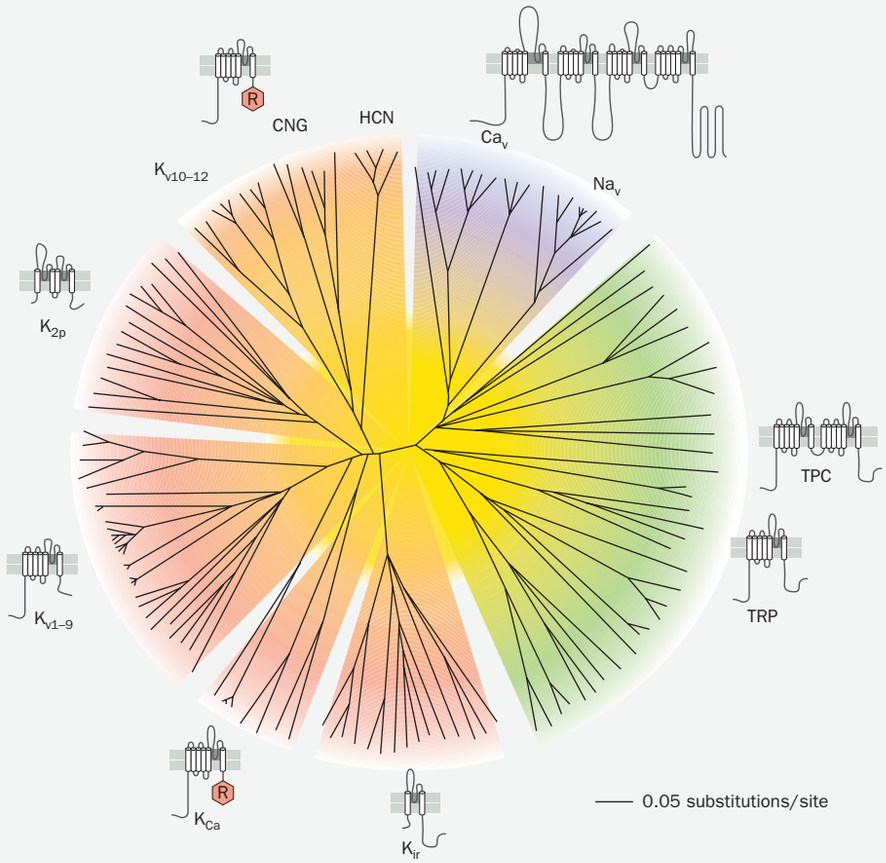

Figure 2-34 Phylogenetic tree of 143 ion channels. This tree is constructed according to similarities in the amino acid sequences of the conserved pore regions of 143 structurally related ion channels, which correspond to a subset of the ion channels listed in Table 2-2; channels that do not show sequence similarity to this superfamily, such as Cl^- channels and neurotransmitter-gated channels, are not included here. The scale bar represents a distance on the tree corresponding to 0.05 amino acid substitutions per site in the sequence. Background shades separate ion channels into families: blue, voltage-gated Na^+ (Na_v) and Ca^{2+} (Ca_v) channels; green, transient receptor potential (TRP) and related channels, including two-pore channels (TPC); red, most K^+ channels, including inward-rectifier K^+ channels (K_{ir}), Ca^{2+}-dependent K^+ channels (K_{Ca}), the first nine subfamilies of voltage-gated K^+ channels (K_{v1-9}), and two-pore domain K^+ channels (K_{2p}); orange, cyclic nucleotide-gated (CNG) channels, including the structurally related hyperpolarization-activated cyclic nucleotide-gated (HCN) channels and the last three subfamilies of voltage-gated K^+ channels (K_{v10-12}), which contain a cyclic-nucleotide-binding domain. The schematics surrounding the tree illustrate the membrane topologies of the channel proteins, with the pore loops shaded in dark gray. R within a red hexagon represents cytoplasmic domains that possess cyclic nucleotide- or Ca^{2+}-binding domains. (From Yu FH & Catterall WA [2004] *Science STKE* 253:re15. With permission from AAAS.)

channels consist of heterogeneous families of proteins with structures distinct from cation channels. One particular family consists of channels containing two subunits, each of which has 18 membrane-embedded helices and an ion conduction pore. In fact, these Cl^- channels are in the same family as bacterial Cl^-/H^+ exchangers, suggesting that ion channels and transporters can share structural similarities. New Cl^- channels are still being identified.

Voltage-gated Ca^{2+} channels constitute another important family of proteins in excitable cells. Their primary structure resembles those of voltage-gated Na^+ channels, with four repeating modules each containing six transmembrane helices. Different voltage-gated Ca^{2+} channels differ in their activation thresholds, single channel conductances, and inactivation speeds. Neurons usually maintain a very low intracellular Ca^{2+} concentration of ~0.1 μM, which is >10,000-fold lower than the extracellular Ca^{2+} concentration (~1.2 mM); this produces a very high E_{Ca} of approximately +120 mV. Opening of voltage-gated Ca^{2+} channels thus leads to depolarization due to Ca^{2+} influx driven by both chemical and electrical gradients. Indeed, action potentials in some neurons and cardiac myocytes are mediated by voltage-gated Ca^{2+} channels instead of voltage-gated Na^+ channels. As we will learn in later chapters, voltage-gated Ca^{2+} channels play important roles in regulating neurotransmitter release at axon terminals. They are also essential for excitation–contraction coupling of muscles, for dendritic integration in some mammalian neurons, for shaping spiking patterns such as rhythmic burst firing (Figure 2-35B), and for regulating gene expression and neuronal differentiation in response to neuronal activity. Other Ca^{2+} channels are present on the membrane of internal Ca^{2+} stores and are gated by intracellular messengers.

Box 2-4: continued

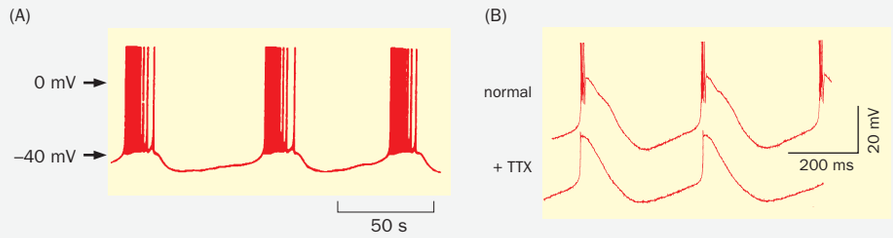

Figure 2-35 Ion channels that contribute to rhythmic burst firing of neurons. (A) Intracellular recording of a marine mollusk pacemaker cell (a neuron that can produce rhythmic output in the absence of input), showing periodic bursts of action potentials. Repeated action potentials result in a cumulative rise in intracellular [Ca^{2+}], which activates Ca^{2+}-dependent K^+ channels that contribute to the hyperpolarization after the burst. As $[Ca^{2+}]_i$ gradually decreases during the interburst intervals, more Ca^{2+}-dependent K^+ channels close, raising the membrane potential until it reaches the threshold for another burst of action potentials. **(B)** Intracellular recording from a cat thalamic neuron in slice in the absence (top) and presence (bottom) of TTX. TTX blocks the action potential firing but not the rhythmic membrane potential change, indicating that voltage-gated Na^+ channels do not contribute to the latter. Further analysis revealed that the rhythmic membrane potential change is mainly a result of interactions between low-threshold voltage-gated Ca^{2+} channels, voltage-gated K^+ channels, and HCN channels. Depolarization opens the Ca^{2+} channels and produces a Ca^{2+} spike. Inactivation of Ca^{2+} channels and opening of K^+ channels cause hyperpolarization, which then activates HCN channels. HCN channel opening causes depolarization until reaching the threshold of the Ca^{2+} channels for the next Ca^{2+} spike. Without TTX, Ca^{2+} spikes depolarize the neuron above the threshold of voltage-gated Na^+ channels, resulting in burst firing. (A, from Smith SJ & Thompson SH [1987] *J Physiol* 382:425–428. B, from McCormick DA & Huguenard JR [1992] *J Neurophysiol* 68:1384–1400.)

Whereas K^+, Cl^-, Na^+, and Ca^{2+} channels are so named because of their ion selectivity, some channels are not as selective for the ions they conduct. For example, most **TRP channels** (named after the founding member, transient receptor potential, a *Drosophila* protein essential for visual transduction) and **CNG channels** (for cyclic nucleotide-gated channels) are *nonselective cation channels*, which means that they are permeable to Na^+, K^+, and sometimes Ca^{2+}. Because the driving force for Na^+ is typically larger than that for K^+ at the resting state, opening of nonselective cation channels causes more Na^+ influx than K^+ efflux and therefore produces a net depolarization. As we will learn in Chapters 4 and 6, CNG channels and TRP channels play important roles in sensory neurons to convert environmental stimuli—including light, odorants, pheromones, temperature, and noxious chemicals—into membrane potential changes. TRP channels also contribute to mechanosensation in *Drosophila* and *C. elegans.* **HCN channels** (for hyperpolarization-activated cyclic nucleotide-gated channels) are activated by hyperpolarization (usually below –55 mV) and cyclic nucleotides and are structurally related to CNG channels. Because HCN channels conduct cations and thus depolarize cells in response to hyperpolarization, they are particularly important for rhythmic neuronal firing and heart beating (Figure 2-35B).

At least 70 genes in the human genome encode ion channels gated by neurotransmitters (Table 2-2); these channels belong to different gene families from those depicted in Figure 2-34. Many neurotransmitter-gated channels are nonselective cation channels and thus their opening depolarizes and causes excitation of postsynaptic neurons. Some neurotransmitter-gated channels are selective for Cl^-; their opening usually mediates inhibition of postsynaptic neurons. We will study the structure and function of these neurotransmitter-gated ion channels in greater detail in Chapter 3.

Since the sequencing of the human genome in early 2000s, we are still discovering new ion channels. For instance, as we will discuss in Chapter 6, ion channels gated by mechanical forces mediate hearing and touch sensation. In mammals, the molecular nature of mechanosensitive channels is still being intensely investigated, as they do not appear to belong to the ion channel families discussed here. For example, a subset of mechanosensitive channels that mediate touch belong to an evolutionarily conserved family of proteins called the **Piezos**, which contain >30 transmembrane segments per subunit with no sequence resemblance to other known ion channels. We expect further additions to the ion channel list (Table 2-2) in the future.

Finally, mutations in many human ion channels cause or increase susceptibility to a variety of nervous system disorders, including epilepsy (Box 12-4), schizophrenia, autism (Section 12.24), migraine, and abnormal pain sensitivity. More than 1000 pathogenic mutations have been identified in voltage-gated Na^+ channels alone. These findings highlight the importance of ion channels in human health.

SUMMARY

Neurons are extraordinarily large cells. They adopt specialized cell biological properties to support their dendrites and axons, whose surface areas and volumes often exceed those of their cell bodies by orders of magnitude. mRNAs, ribosomes, and secretory pathway components are present in dendrites (and axons to a limited extent) so that cytosolic and membrane proteins can be synthesized and

processed locally. Organelles and soma-synthesized proteins are actively transported to axons and dendrites by specific microtubule motors. Axonal microtubules are oriented uniformly with their plus ends facing outward. In vertebrate neurons, dendrites possess both plus-end-out and minus-end-out microtubules. The microtubule polarity difference in axons and dendrites is critical for directing specific cargos to appropriate subcellular compartments. Kinesins are mostly plus-end-directed microtubule motors and mediate axonal transport to deliver membrane proteins (via intracellular vesicles) and cytosolic proteins from the soma to axon terminals. Dynein and minus-end-directed kinesins mediate retrograde transport from axon terminals back to the soma. Kinesins and dynein also transport cargos within dendrites. Whereas microtubules run along the centers of dendritic and axonal processes, F-actin is enriched at the peripheries and can help cargos reach their final destination via myosin-based transport after they leave the microtubule highway.

Electrical signaling in excitable cells is enabled by the properties of the lipid bilayer and the activities of transporters and ion channels on the plasma membrane. Active transporters, such as the Na^+–K^+ ATPase, use energy to transport ions across the membrane against their electrochemical gradients; these transporters maintain ionic concentration differences across the plasma membrane. In most neurons and muscles, the intracellular compartment is high in K^+ but low in Na^+, Ca^{2+}, and Cl^- compared to the extracellular environment. Because the membrane at rest is more permeable to K^+ than to any other ions, the resting membrane potential is close to the K^+ equilibrium potential.

The neuronal plasma membrane can be effectively described as a parallel *R-C* circuit, with conductance paths for each ion representing ion flow through specific channels and a capacitance path representing the lipid bilayer. Electrical signals, such as the change in membrane potential in response to current injection, evolve over time. When electrical signals passively propagate along neuronal fibers, leaky membrane conductance along the way causes the signals to decay across distance. To propagate electrical signals reliably across a long distance, axons employ active properties such as the action potential.

Action potentials are produced by suprathreshold depolarization. Depolarization first opens voltage-gated Na^+ channels, leading to further depolarization and accounting for the rapid rising phase. The falling phase of action potentials is caused by inactivation of Na^+ channels and delayed opening of voltage-gated K^+ channels. This sequence ensures that action potentials are all or none, regenerative events that propagate unidirectionally along the axon from the cell body to the axon terminals. Studies utilizing important techniques developed in the past decades, such as patch clamp recording, molecular cloning, and atomic structural analysis, have revealed the molecular and mechanistic bases of how ion channels conduct ions with exquisite selectivity, how channel opening is controlled by voltage, how inactivation occurs, and how properties of individual ion channels account for macroscopic current in response to membrane potential changes.

Ion channels serve diverse functions. We will study these functions in greater detail in subsequent chapters, starting with the central subjects of the next chapter: neurotransmitter release at the presynaptic terminal and neurotransmitter reception at the postsynaptic specialization.

OPEN QUESTIONS

- How can we predict the neuronal compartment (axon, dendrite, soma) to which a protein is localized based on its amino acid and/or mRNA sequences?
- What mechanisms regulate the loading and unloading of cargo from molecular motors?
- What mechanisms control timing, extent, and neuronal type specificity of myelination of CNS axons?
- How would you discover previously unknown ion channels?

FURTHER READING

Books and reviews

Alberts B, Johnson A, Lewis J, Morgan D, Raff M, Roberts K, & Walter P (2015). Molecular Biology of the Cell, 6th ed. Garland Science.

Catterall WA, Wisedchaisri G, & Zheng N (2017). The chemical basis for electrical signaling. *Nat Chem Biol* 13:455–463.

Hille B (2001). Ion Channels of Excitable Membranes, 3rd ed. Sinauer.

Holt CE, Martin KC, & Schuman EM (2019). Local translation in neurons: visualization and function. *Nat Struct Mol Biol* 26:557–566.

Katz B (1966). Nerve, Muscle, and Synapse. McGraw-Hill.

Miller C (2006). CIC chloride channels viewed through a transporter lens. *Nature* 440:484–489.

Nirschl JJ, Ghiretti AE, & Holzbaur ELF (2017). The impact of cytoskeletal organization on the local regulation of neuronal transport. *Nat Rev Neurosci* 18:585–597.

Cell biological properties of neurons

Allen RD, Metuzals J, Tasaki I, Brady ST, & Gilbert SP (1982). Fast axonal transport in squid giant axon. *Science* 218:1127–1129.

Lasek R (1968). Axoplasmic transport in cat dorsal root ganglion cells: as studied with [3-H]-L-leucine. *Brain Res* 7:360–377.

Park HY, Lim H, Yoon YJ, Follenzi A, Nwokafor C, Lopez-Jones M, Meng X, & Singer RH (2014). Visualization of dynamics of single endogenous mRNA labeled in live mouse. *Science* 343:422–424.

Vale RD, Reese TS, & Sheetz MP (1985). Identification of a novel force-generating protein, kinesin, involved in microtubule-based motility. *Cell* 42:39–50.

Xu K, Zhong G, & Zhuang X (2013). Actin, spectrin, and associated proteins form a periodic cytoskeletal structure in axons. *Science* 339:452–456.

Electrical properties of neurons, action potentials, and ion channels

Armstrong CM & Bezanilla F (1977). Inactivation of the sodium channel. II. Gating current experiments. *J Gen Physiol* 70:567–590.

Doyle DA, Morais Cabral J, Pfuetzner RA, Kuo A, Gulbis JM, Cohen SL, Chait BT, & MacKinnon R (1998). The structure of the potassium channel: molecular basis of K+ conduction and selectivity. *Science* 280:69–77.

Hodgkin AL & Huxley AF (1952a). Currents carried by sodium and potassium ions through the membrane of the giant axon of Loligo. *J Physiol* 116:449–472.

Hodgkin AL & Huxley AF (1952b). A quantitative description of membrane current and its application to conduction and excitation in nerve. *J Physiol* 117:500–544.

Noda M, Shimizu S, Tanabe T, Takai T, Kayano T, Ikeda T, Takahashi H, Nakayama H, Kanaoka Y, Minamino N, et al. (1984). Primary structure of *Electrophorus electricus* sodium channel deduced from cDNA sequence. *Nature* 312:121-127.

Pan X, Li Z, Zhou Q, Shen H, Wu K, Huang X, Chen J, Zhang J, Zhu X, Lei J, et al. (2018). Structure of the human voltage-gated sodium channel Nav1.4 in complex with beta1. *Science* 362:eaau2486.

Schwarz TL, Tempel BL, Papazian DM, Jan YN & Jan LY (1988). Multiple potassium-channel components are produced by alternative splicing at the *Shaker* locus in *Drosophila*. *Nature* 331:137–142.

Sigworth FJ & Neher E (1980). Single Na^+ channel currents observed in cultured rat muscle cells. *Nature* 287:447–449.

Taveggia C, Zanazzi G, Petrylak A, Yano H, Rosenbluth J, Einheber S, Xu X, Esper RM, Loeb JA, Shrager P, et al. (2005). Neuregulin-1 type III determines the ensheathment fate of axons. *Neuron* 47:681–694.

Zagotta WN, Hoshi T & Aldrich RW (1990). Restoration of inactivation in mutants of Shaker potassium channels by a peptide derived from ShB. *Science* 250:568–571.

CHAPTER 3

Signaling across Synapses

Processes which go through the nervous system may change their character from digital to analog, and back to digital, etc., repeatedly.

John von Neumann (1958),
The Computer & the Brain

In this chapter, we continue to explore neuronal communication. We discuss first how arrival of an action potential at the presynaptic terminal triggers neurotransmitter release and then how neurotransmitters affect postsynaptic cells. This process, called **synaptic transmission**, results in information transmission from the presynaptic cell to the postsynaptic cell across the chemical synapse. In the context of studying postsynaptic reception, we will also introduce the fundamentals of signal transduction and study how synaptic inputs are integrated in postsynaptic neurons. Finally, we will discuss the electrical synapse, an alternative to the chemical synapse. Intercellular communication mediated by chemical and electrical synapses is the foundation of all nervous system functions.

HOW DOES NEUROTRANSMITTER RELEASE AT THE PRESYNAPTIC TERMINAL OCCUR?

In Chapter 2, we addressed the basic cell biological and electrical properties of neurons that are required to understand how molecules, organelles, and action potentials get to axon terminals. We now address the main purpose of these movements: to transmit information across synapses to postsynaptic targets, which can be other neurons or muscle cells. To illustrate general principles, we focus first on model synapses and neurotransmitter systems and then expand our discussion to other neurotransmitter systems.

3.1 Arrival of the action potential at the presynaptic terminal triggers neurotransmitter release

Neurotransmitters are molecules released by presynaptic neurons that diffuse across the synaptic cleft and act on postsynaptic target cells. The vertebrate **neuromuscular junction (NMJ)**, the synapse between the motor neuron axon terminals and skeletal muscle, is a model synapse that has been used to understand basic properties of synaptic transmission, many of which were later found to apply to other synapses. The neurotransmitter at the vertebrate NMJ was identified in the 1930s to be **acetylcholine** (**ACh**) (**Figure 3-1**A). An important advantage of studying the neuromuscular synapse is that the postsynaptic muscle cell (also called a muscle fiber) is a giant cell that can easily be impaled by a microelectrode for intracellular recording (see Section 14.21 for details); sensitive and quantitative measurement of synaptic transmission can be achieved by recording the resulting current or membrane potential changes in the muscle fiber. The NMJ is also an unusual synapse in that the motor axon spreads out to form many terminal branches that harbor hundreds of sites releasing ACh onto the target muscle. This property makes the NMJ a strong synapse that reliably converts action potentials in the motor neurons into muscle contraction (to be discussed in more detail in Section 8.1). In the experiments described in this chapter, researchers typically adjusted experimental conditions to prevent muscle contraction, so as to avoid recording artifacts induced by movement.

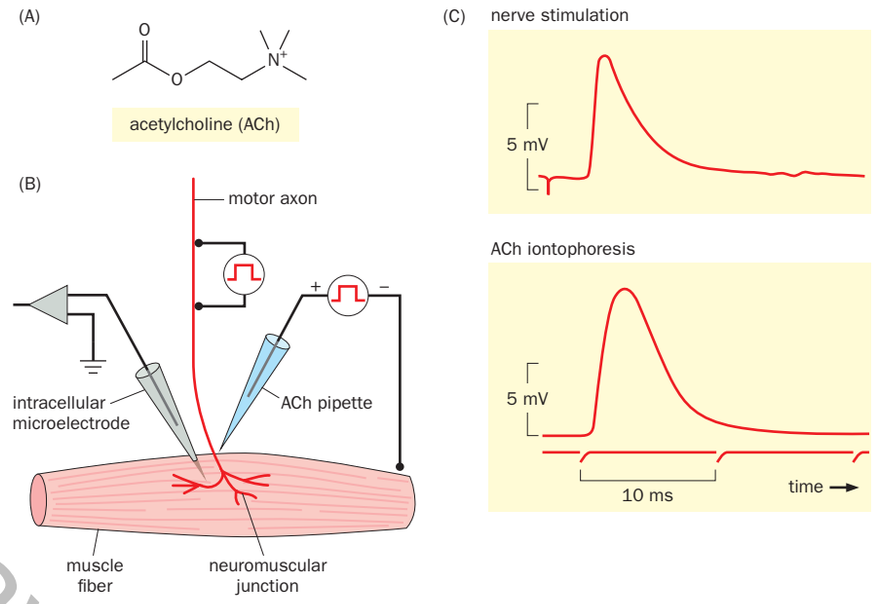

Figure 3-1 Studying synaptic transmission at the vertebrate neuromuscular junction (NMJ). **(A)** Structure of acetylcholine (ACh), the first identified neurotransmitter. **(B)** Measuring depolarization of a muscle fiber in response to motor axon stimulation or ACh iontophoresis in an NMJ *ex vivo*. The intracellular electrode is inserted into the muscle fiber close to the NMJ to record the end-plate potential (EPP). The square wave on the motor axon represents an application of current through a stimulating electrode that depolarizes the motor axon, causing it to fire an action potential. The square wave attached to the ACh pipette represents application of positive current that drives positively charged ACh out of the micropipette and onto the surface of the muscle close to the NMJ. **(C)** EPPs in the muscle fiber in response to motor axon stimulation (top) or focal ACh application (bottom) are similar in waveform. The first downward dip in the top trace indicates the time of axon stimulation. (C, adapted from Krnjevic K & Miledi R [1958] *Nature* 182:805–806. With permission from Springer Nature.)

In a typical setup for studying synaptic transmission across the NMJ, an *ex vivo* preparation containing the muscle and its attached motor nerve is bathed in a solution mimicking physiological conditions. The motor nerve is then stimulated with an electrode to produce an action potential, and the membrane potential of the muscle fiber is recorded with an intracellular electrode at the NMJ (Figure 3-1B). Motor nerve stimulation was found to induce a transient depolarization in the muscle fiber within a few milliseconds (Figure 3-1C, top panel). This transient depolarization is called an **end-plate potential**, or **EPP**, as the postsynaptic area of the muscle fiber is flattened like an end plate. We will study the postsynaptic mechanisms that produce the EPP in greater detail in the second part of this chapter. For now, we simply use the EPP as a readout as we investigate the mechanisms of neurotransmitter release.

How does motor nerve stimulation evoke an EPP? Researchers found that motor nerve stimulation can be mimicked by ACh application through a micropipette at the contact site between motor axon terminals and the muscle (Figure 3-1C, bottom panel). (This method is called **iontophoresis**; here, positively charged ACh is driven out of a micropipette by applying positive current.) Subsequent experiments revealed that application of the tetrodotoxin (TTX; Figure 2-29), which blocks voltage-gated Na^+ channels and thus prevents action potential propagation in motor axons, blocks the muscle EPP in response to motor nerve stimulation. However, ACh iontophoresis could evoke an EPP even when action potentials were blocked or when the motor axon was removed altogether. These results suggested that the ultimate effect of action potentials in the motor axon is to trigger ACh release at the axon terminals, and binding of ACh to the muscle membrane triggers depolarization of the muscle fiber in the form of an EPP.

We now know that fusion of synaptic vesicles with the presynaptic plasma membrane causes release of discrete packets of ACh molecules into the synaptic cleft. As we shall soon see, however, the release of neurotransmitters in discrete packets was deduced before the actual discovery of synaptic vesicles.

3.2 Neurotransmitters are released in discrete packets

In the early 1950s, Bernard Katz and colleagues applied intracellular recording techniques, then newly invented, to muscle cells to study the mechanisms of neuromuscular synaptic transmission. While studying muscle EPPs evoked by nerve stimulation in the frog NMJ, they observed that muscle fibers also exhibited small

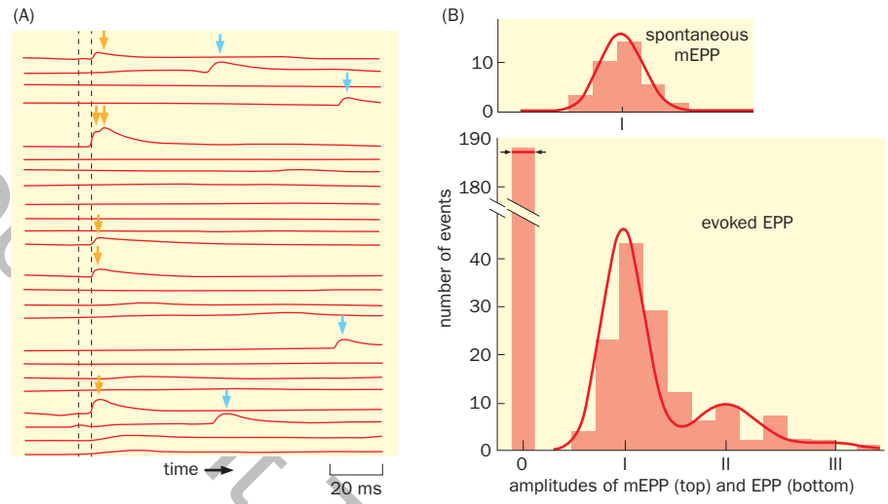

Figure 3-2 Miniature end-plate potentials (mEPPs) and a statistical test of quantal neurotransmitter release. (A) At low extracellular Ca^{2+} concentrations, nerve stimulation (at the time indicated by the first dashed vertical line) infrequently evokes EPPs, each of which follows the nerve stimulus with a specific latency (second dashed vertical line). In the 24 trials shown here (each represented by a horizontal trace), five EPPs (yellow arrows) were evoked. In one case the action potential evoked two quanta. Note also the presence of four depolarization events not linked with nerve stimulation (cyan arrows). **(B)** Using spontaneous mEPPs (top) as the unitary size, the frequency distribution of evoked EPPs (bottom) was predicted by a Poisson distribution (red line). This fits with the experimental data plotted as a histogram showing the number of EPPs (*y* axis) whose amplitudes fell within a certain bin (*x* axis). Note that the mEPP amplitude (top) varies; the sizes of individual neurotransmitter packets are not exactly the same. The evoked EPP amplitude (bottom) is 1×, 2×, or 3× the average mEPP amplitude. The frequency of synaptic failure (trials with an EPP amplitude of 0) also matches well the prediction from the Poisson distribution (red line flanked by two arrows). (Adapted from Del Castillo J & Katz B [1954] *J Physiol* 124:560–573.)

EPPs in the *absence* of any nerve stimulation; these were termed **miniature end-plate potentials**, or **mEPPs**. mEPPs had an intriguing property: for a given neuromuscular preparation, they seemed to have a defined unitary size. The amplitude of mEPPs, hypothesized to be due to spontaneous release of ACh from motor axon terminals, was usually two orders of magnitude lower than EPPs evoked by nerve stimulation. To understand if mEPPs and EPPs are related to each other, Katz and colleagues lowered the concentration of extracellular Ca^{2+}, a condition known then to diminish neurotransmitter release. They reached a condition in which most nerve stimulations did not evoke any EPPs. When stimuli did trigger EPPs under these conditions, the amplitude of those evoked EPPs were usually the same size as mEPPs, and occasionally two or three times the unit size (**Figure 3-2**A). Further reduction of the Ca^{2+} concentration reduced the *frequency* of observing any evoked EPP, but it did not further diminish the EPP *amplitude*. These observations suggested that mEPPs reflected the basic unit of synaptic transmission. EPPs evoked by nerve stimulation under normal conditions were caused by the simultaneous occurrence of hundreds of mEPPs. These results led to the **quantal hypothesis of neurotransmitter release**, which posited that neurotransmitters are released in discrete packets (quanta) of relatively uniform size.

To further test the quantal hypothesis, Katz and his colleagues used statistical methods (see **Box 3-1** for details) to predict the frequencies of releasing no quanta, a single quantum, or multiple quanta in response to nerve stimulation. If the larger evoked potentials are caused by release of multiple quanta, they should occur at frequencies related to the frequency of release of a single quantum. When Ca^{2+} concentration is low and the release probability is small, the frequency (f) that k quanta are released during each nerve stimulation follows the **Poisson distribution**:

$$f = \frac{m^k}{k!} e^{-m}$$

where m is the mean number of units (quanta) that respond to an individual stimulus. Since mEPPs following each spontaneous release correspond to one unit, m can be experimentally determined as the mean EPP amplitude divided by the mean mEPP amplitude. Indeed, the frequency distributions of EPPs calculated earlier and those observed experimentally were an excellent fit: the frequency of **synaptic failures**, cases when nerve stimulation did not cause an EPP, matched precisely with the statistical prediction; there was a prominent peak at around the size of the unitary mEPP and a small peak at twice the mEPP amplitude (Figure 3-2B). Thus, this statistical analysis provided strong support for the notion that neurotransmitters are released in discrete packets.

Box 3-1: Binomial distribution, Poisson distribution, and neurotransmitter release probability

The Poisson distribution and the related **binomial distribution** are both probability distributions describing the frequency of discrete events that occur independently. Let's start our discussion with the binomial distribution. Imagine that we are tossing a coin and that the probability that the coin lands with heads facing up is p. A coin toss is an example of a Bernoulli trial (binomial trial), a trial with exactly two outcomes. The binomial distribution describes the frequency (f) in which k events occur after n trials (that is, k times heads facing up after n coin tosses):

$$f(k; n, p) = \frac{n!}{k!(n-k)!} p^k (1-p)^{n-k}$$

where $k = 0, 1, 2, \ldots n$, ! is factorial (for example, $4! = 4 \times 3 \times 2 \times 1 = 24$), and $n!/k!(n-k)!$ is the binomial coefficient. Suppose you want to know the likelihood of tossing a coin four times and having the heads face up only once. The probability for heads, p, is 0.5 for any given toss of a fair coin. According to the formula, the binomial coefficient for $k = 0, 1, 2, 3, 4$ is respectively 1, 4, 6, 4, 1 (note that $0! = 1$), and the frequency of occurrence (f) for the five k values are calculated to be 0.0625, 0.25, 0.375, 0.25, 0.0625, respectively. In other words, out of four coin tosses, the probability that heads faces up only once (or three times) is 25%; the probability that heads faces up twice is 37.5%, and the probability that heads faces up four times (or never) is 6.25%.

If neurotransmitter release occurs in discrete quanta and if the release of each quantum occurs at a probability of p and if each quantum is independent of the other quanta, then we can think of each spike as initiating a set of simultaneous Bernoulli trials (equal to the number of quanta available for release), and we can calculate the frequency that k quanta out of the total n quanta are released using the binomial formula. However, researchers did not know the actual values for n (how many quanta are available to be released) or for p (how likely is any individual quantum to be released), so it was not possible to apply a binomial distribution. Fortunately, according to probability theory, when n is large (>20) and p is small (<0.05), the binomial distribution can be approximated by the Poisson distribution, in which the frequency (f) that k events occur can be determined by a single parameter λ (which equals the product of n and p in the binomial distribution) according to the following formula:

$$f(k; \lambda) = \frac{\lambda^k}{k!} e^{-\lambda}$$

One can experimentally estimate λ (same as m in Section 3.2) because, as the product of n and p, it equals the mean number of quanta that are released in response to a stimulus and thus is equivalent to the ratio of the mean EPP amplitude and the mEPP amplitude (assumed to be the quantal unit). Thus, researchers can calculate the probability of release in response to nerve stimulation—estimating the likelihood that no release occurs ($k = 0$), that a single quantum is released ($k = 1$), that two quanta are released ($k = 2$), and so on—and can then compare these calculations with the actual experimental data, as shown in Figure 3-2B.

Note that to apply the Poisson distribution, the release probability (p) must be small and the number of available quanta (n) must be large so that p does not change during the measurement of λ. Researchers cannot control n, but it turns out that n is very large in the vertebrate NMJ, because there are typically hundreds of neurotransmitter release sites between a motor axon and its muscle target. Researchers can experimentally reduce p by studying neurotransmitter release in low-Ca^{2+} extracellular solutions. Synaptic transmission at the NMJ also follows closely other assumptions required for the Poisson distribution: independent release of each quantum (because of the large number of release sites), the uniformity of the population (p is the same for all quanta), and the relative uniformity of their size (each vesicle contains a similar amount of neurotransmitter molecules). In many CNS synapses these assumptions either fail (for example, n is often too small) or cannot be tested adequately. Thus, the probability of neurotransmitter release in CNS synapses may not follow the Poisson distribution. Interestingly, recent studies suggest that release probability at some CNS synapses containing a single presynaptic active zone can be fit by binomial distribution with n ranging between 1 and 10, likely representing the number of docking sites for readily releasable synaptic vesicles.

3.3 Neurotransmitters are released when synaptic vesicles fuse with the presynaptic plasma membrane

Physiological and anatomical studies often complement each other in driving neuroscience discoveries. A strong candidate for the physical substrate of quantal neurotransmitter release became evident when electron microscopy (EM) was first applied to the nervous system in the mid-1950s. Thin sections across the nerve terminals revealed that they contain abundant vesicles that are ~40 nm in diameter. At the NMJ, many such vesicles appear stacked near the presynaptic membrane juxtaposed to the muscle membrane (**Figure 3-3**A). These **synaptic vesicles** were immediately hypothesized to be vesicles filled with neurotransmitters. The relatively uniform size of synaptic vesicles could explain why neurotransmitters are released in packets with a uniform quantal size. (The quantal size at the frog NMJ has been estimated to be about 7000 ACh molecules.) The unitary release of neurotransmitters occurs when a single synaptic vesicle fuses with the plasma

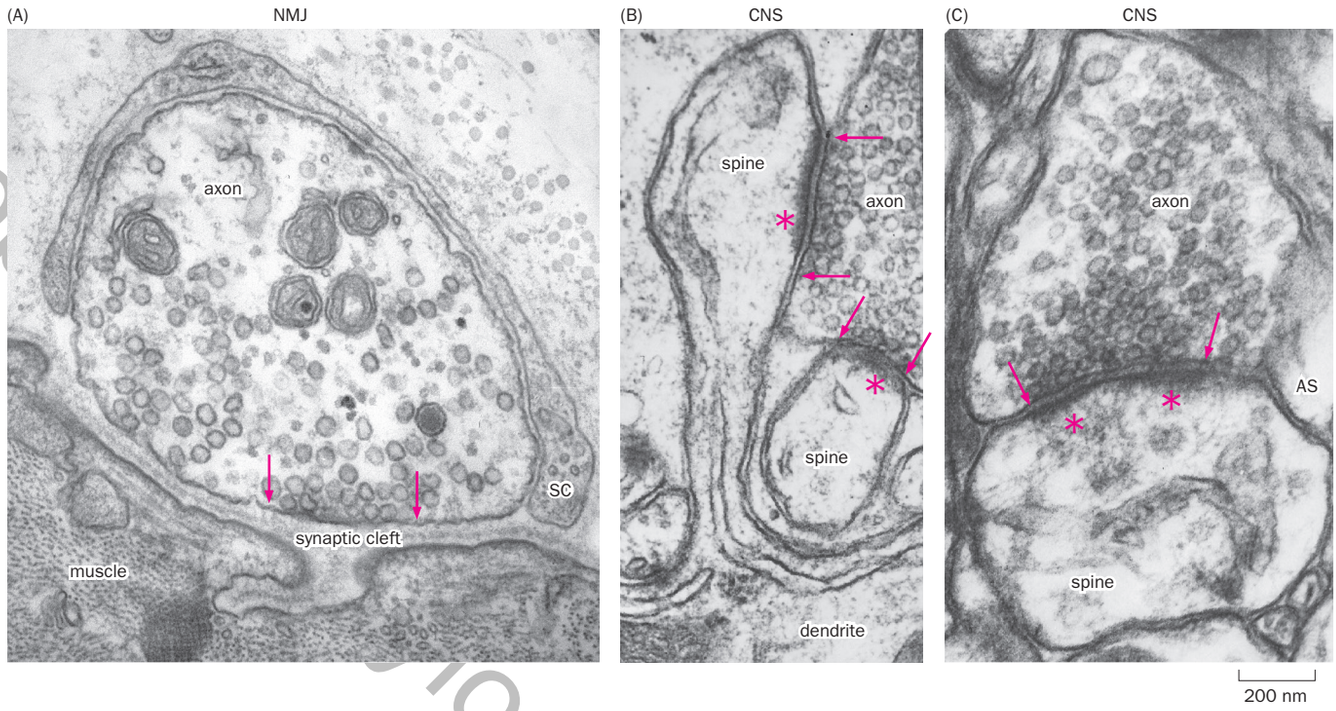

Figure 3-3 Structures of synapses revealed by electron microscopy. Pairs of arrows define the extents of active zones in the presynaptic terminals. Asterisks indicate postsynaptic densities. Note the abundance of ~40 nm diameter synaptic vesicles in each presynaptic terminal; some of these vesicles are docked at the active zone, ready for release. **(A)** A frog NMJ. The synaptic cleft is considerably wider than at the CNS synapses shown in the other two panels. SC indicates a Schwann cell process that wraps around the motor axon terminal. A typical motor axon forms hundreds of such presynaptic terminals onto a muscle fiber. **(B)** Two synapses formed between a single axon and two dendritic spines in rat cerebellar cortex. **(C)** A synapse from human cerebral cortex. AS indicates an astrocyte process wrapped around many CNS synapses. All images share the scale bar. (A, courtesy of Jack McMahan. B & C, courtesy of Josef Spacek and Kristen M. Harris, SynapseWeb.)

membrane, dumping its neurotransmitter content into the synaptic cleft and producing a miniature depolarization in the muscle cell. Nerve stimulation under normal conditions (ordinary external Ca^{2+} rather than low Ca^{2+}) causes hundreds of these vesicle fusion events at a given NMJ, thereby producing EPPs two orders of magnitude larger than mEPPs. Thus, the NMJ has a high **quantal content** (releasing transmitters from several hundred synaptic vesicles per action potential). By contrast, many synapses in the CNS have much lower quantal contents (releasing transmitters from only one or a few synaptic vesicles per action potential).

The basic structural elements of chemical synapses are highly similar across the entire nervous system and in different animal species (Figure 3-3). In all cases presynaptic terminals have clusters of synaptic vesicles "docked" at the presynaptic membrane ready for release at the **active zone**. Across the synaptic cleft from the active zone and at the postsynaptic membrane is an electron-dense structure called **postsynaptic density**. We will study the molecular composition of the active zone and the postsynaptic density later in this chapter.

Although EM studies revealed many vesicles in presynaptic terminals, observing a fusion event in response to stimulation was necessary to confirm the hypothesis that neurotransmitter release is due to fusion of synaptic vesicles and the presynaptic plasma membrane. These events occur very transiently and are thus difficult to detect in typical electron microscopic preparations. To visualize fusion events, researchers stimulated a neuromuscular preparation while the entire sample was falling toward a copper block cooled to 4 Kelvin that froze the tissue immediately upon contact. Fusion events between synaptic vesicles and the presynaptic plasma membrane were indeed caught in action (**Figure 3-4**). Such studies provided definitive evidence that synaptic vesicle fusion with the presynaptic plasma membrane causes neurotransmitter release.

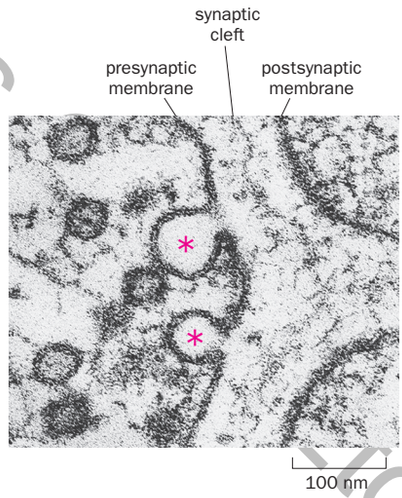

Figure 3-4 Synaptic vesicle fusion caught in action. This electron micrograph was taken from a frog NMJ preserved 3–5 ms after nerve stimulation, revealing the fusion of two synaptic vesicles (asterisks) with the presynaptic plasma membrane. (Courtesy of John Heuser. See also Heuser JE & Reese TS [1981] *J Cell Biol* 88:564–580.)

3.4 Neurotransmitter release is controlled by Ca^{2+} entry into the presynaptic terminal

How does action potential arrival cause synaptic vesicle fusion in the presynaptic terminal? As noted in Section 3.2, external Ca^{2+} facilitates action potential–triggered neurotransmitter release: bathing NMJ preparations in solutions with progressively lower concentrations of Ca^{2+} rendered the stimulation of motor axons increasingly ineffective at generating EPPs in muscle cells. Supplying Ca^{2+} locally at the NMJ in preparations with very low extracellular Ca^{2+} through iontophoresis (Figure 3-1) provided a means to determine when Ca^{2+} is required during action potential–induced synaptic transmission. A brief application of Ca^{2+} enabled neurotransmitter release if it occurred immediately before the depolarization pulse, but not if it occurred after the depolarization pulse. Thus, extracellular Ca^{2+} is required during the brief period when depolarization occurs and preceding transmitter release itself.

How does external Ca^{2+} contribute to neurotransmitter release? Key insights were obtained from studies of the squid giant synapse, whose presynaptic as well as postsynaptic terminals are so large that researchers can insert electrodes into both compartments for intracellular recordings. (One of the postsynaptic target cells is the neuron that extends the giant axon featured in Chapter 2.) It was found that action potentials could be replaced by depolarization, which opens voltage-gated Ca^{2+} channels (Box 2-4) in the presynaptic plasma membrane, causing an inward flux of Ca^{2+} that triggers neurotransmitter release.

Let's study in detail one specific experiment (**Figure 3-5**), which showcased the Ca^{2+} dependence of neurotransmitter release and provided information about the timing of different steps of the process. In this experiment, the voltage clamp technique was applied to both the presynaptic terminal and postsynaptic target of the squid giant synapse in the presence of Na^+ and K^+ channel blockers, such that the only cation that could cross the presynaptic membrane was Ca^{2+}. From a resting potential at –70 mV, a depolarizing voltage step to –25 mV applied to the presynaptic terminal (Figure 3-5A, top) triggered Ca^{2+} influx, as measured by presynaptic current (Figure 3-5A, middle). This resulted in synaptic transmission, as measured by an inward postsynaptic current (Figure 3-5A, bottom; we will study the nature of such postsynaptic currents in later sections).

However, a voltage step to +50 mV applied to the presynaptic terminal did not trigger presynaptic Ca^{2+} influx or postsynaptic currents (Figure 3-5B, left portion). At this potential, voltage-gated Ca^{2+} channels are open, but because +50 mV is close to the equilibrium potential of Ca^{2+} in the presynaptic terminal under the experimental conditions used, there was little driving force for Ca^{2+} influx (Section 2.5). Nonetheless, returning the presynaptic membrane potential from +50 mV

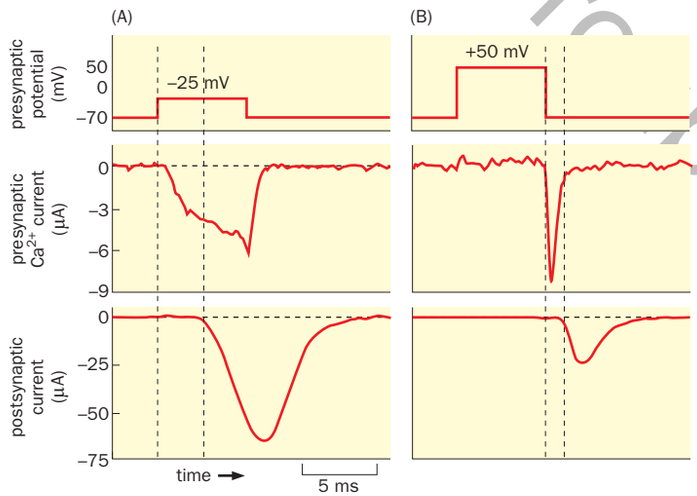

Figure 3-5 Voltage clamp studies of Ca^{2+} entry into the presynaptic terminal of the squid giant synapse. Voltage steps were applied to the presynaptic terminal (top traces) using the voltage clamp technique (Figure 2-21). The current injected into the presynaptic terminal to maintain the clamped voltage is equivalent to the Ca^{2+} current across the presynaptic membrane (middle traces), as Na^+ and K^+ channel blockers were applied in these experiments. Postsynaptic current was simultaneously recorded in a voltage clamp setting as an assay for neurotransmitter release (bottom traces). **(A)** A depolarizing step in the presynaptic terminal triggered the opening of voltage-gated Ca^{2+} channels, which caused Ca^{2+} influx and a subsequent postsynaptic response. **(B)** A larger depolarization step of the presynaptic membrane potential (bringing the membrane close to the Ca^{2+} equilibrium potential) prevented Ca^{2+} entry due to lack of a driving force; no postsynaptic response occurs. A tail current representing Ca^{2+} influx was produced when the presynaptic membrane potential returned to –70 mV, which triggered a postsynaptic response. The pairs of dashed lines represent the presynaptic voltage step (left) and the onset of the postsynaptic response (right). The delay in Panel B includes the time between Ca^{2+} entry and the postsynaptic response. In Panel A, the interval is lengthened by the time required to open Ca^{2+} channels. (Adapted from Augustine GJ, Charlton MP, & Smith SJ [1985] *J Physiol* 367:163–181. See also Llinás RR [1982] *Sci Am* 247(4):56–65.)

to –70 mV produced a presynaptic "tail current" (Figure 3-5B, middle). This is because the membrane potential change was faster than the closure of voltage-gated Ca^{2+} channels; thus there was a transient period with a strong driving force for Ca^{2+} influx while Ca^{2+} channels remained open. Ca^{2+} influx produced a corresponding postsynaptic current response (Figure 3-5B, bottom). Interestingly, the Ca^{2+} tail current after presynaptic depolarization to +50 mV triggered a postsynaptic response more rapidly than did the presynaptic depolarization to –25 mV (compare the time interval between the two dashed lines in the two panels). This suggests that the normal synaptic delay between presynaptic depolarization and postsynaptic response in Panel A consists of two components: a delay due to the time it takes to open voltage-gated Ca^{2+} channels (which was bypassed in the tail current condition, as the channels were already open) and a delay between Ca^{2+} entry and the neurotransmitter-triggered postsynaptic response.

The hypothesis that Ca^{2+} entry triggers neurotransmitter release was further validated by other techniques. In one type of experiment, a chemical dye used to indicate changes in Ca^{2+} concentration (see Section 14.22 for more details) was injected into the presynaptic terminal of the squid giant synapse. Nerve stimulation was found to increase the intracellular Ca^{2+} concentration at the presynaptic terminal (**Figure 3-6**). The Ca^{2+} concentration was highest in specific regions of the presynaptic terminal. As will be discussed in Section 3.7, this is because voltage-gated Ca^{2+} channels are highly concentrated at the active zone, where synaptic vesicles dock and fuse with presynaptic membrane. Another type of experiment featured chemical compounds that "cage" Ca^{2+}, preventing it from interacting with Ca^{2+}-binding proteins, and can be triggered by light to release Ca^{2+}. When caged Ca^{2+} was introduced into the presynaptic terminal of the squid giant axon, light could trigger neurotransmitter release in the absence of action potentials or Ca^{2+} entry from the extracellular solution. This experiment demonstrated that vesicle fusion and neurotransmitter release do not require depolarization or Ca^{2+} entry from the extracellular solution; rather, they are caused by an instantaneous increase in Ca^{2+} concentration in the presynaptic terminal.

Together, these experiments firmly established a sequence of events from action potential to neurotransmitter release:

> *Action potential from the axon → Depolarization of the presynaptic terminal → Opening of voltage-gated Ca^{2+} channels → Ca^{2+} entry into the presynaptic terminal → Fusion of synaptic vesicles with presynaptic plasma membrane → Neurotransmitter release*

This sequence of events, originally worked out in the frog NMJ and the squid giant synapse, has been found to apply to all chemical synapses across the animal kingdom, regardless of the type of synapse and neurotransmitter used.

The short latency between Ca^{2+} entry into the presynaptic terminal and postsynaptic events (~2 ms in Figure 3-5B, and often shorter) indicates that there must be a pool of synaptic vesicles that are ready to fuse with the presynaptic plasma membrane immediately upon a rise in intracellular Ca^{2+} concentration. This is consistent with observations in electron microscopy (Figure 3-3). Furthermore, membrane fusion is energetically unfavorable, as breaking two membranes and resealing them necessitates exposing hydrophobic surfaces to water and thus requires external energy such as ATP hydrolysis. However, the final step of synaptic vesicle fusion is so fast that it is unlikely to involve an ATP hydrolysis-dependent catalytic process. Instead, as we will soon learn, synaptic vesicles are primed for fusion by a specialized protein complex already existing in a high-energy configuration, simply waiting for Ca^{2+} to trigger the sudden conformational change that permits fusion.

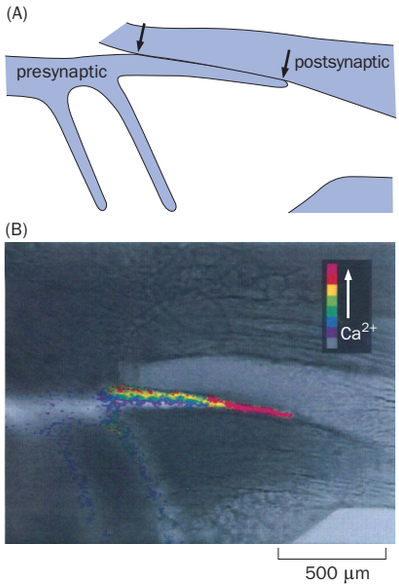

Figure 3-6 Nerve stimulation triggers Ca^{2+} entry into the presynaptic terminal of the squid giant synapse. (A) Schematic of the squid giant synapse image in Panel B. The presynaptic terminals resemble finger-like extensions that contact postsynaptic neurons (one of which is shown). The two arrows indicate the extent of synaptic contact between the two neurons. **(B)** A brief train of presynaptic action potentials caused the Ca^{2+} concentration to increase in the presynaptic terminal, as reported by fluorescence changes of microinjected fura-2, a Ca^{2+} indicator (see Section 14.22 for details). The Ca^{2+} increase is seen as a shift from cool colors to warm ones. (From Smith SJ, Buchanan J, Osses LR, et al. [1993] *J Physiol* 472:573–593. With permission from the Physiological Society.)

3.5 SNARE proteins mediate synaptic vesicle fusion

We now turn to the molecular mechanisms mediating the fusion of synaptic vesicles with the presynaptic plasma membrane (a process also called neurotransmitter

exocytosis). Our current understanding of these mechanisms comes from a convergence of multiple experimental approaches:

- *Biochemical purification* to identify presynaptic protein components. Because of the uniform size and buoyancy of synaptic vesicles and their abundance, researchers can purify them to a high degree, which permits the identification of their key components. Indeed, the synaptic vesicle is one of the best-characterized organelles in the cell, with quantitative information about its protein and lipid composition (**Figure 3-7**; **Movie 3-1**). We will study key synaptic vesicle proteins in this and subsequent sections.
- *Genetic studies in yeast* that identified genes required for membrane fusion in the secretion pathway (Figure 2-2).
- *Biochemical reconstitution* of mammalian vesicle fusion reactions *in vitro*, which identified the minimal components sufficient for membrane fusion. Strikingly, these and yeast genetic studies identified a common set of evolutionarily conserved proteins (which we will soon discuss) and demonstrated that neurotransmitter exocytosis is a specialized form of membrane fusion that occurs in all eukaryotic cells and in many parts of the cell (Figure 2-2; see also Figure 13-13).
- *Genetic tests for the necessity* of these evolutionarily conserved proteins in synaptic transmission in *C. elegans, Drosophila,* and mice *in vivo*.
- *Studies of toxins* that block specific steps of neurotransmitter release and identification of their protein targets.

Together, these approaches have given rise to our current understanding of the neurotransmitter release mechanisms summarized in the following.

At the core of vesicle fusion are three **SNARE** proteins and **SM proteins**. (We will introduce the origin of the SNARE acronym later. SM stands for Sec1/Munc18-like proteins—Sec1 was originally identified in yeast for its requirement in secretion; Munc18 is the mammalian homolog of Unc18, originally identified in *C. elegans* as mutants that exhibit an uncoordinated phenotype). The first SNARE is a transmembrane protein on the synaptic vesicle called **synaptobrevin** (also called VAMP for vesicle-associated membrane protein), which is the most abundant synaptic vesicle protein. Since synaptobrevin is associated with the synaptic vesicle, it is designated as a **v-SNARE**. The second SNARE is a transmembrane protein on the plasma membrane called **syntaxin**. Owing to its location on the target membrane for vesicle fusion, syntaxin is called a **t-SNARE**. The third SNARE, named **SNAP-25** (synaptosomal-associated protein with a molecular weight of 25 kDa), is a t-SNARE anchored to the cytoplasmic face of the plasma membrane via a lipid modification. Once the synaptic vesicle is in the vicinity of the presynaptic plasma membrane, the cytoplasmic domains of synaptobrevin, syntaxin, and SNAP-25 assemble into a very tight complex. Current data indicate that the assembly of the SNARE complex proceeds from binding of v- and t-SNAREs from the ends farthest from the membrane to the ends closest to the membrane, like a zipper that zips up. The force generated by the assembly of the SNARE complex pulls the synaptic vesicle membrane even closer to the plasma membrane, leading the lipid bilayers to fuse, such that the contents of the synaptic vesicle are exposed to the extracellular space (**Figure 3-8**A; **Movie 3-2**).

The structure of the SNARE complex has been determined at atomic resolution by X-ray crystallography. Three SNARE proteins form a four-helix bundle, with synaptobrevin and syntaxin each contributing one helix and SNAP-25 contributing two helices (Figure 3-8B). Many naturally occurring protease toxins that inhibit neuronal communication target these three SNARE proteins at specific amino acid residues (**Box 3-2**). Proteolytic cleavage by these proteases is predicted to inhibit the attachment of the four-helix bundle to the membrane, thereby blocking neurotransmitter release.

The SNARE-based mechanism of membrane fusion applies to many fusion reactions in intracellular vesicle trafficking. The v- and t-SNAREs for other specific fusion events (for example, fusion of ER-derived vesicles with the Golgi mem-

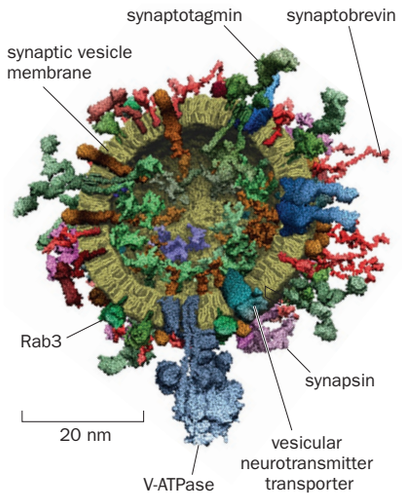

Figure 3-7 The molecular anatomy of a synaptic vesicle. This model is based on quantitative determination of the protein components associated with synaptic vesicles. Each colored structure in this cross section of the synaptic vesicle represents a synaptic vesicle protein. The synaptic vesicle membrane and six synaptic vesicle proteins whose functions are discussed in this and subsequent sections are indicated (see also Table 3-1). (Adapted from Takamori S, Holt M, Stenius K, et al. [2006] *Cell* 127:831–846. With permission from Elsevier Inc.)

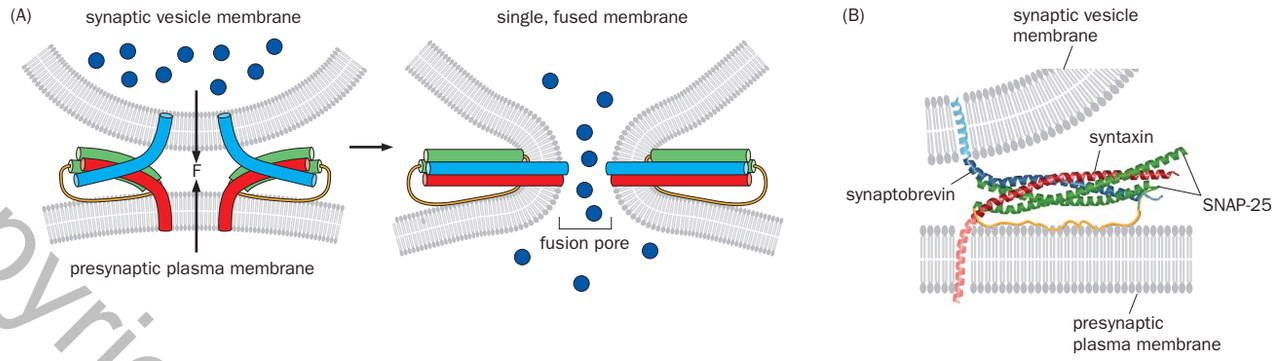

Figure 3-8 Model and structural basis of synaptic vesicle fusion. **(A)** Schematic models of SNARE complexes before and after membrane fusion. Before fusion (left), the vesicular and target SNAREs are on separate membranes (the synaptic vesicle membrane and the presynaptic plasma membrane, respectively). The strong binding of their cytoplasmic domains, in a zipper-like fashion starting from the two sides and progressing toward the center, produces a force (F) that brings the vesicle and target membranes together, causing them to fuse (right). Colored rods represent helices from the SNARE proteins detailed in Panel B. **(B)** Structure of the SNARE complex for synaptic vesicle fusion determined by X-ray crystallography. Blue, red, and green represent α helices from the cytoplasmic domains of synaptobrevin, syntaxin, and SNAP-25, respectively. Faded blue and red represent transmembrane domains of synaptobrevin and syntaxin, respectively, which were not part of the solved crystal structure. The orange strand links the two SNAP-25 helices and is attached to the presynaptic plasma membrane through a lipid modification, which was also not part of the crystal structure. (A, adapted from Südhof TC & Rothman JE [2009] *Science* 323:474–477. B, from Sutton, RB, Fasshauer D, Jahn R, et al. [1998] *Nature* 395:347–353. With permission from Springer Nature.)

brane; Figure 2-2) resemble the v- and t-SNAREs for synaptic vesicle exocytosis. These findings suggest that the mechanism of synaptic vesicle exocytosis was co-opted from general vesicle trafficking (see Section 13.9 for more discussions).

In all of these reactions, including synaptic vesicle fusion, however, SNARE proteins were found to be insufficient to mediate fusion. A partner for SNARE proteins in all fusion reactions is an SM protein called Munc18 in mammals. Munc18

Box 3-2: From toxins to medicines

Research in neurobiology has greatly benefited from naturally occurring toxins that have evolved to block specific steps of neuronal communication. These toxins are produced by organisms from a wide range of phylogenetic groups, including bacteria, protists, plants, fungi, and animals. Despite the energetic costs of producing toxins, they offer adaptive advantages such as deterring herbivores, fending off predators, and immobilizing prey. Scientists have used these toxins to study the biological functions and mechanisms of action of their target proteins. Some of these toxins have even been developed into medicines.

Virtually all steps of neuronal communication are targets for toxins. Action potentials are potently blocked by tetrodotoxin (Figure 2-29), an inhibitor of voltage-gated Na^+ channels produced by symbiotic bacteria in puffer fish, rough-skinned newts, and certain octopi. The presynaptic voltage-gated Ca^{2+} channels essential for neurotransmitter release are specifically blocked by a small peptide, ω-conotoxin, from marine snails. Synaptic vesicle fusion is blocked by a number of proteases produced by the bacteria *Clostridium tetani* and *Clostridium botulinum.* **Tetanus** and **botulinum toxins** specifically cleave SNARE proteins, with each toxin cleaving a specific SNARE at a specific amino acid residue, thereby preventing synaptic vesicle fusion with presynaptic membrane (Figure 3-8). Indeed, identification of the protein targets of tetanus and botulinum toxins was instrumental in establishing that SNARE proteins play a central role in synaptic vesicle fusion. Toxins that target neurotransmitter receptors will be discussed later in this chapter. For instance, **curare**, a plant toxin used by Native Americans on poisonous arrows, and **α-bungarotoxin** and cobratoxin from snakes are all potent competitive inhibitors of acetylcholine receptors at the vertebrate NMJ and thereby block motor neuron–triggered muscle contraction. **Picrotoxin**, another plant toxin, is a potent blocker of the $GABA_A$ receptors that mediate fast inhibition in vertebrates and invertebrates alike. **Muscimol**, produced by toxic mushrooms, is a potent activator of these $GABA_A$ receptors. The venoms of predators such as snakes, scorpions, cone snails, and spiders have been a rich source of tools for investigating neuronal communication. The fact that most toxins affect many different animal species also indicates that the molecular machinery of neuronal communication is highly conserved across the animal kingdom.

Natural toxins and their derivatives have also been used extensively in medicine. Channel blockers are used to treat epilepsy and intractable pain. Synaptic transmission blockers are used as muscle relaxants. For example, botulinum toxin A, commonly known as Botox, can be injected into specific eye muscles to treat strabismus (misaligned eyes). Botox injections have also become a popular cosmetic procedure to temporarily remove wrinkles.

binds to SNAREs throughout the fusion reaction and is essential for fusion, although its exact role in mediating vesicle fusion remains unclear.

3.6 Synaptotagmin acts as a Ca^{2+} sensor to trigger synaptic vesicle fusion

How does Ca^{2+} entry regulate neurotransmitter exocytosis? A prime candidate linking these two events is a class of transmembrane proteins on the synaptic vesicle called **synaptotagmins** (Figure 3-7), which possess five or six Ca^{2+} binding sites on their cytoplasmic domains. To test the function of synaptotagmin in synaptic transmission, **knockout** mice were created in which synaptotagmin-1, the predominant form of synaptotagmin expressed in forebrain neurons, was disrupted using the gene targeting method (see Section 14.7 for details). To assay for synaptic transmission, embryonic hippocampal neurons from control or knockout mice were dissociated and cultured *in vitro* to allow synapse formation and subjected to a variation of the patch clamp technique called **whole-cell patch recording** (**whole-cell recording** in short). (In whole-cell recordings, the membrane underneath the patch pipette is ruptured such that the patch pipette is connected to the entire neuron; see Section 14.21 and Box 14-3 for details.) Pairs of cultured neurons were recorded simultaneously to test for synaptic connections between each pair. In a connected wild-type pair, depolarization of the presynaptic neuron, which caused it to fire action potentials, resulted in inward currents in the postsynaptic neuron, indicating successful synaptic transmission. By contrast, in knockout pairs, depolarization of the presynaptic neuron elicited much smaller postsynaptic responses, indicating that synaptotagmin-1 is required for normal synaptic transmission (**Figure 3-9**A). Parallel studies in *Drosophila* and *C. elegans* indicated that disruption of synaptotagmin homologs in these invertebrate model organisms (see Section 14.2) also impaired synaptic transmission.

The knockout experiment did not prove that synaptotagmin acts as a Ca^{2+} sensor, as disrupting other genes encoding proteins essential for synaptic transmission, such as the v-SNARE synaptobrevin, similarly blocked synaptic transmission. Subsequent experiments have provided strong evidence that synaptotagmin is a major Ca^{2+} sensor that regulates neurotransmitter release. For example, a mutant synaptotagmin-1 with a single amino acid change that reduces Ca^{2+} binding by 50% in an *in vitro* biochemical assay was identified. When researchers replaced the endogenous synaptotagmin-1 with this mutant synaptotagmin-1 in a varia-

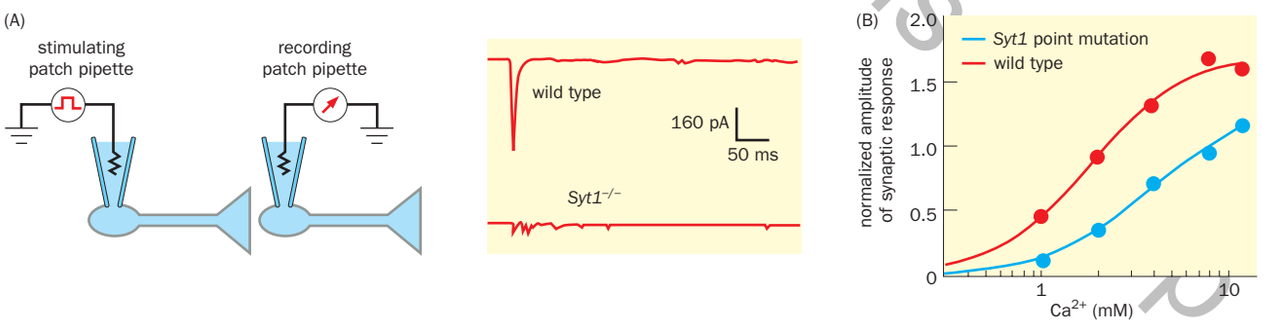

Figure 3-9 Synaptotagmin, a Ca^{2+} sensor that functions in synaptic transmission. (A) Left, schematic of experimental preparation to examine the role of synaptotagmin-1 (Syt1) in synaptic transmission. Pairs of cultured hippocampal neurons were subjected to simultaneous whole-cell recording. Depolarizing currents were injected into presynaptic neurons to cause them to fire action potentials, and postsynaptic responses were recorded as inward currents when the membrane potential was clamped at –70 mV. Right, compared with the inward current triggered by a presynaptic action potential between a pair of wild-type neurons (top trace), the synaptic response between a pair of neurons from *Syt1* knockout mice (lacking both copies of the *Syt1* gene) was greatly diminished (bottom trace). **(B)** A point mutation in *Syt1* that reduced Ca^{2+} binding by 50% also reduced the sensitivity of neurotransmitter release in cultured hippocampal neurons to Ca^{2+} by about 50%, as indicated by the downward shift of the mutant curve relative to the wild-type curve; each curve depicts normalized synaptic transmission amplitude against Ca^{2+} concentration. This finding suggests that synaptotagmin-1 acts as a Ca^{2+} sensor for synaptic vesicle fusion in hippocampal neurons. (A, adapted from Geppert M, Goda Y, Hammer RE, et al. [1994] *Cell* 79:717–727. With permission from Elsevier Inc. B, adapted from Fernández-Chacón R, Königstorfer A, Gerber SH, et al. [2001] *Nature* 410:41–49. With permission from Springer Nature.)

tion of the knockout procedure called **knock-in** (Section 14.7), neurons derived from the knock-in mice exhibited a corresponding 50% reduction in the Ca^{2+} sensitivity of neurotransmitter release (Figure 3-9B), consistent with synaptotagmin-1 acting as a Ca^{2+} sensor. Another protein involved in neurotransmitter release is complexin, which has a complex role, both activating the SNARE complex and blocking it in an intermediate step. One current model is that synaptotagmin releases the inhibitory block of complexin in a Ca^{2+}-dependent manner, thus allowing SNAREs to complete the vesicle fusion reaction in response to a rise in intracellular Ca^{2+} concentration.

At fast mammalian CNS synapses at physiological temperatures, action potential arrival can cause postsynaptic depolarization within as little as 150 μs. This interval includes about 90 μs for the opening of voltage-gated Ca^{2+} channels during the action potential upstroke, allowing Ca^{2+} influx, and 60 μs in total for Ca^{2+}-triggered vesicle fusion, neurotransmitter diffusion across the synaptic cleft, and the postsynaptic physiological response. To enable this rapid action, synaptic vesicles are docked at the active zone ready for release (Figure 3-3), with their SNARE proteins partially preassembled in high-energy configurations, yet blocked, waiting for the action of a Ca^{2+} sensor to release the break and complete SNARE assembly, which drives membrane fusion.

The rapidity of neurotransmitter release following Ca^{2+} entry described earlier, as well as its transience, allows the presynaptic terminal to respond to future action potentials with more neurotransmitter release. This requires the presynaptic concentration of free Ca^{2+} to be rapidly reduced after Ca^{2+} entry stops; this is accomplished by proteins that rapidly sequester Ca^{2+} or pump it out of the cytoplasm. It is also important that the presynaptic Ca^{2+} sensor has a low binding affinity for Ca^{2+}, as a high-affinity sensor would be bound for a longer time period. Indeed, synaptotagmin employs multiple low-affinity Ca^{2+}-binding sites that bind Ca^{2+} cooperatively (that is, binding of one Ca^{2+} facilitates binding of a second); only when multiple sites bind to Ca^{2+} is it able to trigger neurotransmitter release. Together, these mechanisms ensure that neurotransmitter release is triggered only transiently and locally at the site of Ca^{2+} entry.

3.7 The presynaptic active zone is a highly organized structure

The rapidity and transience of Ca^{2+}-induced neurotransmitter release relies on the proximity of voltage-gated Ca^{2+} channels and docked synaptic vesicles in the active zone. Indeed, Ca^{2+} imaging of presynaptic terminals (e.g., Figure 3-6) suggested that the rise in intracellular Ca^{2+} concentration in response to depolarization is highly restricted to microdomains near the active zone. Although the intracellular Ca^{2+} concentration is normally very low (~0.1 μM), it can shoot up transiently several orders of magnitude in the microdomain; this facilitates cooperative binding of Ca^{2+} to multiple Ca^{2+}-binding sites of synaptotagmin, allowing it to achieve the conformational change necessary for triggering vesicle fusion.

The molecular machinery that organizes the active zone has been extensively characterized (**Figure 3-10**). A central player is a protein called Unc13. Unc13 binds and activates the t-SNAREs and also reaches up and tethers the v-SNARE synaptobrevin and synaptic vesicle to the release site. Voltage-gated Ca^{2+} channels are recruited by two other active zone core components, RIM (Rab3-interacting molecule) and RIM-BP (RIM-binding protein). RIM binds Rab3, a synaptic vesicle–associated small GTPase, and thus brings synaptic vesicles close to voltage-gated Ca^{2+} channels. RIM and RIM-BP also interact with other active zone proteins, which in turn associate with the actin cytoskeleton that supports the structural integrity of the presynaptic terminal and transports molecules into the presynaptic terminal (Figure 2-6).

The speed of neurotransmission requires neurotransmitters to diffuse only a short distance to neurotransmitter receptors on the postsynaptic cell. The active zone has many synaptic adhesion molecules linking it to the postsynaptic membrane rich for neurotransmitter receptors. These include the presynaptic **neurexins**, which bind postsynaptic **neuroligins** (called **heterophilic binding**), and

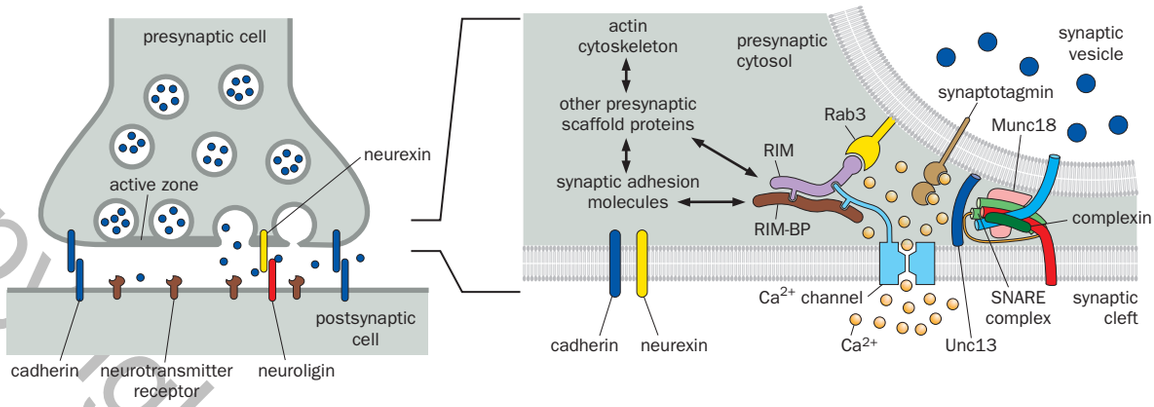

Figure 3-10 Molecular organization of the presynaptic terminal. Left, a lower-magnification model of a chemical synapse showing presynaptic and postsynaptic cells. Transsynaptic adhesion molecules, such as neurexin (yellow), neuroligin (red), and cadherin (blue), align the active zone with a postsynaptic density enriched in neurotransmitter receptors, facilitating the rapid action of neurotransmitters. Right, a magnified model of the presynaptic active zone. Unc13 binds both t- and v-SNAREs and thus brings the synaptic vesicle close to the presynaptic plasma membrane. The RIM/RIM-BP protein complex binds to voltage-gated Ca^{2+} channels directly and to synaptic vesicles via the Rab3 protein; this allows Ca^{2+} entry to activate synaptotagmin with minimal diffusion, which in turn releases the complexin inhibitory block on the SNARE/SM complex and causes neurotransmitter release (the SNARE complex is represented as in Figure 3-8A; Munc18 is the SM protein in mammalian synapses). RIM and RIM-BP are also associated with other presynaptic scaffold proteins, which are in turn associated with the actin cytoskeleton and with synaptic adhesion molecules. (Adapted from Südhof TC [2012] *Neuron* 75:11–25. With permission from Elsevier Inc.)

cadherins (Ca^{2+}-dependent cell adhesion proteins), present both pre- and postsynaptically, which bind each other (called **homophilic binding** in the case that the pre- and postsynaptic cadherins are the same isoform). These and other cell-adhesion molecules bring the presynaptic and postsynaptic plasma membranes within 20 nm of each other (Figure 3-10) and align the active zone with the portion of the postsynaptic membrane rich in neurotransmitter receptors.

Recent studies using super-resolution fluorescent microscopy (see Section 14.17 for more details) have begun to reveal how pre- and postsynaptic units are organized to form a functional synapse. For example, super-resolution localization of molecules in the *Drosophila* NMJ (**Figure 3-11**) indicated that RIM-BP proteins form a ring around a cluster of voltage-gated Ca^{2+} channels at the active zone presynaptic membrane. An active zone scaffold protein called Bruchpilot (similar to a mammalian protein called ELKS) extends from the center of the active zone to the periphery. Glutamate receptors are enriched in the postsynaptic density, which is aligned with the presynaptic active zone (glutamate is used as a neurotransmitter in the *Drosophila* NMJ; see Section 3.11 for details). A similar subsynaptic molecular architecture aligns presynaptic vesicle fusion with postsynaptic neurotransmitter receptors in vertebrates.

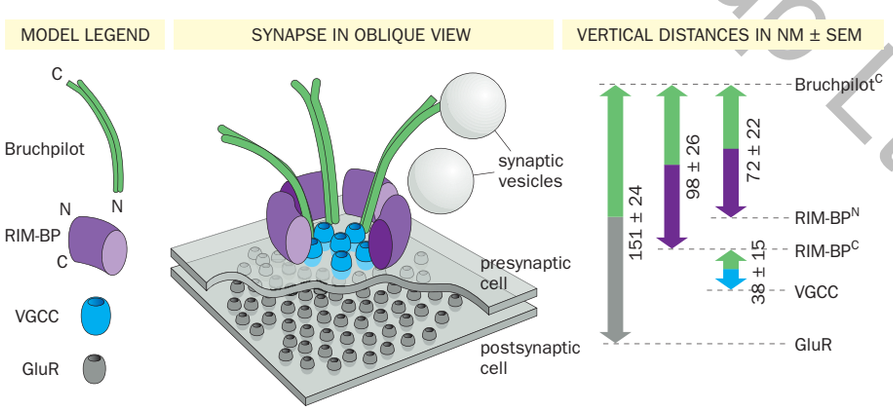

Figure 3-11 The organization of selected proteins in the *Drosophila* NMJ. This model is based on two-color labeling of different pairs of proteins (shown at right) and measurement of their distances using a technique called stimulated emission depletion microscopy, which can resolve structures ~50 nm apart (see Section 14.17 for details). For instance, the distance between the C-terminal of Bruchpilot and postsynaptic glutamate receptors was estimated by measuring the distance between the fluorescence signal from an antibody against the C-terminus of Bruchpilot and that from an antibody against the glutamate receptor (151 ± 24 nm apart). RIM-BP, Rab3-interacting-molecule binding protein; VGCC, voltage-gated Ca^{2+} channel; GluR, glutamate receptor; N, amino terminus; C, carboxy terminus; SEM, standard error of the mean. (From Liu KSY, Siebert M, Mertel S, et al. [2011] *Science* 334: 1565–1569. With permission from AAAS.)

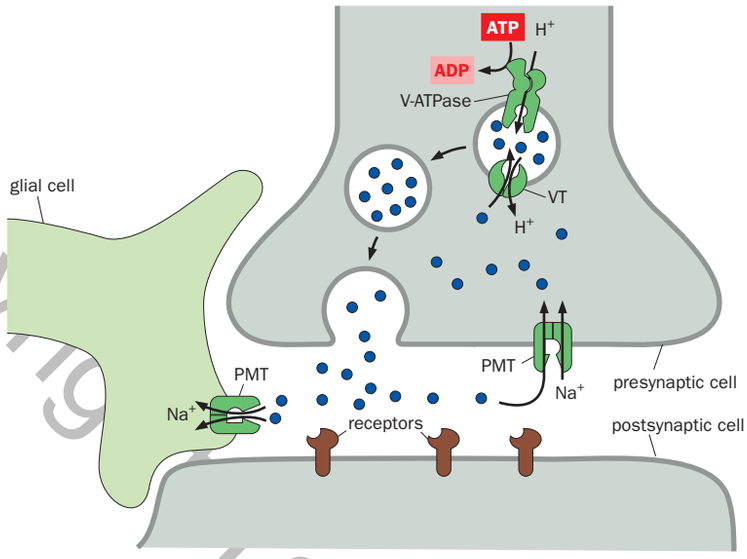

Figure 3-12 Clearance and recycling of neurotransmitters. After being released into the synaptic cleft, excess transmitters are taken up by plasma membrane transporters (PMTs) on the presynaptic or nearby glial plasma membranes; both are symporters that utilize energy from Na^+ entry. Within the presynaptic cytosol, neurotransmitters are transported into synaptic vesicles by vesicular neurotransmitter transporters (VTs), antiporters that use energy from transport of protons (H^+) out of the synaptic vesicle down their electrochemical gradient. The V-ATPase on the synaptic vesicle membrane establishes the H^+ gradient across the vesicular membrane using energy from ATP hydrolysis. (Based on Blakely RD & Edwards RH [2012] *Cold Spring Harb Perspect Biol* 4:a005595.)

3.8 Neurotransmitters are cleared from the synaptic cleft by degradation or transport into cells

For postsynaptic neurons to continually respond to firing of presynaptic neurons, neurotransmitters released in response to each presynaptic action potential must be efficiently cleared from the synaptic cleft. Although neurotransmitters can diffuse out of the synaptic cleft, additional mechanisms are employed to speed up neurotransmitter clearance.

Acetylcholine at the NMJ is rapidly degraded by **acetylcholinesterase**, an enzyme enriched in the synaptic cleft. Indeed, this enzyme is so active that most acetylcholine molecules released by motor axon terminals are degraded while diffusing across the short distance of the synaptic cleft. Some of the physiology experiments described in earlier sections involving mEPP measurements actually included acetylcholinesterase inhibitors in the saline to boost the mEPP amplitude.

In most other neurotransmitter systems, transmitter molecules are recycled after they are released, rather than being degraded. In a process called **neurotransmitter reuptake**, excess neurotransmitters are first taken back into the presynaptic cytosol via **plasma membrane neurotransmitter transporters**. These are symporters that move Na^+ into the cell along with the neurotransmitter itself; because Na^+ is moving down its electrochemical gradient as it enters the cell, the energy stored in the Na^+ gradient is harnessed to drive neurotransmitter reuptake (**Figure 3-12**; Movie 3-1). Once in the cytosol, neurotransmitters refill new and recycled synaptic vesicles (see Section 3.9) via a second transporter, the **vesicular neurotransmitter transporter** on the synaptic vesicle (Figure 3-7). The energy for vesicular transporters derives from transport of protons out of the synaptic vesicle down their electrochemical gradient. The electrochemical gradient of protons (high in vesicles and low in the cytosol) is created by the **V-ATPase**, which hydrolyzes ATP to pump protons (H^+) into the synaptic vesicle. In some neurotransmitter systems, including glutamate, secreted transmitters are cleared from the synaptic cleft by neurotransmitter transporters on the plasma membrane of glial cells, which wrap around many synapses (Figure 3-3). In Chapter 12, we will learn more about neurotransmitter reuptake mechanisms, as drugs altering these mechanisms are widely used to treat psychiatric disorders.

3.9 Synaptic vesicle recycling by endocytosis is essential for continual synaptic transmission

To maintain the ability to respond to sustained neuronal firing, presynaptic terminals must be able to replenish the stockpile of synaptic vesicles filled with

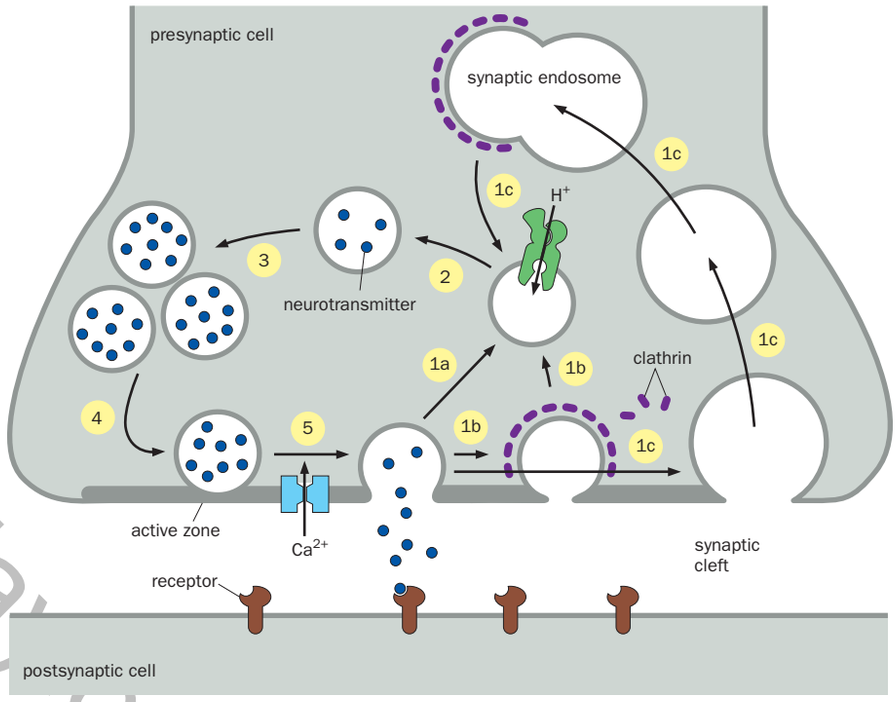

Figure 3-13 The synaptic vesicle cycle. After membrane fusion between the synaptic vesicle and the presynaptic membrane and release of neurotransmitters into the synaptic cleft, synaptic vesicles can be recycled via three pathways. In the kiss-and-run pathway, synaptic vesicles reform after a very transient fusion with limited exchange of proteins and lipids with the presynaptic plasma membrane (1a). In clathrin-mediated endocytosis, the synaptic vesicle membrane fuses fully with the presynaptic plasma membrane and is then retrieved via clathrin-mediated endocytosis (1b). In ultrafast endocytosis, the presynaptic plasma membrane is rapidly endocytosed, forming vesicles larger than synaptic vesicles; synaptic vesicles are produced subsequently from endosomes via a clathrin-mediated process (1c). The interior of vesicles is acidified by pumping protons (H^+) inside using the V-ATPase on the synaptic vesicle membrane; the synaptic vesicle is then ready to be filled with neurotransmitter by the proton export-coupled vesicular transporter (2; Figure 3-12). Synaptic vesicles filled with neurotransmitters join the pool of vesicles in the presynaptic terminal (3). Some vesicles transit into the readily releasable pool and are docked at the active zone (4) ready for exocytosis. Finally, Ca^{2+} entry through voltage-gated Ca^{2+} channels at the active zone triggers vesicle fusion (5). (Based on Südhof TC [2004] *Ann Rev Neurosci* 27:509–547; Watanabe S, Trimbuch T, Camecho-Pérez M, et al. [2014] *Nature* 515:228–233.)

neurotransmitters. The synaptic vesicle membrane and proteins are mostly synthesized in the soma. Because the distance between synaptic terminals and the soma can be up to 1 meter, synaptic vesicles must be rapidly recycled at the synapse to support future rounds of synaptic transmission. Two components of synaptic vesicles must be recycled and sorted into new vesicles: membranes and proteins.

Several mechanisms have been proposed for retrieving synaptic vesicle membranes (**Figure 3-13**). The first mechanism, "kiss and run," involves a very transient fusion of the synaptic vesicle with the presynaptic plasma membrane for neurotransmitter release, followed by closure of the pore so that mixing of the vesicle's protein and lipid content with the presynaptic plasma membrane is limited. In the second mechanism, the synaptic vesicle collapses into the presynaptic plasma membrane after fusion and is retrieved in the presynaptic terminal by clathrin-mediated endocytosis. (Clathrin is a protein that assembles into a cage on the cytoplasmic side of a membrane to form a coated pit, which buds off to form a clathrin-coated vesicle.) More recently, a third mechanism has been described, in which endocytic vesicles larger than synaptic vesicles are produced from the presynaptic membrane surrounding the active zone; these large endocytic vesicles then become part of synaptic endosomes, from which synaptic vesicles are subsequently produced by a clathrin-mediated process. Time-resolved electron microscopy revealed that large endocytic vesicles form within 100 ms after vesicle fusion; this is much faster than clathrin-mediated endocytosis, which usually takes seconds, potentially allowing more rapid production of synaptic vesicles for repeated use. Which of these mechanisms predominates at any given synapse is not known.

Proteins must be properly sorted to regenerate functional synaptic vesicles. Most importantly, the SNARE proteins must be pulled apart and sorted to the plasma and vesicle membranes. The SNARE complexes are disassembled by NSF in an ATP-dependent manner. (NSF stands for *N*-ethylmaleimide-sensitive fusion protein, named after a chemical inhibitor that blocks vesicle fusion reactions *in vitro*; SNARE stands for soluble NSF-attachment protein receptor.) Syntaxin and SNAP-25 remain in the presynaptic plasma membrane, whereas synaptobrevin is returned to the synaptic vesicle. Synaptobrevin and other vesicle proteins, such as synaptotagmin and the vesicular transporters, are recruited to the site of vesicle

formation by specialized adaptor proteins that interact with the clathrin machinery. Once assembly of the vesicle is complete, the neck attaching it to the membrane narrows and is cleaved by a protein called **dynamin**. The clathrin coat is then stripped off the vesicle.

Fully regenerated vesicles are then acidified by the proton pump V-ATPase and refilled with neurotransmitters (Figure 3-12). Filled vesicles join the synaptic vesicles in the presynaptic terminal. A synaptic vesicle-associated protein called synapsin, a marker widely used to identify synapses, links vesicles together at the synapse to maintain their proximity to the presynaptic zone. A small subset of synaptic vesicles constitutes the **readily releasable pool**, operationally defined as the pool of vesicles most easily released. Readily releasable vesicles may be the vesicles docked at active zones in the high-energy configuration of a preassembled SNARE complex and readied for further rounds of neurotransmitter release in response to depolarization-induced Ca^{2+} entry (Figure 3-13).

We use a specific example to illustrate the importance of synaptic vesicle retrieval for continued synaptic transmission and neuronal communication. To identify genes necessary for neuronal communication, forward genetic screens (see Section 14.6 for details) were carried out in the fruit fly *Drosophila* to isolate mutations causing paralysis in flies kept at high temperatures. This led to the discovery of a temperature-sensitive mutation called *Shibire^{ts}*. Mutant flies behave normally at room temperature (~20°C) but are paralyzed shortly after shifting to elevated temperatures (>29°C); their motility returns within a few minutes after flies are returned to 20°C. Molecular-genetic analysis revealed that the *Shibire* gene encodes dynamin, the previously mentioned protein that cleaves vesicles from the membrane. Dynamin is essential for both clathrin-mediated endocytosis of synaptic vesicles and ultrafast endocytosis. The *Shibire^{ts}* mutation causes the dynamin collar to become locked and unable to cleave vesicles from the membrane at elevated temperatures. Without vesicle recycling, presynaptic terminals are rapidly deprived of synaptic vesicles (**Figure 3-14**) and became unable to release neurotransmitters in response to further action potentials, thus causing paralysis. The *Shibire^{ts}* mutation has proven to be a useful tool for rapidly and reversibly silencing specific neurons *in vivo* to analyze their function in information processing within neural circuits (Section 14.23).

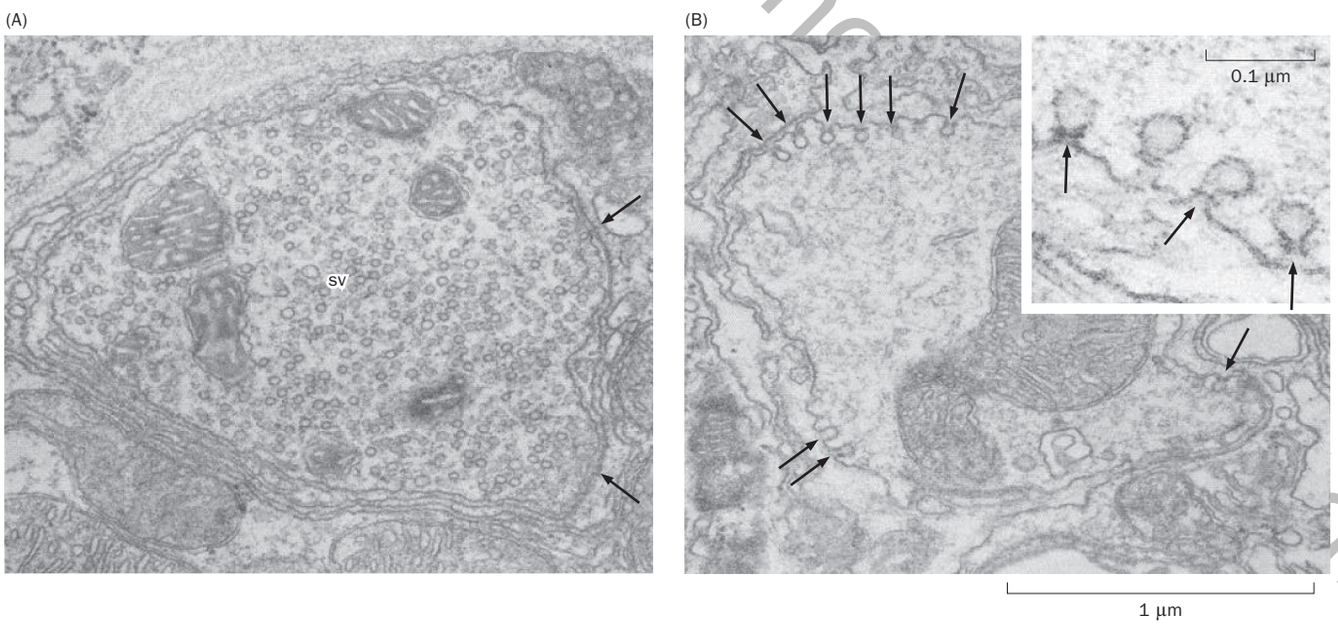

Figure 3-14 Electron micrographs of synapses in temperature-sensitive *Shibire^{ts}* mutant fruit flies. (A) A neuromuscular junction from a *Shibire^{ts}* mutant fly fixed at 19°C. The presynaptic terminal is abundant in synaptic vesicles (sv). Arrows indicate active zones. **(B)** An NMJ fixed 8 minutes after raising the temperature to 29°C. Note the reduced number of synaptic vesicles in the presynaptic terminal compared with Panel A and the presence of "collared" vesicles (arrows, higher magnification in inset), indicating a block of the last step of endocytosis. (From Koenig JH & Ikeda K [1989] *J Neurosci* 9:3844–3860. Copyright ©1989 Society for Neuroscience.)

Table 3-1: A molecular cast for neurotransmitter release

Molecule	Location	Functions
Synaptic vesicle fusion with presynaptic membrane		
Synaptobrevin/VAMP	Synaptic vesicle	Mediates vesicle fusion (v-SNARE)
Syntaxin	Presynaptic plasma membrane	Mediates vesicle fusion (t-SNARE)
SNAP-25	Presynaptic plasma membrane	Mediates vesicle fusion (t-SNARE)
Sec1/Munc18 (SM)	Presynaptic cytosol	Binds to SNARE complex and essential for vesicle fusion
Unc13	Active zone	Promotes assembly of SNARE complex
Ca^{2+} regulation of synaptic transmission		
Voltage-gated Ca^{2+} channel	Active zone of presynaptic membrane	Allows Ca^{2+} entry in response to action potential-triggered depolarization
Ca^{2+}	Entering from extracellular space to presynaptic cytosol	Triggers synaptic vesicle fusion
Synaptotagmin	Synaptic vesicle	Senses Ca^{2+} to trigger vesicle fusion
Complexin	Presynaptic cytosol	Binds and regulates SNARE-mediated vesicle fusion
Organization of presynaptic terminal (and alignment with postsynaptic density)		
RIM	Active zone	Organizes presynaptic scaffold
RIM-BP	Active zone	Organizes presynaptic scaffold
ELKS/Bruchpilot	Active zone	Organizes presynaptic scaffold
Rab3	Synaptic vesicle	Interacts with active zone components
Cadherin	Presynaptic and postsynaptic plasma membranes	Trans-synaptic adhesion
Neurexin	Presynaptic plasma membrane	Trans-synaptic adhesion
Neuroligin	Postsynaptic plasma membrane	Trans-synaptic adhesion
Neurotransmitter and vesicle recycling		
Acetylcholinesterase	Synaptic cleft	Degrades neurotransmitter acetylcholine
Plasma membrane neurotransmitter transporter (PMT)	Presynaptic plasma membrane, glial plasma membrane	Transports excess neurotransmitter molecules back to presynaptic cytosol or to nearby glia
Vesicular neurotransmitter transporter (VT)	Synaptic vesicle	Transports neurotransmitters from presynaptic cytosol to the synaptic vesicle
V-ATPase	Synaptic vesicle	Establishes proton gradient within the synaptic vesicle
Synapsin	Synaptic vesicle	Maintain vesicles in the vicinity of the active zone
Clathrin	Presynaptic cytosol	Shapes recycled vesicles from presynaptic plasma membrane or endosome membrane during endocytosis
Shibire/dynamin	Presynaptic cytosol	Retrieves vesicles from presynaptic plasma membrane via endocytosis
NSF	Presynaptic cytosol	Disassembles SNARE complex after fusion

As a summary of what we have learned so far, **Table 3-1** provides a list of molecules that play key roles in mediating and regulating the sequence of events essential for neurotransmitter release.

3.10 Synapses can be facilitating or depressing

Because synaptic transmission is the key mode of interneuronal communication, the **efficacy of synaptic transmission**, measured by the magnitude of the postsynaptic response to a presynaptic stimulus, is regulated in many ways. **Synaptic plasticity**, the ability to change the efficacy of synaptic transmission, is an extremely important property of the nervous system. Synaptic plasticity is usually

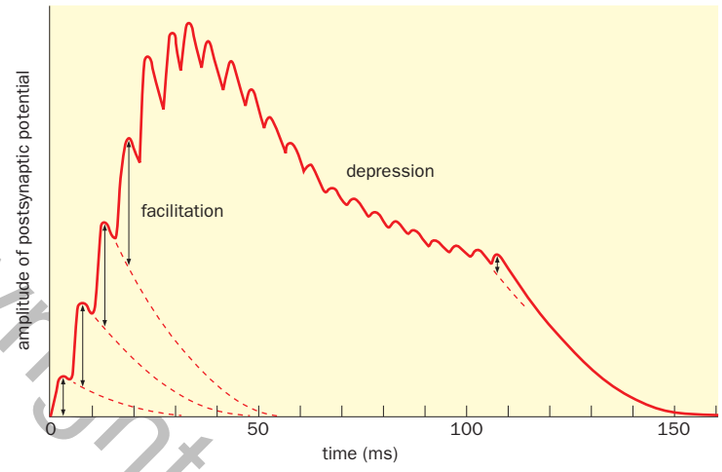

Figure 3-15 Synaptic facilitation and depression. In this schematic, the amplitudes of postsynaptic potentials, indicated by the lengths of the double arrows parallel to the *y* axis, change in response to a train of action potentials. The first series exhibits facilitation, as each successive action potential produces a larger response; the latter series exhibits depression as responses become smaller and smaller for each successive action potential. The dashed lines represent the natural decay of postsynaptic potentials, had there not been follow-up action potentials, and were used to determine the amplitude of postsynaptic potentials in response to successive action potentials. (From Katz B [1966] Nerve, Muscle, and Synapse. With permission from McGraw Hill.)

divided into **short-term synaptic plasticity**, which occurs within milliseconds to minutes, and **long-term synaptic plasticity**, which can extend from hours to the lifetime of an animal. We discuss in the following the two simplest forms of short-term plasticity, which involve changes in neurotransmitter release probability. Long-term synaptic plasticity will be examined in Chapter 11 in the context of memory and learning.

Although Ca^{2+}-dependent synaptic vesicle fusion provides an essential link between action potential arrival and neurotransmitter release, not every action potential produces the same neurotransmitter release probability. As discussed earlier, the quantal content of CNS synapses is much lower than that of the NMJ, as presynaptic axons typically form at most a few active zones onto any given postsynaptic partner neuron. In most mammalian CNS synapses *in vivo,* the average **release probability** (defined as the probability that an active zone of a presynaptic terminal releases the transmitter contents of one or more synaptic vesicles following an action potential) is estimated to be far smaller than 1. If many active zones exist between a presynaptic cell and a postsynaptic cell, as is the case at the vertebrate NMJ, the probability that at least one active zone releases a vesicle approaches 1; however, the magnitude of the postsynaptic response still depends on the release probability of each active zone.

The release probability can be affected by prior synaptic activity. At **facilitating synapses**, successive action potentials trigger larger and larger postsynaptic responses. By contrast, at **depressing synapses**, successive action potentials result in smaller and smaller postsynaptic responses (**Figure 3-15**). Fast facilitation and depression are most often due to presynaptic factors, such as altered amounts of neurotransmitter release. The same synapse can be facilitating or depressing, depending on its intrinsic properties and recent activity.

In the simplest case, facilitating synapses have low starting release probabilities. The amount of release increases during repeated action potentials as active zone Ca^{2+} builds up. Depressing synapses, on the other hand, are usually characterized by high starting release probabilities that result in substantial release at the beginning of a stimulus train; this exhausts the pool of readily releasable vesicles, leading to a decline in the amount of release per spike as the stimulus train proceeds. Typically, large numbers of vesicles in the presynaptic terminal can replenish depleted vesicles in the readily releasable pool, so this sort of depression can recover in seconds. In the course of this book, we will encounter additional mechanisms for adjusting synaptic strength via distinct processes and at different temporal scales.

3.11 Nervous systems use many neurotransmitters

To illustrate the basic principles of synaptic transmission, we have focused primarily on the vertebrate NMJ, which employs the neurotransmitter acetylcholine.

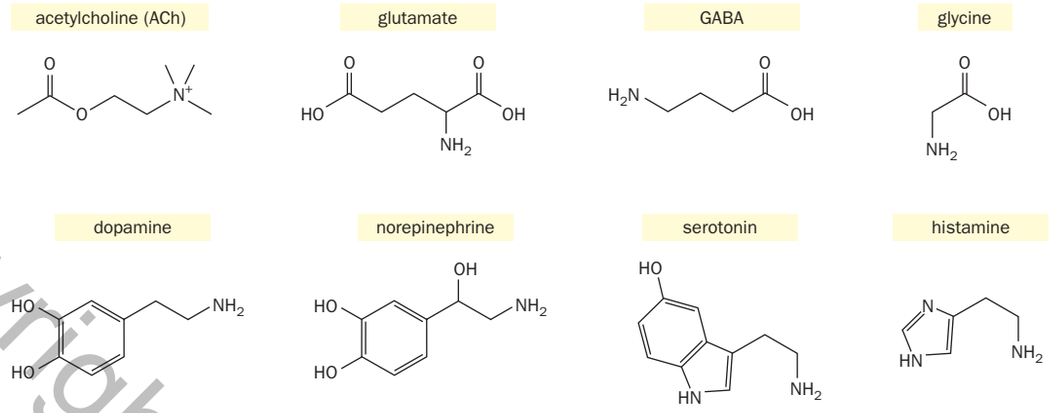

Figure 3-16 Structures of widely used small-molecule neurotransmitters. Acetylcholine is produced from choline and acetyl-CoA. Glutamate and glycine are natural amino acids. GABA (γ-amino butyric acid) is produced from glutamate. Dopamine is derived from the amino acid tyrosine. Norepinephrine is produced from dopamine and is a precursor for the hormone epinephrine. Serotonin is derived from the amino acid tryptophan. Histamine is derived from the amino acid histidine. See Figure 12-20 for the biosynthetic pathway that produces dopamine, norepinephrine, and epinephrine.

The principles learned thus far apply to virtually all chemical synapses, regardless of the neurotransmitter they use (**Figure 3-16**; **Table 3-2**). Two major neurotransmitters used in the vertebrate CNS are **glutamate** (glutamic acid), a natural amino acid, and **GABA** (γ-amino butyric acid), which is converted from glutamate by the enzyme **glutamic acid decarboxylase** (**GAD**). Glutamate is the predominant **excitatory neurotransmitter** in the vertebrate nervous system because its release depolarizes postsynaptic neurons, making them more likely to fire action potentials. GABA is an **inhibitory neurotransmitter** because its release usually renders postsynaptic neurons less likely to fire action potentials. The amino acid **glycine**, another inhibitory neurotransmitter, is used by a subset of inhibitory neurons in the vertebrate brainstem and spinal cord.

GABA is the major inhibitory neurotransmitter in diverse species, including invertebrates such as the nematode *C. elegans,* the fruit fly *Drosophila melanogaster,* and crustaceans. Indeed, GABA's inhibitory action was first established in the crab. Like vertebrates, *C. elegans* also uses ACh as the excitatory transmitter at its NMJ and glutamate as the major neurotransmitter in its CNS. Curiously,

Table 3-2: Widely used neurotransmitters

Neurotransmitter	Major uses in the vertebrate nervous system[a]
Acetylcholine	Motor neurons that excite muscle; ANS[b] neurons; CNS excitatory and modulatory neurons
Glutamate	Most CNS excitatory neurons; most sensory neurons
GABA	Most CNS inhibitory neurons
Glycine	Some CNS inhibitory neurons (mostly in the brainstem and spinal cord)
Serotonin (5-HT)	CNS modulatory neurons; neurons in the gastrointestinal tract
Dopamine	CNS modulatory neurons
Norepinephrine	CNS modulatory neurons; ANS[b] neurons
Histamine	CNS modulatory neurons
ATP, adenosine	Some sensory and CNS neurons
Neuropeptides	Usually co-released from excitatory, inhibitory, or modulatory neurons; neurosecretory cells

[a] See text for variations in invertebrate nervous systems.

[b] ANS, autonomic nervous system; as will be discussed in more detail in Chapter 9, acetylcholine and norepinephrine are used in different types of ANS neurons.

Drosophila utilizes ACh as the major excitatory neurotransmitter in its CNS and glutamate as the transmitter at its NMJ (Figure 3-11).

Although we often identify neurotransmitters as excitatory or inhibitory, it is important to note that neurotransmitters do not possess such qualities intrinsically—they are just molecules. The excitatory or inhibitory quality arises from the ion conductances these molecules activate in the postsynaptic neuron. Thus, we consider glutamate and acetylcholine excitatory neurotransmitters because of their actions on most postsynaptic neurons, but in some cases they can be inhibitory, as we will see in the next part of this chapter.

Another important class of neurotransmitters plays a predominantly modulatory role. **Modulatory neurotransmitters** (also called **neuromodulators**) typically act on longer time scales and/or larger spatial scales than the classical neurotransmitters described so far. Neuromodulators can shift the membrane potential up or down, thereby influencing neuronal **excitability** (how readily a neuron fires an action potential). Classic neuromodulators include **serotonin** (also called **5-HT** for 5-hydroxytryptamine), **dopamine**, **norepinephrine** (also called noradrenaline), and **histamine** (Figure 3-16); these are all derived from aromatic amino acids and are collectively called **monoamine neurotransmitters**. In addition to being released into the synaptic cleft, these neurotransmitters can be released into the extracellular space outside of morphologically defined synapses to affect nearby cells; this process is called **volume transmission**. In vertebrates, the cell bodies of neurons that synthesize monoamine neurotransmitters are mostly clustered in discrete nuclei in the brainstem or hypothalamus. They send profuse axons that collectively innervate a large fraction of the CNS (see Box 9-1 for details). Dopamine and serotonin act as neuromodulators throughout the animal kingdom. In place of norepinephrine, a chemically similar molecule called **octopamine** is used in some invertebrate nervous systems. Finally, ATP and its derivative adenosine can act as neurotransmitters in some sensory neurons and in the CNS.

Some neurotransmitters have different roles in different parts of the nervous system (Table 3-2). In vertebrates, ACh is used as an excitatory neurotransmitter by motor neurons to control skeletal muscle contraction at the NMJ. It is also one of two neurotransmitters employed by the **autonomic nervous system** for neural control of visceral processes such as heartbeat, respiration, and digestion. In the brain, ACh can act as both an excitatory neurotransmitter and a neuromodulator. Likewise, norepinephrine functions as the autonomic nervous system's other neurotransmitter, but acts as a neuromodulator in the brain.

The type of neurotransmitter a neuron releases is often used as a major criterion for neuronal classification: glutamatergic, GABAergic, cholinergic, etc. Neurons of a given neurotransmitter type express a specific set of genes associated with that type, including enzyme(s) that synthesize the neurotransmitter, a vesicular transporter that pumps the neurotransmitter into synaptic vesicles, and in many cases a plasma membrane transporter that retrieves the neurotransmitter from the synaptic cleft after release (Figure 3-12). However, recent studies have identified an increasing number of cases in which the same neuron releases more than one neurotransmitter. For example, some serotonin or dopamine neurons co-release glutamate or GABA. Some cholinergic neurons co-release GABA. These findings muddy the definition of neuronal types by the neurotransmitter they release. In most cases, it remains unclear whether two transmitters are released from the same synaptic vesicle or distinct vesicles, and whether they are released from the same presynaptic terminal or distinct terminals. These are important questions to be addressed in the future.

In addition to the small-molecule neurotransmitters we have discussed thus far, some neurons also secrete **neuropeptides** that act as neurotransmitters. The mammalian nervous system utilizes dozens of neuropeptides, with lengths ranging from a few amino acids to several dozen. As we will learn in Chapters 9 and 10, neuropeptides regulate diverse and vital physiological functions such as eating, sleeping, and sexual behaviors. Neuropeptides are usually produced by proteolytic cleavage of precursor proteins in the secretory pathway (Figure 2-2). They are packaged into **large dense-core vesicles** (which are larger than synaptic vesicles

and contain electron-dense materials) that bud off from the Golgi apparatus and are delivered to axons and presynaptic terminals via fast axonal transport. Neuropeptides cannot be locally synthesized or recovered after release and must be transported across long distances from the soma to axon terminals. This may account for their more sparing use: the probability of neuropeptide release seems to be much lower than that of small-molecule neurotransmitters in the same terminals. We know far less about the mechanisms controlling neuropeptide release from large dense-core vesicles than we do about the mechanisms controlling the release of small-molecule neurotransmitters from synaptic vesicles. In most cases, neuropeptides play modulatory roles and are released by neurons that also use a small-molecule neurotransmitter. Indeed, large dense-core vesicles can contain not only peptides but also small-molecule neuromodulators like monoamines. As we will learn in Chapter 9, some neurons and neuroendocrine cells secrete neuropeptides into the bloodstream; in these cases, neuropeptides act as **hormones** to influence the physiology of remote recipient cells.

The reason different neurotransmitters have different effects is that their postsynaptic receptors have different properties. We now turn to the next step of neuronal communication: mechanisms by which neurotransmitters influence postsynaptic neurons.

HOW DO NEUROTRANSMITTERS ACT ON POSTSYNAPTIC NEURONS?

In the first part of the chapter, we used postsynaptic responses, such as the end-plate potential (Figure 3-1) and postsynaptic inward current (Figures 3-5 and 3-9), as assays to investigate the mechanisms of presynaptic neurotransmitter release. In the following sections, we study the mechanisms by which postsynaptic neurons produce these responses. We first discuss rapid responses, occurring within milliseconds, caused by direct changes in ionic conductances. We then study responses occurring in tens of milliseconds to seconds mediated by intracellular signaling pathways. We further highlight responses occurring in hours to days and involving expression of new genes. Finally, we summarize how postsynaptic neurons integrate different inputs to determine their own firing patterns and neurotransmitter release properties, thus completing a full round of neuronal communication.

3.12 Acetylcholine opens a nonselective cation channel at the neuromuscular junction

We begin our journey across the synaptic cleft by returning to the vertebrate neuromuscular junction (NMJ). In Section 3.1, we learned that acetylcholine (ACh) released from motor axon terminals depolarizes the muscle membrane and that iontophoretic application of ACh to muscle mimics ACh release from presynaptic terminals (Figure 3-1). How does ACh accomplish this? By locally applying ACh to different regions of muscle fibers, researchers found that exogenous ACh produced the most effective depolarization near motor axon terminals. These experiments implied that receptors for ACh must be present on the muscle membrane and concentrated at the NMJ. Upon ACh binding, ACh receptors trigger a change in the muscle membrane's ionic conductances within a few milliseconds.

To explore the underlying mechanisms, voltage clamp experiments analogous to those carried out on squid giant axons (Section 2.10) were performed on muscle fibers. These experiments enabled researchers to test how ACh release induced by motor axon stimulation changes ion flow across the muscle membrane (**Figure 3-17**A). In these experiments, two electrodes were inserted into the muscle cell, one to measure the membrane potential (V_m) and compare it to a desired command voltage (V_{CMD}) and the other to pass feedback current into the muscle to maintain V_m at the same value as V_{CMD}. The current injected into the muscle, which can be experimentally measured, equals the current that passes through the muscle membrane in response to ACh release, or the **end-plate cur-**

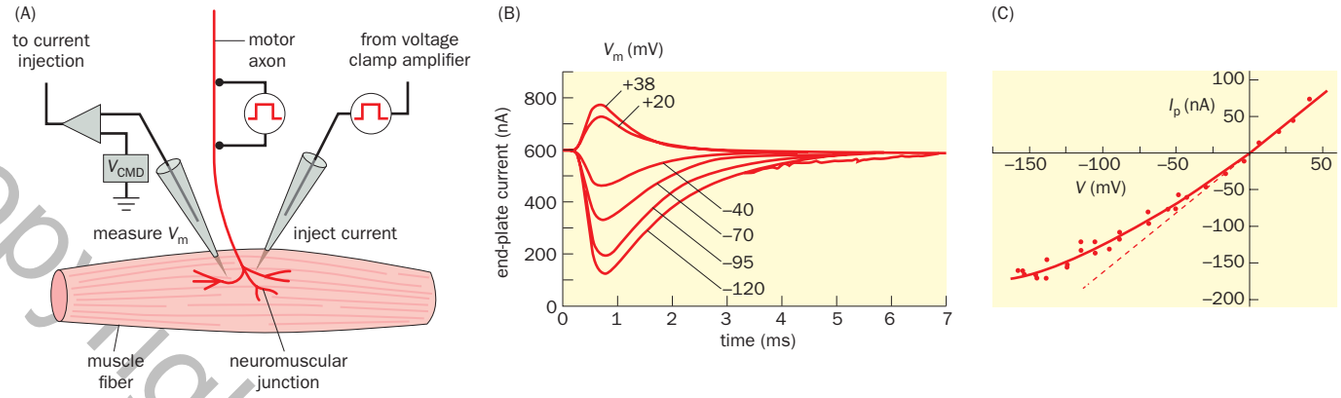

Figure 3-17 Properties of an acetylcholine-induced current studied by voltage clamp. (A) Experimental setup. Two intracellular electrodes were inserted into a muscle cell at the frog NMJ. The first (left) was to record the membrane potential (V_m), which was compared with an experimenter-determined command potential (V_{CMD}). The second electrode injected feedback current into the muscle to maintain V_m at V_{CMD}. The end-plate current in response to ACh release caused by motor axon stimulation was determined from the feedback current injected into the muscle cell to hold V_m at V_{CMD}. See Figure 2-21 for more details of voltage clamp. **(B)** The end-plate current elicited by single motor axon stimulation was measured at the six different membrane potentials indicated. At negative potentials the end-plate current was inward (positive ions flowing into the muscle cell), whereas at positive potentials the end-plate current was outward. **(C)** Peak end-plate current (I_p, *y* axis) as a function of the muscle membrane potential (V, *x* axis). Experimental data (represented as dots) fell on a curve (the *I–V* curve) that is close to linear (dashed line), indicating that the conductance (represented by the slope of the *I–V* curve) is mostly unaffected by voltage. The current switches signs between negative (inward) and positive (outward) at 0 mV, the reversal potential of the channel opened by ACh. (B & C, adapted from Magleby KL & Stevens CF [1972] *J Physiol* 223:173–197.)

rent. ACh release was found to cause an inward current at negative membrane potentials, but an outward current at positive membrane potentials (Figure 3-17B). The current–voltage relationship (plotted on an ***I–V* curve**) was nearly linear, and the membrane potential at which the current flow reversed direction (called the **reversal potential**) was approximately 0 mV (Figure 3-17C).

If the ACh-induced current were carried by a single ion, the reversal potential would equal the equilibrium potential of that ion, as both reversal potential and equilibrium potential define a state in which net current is zero. However, the reversal potential of the ACh-induced current is unlike the Na^+, K^+, or Cl^- currents we discussed in Section 2.5. These three ions have equilibrium potentials around +58 mV, –85 mV, and –79 mV, respectively. Thus, we can infer that the ACh-induced current is carried by more than one ion. Indeed, when researchers performed experiments measuring the reversal potential of the ACh-induced current while varying extracellular ion concentrations, they found that ACh opens a channel permeable to K^+, Na^+, and other cations but not to anions such as Cl^-. Further evidence indicated that ACh acts on a single channel permeable to both Na^+ and K^+. At positive membrane potentials, the driving force for K^+ efflux exceeds that for Na^+ influx (because V_m is further from E_K than from E_{Na}), so K^+ efflux exceeds Na^+ influx, causing a net outward current. At negative membrane potentials, the driving force for Na^+ influx exceeds that for K^+ efflux, causing a net inward current. Ca^{2+} influx also makes a small contribution to the inward current. Importantly, since the reversal potential of 0 mV is far above the muscle membrane's resting potential (around –75 mV) and the threshold for action potential production (usually 10–20 mV more depolarized than the resting potential), the end-plate current under physiological conditions is always inward, carried by more Na^+ influx than K^+ efflux (**Figure 3-18**A). This depolarizes the muscle membrane, resulting in the end-plate potential (EPP) we introduced in Section 3.1.

The action of the ACh-induced current can be represented by an electrical circuit model of the muscle membrane, in which the ACh-induced current is represented in parallel with the resting current (Figure 3-18B). Immediately after the switch is on (representing ACh release), $I_{Na} = g_{Na}(V_m - E_{Na})$, and $I_K = g_K(V_m - E_K)$. Because at rest V_m is around –75 mV, the absolute value $|V_m - E_{Na}|$ far exceeds $|V_m - E_K|$. Assuming the ACh-activated channel has similar conductances for Na^+ and K^+ (see the following), the inward current on the Na^+ branch will far exceed

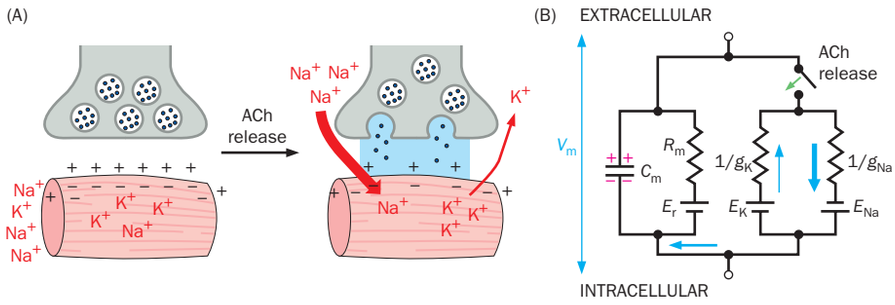

Figure 3-18 ACh opens a nonselective cation channel on the muscle membrane. **(A)** Schematic of how ACh release causes depolarization of the muscle membrane. At rest (left), the membrane potential of the muscle cell is around –75 mV, similar to the resting membrane potential of many neurons, with higher K^+ concentration inside the cell and higher Na^+ concentration outside. ACh binding opens a cation channel on the muscle membrane permeable to both Na^+ and K^+. This produces more Na^+ influx than K^+ efflux because of the larger driving force on Na^+, and so the muscle membrane is depolarized. **(B)** An electrical circuit model. The left part represents the resting muscle membrane, which includes a membrane capacitance branch (C_m) and a membrane resistance branch (R_m) with a battery representing the resting potential (E_r) (Sections 2.7 and 2.8). The right part represents the ACh-induced current, with the K^+ and Na^+ paths (with resistances of $1/g_K$ and $1/g_{Na}$, respectively) in parallel. After the switch is turned on (green arrow) by ACh release, the current passing through the Na^+ path is much larger than the current passing through the K^+ path because the driving force for Na^+ (= $E_{Na} - V_m$; Section 2.5) is far greater than the driving force for K^+ (= $V_m - E_K$). A net inward current discharges the membrane capacitance, and depolarizes the membrane potential.

the outward current on the K^+ branch. Thus, ACh release will activate a net inward current.

The reversal potential, designated $\boldsymbol{E_{rev}}$, is an important property of ion channels permeable to multiple ions and is determined by the relative conductances and equilibrium potentials of each ion. Using the electrical circuit model in Figure 3-18B, we can determine their relationship as follows: at the reversal potential ($V_m = E_{rev}$), Na^+ influx equals K^+ efflux, thus $I_K = -I_{Na}$. Since $I_K = g_K(V_m - E_K)$ and $I_{Na} = g_{Na}(V_m - E_{Na})$, we have

$$E_{rev} = \frac{g_{Na}E_{NA} + g_K E_K}{g_{Na} + g_K} = \frac{\frac{g_{Na}}{g_K}E_{Na} + E_K}{\frac{g_{Na}}{g_K} + 1}$$

We can see from this formula that if the conductances for Na^+ and K^+ were equal ($g_{Na}/g_K = 1$), E_{rev} would simply be an average of E_{Na} and E_K. If the ionic concentrations across the muscle membrane were the same as our model neuron in Figure 2-12A, with E_K = –85 mV and E_{Na} = +58 mV, then E_{rev} would be –13.5 mV. However, since E_{rev} = 0 mV, as shown in Figure 3-17C, we can calculate that g_{Na}/g_K is approximately 1.5 (i.e., 85/58); in other words, the channel opened upon ACh binding has a higher conductance for Na^+ than for K^+.

3.13 The skeletal muscle acetylcholine receptor is a ligand-gated ion channel

A deeper understanding of the ACh-induced conductance change required identification of the postsynaptic **acetylcholine receptor** (**AChR**) and the ion channel whose conductance is coupled to ACh binding. Further studies indicated that the muscle AChR is itself the ion channel. Just as the NMJ served as a model synapse because of its experimental accessibility, the AChR served as a model neurotransmitter receptor because of its abundance, particularly in the electric organ of the *Torpedo* ray, which is highly enriched for an AChR similar to that from the skeletal muscle. Biochemical purification and subsequent cloning of the *Torpedo* AChR revealed that it consists of five subunits: two α, one β, one γ, and one δ (**Figure 3-19**A). Each AChR contains two ACh binding sites, located at the α–γ and α–δ subunit interfaces, respectively. Both sites need to bind ACh for the channel to open. Evidence that this heteropentameric receptor was the ACh-activated channel came from a reconstitution experiment: co-injection of mRNAs encoding all four AChR subunits into the *Xenopus* oocyte caused the oocyte, which normally does not respond to ACh, to produce an inward current in response to ACh iontophoresis in voltage clamp experiments. This ACh-induced inward current was reversibly blocked by curare (Box 3-2), an AChR **antagonist** (agent that acts to counter the action of an endogenous molecule); washing out the curare restored the inward current (Figure 3-19B). Omitting an mRNA of any of the AChR subunits abolished the ACh-induced inward current in the oocyte expression system.

The three-dimensional structure of the *Torpedo* AChR has been determined by high-resolution electron microscopy (**Figure 3-20**). All AChR subunits contain four transmembrane helices, with the M2 helices from all subunits lining the ion

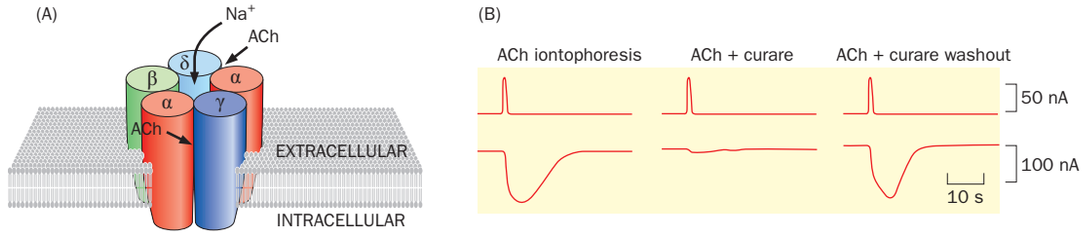

Figure 3-19 Composition of the acetylcholine receptor (AChR). **(A)** Schematic illustrating the subunit composition of the AChR. The two ACh binding sites are at the α–γ and α–δ subunit interfaces. **(B)** Functional expression of AChR was achieved by injecting mRNAs encoding the four AChR subunits into *Xenopus* oocytes. Top traces, current used for iontophoresis of ACh. Bottom traces, inward current in response to ACh application measured in a voltage clamp setup. ACh application led to an inward current (left) blocked by curare, an AChR inhibitor (middle), that was restored after curare was washed out (right). The membrane potential was held at –60 mV. (B, adapted from Mishina M, Kurosaki T, Tobimatsu T, et al. [1984] *Nature* 307:604–608. With permission from Springer Nature.)

conduction pore. The transmembrane helices form a hydrophobic barrier or "gate" when AChR is closed, preventing ion flow. ACh binding causes rotation of the α subunits, inducing an alternative conformation of the M2 helices and opening the gate to allow cation passage.

To summarize synaptic transmission at the vertebrate NMJ: action potentials trigger ACh release from motor axon terminals; ACh molecules diffuse across the synaptic cleft and bind to postsynaptic AChRs, which are highly concentrated on the muscle membrane directly apposing the motor axon terminal; upon ACh binding, muscle AChRs open a nonselective cation channel that allows more Na^+ influx than K^+ efflux, thus depolarizing the muscle cell in the form of an EPP; when this depolarization reaches threshold, the muscle cell fires action potentials, resulting in muscle contraction. We will study the mechanisms of muscle contraction in Section 8.1.

Whereas the open probability of the voltage-gated Na^+ and K^+ channels we studied in Chapter 2 is increased by depolarization, the open probability of muscle AChR channels is not affected by membrane potential changes; its conductance (I/V) is mostly constant across different voltages, as can be seen by the near

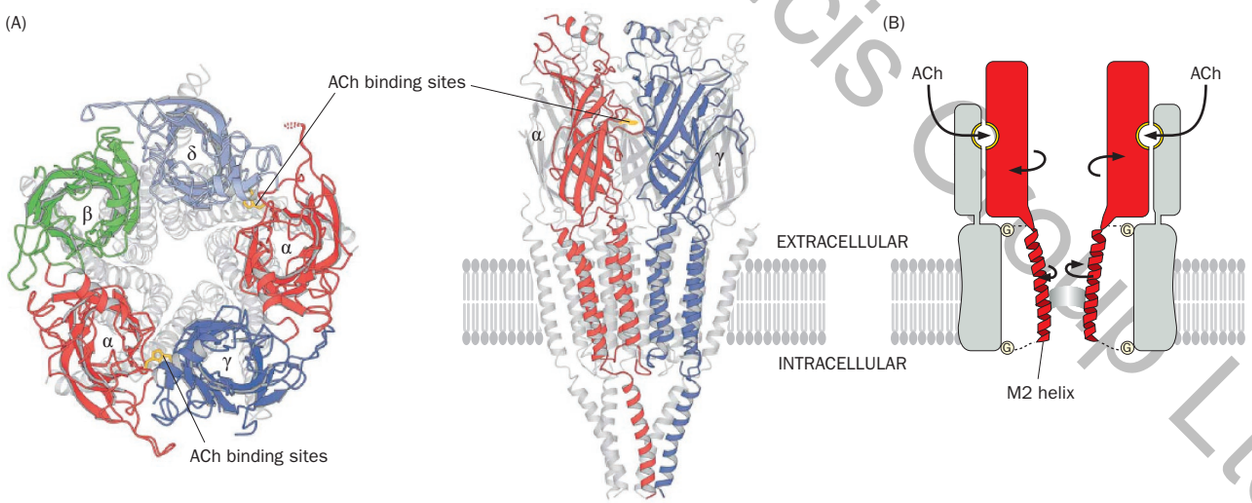

Figure 3-20 AChR structure and gating model. (A) Structure of *Torpedo* AChR in a closed state at a resolution of 4 Å by electron microscopy. Left, a surface view from the extracellular side. The tryptophan in the α subunit implicated in ACh binding is highlighted in gold. Only the extracellular portions are colored. Right, a side view showing the transmembrane helices. The front α and γ subunits are highlighted in color. **(B)** A model of AChR activation. ACh binding induces a rotation of part of the extracellular domain of the α subunit (red). This rotation triggers a conformational change in the transmembrane helix M2 that lines the ion conduction pore, leading to the opening of the ion gate. Dotted lines with circled Gs (for glycine residues) denote the flexible loops connecting M2 to the rest of the protein. (A, from Unwin N [2005] *J Mol Biol* 346:967–989. With permission from Elsevier Inc. B, adapted from Miyazawa A Fujiyoshi Y, & Unwin N [2003] *Nature* 423:949–955. With permission from Springer Nature.)

linear *I–V* curve in Figure 3-17C. Rather, the open probability of muscle AChR channels is increased by ACh binding. The muscle AChR is therefore called a **ligand-gated ion channel** and is the prototype of a large family of such channels (Table 2-2). Most ligands of these channels are extracellular neurotransmitters such as ACh; however, some channels are gated by intracellular signaling molecules.

3.14 Neurotransmitter receptors are either ionotropic or metabotropic

Following the pioneering work on vertebrate skeletal muscle AChRs, receptors for several other neurotransmitters were found to be ion channels. All neurotransmitter-gated ion channels in vertebrates belong to one of three families. GABA-, glycine-, and serotonin-gated ion channels are in the same family as muscle AChRs (**Figure 3-21**, left), with five subunits each possessing four transmembrane segments. Glutamate-gated ion channels constitute a second family, with four subunits each possessing three transmembrane segments (Figure 3-21, middle). Finally, some neurons use ATP as a neurotransmitter, and ATP-gated ion channels are trimers, with each subunit having just two transmembrane segments (Figure 3-21, right).

Neurotransmitter receptors that function as ion channels, allowing rapid communication across the synapse, are also called **ionotropic receptors** (**Figure 3-22**A). For example, the direct gating of muscle AChR channels by ACh allows transmission of electrical signals from presynaptic neuron to postsynaptic muscle within a few milliseconds (Figure 3-1C). Ionotropic receptors are synonymous with the ligand-gated ion channels introduced in the previous section. Both terms encompass receptors that are gated by ligands (neurotransmitters) and conduct ions across the membrane; the decision of which term to use depends on whether channel- or receptor-relevant properties are under discussion.

In contrast to fast-acting ionotropic receptors, **metabotropic receptors** (Figure 3-22B), when activated by neurotransmitter binding, modulate the membrane potential indirectly by triggering intracellular signaling cascades that regulate ion channel conductances. (The intracellular signaling molecules are often referred to as second messengers, as opposed to the first messengers—the extracellular ligands.) Accordingly, they operate over a longer time scale, ranging from tens of milliseconds to seconds. In addition, unlike ionotropic receptors, which are mostly concentrated in the postsynaptic density across the synaptic cleft from the

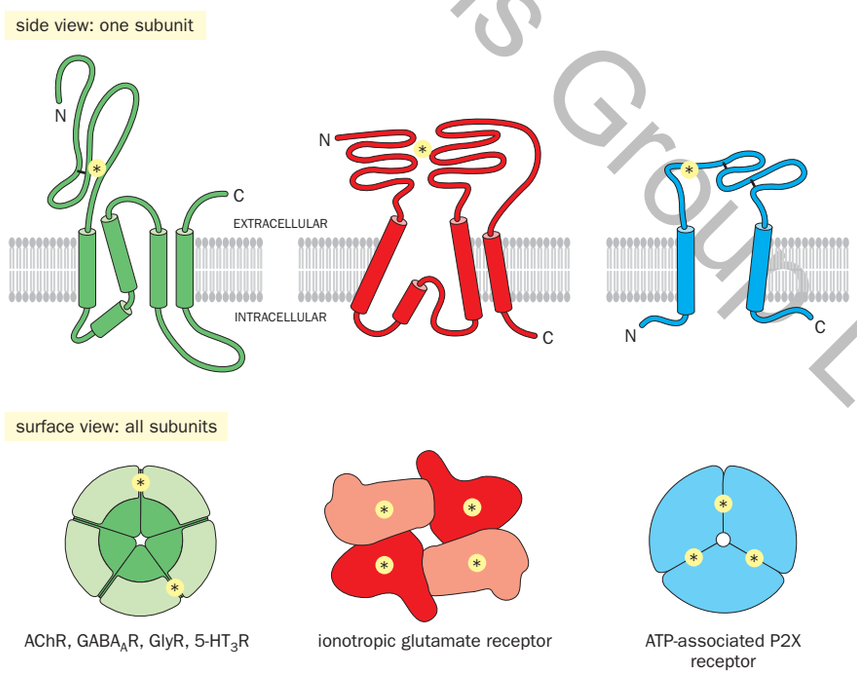

Figure 3-21 Three families of ionotropic receptors in vertebrates. Left, like subunits of the ionotropic AChR (Figure 3-20), subunits of the ionotropic GABA, glycine, and serotonin receptors span the membrane four times. Five subunits constitute a functional receptor with two neurotransmitter-binding sites (stars). Middle, an ionotropic glutamate receptor has four subunits and four neurotransmitter/agonist-binding sites; each subunit spans the membrane three times. Right, an ionotropic P2X receptor consists of three subunits, each spanning the membrane twice. (From Hille [2001] Ion Channels of Excitable Membranes. With permission from Sinauer.)

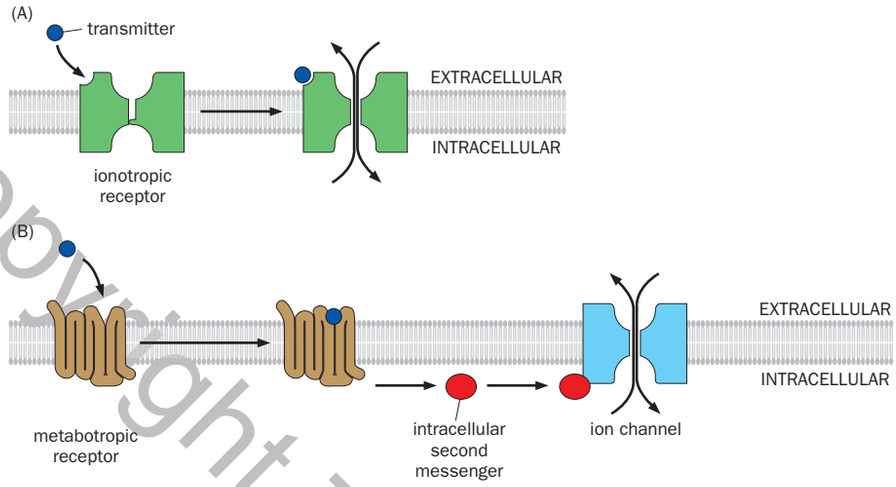

Figure 3-22 Ionotropic and metabotropic neurotransmitter receptors. (A) Ionotropic receptors are ion channels gated by neurotransmitters. Neurotransmitter binding causes membrane potential changes within a few milliseconds. **(B)** Metabotropic receptors act through intracellular second messenger systems to regulate ion channel conductance. Neurotransmitter binding causes membrane potential changes in tens of milliseconds to seconds.

presynaptic active zone, metabotropic receptors are typically not concentrated at the postsynaptic membrane apposing the presynaptic active zone and therefore are termed *extrasynaptic*.

Many neurotransmitters have both ionotropic and metabotropic receptors (**Table 3-3**). For example, ACh can act on metabotropic receptors in addition to the ionotropic AChR we just studied. To distinguish between the two receptor types, we refer to them according to their specific **agonists** (an agonist is an agent that activates a biological process by interacting with a receptor, often mimicking the action of an endogenous molecule). Hence, ionotropic AChRs are also called **nicotinic AChRs** because they are potently activated by nicotine. Nicotinic AChRs are expressed not only in muscles but also in many neurons in the brain, where nicotine acts as an addictive stimulant. Metabotropic AChRs are also called **muscarinic AChRs** because they are activated by muscarine, a compound enriched in certain mushrooms.

In the following sections, we highlight the actions of key ionotropic and metabotropic receptors for major neurotransmitters in the CNS (Table 3-3).

Table 3-3: Ionotropic and metabotropic neurotransmitter receptors encoded by the human genome

Neurotransmitter	Ionotropic		Metabotropic	
	Name	Number of genes	Name	Number of genes
Acetylcholine	Nicotinic ACh receptor	16	Muscarinic ACh receptor	5
Glutamate	NMDA receptor	7	Metabotropic glutamate receptor (mGluR)	8
	AMPA receptor	4		
	Others	7		
GABA	$GABA_A$ receptor	19	$GABA_B$ receptor	2
Glycine	Glycine receptor	5		
ATP	P2X receptor	7	P2Y receptor	8
Serotonin (5-HT)	$5\text{-}HT_3$ receptor	5	$5\text{-}HT_{1,2,4,6,7}$ receptors	13
Dopamine			Dopamine receptor	5
Norepinephrine (epinephrine)			α-adrenergic receptor	6
			β-adrenergic receptor	3
Histamine			Histamine receptor	4
Adenosine			Adenosine receptor	4
Neuropeptides			Neuropeptide receptors	Dozens

Based on the Guide to Pharmacology database (www.guidetopharmacology.org). Abbreviations: GABA, γ-aminobutyric acid; P2X receptor, ATP-gated ionotropic receptor; P2Y, ATP-gated metabotropic receptor; 5-HT# receptor, serotonin (5-hydroxytryptamine) receptor subtype #; ACh, acetylcholine; NMDA, N-methyl-d-aspartate; AMPA, 2-amino-3-hydroxy-5-methylisoxazol-4-propanoic acid.

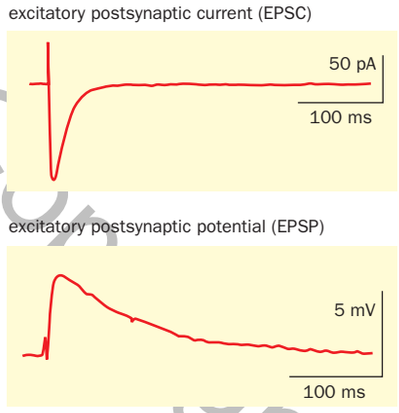

Figure 3-23 Excitatory postsynaptic current and excitatory postsynaptic potential at a glutamatergic synapse. Representative EPSC (top) and EPSP (bottom) recorded using whole-cell patch clamping from hippocampal pyramidal neurons in an *in vitro* slice preparation, in response to electrical stimulation of glutamatergic input axons. The EPSC was recorded in a voltage clamp mode with the membrane potential held at –90 mV, and the EPSP was recorded in a current clamp mode (see Section 14-21 for details). The vertical ticks before the EPSC and EPSP are electrical stimulation artifacts. (Adapted from Hestrin S, Nicoll RA, Perkel DJ, et al. [1990] *J Physiol* 422:203–225.)

3.15 AMPA and NMDA glutamate receptors are activated by glutamate under different conditions

Ionotropic glutamate receptors mediate the fast actions of glutamate, the major excitatory neurotransmitter in the vertebrate CNS. Indeed, glutamatergic excitatory synapses account for the vast majority of synapses in the vertebrate CNS: virtually all neurons—whether they are themselves excitatory, inhibitory, or modulatory—express ionotropic glutamate receptors and are thus excited by glutamate.

Like muscle AChRs, ionotropic glutamate receptors are cation channels permeable to both Na^+ and K^+, with a reversal potential near 0 mV. Under physiological conditions, glutamate binding to ionotropic glutamate receptors produces an inward current called the **excitatory postsynaptic current** (**EPSC**) (**Figure 3-23**, top), as more positively charged ions flow into the cell than out of it. This is analogous to the end-plate current we saw at the NMJ (Figure 3-17). The inward current produces a transient depolarization in the postsynaptic neuron called the **excitatory postsynaptic potential** (**EPSP**) (Figure 3-23, bottom), analogous to the EPP at the NMJ. The recordings shown in Figure 3-23 were made in acutely prepared **brain slices** (fresh sections of brain tissue a few hundred micrometers thick) that preserve local three-dimensional architecture and neuronal connections while allowing experimental access, such as whole-cell recording of individual neurons and control of extracellular solutions.

Historically, ionotropic glutamate receptors have been divided into three subtypes named for their selective responses to three agonists: AMPA (2-amino-3-hydroxy-5-methylisoxazol-4-propanoic acid), kainate (kainic acid), and NMDA (*N*-methyl-D-aspartate). Molecular cloning of these receptors revealed that they are encoded by distinct gene subfamilies of ionotropic glutamate receptors (Table 3-3). Because the properties of **AMPA receptors** and **kainate receptors** are more similar to each other, they are collectively called non-NMDA receptors; **NMDA receptors** have distinctive properties. In the following we use the AMPA and NMDA receptors to illustrate these differences.

AMPA receptors are fast glutamate-gated ion channels that conduct Na^+ and K^+; depending on subunit composition, some AMPA receptors are also permeable to Ca^{2+} (see the next section). They mediate synaptic transmission at most glutamatergic synapses when the postsynaptic neuron is near the resting potential. Because the driving force of Na^+ is much greater than that of K^+ near the resting potential, AMPA receptor opening causes a net influx of positively charged ions, resulting in depolarization of postsynaptic neurons (**Figure 3-24**A).

NMDA receptors have two unusual properties. First, they must be bound to two distinct ligands (glutamate and glycine) to open. However, their glycine binding site is a high-affinity site and so may already be bound at ambient extracellular glycine levels. Second, NMDA receptors do not open unless the postsynaptic membrane is depolarized. The mechanism of voltage dependence is different from that of the voltage-gated Na^+ and K^+ channels discussed in Chapter 2. At the extracellular face of the membrane, the mouth of the NMDA receptor is blocked by Mg^{2+} at negative membrane potentials, such that the channel remains closed despite glutamate binding (Figure 3-24A). However, depolarization of the postsynaptic membrane relieves the Mg^{2+} block (Figure 3-24B). In the absence of external Mg^{2+}, the NMDA receptor conductance is not affected by the membrane potential, as can be seen by the nearly linear *I–V* curve (Figure 3-24C, blue line), similar to the *I–V* curve for nicotinic AChR (Figure 3-17C). By contrast, under physiological external Mg^{2+} conditions, the conductance is greatly reduced when the membrane potential is negative (Figure 3-24C, red line). Thus, the NMDA receptor acts as a **coincidence detector**, opening only in response to concurrent presynaptic glutamate release *and* postsynaptic depolarization. This property is very important for synaptic plasticity and learning, as well as for activity-dependent wiring of the nervous system, as we will learn in Chapters 5 and 11. Once opened, NMDA receptors have high Ca^{2+} conductance. While AMPA receptors provide initial depolarizations to release the Mg^{2+} block of nearby NMDA receptors—these

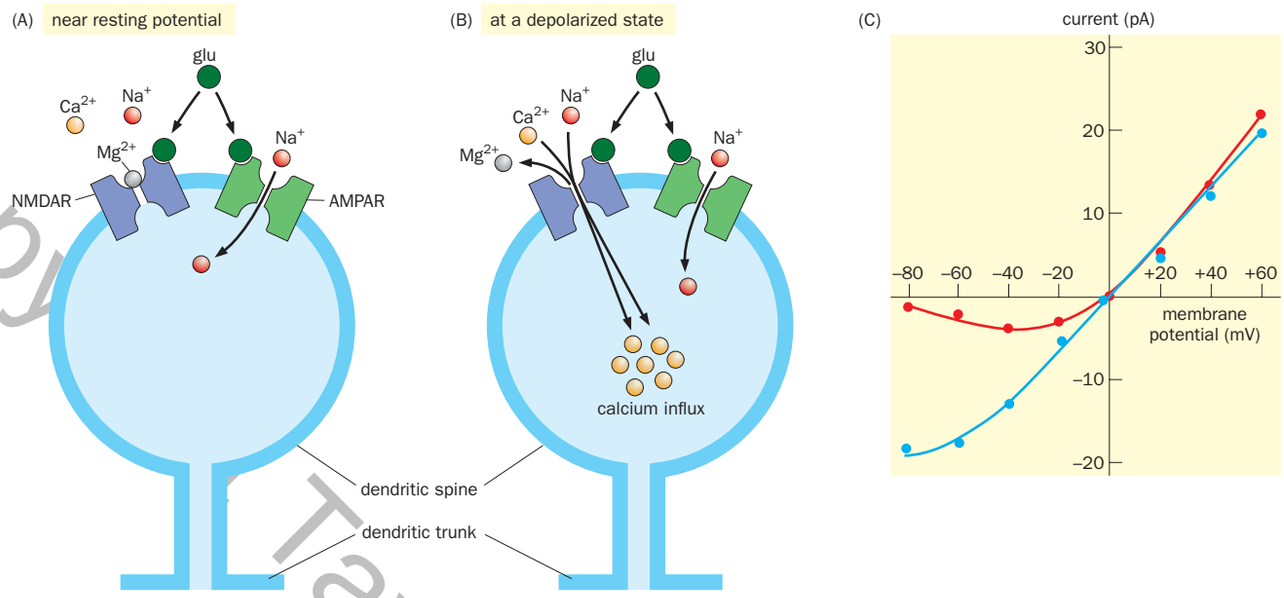

Figure 3-24 Properties of AMPA and NMDA glutamate receptors. **(A)** When the postsynaptic neuron (represented by a dendritic spine) is near the resting potential, glutamate (glu) released from the presynaptic neuron opens only the AMPA receptor (AMPAR), causing Na^+ entry and producing excitatory postsynaptic potentials (EPSPs). The NMDA receptor (NMDAR) is blocked by external Mg^{2+} and therefore cannot be opened by glutamate binding alone. **(B)** When the postsynaptic neuron is depolarized, the Mg^{2+} block is relieved. Both NMDAR and AMPAR can now be opened by glutamate binding. The NMDAR is highly permeable to Ca^{2+}. For simplicity, the small K^+ efflux through open AMPARs and NMDARs is omitted. **(C)** Current–voltage relationship of the NMDAR in the presence or absence of external Mg^{2+}. Blue curve, the nearly linear slope of the *I–V* curve indicates that the conductance of the NMDAR in Mg^{2+}-free media is nearly constant between –60 mV and +60 mV, revealing that the NMDAR is not gated by voltage per se. Red curve, physiological concentrations of extracellular Mg^{2+} markedly diminish the inward current at negative membrane potentials, as Mg^{2+} blocks cation influx. Data were obtained using whole-cell recording of cultured mouse embryonic neurons. (A & B, adapted from Cowan WM, Südhof TC, & Stevens CF [2001] Synapses. Johns Hopkins University Press. C, adapted from Nowak L Bregestovski P, & Ascher P [1984] *Nature* 307:462–465. With permission from Springer Nature. See also Mayer ML, Westbrook GL, & Guthrie PB [1984] *Nature* 309:261–263.)

two glutamate receptors are often co-localized to the same postsynaptic site—NMDA receptors contribute additional depolarization alongside AMPA receptors. Furthermore, Ca^{2+} influx via NMDA receptors contributes to many biochemical changes in postsynaptic cells, as will be discussed later in the chapter.

3.16 Properties of individual ionotropic glutamate receptors are specified by their subunit compositions

All ionotropic glutamate receptors have four subunits (Figure 3-21). Each subunit consists of several modular domains (**Figure 3-25A**): an amino terminal domain, a ligand-binding domain, a transmembrane domain comprising three membrane-spanning helices (M1, M3, and M4) and an additional pore loop (M2), and a carboxy-terminal intracellular domain. AMPA receptors can form functional homotetramers (composed of four identical subunits) although they are usually found *in vivo* as heterotetramers of two or more of the four variants, GluA1, GluA2, GluA3, and GluA4. Comparisons of cryo-EM structures of GluA2 homotetramers in closed and open states revealed that glutamate binding results in a large conformational change featuring closing of the clamshell-like structure of the ligand-binding domain. This change leads the opening of two gates in the ion conductance pore formed by the M3 and M2 helices, respectively (Figure 3-25B).

NMDA receptors are obligatory heterotetramers composed of two **GluN1** subunits and two **GluN2** subunits. (Some neurons express NMDA receptors containing GluN3 subunits instead of GluN2 subunits.) GluN1 is encoded by a single gene, whereas GluN2 has four variants, GluN2A, GluN2B, GluN2C, and GluN2D, encoded by four separate genes. Glutamate and glycine bind to GluN2 and GluN1 subunits, respectively, which triggers the opening of the ion channel.

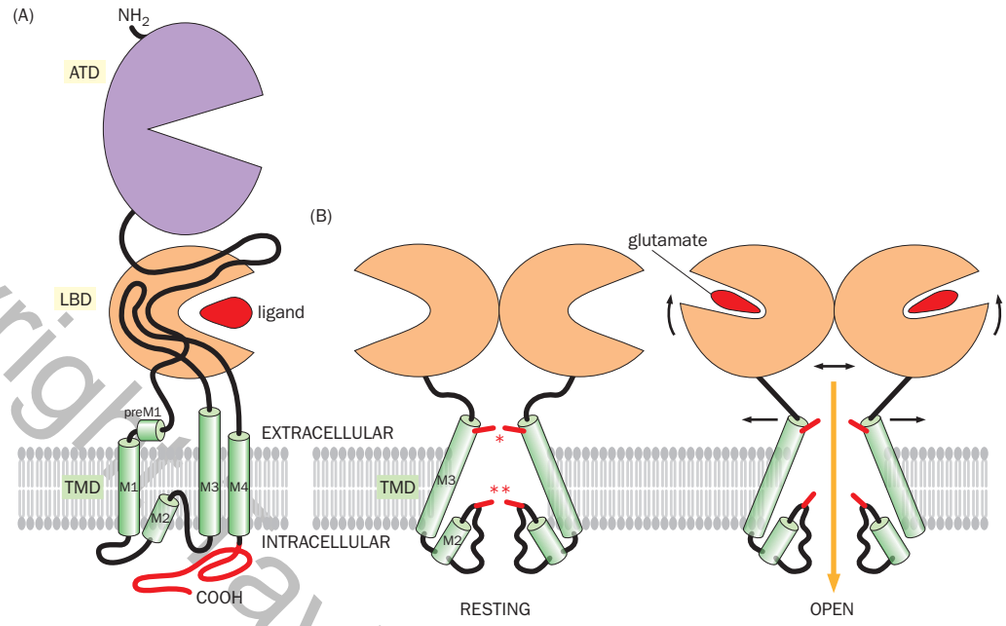

Figure 3-25 AMPA receptor structure and activation mechanism. **(A)** All ionotropic glutamate receptor subunits comprise an amino-terminal domain (ATD), a ligand-binding domain (LBD), a transmembrane domain (TMD), and a carboxy-terminal intracellular domain (red). The line represents the polypeptide chain from the extracellular amino terminus (NH_2) to the intracellular carboxy-terminus (COOH). The M1–M4 cylinders represent helices that span across (M1, M3, M4) or loop into (M2) the plasma membrane. The schematic is based on the crystal structure of a homotetramer of GluA2. **(B)** Schematic summary of the AMPA receptor activation mechanism, based on comparisons of cryo-EM structures of homotetrameric GluA2 structures with the ion conduction pore in the closed and open states (these states were trapped when GluA2 was in complex with different auxiliary proteins in the absence or presence of agonists). Glutamate binding induces closure of the LBD clamshells, leading to conformational changes (indicated by arrows) transduced to the M3 and M2 membrane helices and opening of the upper (*) and lower (**) gates of the ion conduction pore. Only two subunits are shown; ATDs are omitted from this schematic. (A, adapted from Sobolevsky AI, Rosconi MP, & Gouaux E [2009] *Nature* 462:745–756. With permission from Springer Nature. B, adapted from Twomey EC, Yelshanskaya MV, Grassucci RA, et al. [2017] *Nature* 549:60–65. With permission from Springer Nature. See also Chen S, Zhao Y, Wang Y, et al. [2017] *Cell* 170:1234–1246.)

The subunit composition of both AMPA and NMDA receptors has important functional consequences. For example, most AMPA receptors contain the GluA2 subunit; most GluA2-containing AMPA receptors are impermeable to Ca^{2+} due to a posttranscriptional modification called **RNA editing**, which changes the mRNA sequence encoding a key residue in GluA2's channel pore (see Figure 3-26A). AMPA receptors lacking GluA2 or containing unedited GluA2 subunits are permeable to Ca^{2+} (though not as permeable as NMDA receptors). AMPA receptors lacking GluA2 are also susceptible to voltage-dependent block by intracellular polyamines, preventing Na^+ influx when the neuron becomes depolarized. These AMPA receptors are thus inwardly rectified, like the inward-rectifier K^+ channels we discussed in Box 2-4. NMDA receptors containing different GluN2 variants also have distinct channel conductances and cytoplasmic signaling properties, and bind differentially to postsynaptic scaffold proteins (see the next section). Combining different subunits thus allows both AMPA and NMDA receptors to exhibit a rich repertoire of functional and regulatory properties. Indeed, the subunit compositions of AMPA and NMDA receptors differ in different types of neurons. The subunit composition of these receptors within the single neuronal type also undergoes developmental changes and can be regulated by synaptic activity.

Cell-surface expression and physiological properties of AMPA receptors are regulated by **transmembrane AMPA receptor regulatory proteins** (**TARPs**), which are intimately associated with the pore-forming subunits of the AMPA receptor channel and are thus called auxiliary subunits of the AMPA receptor (**Figure 3-26**A). The first TARP was discovered by investigating the physiological

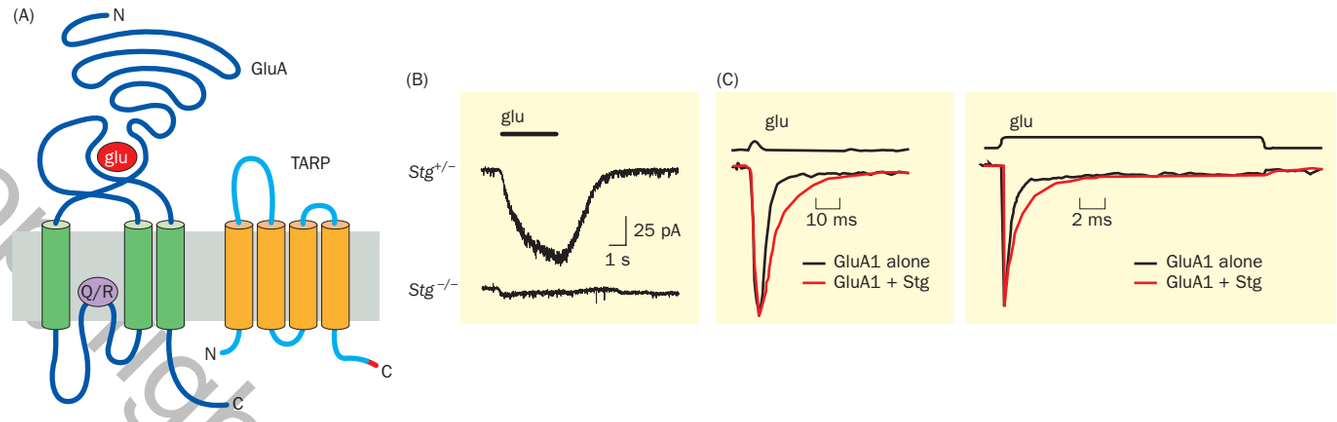

Figure 3-26 Transmembrane AMPA receptor regulator proteins (TARPs). (A) Schematic of TARP next to a pore-forming subunit of the AMPA receptor (GluA). Each TARP subunit consists of four transmembrane segments. The C-terminal tip contains a PDZ binding motif (red; see Section 3.17 for PDZ proteins). Recent cryo-EM-based structural studies indicate that each tetrameric AMPA receptor can associate with 1–4 TARP subunits. The Q/R site represents the amino acid change from glutamine (Q) to arginine (R) due to RNA editing. **(B)** Whole-cell recordings of cerebellar granule cells in slice; membrane potential was held at –80 mV. Glutamate (glu) application results in a large EPSC in the *Stargazer* heterozygous ($Stg^{+/-}$) neuron. EPSC is largely absent in the homozygous mutant ($Stg^{-/-}$) neuron. **(C)** Excised patch recordings (see Box 14-3 for details of this method) from *Xenopus* oocyte expressing GluA1 alone or co-expressing GluA1 and Stargazin (Stg). Stargazin slows down deactivation (how fast the channel closes after a short pulse of glutamate; left) and desensitization (how fast the channel closes in response to prolonged glutamate application; right) of the AMPA receptor channel. (A, adapted from Jackson AC & Nicoll AN [2011] *Neuron* 70:178–199. With permission from Elsevier. B, adapted from Chen L, Chetkovich DM, Petralia RS, et al. [2000] *Nature* 408:936–943. With permission from Springer Nature. C, from Tomita S, Adesnik H, & Sekiguchi M, et al. [2005] *Nature* 435:1052–1058.)

deficits in the *Stargazer* mutant mouse, so named because mutant mice exhibit unusual, repeated head elevations. AMPA receptor-mediated excitatory postsynaptic currents were found to be virtually absent in *Stargazer* mutant cerebellar granule cells (Figure 3-26B). Further investigation indicated that Stargazin, the protein encoded by the *Stargazer* gene, has a multitude of functions: (1) it regulates the trafficking of the AMPA receptor from ER to the cell surface, (2) it helps anchor the AMPA receptor to the postsynaptic density scaffold (see the next section), and (3) it regulates a variety of physiological properties of the AMPA receptor, such as slowing the deactivation and desensitization time course (Figure 3-26C), allowing more inward current through the channel in response to the same amount of glutamate release. Most neurons express multiple TARPs. Cerebellar granule cells are an exception in that Stargazin is the only TARP expressed there; thus mutation of this single gene led to dramatic effects. TARPs have also been found in *C. elegans*. *C. elegans* TARPs can substitute for Stargazin in modifying receptor function, suggesting evolutionary conservation of TARPs. AMPA receptor auxiliary subunits belonging to gene families other than TARPs have since been identified, as have auxiliary proteins for the NMDA and kainate receptors.

3.17 The postsynaptic density is organized by scaffold proteins

Just as the presynaptic terminal is highly organized by active-zone scaffold proteins, the postsynaptic density is highly organized by postsynaptic proteins. At glutamatergic synapses, for example, the postsynaptic density consists of not only glutamate receptors but also other associated proteins (**Figure 3-27**). These include (1) trans-synaptic adhesion proteins that align active zones with postsynaptic densities (see also Section 3.7), (2) proteins that participate in signal transduction cascades, and (3) a diverse array of scaffold proteins that connect glutamate receptors and trans-synaptic adhesion molecules to signaling molecules and cytoskeletal elements. The resulting protein network controls glutamate receptor localization, density, trafficking, and signaling, all of which affect synaptic transmission and synaptic plasticity. Synaptic scaffolds are also present in

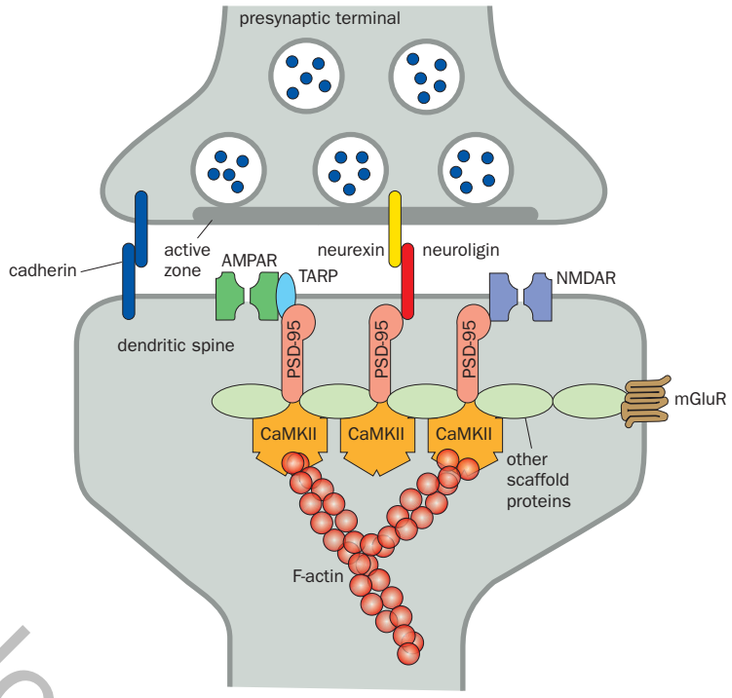

Figure 3-27 The organization of the postsynaptic density at glutamatergic synapses. At the cell surface, the postsynaptic density of a mature glutamatergic synapse is enriched in AMPA and NMDA receptors (AMPAR and NMDAR) as well as trans-synaptic cell adhesion molecules like cadherins and neuroligins (which, respectively, bind presynaptic cadherins and neurexins; Figure 3-10). The scaffold proteins of the PSD-95 family, named for their localization to the postsynaptic density and molecular weight, bind many proteins, including the GluN2 subunit of the NMDAR, AMPAR-associated TARPs, the neuroligin synaptic adhesion molecules, the signal-transducing enzyme CaMKII, and other scaffold proteins that bind metabotropic glutamate receptors (mGluRs) and other postsynaptic density proteins (not shown). The diagram depicts only a small subset of known components and interactions in the postsynaptic density. (Adapted from Sheng M & Kim E [2011] *Cold Spring Harb Perspect Biol* 3:a005678.)

GABAergic postsynaptic terminals; GABAergic and glutamatergic postsynaptic densities utilize common as well as unique scaffold proteins. We will learn more about the postsynaptic density protein network in the contexts of development and synaptic plasticity in Chapters 7 and 11, respectively, and how its dysfunction contributes to brain disorders in Chapter 12.

We use one of the most abundant scaffold proteins at the glutamatergic synapse, **PSD-95** (postsynaptic density protein-95 kDa), to illustrate the organizational role of scaffold proteins in dendritic spines, where glutamatergic synapses are usually located (Figure 3-27). PSD-95 contains multiple protein–protein interaction domains, including three **PDZ domains**, which bind C-terminal peptides with a sequence motif that occurs in many transmembrane receptors. (PDZ is an acronym for three proteins that share this domain: PSD-95, identified from biochemical analysis of the postsynaptic density; Discs-large, which regulates cell proliferation in *Drosophila* and is also associated with the postsynaptic density; and ZO-1, an epithelial tight junction protein.) These protein–protein interaction domains enable PSD-95 to bind directly to the GluN2 subunit of the NMDA receptor, AMPR receptor auxiliary subunits (TARPs; Figure 3-26), the trans-synaptic adhesion molecule neuroligin, and Ca^{2+}/calmodulin-dependent protein kinase II (CaMKII, an enzyme highly enriched in postsynaptic densities, whose role in signal transduction will be introduced in Section 3.20). PSD-95 also binds other PDZ-domain-containing scaffold proteins that in turn associate with other postsynaptic components such as metabotropic glutamate receptors and the actin cytoskeleton. Thus, the scaffold protein network stabilizes neurotransmitter receptors at the synaptic cleft by placing them close to the trans-synaptic adhesion complex apposing the active zone (Figure 3-10). It also brings enzymes (for example, CaMKII) close to their upstream activators (for example, Ca^{2+} entry through NMDA receptors) and downstream substrates, and organizes the structure of the dendritic spine by bridging the trans-synaptic adhesion complex and the underlying actin cytoskeleton. Recent studies suggest that PSD scaffold proteins exhibit a property called "liquid–liquid phase separation," where multivalent interactions among PSD proteins cause them to self-organize into a separate phase in solution. This property likely contributes to the PSD organization *in vivo*.

3.18 Ionotropic GABA and glycine receptors are Cl^- channels that mediate inhibition

The role of inhibition in nervous system function was first established in the study of spinal cord reflexes over a century ago (Section 1.9). In the 1950s, when intracellular recording techniques were applied to the study of spinal motor neurons, it was found that stimulating certain input resulted in a rapid hyperpolarization (termed an **inhibitory postsynaptic potential** or **IPSP**) due to outward current flow across the motor neuron membrane (called an **inhibitory postsynaptic current** or **IPSC**). In a revealing experiment (**Figure 3-28**), researchers set the membrane potential of the motor neuron at different initial values by injecting different constant currents through an electrode, and the membrane potential was measured by a second electrode in response to stimulation of an inhibitory input. When the initial membrane potential was equal to or more depolarized than the resting potential of about –70 mV, stimulation of the inhibitory input caused hyperpolarization, but when the initial membrane potential was more hyperpolarized than –80 mV, stimulation of the inhibitory input produced depolarization. The reversal potential of around –80 mV is close to the equilibrium potential for Cl^- (E_{Cl}), suggesting that the IPSC is carried by Cl^- flow. Indeed, by increasing intracellular Cl^- concentration, the reversal potential became less negative following the change in E_{Cl}, as predicted by the Nernst equation. This experiment suggested that inhibition of the spinal motor neuron is mediated by an increase in Cl^- conductance across the motor neuron membrane.

Subsequent studies have shown that the fast IPSC/IPSP is mediated by the neurotransmitters glycine (used by a subset of inhibitory neurons in the spinal cord and brainstem) and GABA (used by most inhibitory neurons), which act on ionotropic **glycine receptors** and **$GABA_A$ receptors**, respectively. The structure of $GABA_A$ receptors is similar to that of nicotinic AChRs (Figure 3-20), comprising a pentamer with two α subunits, two β subunits, and one γ subunit. Each subunit has multiple isoforms encoded by different genes (Table 3-3), and other subunits such as δ and ε can be used in lieu of γ. Many pharmaceutical drugs act on $GABA_A$ receptors to modulate inhibition in the brain. As we will learn in Chapter 12, the most widely used anti-epilepsy, anti-anxiety, and sleep-promoting drugs all bind to and enhance the functions of $GABA_A$ receptors. Glycine receptors also make up a pentamer. Both $GABA_A$ and glycine receptors are ligand-gated ion channels selective for anions, primarily Cl^-.

How does an increase in Cl^- conductance resulting from the opening of $GABA_A$ or glycine receptor channels on postsynaptic neurons cause inhibition? In most neurons, E_{Cl} is slightly more hyperpolarized than the resting potential, as in the spinal motor neurons we just studied. Thus, an increase in Cl^- conductance causes Cl^- influx (which is equivalent to an outward current because Cl^- carries a negative charge), resulting in a small hyperpolarization (**Figure 3-29**A, left panel). Importantly, if the neuron also simultaneously receives an excitatory input that produces an EPSP (for example, via opening of glutamate receptor channels), the more depolarized membrane potential enhances the driving force for Cl^- influx. This increases the outward current triggered by GABA, which counters the EPSP-producing inward current, making it more difficult for the cell's membrane potential to reach the threshold for firing action potentials (Figure 3-29A, middle and right panels).

The interaction of excitatory and inhibitory input can also be modeled by an electrical circuit wherein each input is represented by a branch consisting of a switch (representing neurotransmitter release), a conductance (g_e or g_i, representing EPSC or IPSC conductance), and a battery (representing the reversal potential for the excitatory glutamate receptors, $E_{e\text{-}rev}$, or the $GABA_A$ receptor, E_{Cl}). When only the inhibitory input is switched on, because E_{Cl} is more hyperpolarized than the resting potential (E_r), a small outward current will be produced by the g_i branch, resulting in a small hyperpolarizing IPSP (Figure 3-29B, left). When only the excitatory input is switched on, a large inward current will be produced by the g_e branch, as $E_{e\text{-}rev}$ is much more depolarized than E_r, resulting in a large depolarizing EPSP (Figure 3-29B, middle). When both the excitatory and inhibitory

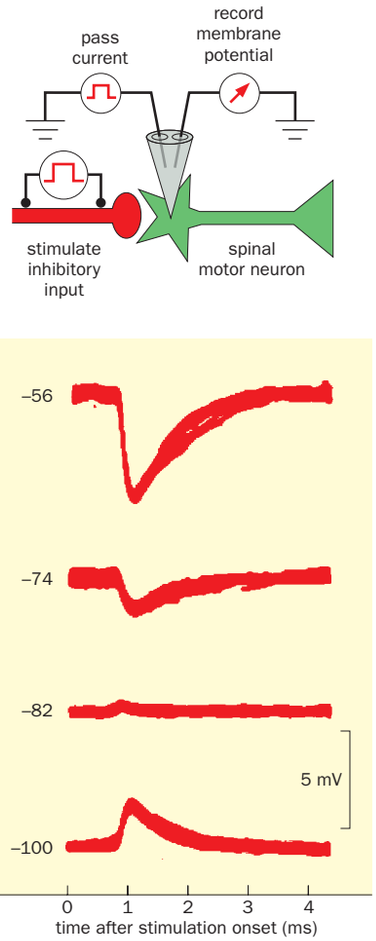

Figure 3-28 Inhibitory postsynaptic potentials (IPSPs). Top, experimental setup. Two electrodes were inserted into a spinal motor neuron, one for passing current to change the holding membrane potential and the other to measure the membrane potential in response to electrical stimulation of an inhibitory input. (The schematic is simplified; the sensory afferent from an antagonist muscle was stimulated, which inhibits the recorded motor neuron through intermediate inhibitory interneurons; see Figure 1-19.) Bottom, IPSPs recorded at four different holding membrane potentials. Each record represents the superposition of about 40 traces. At membrane potentials of –74 mV or above, stimulation of inhibitory input resulted in hyperpolarizing IPSPs, with increasing amplitudes as holding membrane potentials became less negative. At membrane potentials of –82 mV or below, stimulation of inhibitory input resulted in depolarizing IPSPs, with increasing amplitudes as holding membrane potentials became more negative. (Graphs adapted from Coombs JS, Eccles JC, & Fatt P [1955] *J Physiol* 130:326–373.)

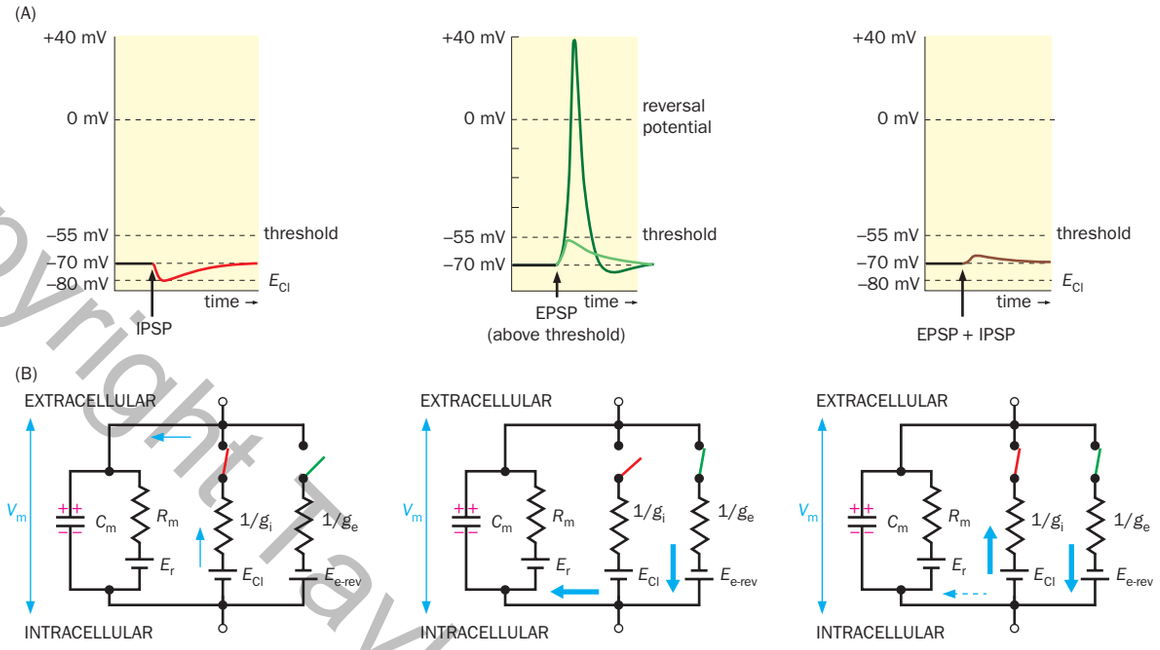

Figure 3-29 The inhibitory effect of Cl^- conductance mediated by $GABA_A$ receptors. (A) In this neuron, the Cl^- equilibrium potential, E_{Cl}, is slightly more hyperpolarized than the resting potential. Left, an IPSP from $GABA_A$ receptors causes hyperpolarization of this postsynaptic neuron toward E_{Cl}. Middle, an EPSP from glutamate receptors causes depolarization of the postsynaptic neuron, as the reversal potential (~0 mV) is far above the resting potential. If the EPSP amplitude exceeds the threshold, it produces an action potential. Right, an IPSP can cancel the effect of an EPSP when excitatory and inhibitory inputs are present at the same time, thus preventing postsynaptic firing. **(B)** Circuit models for the three scenarios in Panel A. Two branches, representing inhibitory and excitatory neurotransmitter receptors with conductances of g_i and g_e when neurotransmitter binding opens the receptor channels, are added to the resting neuronal model represented by the membrane capacitance (C_m), resistance (R_m), and resting potential (E_r). Left, when only the inhibitory branch is switched on (GABA release activating $GABA_A$ receptors), a small outward current results (upward arrow) because E_{Cl} is more hyperpolarized than E_r. This causes more charge to build up at C_m, thus hyperpolarizing the membrane potential (V_m). Middle, when only the excitatory branch is switched on (glutamate release activating glutamate receptors), a large inward current results (downward arrow) because the reversal potential for the excitatory ionotropic glutamate receptors ($E_{e\text{-}rev}$) is far more depolarized than E_r. This causes discharge of C_m, thus depolarizing the membrane potential. Right, when both the inhibitory and excitatory branches are switched on (GABA and glutamate released at the same time), a large fraction of the inward current in the excitatory branch is diverted by the outward current in the inhibitory branch. As a result, the current discharging C_m (dashed arrow) is smaller. (Note that the more depolarized V_m is, the larger the outward current is, because of the larger driving force for Cl^-).

inputs are switched on, part of the inward current in the g_e branch will flow outward through the g_i branch (Figure 3-29B, right), leading to a smaller depolarization than when the g_e branch is active alone. Indeed, as can be seen from the circuit model, even when E_{Cl} equals E_r, meaning that no net Cl^- influx or efflux occurs at rest, $GABA_A$ receptor opening creates an extra path (an extra conductance) that tends to hold the membrane potential near E_{Cl}, counteracting the inward current created by excitatory inputs, and thereby diminishing the voltage change across the membrane. This so-called shunting contributes to GABA's potent inhibitory effect.

A noteworthy exception to GABA's inhibitory effects can occur in developing neurons. The intracellular Cl^- concentration is high in many developing neurons because their Cl^- transporters (Figure 2-12B) are not yet expressed at a high level as in mature neurons. When the intracellular Cl^- concentration is high, E_{Cl} is substantially more depolarized than the resting potential, such that an increase in Cl^- conductance results in Cl^- efflux, causing depolarization that can exceed the threshold for action potential generation. Under these circumstances, GABA may thus act as an excitatory neurotransmitter.

As we will learn soon, another inhibitory action of GABA is mediated by metabotropic **$GABA_B$ receptors**, which act through intracellular signaling pathways to cause the opening of K^+ channels. Because E_K is always more negative than the resting potential, opening of K^+ channels always causes hyperpolariza-

tion, making the neurons less likely to reach the threshold for an action potential in response to excitatory input.

3.19 Metabotropic neurotransmitter receptors trigger G protein cascades

We now turn to metabotropic receptors, which act through intracellular signaling pathways rather than mediating ion conduction directly (Figure 3-22B). These receptors, which belong to the **G-protein-coupled receptor** (**GPCR**) superfamily, participate in signaling cascades involving a heterotrimeric guanine nucleotide-binding protein (**trimeric GTP-binding protein**, or simply **G protein**). ACh, glutamate, and GABA all bind to their own metabotropic receptors: muscarinic AChRs, metabotropic GluRs (mGluRs), and $GABA_B$ receptors, respectively, each with several variants. Other GPCRs include the receptors for dopamine, norepinephrine, serotonin (most subtypes), ATP (P2Y subtypes), adenosine, and neuropeptides (Table 3-3) as well as sensory receptors for vision and olfaction and a subset of taste receptors, which we will study in Chapters 4 and 6. Indeed, GPCRs, encoding receptors with diverse functions, constitute the largest gene family in mammals (**Figure 3-30**). GPCRs are crucial for neuronal communication, responses to external stimuli, and many other physiological processes. As a result, they are targets of many pharmaceutical drugs.

All GPCRs possess seven transmembrane helices (**Figure 3-31**A), and almost all are activated by binding of specific extracellular ligands. (A notable exception is rhodopsin in photoreceptors, which is activated by light absorption, as will be discussed in greater detail in Chapter 4.) Ligand binding triggers conformational changes in the transmembrane helices and allows the cytoplasmic domain to associate with a trimeric G protein complex consisting of three different subunits: **Gα**, **Gβ**, and **Gγ** (Figure 3-31B).

Before GPCR activation, the G protein heterotrimer preassembles and binds GDP via the Gα nucleotide-binding site (Figure 3-31C, Resting state). Because Gα and Gγ are both lipid-modified, this ternary complex associates with the plasma membrane. Ligand activation of the GPCR triggers the binding of its cytoplasmic domain to Gα. This stabilizes a nucleotide-free conformation of Gα and thereby catalyzes the replacement of GDP with GTP (Figure 3-31C, Steps 1 and 2). Next, GTP binding causes Gα to dissociate from Gβγ. Depending on the cellular context, Gα-GTP, Gβγ, or both can trigger downstream signaling cascades (Figure 3-31C, Step 3). Gα not only binds to GDP and GTP but also is a **GTPase**, hydrolyzing GTP to GDP. This GTPase activity provides a built-in termination mechanism for G protein signaling (Figure 3-31C, Step 4) and is often facilitated by additional proteins. GDP-bound Gα has a strong affinity for Gβγ, which promotes reassembly of the ternary complex, thereby returning to the resting state (Figure 3-31C, Step 5) and readying the trimeric G protein for the next round of GPCR activation (**Movie 3-3**).

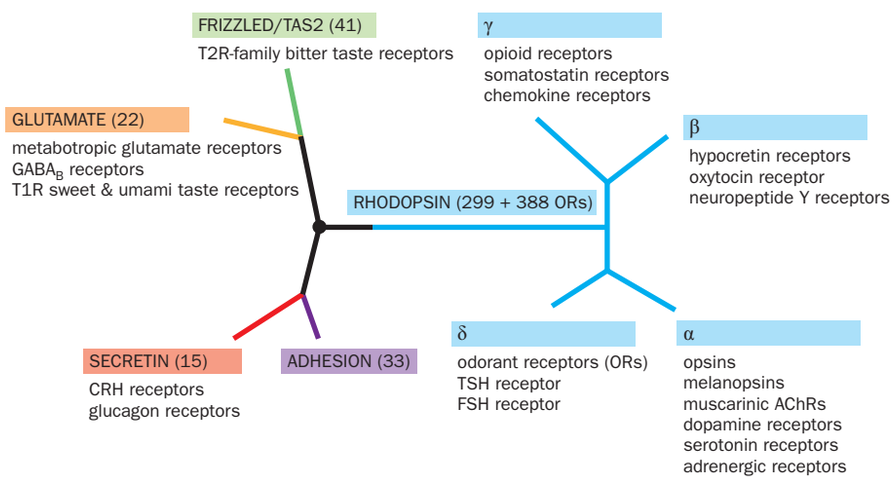

Figure 3-30 G-protein-coupled receptors (GPCRs) in the human genome. The human genome contains about 800 GPCRs separated into five major branches according to the sequence similarities in their transmembrane domains. The dot at the center represents the root of the branches. Numbers in parentheses indicate the number of genes within a specific branch. Names of some representative GPCRs discussed in this book are given. The glutamate branch includes mGluRs and $GABA_B$ receptors as well as sweet and umami taste receptors. The frizzled/TAS2 branch includes bitter taste receptors. The secretin branch includes neuropeptide corticotropin-releasing factor (CRF) receptors involved in stress response. The adhesion branch includes receptors that signal across the synaptic cleft. The largest branch, rhodopsin, is further divided into four clusters. These include many GPCRs important in neurobiology: opsins and melanopsins for vision and receptors for serotonin, dopamine, acetylcholine (muscarinic), and epinephrine/norepinephrine (α cluster); many neuropeptide receptors (β and γ clusters); receptors for thyroid-stimulating hormone (TSH), follicle-stimulating hormones (FSH), and a large number of rapidly evolving odorant receptors (δ cluster). (Based on Fredriksson R, Lagerstrom MC, Lundin LG, et al. [2003] *Mol Pharmacol* 63:1256–1272; Alexander SPS, Christopoulos A, Davenport AP, et al. [2017] *Br J Pharmacol* 174 Suppl 1:S17.)

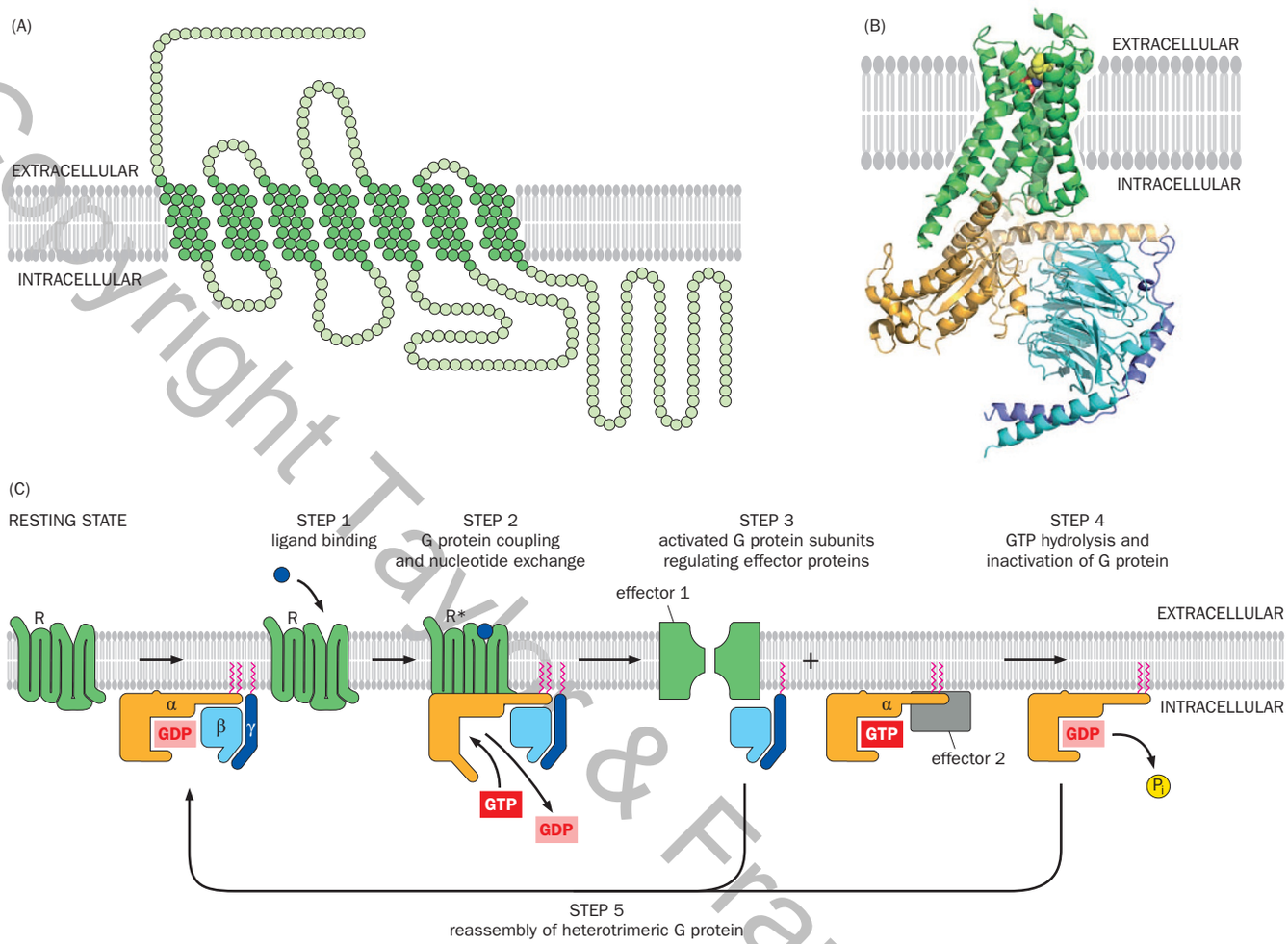

Figure 3-31 Structure and signaling cascade of GPCRs. (A) Primary structure of the β2-adrenergic receptor, the first cloned ligand-gated GPCR. Each circle represents an amino acid. All GPCRs span the lipid membrane seven times, with N-termini on the extracellular side and C-termini on the intracellular side. **(B)** Crystal structure of the β2-adrenergic receptor in complex with trimeric G proteins. Green, β2-adrenergic receptor, with seven transmembrane helices spanning the lipid bilayer; yellow, agonist in its binding pocket; orange, Gα; cyan, Gβ; blue, Gγ. The Gα part in the foreground contains binding sites for GDP/GTP, Gβ, and the β2-adrenergic receptor. The Gα part in the background can swing relative to the part in the foreground, allowing exchange of GDP and GTP. **(C)** Schematic of the GPCR signaling cascade. Resting state, the preassembled trimeric G protein complex in the GDP-bound state associates with the plasma membrane because Gα and Gγ are covalently attached to lipids (zigzag lines). Step 1, ligand binding. Step 2, a conformational change of the GPCR induced by ligand binding (R → R*) creates a binding pocket for Gα. R* (activated GPCR) catalyzes the exchange of GDP for GTP on Gα. Step 3, GTP-bound Gα dissociates from R*, releasing Gα-GTP and Gβγ to trigger their respective effector proteins that transduce and amplify signals; here, effector 1 is an ion channel that binds Gβγ and effector 2 is an enzyme that binds Gα-GTP. Step 4, the intrinsic GTPase activity of Gα converts Gα-GTP to Gα-GDP. Step 5, Gα-GDP reassociates with Gβγ, returning to the resting state. (A, adapted from Dohlman HG, Caron MG, & Lefkowitz RJ [1987] *Biochemistry* 26:2657–2668. B & C, adapted from Rasmussen SG, DeVree BT, Zou Y, et al. [2011] *Nature* 477:549–555. With permission from Springer Nature.)

Such cycling between GTP- and GDP-bound forms is a general signaling mechanism employed by a superfamily of G proteins (**Box 3-3**).

3.20 A GPCR signaling paradigm: β-adrenergic receptors activate cAMP as a second messenger

β-adrenergic receptors (Figure 3-31A, B) have been the most extensively studied ligand-activated GPCRs. They are activated by epinephrine and norepinephrine (also known as adrenaline and noradrenaline, from which the name of the receptors originates). Whereas norepinephrine is produced by neurons and acts as a neurotransmitter in both the CNS and the autonomic nervous system (Section 3.11), **epinephrine** is produced primarily by adrenal chromaffin cells; it circulates through the blood and acts as a hormone, mediating systemic responses to

Box 3-3: G proteins are molecular switches

The G protein cycle outlined in Figure 3-31C is a universal signaling mechanism of GPCRs, which are used in many biological contexts. Indeed, the switch between a GDP-bound form and a GTP-bound form defines the G protein superfamily, which includes not only trimeric G proteins but also small monomeric GTPase families such as the **Rab**, **Ras**, and **Rho** families. These small GTPases resemble part of the Gα subunit of the trimeric G protein. Rab GTPases regulate different steps of intracellular vesicular trafficking (Section 2.1); we encountered a family member, Rab3, in the context of bridging the synaptic vesicle with the presynaptic active zone scaffold proteins (Figure 3-10). The Ras family of GTPases contains key signaling molecules involved in cell growth and differentiation. As will be discussed in Box 3-4, Ras GTPases play crucial roles in transducing signals from the cell surface to the nucleus. Rho GTPases are pivotal regulators of the cytoskeleton; we will study them in the context of growth cone signaling and neuronal wiring in Chapter 5.

All members of the G protein superfamily are molecular switches. For the trimeric G proteins as well as the Ras and Rho families of GTPases, the GDP-bound form is inactive and the GTP-bound form is active in downstream signaling. The transitions between the GTP-bound and GDP-bound forms are usually facilitated by two types of proteins: the **guanine nucleotide exchange factors** (**GEFs**), which switch GTPases *on* by catalyzing the exchange of GDP for GTP, and **GTPase activating proteins** (**GAPs**), which switch GTPases *off* by speeding up the endogenous GTPase activity, converting GTP to GDP (**Figure 3-32**; **Movie 3-4**). As will be discussed in Section 3.23, proper signal termination is an important aspect of signaling.

In the context of trimeric G protein signaling discussed in Section 3.19, ligand-activated GPCRs act as GEFs for the trimeric G proteins. By stabilizing the transition state of the nucleotide-free conformation of Gα (Figure 3-31B), GPCRs catalyze the exchange of GDP for GTP on Gα (Step 2 of Figure 3-31C). The reaction is driven in the direction of Gα-GTP production by the dissociation of Gα-GTP from the GPCR and from Gβγ. We will learn more about GAPs in GPCR signaling in the context of visual transduction in Chapter 4.

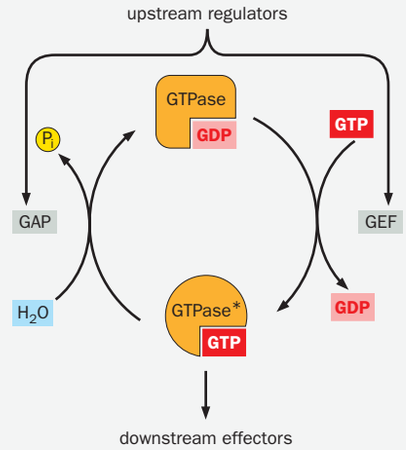

Figure 3-32 The GTPase cycle. GTPases cycle between a GDP-bound form and a GTP-bound form. For signaling GTPases such as trimeric G proteins as well as Ras and Rho subfamilies of small GTPases, the GTP-bound form usually binds effectors and activates downstream signaling. The guanine nucleotide exchange factor (GEF) catalyzes the exchange of GDP for GTP, thus activating the GTPases. The GTPase activating protein (GAP) accelerates the G protein's endogenous GTPase hydrolysis of the bound GTP, thus inactivating the GTPases. GEFs and GAPs are regulated by upstream signals.

extreme conditions, the so-called fright, fight, and flight responses. (A small number of CNS neurons also use epinephrine as a modulatory neurotransmitter.) Classic biochemical studies demonstrated that epinephrine activates β-adrenergic receptors to produce an intracellular second messenger called **cyclic AMP** (**cAMP**). cAMP is synthesized from ATP by a membrane-associated enzyme called **adenylate cyclase** (**Figure 3-33**). In fact, studies of mechanisms by which β-adrenergic receptors activate adenylate cyclase, together with parallel investigations of the signal transduction pathways downstream from rhodopsin activation (to be discussed in Section 4.4), led to the discovery that trimeric G proteins are essential intermediates in GPCR signaling.

Originally identified as a second messenger in the context of epinephrine action, cAMP is a downstream signal for many GPCRs. cAMP can directly gate ion channels, as will be discussed below as well as in Chapters 4 and 6. However, the most widely used cAMP effector is the **cAMP-dependent protein kinase** (also called A-kinase, **protein kinase A**, or **PKA**). PKA is a **serine/threonine kinase**, which means that it adds phosphates onto specific serine or threonine residues of target proteins, thereby changing their properties. PKA comprises two regulatory and two catalytic subunits; in the absence of cAMP, these subunits form an inactive tetramer usually associated with various **AKAPs** (for A-kinase anchoring proteins) located in specific parts of the cell. cAMP binding to the regulatory subunits triggers the dissociation of the catalytic subunits from the regulatory subunits; the catalytic subunits become free to phosphorylate their substrates

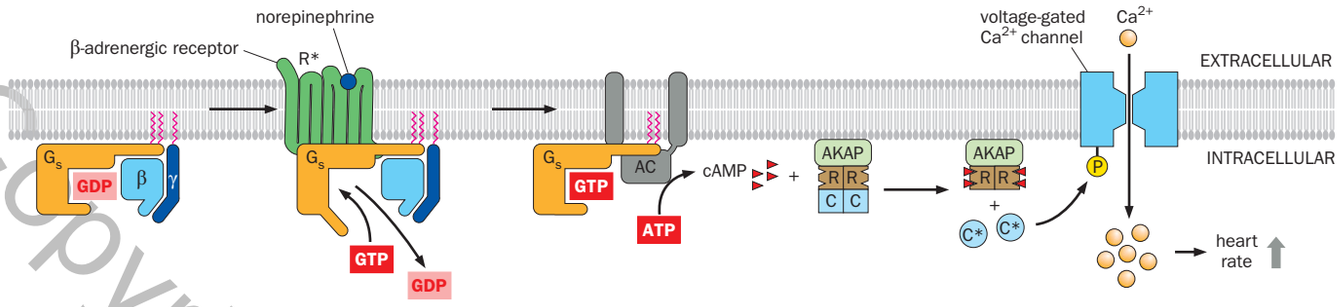

Figure 3-33 Norepinephrine speeds up the heart rate: GPCR signaling through cyclic AMP (cAMP) and protein kinase A (PKA). From left, norepinephrine binding to a β-adrenergic receptor activates G_s, a Gα variant, in cardiac pacemaker cells. G_s-GTP associates with and activates the membrane-bound adenylate cyclase (AC). AC catalyzes the production of cAMP from ATP. cAMP activates PKA. Each PKA consists of two regulatory (R) and two catalytic (C) subunits. Each regulatory subunit contains two cAMP binding sites and is associated with the A-kinase anchoring protein (AKAP). When all four cAMP binding sites on the regulatory subunits are occupied, the catalytic subunits of PKA are released from the complex, become active (C*), and phosphorylate their substrates, such as voltage-gated Ca^{2+} channels. PKA phosphorylation of Ca^{2+} channels increases their open probabilities, facilitates Ca^{2+} influx and depolarization of the pacemaker cells, and thus speeds up heart rate. Note that the central portion of this pathway, from G_s to PKA activation, is widely used in other cellular contexts.

(Figure 3-33; **Movie 3-5**). PKA phosphorylates many substrates with short- or long-lasting effects on neuronal excitability.

As a specific example, we discuss the mechanism by which norepinephrine released from the axon terminals of neurons in the **sympathetic nervous system** (an arm of the autonomic nervous system) speeds up heart rate. In cardiac pacemaker cells, a special type of cardiomyocytes located in the sinoatrial node, norepinephrine binds to and activates a β-adrenergic receptor, which associates with a Gα variant called $\mathbf{G_s}$ (for **stimulatory G protein**). G_s-GTP triggers cAMP production by binding to and activating an adenylate cyclase. Elevated cAMP levels lead to PKA activation. PKA phosphorylates a variety of substrates, including voltage-gated Ca^{2+} channels on the plasma membrane of pacemaker cells, which increases their open probability. Ca^{2+} entry depolarizes pacemaker cells, shortens the duration between action potentials they produce, and thus speeds up heart rate (Figure 3-33). In parallel to PKA activation, cAMPs also bind directly to and open hyperpolarization-activated cyclic nucleotide-gated channels (HCN channels; Box 2-4) in pacemaker cells. Since HCN channels are nonselective cation channels, their opening leads to depolarization of pacemaker cells and increased heart rate. In summary, this signaling cascade provides a paradigm relating how a neurotransmitter (norepinephrine) elicits a physiological response (an increase in heart rate) by binding a metabotropic receptor (β-adrenergic receptor), leading to the activation of a second messenger (cAMP) and its downstream effectors (PKA, voltage-gated Ca^{2+} channels, and HCN channels).

3.21 α and βγ G protein subunits trigger diverse signaling pathways that alter membrane conductance

The human genome encodes 16 Gα, 5 Gβ, and 13 Gγ variants. Their different combinations give rise to myriad trimeric G proteins coupled to different GPCRs that can trigger diverse signaling pathways. For example, in addition to the G_s we just discussed, a variant of Gα called $\mathbf{G_i}$ (for **inhibitory G protein**) also binds adenylate cyclase, but inhibits its activity, causing a decline in intracellular cAMP concentration. Different Gα variants are associated with different receptors and regulate distinct downstream signaling pathways. In postsynaptic neuronal compartments, the ultimate effectors of GPCRs are usually ion channels that regulate membrane potential or neurotransmitter release, most notably K^+ and Ca^{2+} channels (Box 2-4). In the previous section, we discussed a classic example of how norepinephrine activates a Ca^{2+} channel via cAMP and PKA to increase heart rate. In the next two sections, we examine more examples to highlight the diverse outcomes of GPCR signaling.

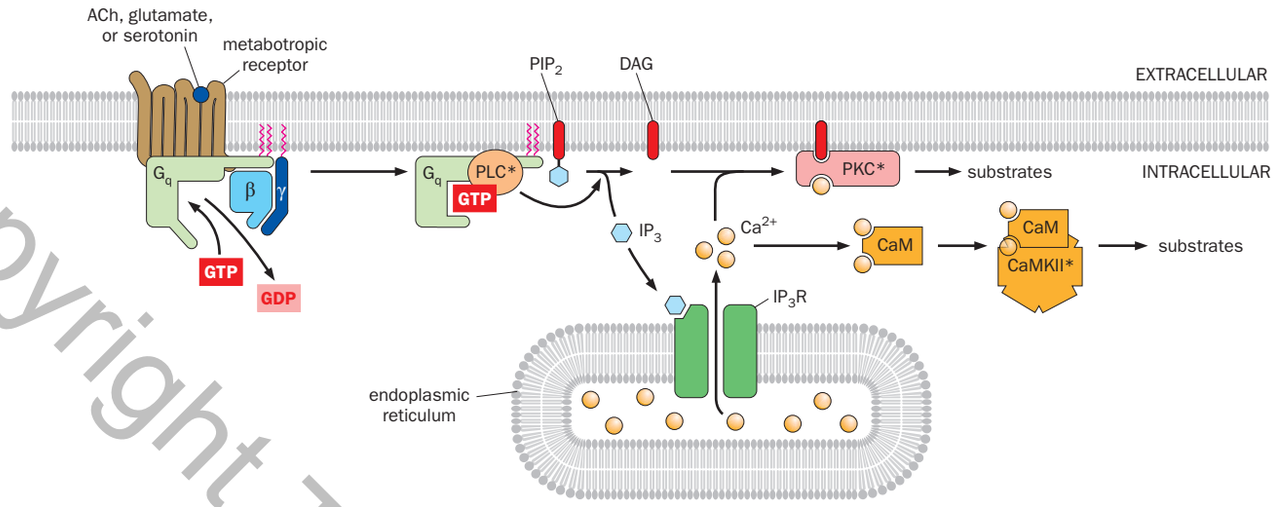

Figure 3-34 GPCR signaling through phospholipase C (PLC) and Ca^{2+}. From left, activation of a variety of metabotropic receptors can activate G_q, a variant of Gα. G_q-GTP in turn activates PLC, which catalyzes the conversion of PIP_2 to DAG and IP_3. IP_3 activates the IP_3 receptor (IP_3R, an IP_3-gated Ca^{2+} channel) on the ER membrane, allowing Ca^{2+} release from ER to the cytosol. DAG and Ca^{2+} co-activate PKC. Ca^{2+} also binds to calmodulin (CaM), and the resulting complex activates CaMKII and other CaM kinases. Asterisks represent activated components.

An important G protein effector of many metabotropic receptors (for example, receptors for acetylcholine, glutamate, and serotonin) is a membrane-associated enzyme called **phospholipase C** (**PLC**) (**Figure 3-34**; **Movie 3-6**). PLC is activated by $\mathbf{G_q}$, a Gα variant. Activated PLC cleaves a membrane-bound phospholipid called PIP_2 (phosphatidyl 4,5-bisphosphate) to produce two important second messengers: **diacylglycerol** (**DAG**) and **inositol 1,4,5-triphosphate** ($\mathbf{IP_3}$). DAG binds to and activates **protein kinase C** (**PKC**), a serine/threonine kinase. PKC activation also requires a rise in intracellular Ca^{2+} concentration. This is achieved via IP_3, which binds to an IP_3-gated Ca^{2+} channel (the **IP_3 receptor**) on the membrane of the endoplasmic reticulum (ER), triggering release of ER-stored Ca^{2+} into the cytosol. In addition to activating PKC, Ca^{2+} interacts with many additional effectors. A key effector is a protein called **calmodulin**. The Ca^{2+}/calmodulin complex can regulate diverse signaling pathways, including the activation of Ca^{2+}/calmodulin-dependent protein kinases (CaM kinases), another important class of serine/threonine kinases. Like PKA, both PKC and CaM kinases phosphorylate many downstream target proteins, including ion channels and receptors, to modulate their activity. A specific subtype of CaM kinases, **CaM kinase II** (**CaMKII**), is one of the most abundant proteins in the postsynaptic density (Section 3.17). Ca^{2+} can also directly increase the open probability of Ca^{2+}-dependent K^+ channels (Box 2-4). Thus, activation of PLC activates PKC and at the same time causes a rise in intracellular Ca^{2+} concentration, both of which can alter neuronal excitability (Figure 3-34).

Historically, Gα was identified as the first signaling intermediate between the GPCR and any effectors. Subsequently, it was found that Gβγ can also mediate signaling, as in the case of acetylcholine regulation of heart rate. In fact, the concept of a chemical neurotransmitter was first established in this context in a classic experiment conducted in 1921 by Otto Loewi. It was known that stimulating the **vagus nerve**, a cranial nerve connecting the medulla to internal organs, slows heart rate. Loewi collected fluid from a frog heart whose vagus nerve had been stimulated, added it to an unstimulated heart, and found that beating of the second heart also slowed. This experiment showed that vagus nerve stimulation released a chemical transmitter, later identified to be acetylcholine, to slow heart rate. (According to Loewi, the initial idea for this experiment came from a dream in the middle of the night. He wrote it down on a piece of paper and went back to sleep. The next morning he remembered dreaming about something important but could not remember what it was or decipher what he had written. The

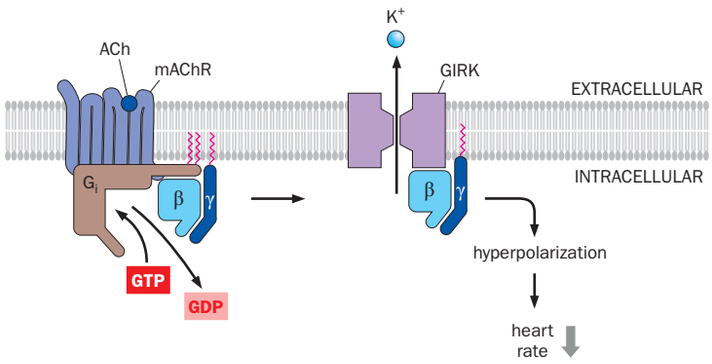

Figure 3-35 Acetylcholine slows down the heart rate: direct action of Gβγ on a K^+ channel. From left, ACh activation of a muscarinic ACh receptor (mAChR) on a cardiac pacemaker cell causes the dissociated Gβγ to bind directly to and activate a G-protein-coupled inward-rectifier K^+ (GIRK) channel, leading to K^+ efflux and hyperpolarization of the pacemaker cell, which slows down heart rate. Based on Clapham DE & Neer EJ [1997] *Annu Rev Pharmacol Toxicol* 37:167–203.)

next night, the dream returned, and this time he got up immediately and went to the lab to perform the experiment.)

Subsequent work has shown that ACh binds to a specific muscarinic AChR and triggers the dissociation of the trimeric G protein complex. βγ subunits then bind to and activate a class of K^+ channels called GIRKs (G-protein-coupled inward-rectifier K^+) channels, resulting in K^+ efflux, hyperpolarization of cardiac pacemaker cells, and a slowing of heart rate (**Figure 3-35**). In addition, the Gα activated by the muscarinic AChR is a G_i variant, which inhibits adenylate cyclase and counteracts the effect of β-adrenergic receptors discussed in Section 3.20.

We have seen that two different neurotransmitters, norepinephrine and ACh, act on different GPCRs, G proteins, and effectors on the same cell to speed up or slow down heart rate, respectively (compare Figures 3-33 and 3-35). These neurotransmitters are used in the two opposing arms of the autonomic nervous system. The sympathetic arm, which uses norepinephrine as a neurotransmitter, and the **parasympathetic** arm, which uses ACh as a neurotransmitter, often have antagonistic functions (see Section 9.1 for more details).

3.22 Metabotropic receptors can act on the presynaptic terminal to modulate neurotransmitter release

In addition to acting on dendrites and cell bodies, metabotropic receptors can also act directly on presynaptic terminals to modulate neurotransmitter release. In the simplest case, neurons can use metabotropic receptors to modulate their own neurotransmitter release, as in the case of sympathetic neurons that release norepinephrine (**Figure 3-36**). The presynaptic terminals of these neurons express α-adrenergic receptors that bind norepinephrine released into the synaptic cleft. Activation of these presynaptic α-adrenergic receptors rapidly inhibits voltage-gated Ca^{2+} channels at the active zone by direct binding of Gβγ to the Ca^{2+} channel, which reduces the depolarization-induced Ca^{2+} entry essential for triggering neurotransmitter release. This negative feedback loop results in diminishing levels of neurotransmitter release, leading to presynaptic depression. This is one of multiple mechanisms of short-term plasticity that alters the probability of neurotransmitter release, as noted in Section 3.10.

A presynaptic terminal of a given neuron can also contain metabotropic receptors for neurotransmitters produced by other neurons. In this case, the presynaptic terminal of a neuron acts as the postsynaptic site for these other neurons (**Figure 3-37**). Depending on the nature of the neurotransmitter, the type of receptor, the signaling pathway, and the final effector, the net effect can either be facilitation or inhibition of neurotransmitter release. Accordingly, these effects are called **presynaptic facilitation** or **presynaptic inhibition**. Presynaptic facilitation can be achieved by closing K^+ channels, which depolarizes the presynaptic membrane potential and facilitates activation of voltage-gated Ca^{2+} channels so that Ca^{2+} entry can trigger neurotransmitter release; we will see an example of this in Chapter 11 where serotonin mediates presynaptic facilitation in the sea slug *Aplysia* to enhance the magnitude of a reflex to a noxious stimulus. Presynaptic

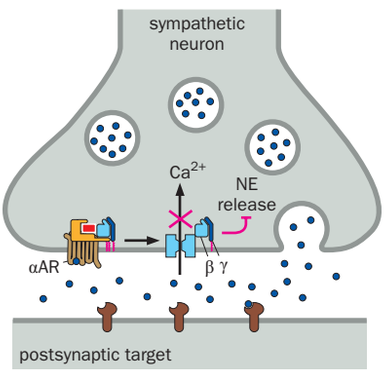

Figure 3-36 Action of norepinephrine on a presynaptic Ca^{2+} channel. From left, released norepinephrine (NE, blue dots) binds and activates a presynaptic α-adrenergic receptor (αAR). Activated Gβγ binds and inhibits the presynaptic voltage-gated Ca^{2+} channel, reducing Ca^{2+} influx in response to depolarization and thereby inhibiting neurotransmitter release.

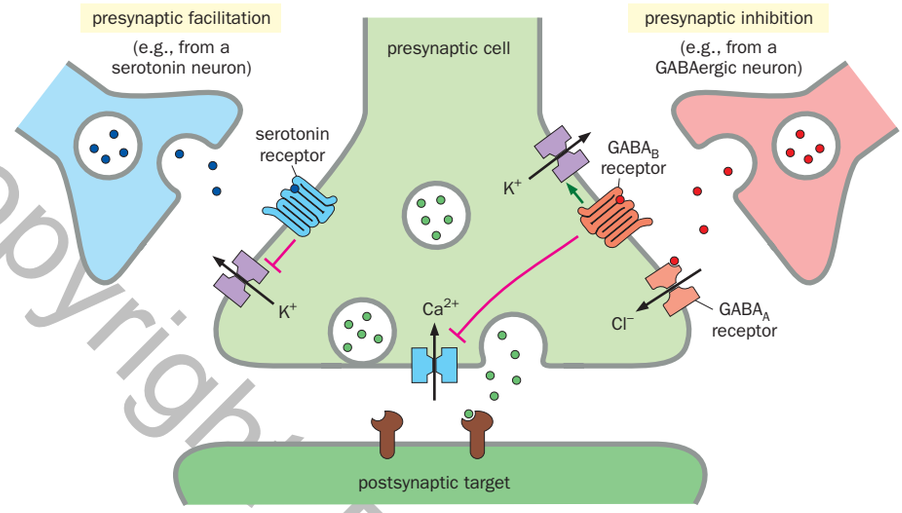

Figure 3-37 Presynaptic facilitation and inhibition. Left, an example of presynaptic facilitation by activation of a metabotropic receptor, such as a serotonin receptor; facilitation can be achieved by decreasing K^+ conductance (red inhibitory sign). Right, examples of presynaptic inhibition by GABA. Activation of the $GABA_A$ receptor increases Cl^- conductance and thereby counters depolarization. Activation of the $GABA_B$ receptor can act by increasing K^+ conductance (green arrow) or decreasing Ca^{2+} conductance (red inhibitory sign).

inhibition can be achieved by opening K^+ channels or closing voltage-gated Ca^{2+} channels, both of which inhibit neurotransmitter release. For example, in Chapter 6, we will learn that *Drosophila* olfactory receptor neurons (ORNs) activate GABAergic local interneurons, which synapse back onto ORN axon terminals to provide negative feedback control of ORN neurotransmitter release. (Presynaptic inhibition can also be achieved through GABA acting on ionotropic $GABA_A$ receptors present on the presynaptic terminals of some neurons.) Presynaptic facilitation and inhibition are also widely used in vertebrate nervous systems.

3.23 GPCR signaling features multiple mechanisms of signal amplification and termination

As we have seen in previous sections, metabotropic neurotransmitter receptors have diverse functions that depend on their locations and their coupling to different G proteins, signaling pathways, and effectors. Their effects unfold more slowly than the rapid effects of ionotropic receptors. However, second messenger systems feature an important property: signal amplification. For example, activation of a single adrenergic receptor can trigger multiple rounds of G protein activation, each activated adenylate cyclase can produce many cAMP molecules, and each activated PKA can phosphorylate many substrate molecules.

Signals must be properly terminated in order for cells to respond to future stimuli. Indeed, all signaling events we have discussed so far are associated with built-in termination mechanisms. The GPCR is deactivated when its ligand dissociates; Gα-GTP is deactivated by its intrinsic GTPase activity, often facilitated by GAPs; Gβγ is deactivated by reassociation with Gα-GDP; adenylate cyclase is deactivated in the absence of Gα-GTP; cAMP produced by adenylate cyclase is metabolized into AMP by an enzyme called **phosphodiesterase**; the catalytic subunits of PKA reassociate with regulatory subunits and become inactive when cAMP concentration declines; and **protein phosphatases** remove phosphates from phosphorylated proteins, thus counteracting the actions of kinases. While some of these termination mechanisms are constitutive, others are regulated by signals.

Another important mechanism of terminating G protein signaling is via the binding of **arrestin**, first discovered in the context of rhodopsin signaling but subsequently found to apply widely to GPCR signaling. Specifically, activated GPCRs are phosphorylated by a GPCR kinase. Phosphorylated GPCRs allow arrestin binding, which competes with GPCR binding to G proteins. In addition, arrestin binding facilitates endocytosis of GPCRs, thus reducing the number of GPCRs on the cell surface. Interestingly, arrestin binding to GPCRs, while terminating GPCR signaling through the G protein, can activate separate downstream signaling pathways.

Signal amplification and termination apply generally to signal transduction pathways (**Box 3-4**). In Chapter 4, we will see a salient example of signal amplification and termination when we study how photons are converted to electrical signals in vision.

Box 3-4: Signal transduction and receptor tyrosine kinase signaling

In response to extracellular signals, cells utilize many pathways to relay such signals to varied effectors to produce specific biological effects; this process is generally referred to as **signal transduction**. In the context of synaptic transmission, we have focused on the actions of ionotropic and metabotropic receptors that change the membrane potential of the postsynaptic cell. In this box, we expand our scope by placing neurotransmitter receptor signaling in the general framework of signal transduction and by discussing receptor tyrosine kinase signaling pathways, which are crucial for nervous system development and function.

In a typical signal transduction pathway (**Figure 3-38**A), an extracellular signal (a **ligand**) is detected by a **cell-surface receptor** in the recipient cell. (We will learn of an exception in Chapter 10: steroid hormones diffuse across the cell membrane to bind receptors *within* the cell.) The extracellular signal is then relayed through one or a series of intracellular signaling proteins to reach the effector(s), producing cellular responses to the extracellular signal. The final effectors are diverse, but usually fall into one of the following categories: (1) enzymes that change cellular metabolism; (2) regulators of gene expression that alter chromatin structure, gene transcription, mRNA metabolism, or protein translation and degradation; (3) cytoskeletal proteins that regulate cell shape, cell movement, and intracellular transport; or (4) ion channels that alter the cell's membrane potential and excitability. Indeed, we can map what we have learned about metabotropic and ionotropic receptor signaling onto this general framework of signal transduction (Figure 3-38B).

The extracellular signal can come from different sources. If the signal is produced by the recipient cell itself (as is the case of presynaptic norepinephrine receptor signaling; Figure 3-36), it is called an **autocrine** signal. If the signal comes from nearby cells, it is called a **paracrine** signal; neurotransmitters can be considered specialized paracrine signals

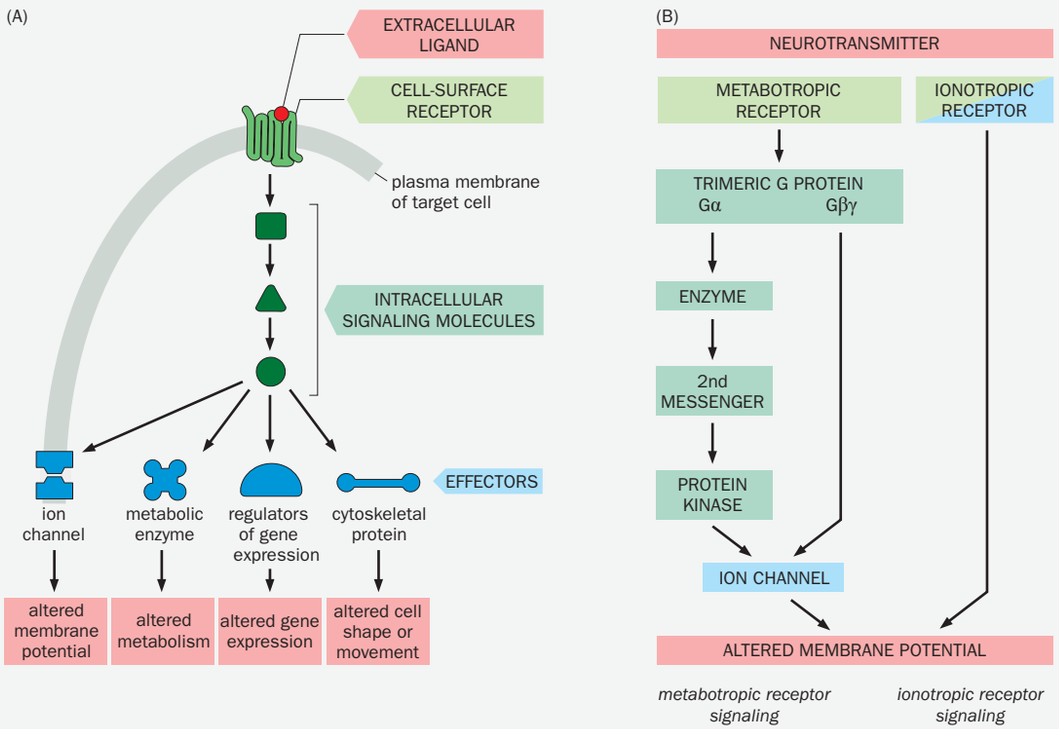

Figure 3-38 Signal transduction pathways. (A) A schematic of a generic signaling pathway. Binding of extracellular ligands to their cell-surface receptors elicits signals transduced by intracellular signaling molecules to various effectors, such as enzymes that modify metabolism, gene regulatory proteins that alter gene expression, cytoskeletal proteins that affect cell shape or motility, and ion channels that influence membrane potential. **(B)** Metabotropic and ionotropic receptor signaling pathways are mapped onto the generic signaling pathway in Panel A, with colors indicating the components of the signaling pathway. Note that ionotropic receptors are simultaneously receptors and effectors that change the membrane potential, thus representing the shortest and fastest (within milliseconds) signaling pathway. (A, adapted from Alberts B, Johnson A, Lewis J, et al. [2015] Molecular Biology of the Cell, 6th ed. Garland Science.)

Box 3-4: continued

with postsynaptic neurons corresponding to target cells. If the signal comes from a remote cell through circulating blood, it is called an **endocrine** signal or a **hormone** (as is the case of epinephrine). When the signal comes from a neighboring cell, it can either be a diffusible molecule such as a neurotransmitter or a secreted protein or be a membrane-bound protein that requires cell–cell contact for signal transduction. Secreted and membrane-bound protein ligands are widely used in cell–cell communication during development, which will be discussed in detail in Chapters 5 and 7.

In addition to the ionotropic and metabotropic receptors, many cell-surface receptors used in the nervous system feature intracellular domains with enzymatic activity. As an example, we discuss here a widely used family of enzyme-coupled receptors called **receptor tyrosine kinases** (**RTKs**)—transmembrane proteins with an N-terminal extracellular ligand-binding portion and a C-terminal intracellular portion possessing a **tyrosine kinase** domain as well as tyrosine phosphorylation sites (**Figure 3-39**A). About 60 genes in the mammalian genome encode RTKs. We focus here on RTK signaling involving the neurotrophin receptors, but the principles are generally applicable to other RTK signaling pathways.

Neurotrophins are a family of secreted proteins that regulate the survival, morphology, and physiology of target neurons (we will discuss the biological effects of these proteins in Section 7.15). They bind to and activate the **Trk receptor** family of RTKs. How does neurotrophin binding to Trk activate signaling? Neurotrophins naturally form dimers. When each neurotrophin binds a Trk receptor, the neurotrophin dimer brings two Trk receptors into close proximity, such that the kinase domain of one Trk can phosphorylate tyrosine residues on the other Trk. Phosphorylation of key tyrosine residues creates binding sites for specific adaptor proteins. These adaptor proteins contain either an SH2 (src homology 2) domain or a PTB (phosphotyrosine binding) domain, which enables the adaptors to bind phosphorylated tyrosines in the context of specific amino acid sequences and thereby initiate downstream signaling. In the Trk receptors, for instance, two key tyrosine residues recruit the binding of several specific adaptor proteins, eliciting separate transduction pathways that can also cross-talk with each other (Figure 3-39A).

One such signaling pathway is initiated by binding of the adaptor Shc (Figure 3-39B), which binds tyrosine-phosphorylated Trk via its PTB domain and becomes tyrosine phosphorylated by Trk. This further recruits the binding of Grb2, an SH2-domain-containing adaptor protein. Grb2 is associated with Sos, a guanine nucleotide exchange factor for the small GTPase Ras (Box 3-3). Ras normally associates with the membrane due to lipid modification like that of Gα. Thus, Trk activation recruits Sos to the plasma membrane to catalyze the exchange of GDP for GTP on Ras. Ras-GTP binds a downstream effector called Raf, a serine/threonine protein kinase. Raf phosphorylates and activates another

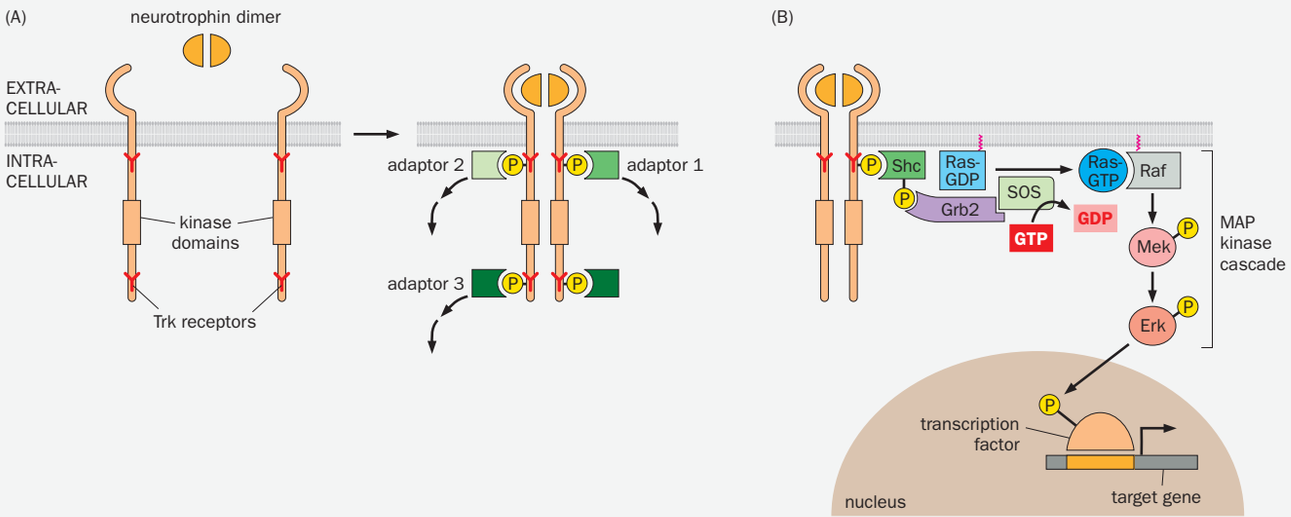

Figure 3-39 Neurotrophin receptor signaling as an example of receptor tyrosine kinase signaling. (A) In the absence of neurotrophin, Trk receptors are present as monomers with unphosphorylated tyrosine residues (Y). Binding of a neurotrophin dimer brings two Trk receptors into close proximity, allowing the kinase domain of each Trk to phosphorylate specific tyrosine residues on the other Trk. Tyrosine phosphorylation recruits binding of specific adaptor proteins, each eliciting a downstream signaling event. Different adaptors can bind the same phosphorylated tyrosine (as in the case of adaptor 1 and adaptor 2). **(B)** Details of one adaptor pathway. Shc binds to a membrane-proximal phosphorylated tyrosine on Trk, leading to tyrosine phosphorylation of Shc. This helps recruit the binding of the Grb2-Sos complex. Sos acts as a guanine nucleotide exchange factor that catalyzes the conversion of Ras-GDP to Ras-GTP (red zigzag lines indicate lipid modification of Ras). Ras-GTP binds to and activates the MAP kinase cascade, including Raf, Mek, and Erk. Activated Erk phosphorylates a number of transcription factors, which activate or repress transcription of target genes.

(*Continued*)

Box 3-4: continued

serine/threonine protein kinase Mek, which in turn phosphorylates and activates a third serine/threonine kinase Erk. Activated Erk phosphorylates and activates a number of **transcription factors** (DNA-binding proteins that activate or repress transcription of target genes), which leads to transcription of specific genes that promote neuronal survival and differentiation, two major biological effects of neurotrophin signaling during development.

Erk is also called MAP kinase (mitogen-activated protein kinase), and therefore Mek is a MAP kinase kinase (since it phosphorylates MAP kinase), and Raf is a MAP kinase kinase kinase. The Raf-Mek-Erk kinase cascade is often referred to as the **MAP kinase cascade**, which acts downstream of Ras and other signaling molecules, such as arrestin (Section 3.23). The Ras-MAP kinase cascade is a widely used signaling pathway that serves many functions, including cell survival and differentiation, as discussed earlier; cell fate determination (Section 5.17); and cell proliferation. It is also used in activity-dependent transcription (Section 3.24).

3.24 Postsynaptic depolarization can induce new gene expression

In addition to changing the membrane potentials and excitability of postsynaptic neurons at the time scales of milliseconds (through ionotropic receptors) or tens of milliseconds to seconds (through metabotropic receptors), neurotransmitters can also trigger long-term (hours to days) changes in the physiological states of postsynaptic neurons by inducing expression of new genes. For example, transcription of ***Fos*** was induced by ionotropic AChR activation within 5 minutes of nicotine application to cultured cells (**Figure 3-40**). *Fos* encodes a transcription factor, and its transient activation can change the expression of many downstream target genes.

Fos is the prototype of a class of genes called **immediate early genes** (**IEGs**), whose transcription is rapidly induced by external stimuli in the presence of protein synthesis inhibitors; this means that no new protein synthesis is required to turn on IEGs. In neurons, IEGs can be rapidly induced by depolarization of postsynaptic neurons in response to presynaptic neurotransmitter release. Some IEGs, such as *Fos* or *Egr1* (early growth response-1), encode transcription factors that regulate the expression of other genes. Other IEGs encode regulators of neuronal communication that act more directly. Among them, **brain-derived neurotrophic factor** (**BDNF**) is a secreted neurotrophin that regulates the morphology and physiology of target neurons (Box 3-4). **Arc** (activity-regulated cytoskeleton-associated protein) is a cytoskeletal protein present at the postsynaptic density that regulates trafficking of glutamate receptors, thus contributing to synaptic plasticity. As will be discussed in later chapters, **activity-dependent transcription** (regulation of gene expression by neuronal activity) plays a prominent role in the maturation of synapses and neural circuits during development and in their modulation by experience in adulthood. Because of the rapid induction of IEGs by neuronal activity, their expression has also been used to identify and manipulate neurons activated by specific experiences, behavioral episodes, and internal states (see Section 14.11 for details).

Many signaling pathways linking neurotransmitter receptors to transcription have been identified. A rise in intracellular Ca^{2+} concentration ($[Ca^{2+}]_i$) is often a key step. $[Ca^{2+}]_i$ increases can be accomplished by several means: via the NMDA receptor at the postsynaptic density in dendritic spines (Figure 3-24), via voltage-gated Ca^{2+} channels enriched on the dendritic trunk and cell body, and via IP_3 receptors (Figure 3-34) or the related **ryanodine receptors** on the ER membrane. (Instead of being activated by IP_3, ryanodine receptors are activated by a rise in $[Ca^{2+}]_i$ and thus amplify the Ca^{2+} signal; ryanodine is a plant-derived agonist of this ER-resident Ca^{2+} channel.) Although free Ca^{2+} ions usually do not diffuse far from the source of entry into the cytosol, they can associate with various Ca^{2+}-binding proteins, most notably calmodulin (CaM) (Figure 3-34), and initiate signals that can be transduced to the nucleus (**Figure 3-41**). For example, Ca^{2+}/CaM activates CaM kinases, such as CaMKII, which is enriched in postsynaptic densities, and

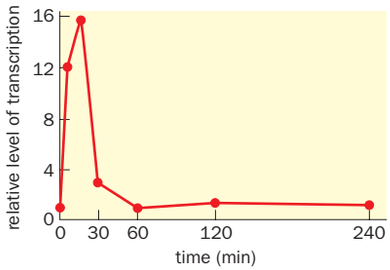

Figure 3-40 Nicotinic AChR activation induces transcription of *Fos*, an immediate early gene. Nicotine application to a cultured neuronal cell line at time 0 induces rapid and transient transcription of *Fos*, indicated by relative levels of newly synthesized *Fos* RNA. (From Greenberg ME, Ziff EB, & Greene LA [1986] *Science* 234:80–83. With permission from AAAS.)

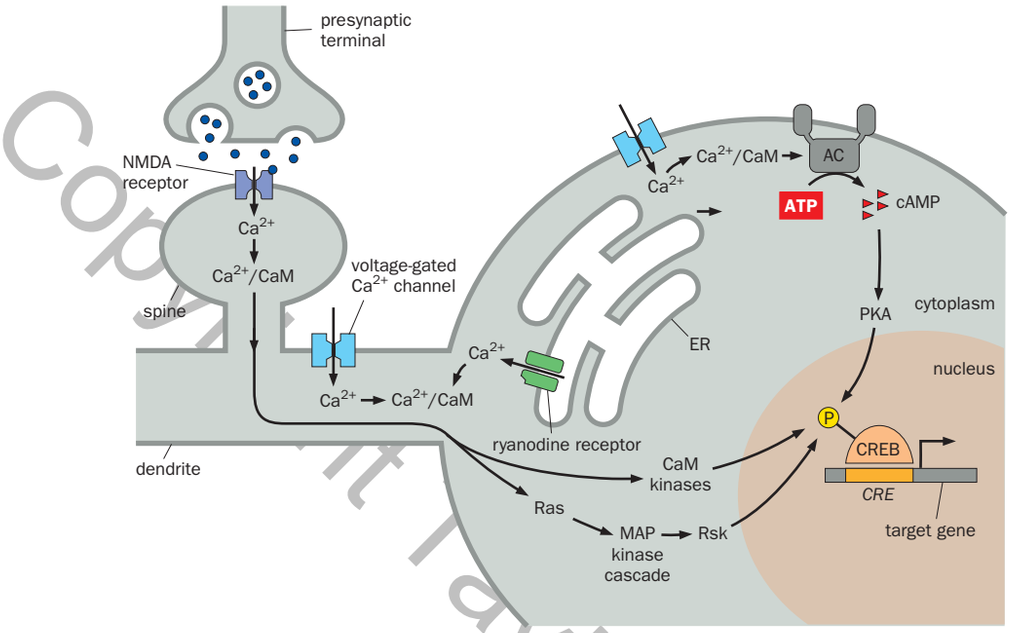

Figure 3-41 Signaling pathways from the synapse to the nucleus. Shown are pathways from postsynaptic terminals and the somatodendritic plasma membrane to the nucleus that involve Ca^{2+} and lead to the phosphorylation and activation of a transcription factor, CREB. An increase in $[Ca^{2+}]_i$ can result from an influx of extracellular Ca^{2+} through NMDA receptors concentrated in dendritic spines or voltage-gated Ca^{2+} channels enriched on the somatodendritic plasma membrane or can be mediated by the release of Ca^{2+} from internal stores in the ER through ryanodine receptors. Ca^{2+} bound to calmodulin (CaM) activates CaM kinases, Rsk (via the Ras-MAP kinase cascade), and PKA (via Ca^{2+}-activated adenylate cyclase and cAMP production). CaM kinases, Rsk, and PKA can all phosphorylate CREB, promoting its activity to induce transcription of target genes with cAMP-response elements (*CRE*s) in their promoters. (Based on Cohen S & Greenberg ME [2008] *Annu Rev Cell Dev Biol* 24:183–209 and Deisseroth K, Mermelstein PG, Xia H, et al. [2003] *Curr Opin Neurobiol* 13:354–365.)

CaMKIV, which is enriched in nuclei. A specific isoform, γCaMKII, can transport Ca^{2+}/CaM from the plasma membrane near voltage-gated Ca^{2+} channels to the nucleus so that Ca^{2+}/CaM can activate nuclear effectors such as CaMKIV. In addition, Ca^{2+}/CaM can activate several adenylate cyclase subtypes, leading to the production of cAMP and activation of PKA. The Ras-MAP kinase cascade (Box 3-4) is yet another signaling pathway that can be activated by Ca^{2+}/CaM.

As a specific example, we discuss how these pathways lead to activation of a transcription factor called **CREB**. CREB was originally identified because it binds to a DNA element (***CRE***) in the promoter of the gene that produces the neuropeptide somatostatin, rendering somatostatin's transcription responsive to cAMP regulation. (*CRE*, for cAMP response element; CREB, for *CRE* binding protein.) *CRE* was subsequently found in the promoter of many IEGs including *Fos*. Biochemical studies indicate that phosphorylation of a particular serine residue is crucial for the activity of CREB as a transcriptional activator. This serine can be phosphorylated by several kinases, including PKA, CaMKIV, and a protein kinase called Rsk (ribosomal protein S6 kinase), a substrate of MAP kinase. Although each of these kinases can be activated by Ca^{2+} (Figure 3-41), each pathway has unique properties. For example, the CaM kinase–mediated pathway is more rapid, resulting in CREB phosphorylation that peaks within minutes after a transient neuronal depolarization, whereas the MAP kinase pathway mediates a gradual increase in CREB phosphorylation over an hour following a transient neuronal depolarization.

In addition to CREB, other Ca^{2+}-responsive transcription factors bind different IEG promoters. Thus, neuronal activity can reach nuclei and change the transcriptional programs of postsynaptic cells via many routes. Furthermore, neuronal activity and Ca^{2+} can also affect chromatin structures through enzymes that control methylation of DNA and posttranslational modifications of histones (for example, methylation, demethylation, acetylation, and deacetylation), the protein component of chromatin. These **epigenetic modifications** (so named because they do not alter DNA sequence) also alter gene expression patterns through regulation of chromatin structures and accessibility of promoters to specific transcription factors. Another form of epigenetic modification is methylation of mRNAs, which can alter their stability and translation efficiency—for example, methylation promotes translation from mRNAs induced by neuronal activity. As will be discussed in Chapter 12, mutations in many components of synapse-to-nucleus signaling pathways have been found to cause human brain disorders,

highlighting the important role of activity-dependent transcription in human brain functions.

3.25 Dendrites are sophisticated integrative devices

Aside from regulating gene expression, the primary function of synaptic transmission is to influence the firing patterns of postsynaptic neurons. This is the means by which information is propagated from one neuron to the next within a neural circuit. As a way of integrating what we've learned about neuronal communication in Chapter 2 and this chapter, in the final two sections we discuss how a postsynaptic neuron integrates synaptic inputs to produce its firing pattern, thus completing a full round of neuronal communication (Figure 1-18). We start our discussion with excitatory inputs.

Most excitatory inputs to a neuron increase its membrane conductance (for example, by opening ionotropic glutamate receptor channels), producing EPSCs and thus EPSPs (Figure 3-23). To influence the postsynaptic cell's firing pattern, these electrical signals need to travel to the axon initial segment, where action potentials are usually initiated. As we learned in Section 2.8, electrical signals evolve over time and decay over distance, specified by the passive (cable) properties of neuronal fibers such as the time (τ) and length constants (λ). Theoreticians have used model neurons to predict amplitudes of somatic EPSPs produced by synaptic input at different locations in dendrites. In the model neuron shown in **Figure 3-42**A, for example, the complex dendritic tree is simplified to 10 compartments with varying distances from the soma in order to predict the amplitudes of somatic EPSPs in response to dendritic inputs. A fixed transient increase in synaptic conductance, equivalent to a transient opening of ionotropic glutamate receptors, produces somatic EPSPs with different shapes and amplitudes when applied to different locations in the dendrites (Figure 3-42B). More distant synapses produce smaller, slower, and broader EPSPs. This is because EPSPs produced at more distant synapses decay more substantially, as they need to travel longer distances to reach the soma. In this model neuron, synaptic inputs given at compartments 4 and 8 produce peak somatic EPSP amplitudes only 29% and 10% of the somatic EPSP amplitude when the same input is given at the soma (Figure 3-42B).

A mammalian CNS neuron receives on average thousands of excitatory synaptic inputs along its dendritic tree. A single EPSP at one synapse is usually insufficient to depolarize the postsynaptic neuron above the action potential firing threshold, due to the small size of an individual EPSP when it arrives at the axon initial segment. Indeed, at any given time, the postsynaptic neuron integrates many excitatory inputs in order to reach the firing threshold. Such integration takes two forms. In **spatial integration**, nearly simultaneously activated synapses at different spatial locations sum their excitatory postsynaptic currents when they converge along the path to the soma, producing a larger EPSP (**Figure 3-43**A). In

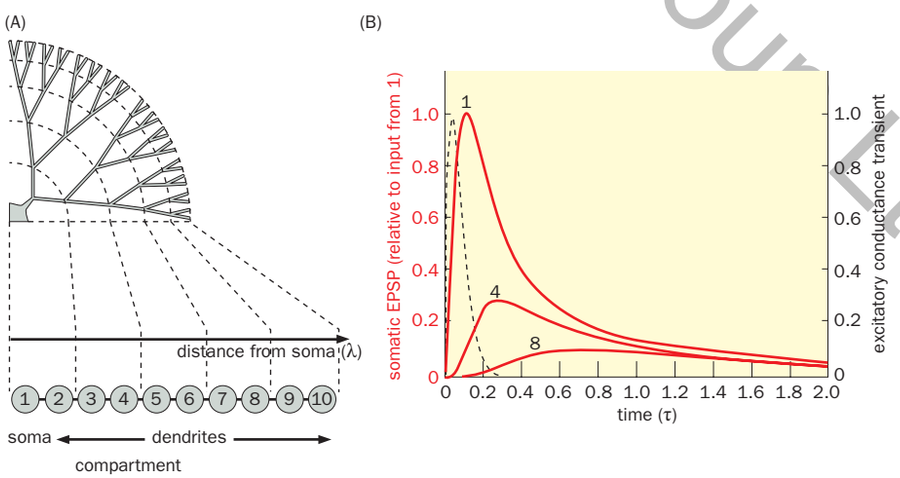

Figure 3-42 Somatic EPSPs from dendritic inputs in a model neuron.
(A) The soma and dendritic tree of this neuron are simplified to 10 compartments for the purpose of mathematical modeling. Compartment 1 represents the soma, and compartments 2–10 represent dendritic segments with increasing distance from the soma, with the length constant (λ) as the unit. Dashed lines illustrate divisions between every two compartments.
(B) When a transient excitatory input of the same size and shape (dashed curve, with *y* axis to the right) is provided at compartments 1, 4, or 8, the shapes of EPSPs at the soma show distinct profiles. The somatic EPSP produced by the somatic input has the largest amplitude and fastest rising and decay time, the somatic EPSP produced by the input given at compartment 8 has the smallest amplitude and slowest rising and decay times, and the somatic EPSP produced by the input given at compartment 4 has the intermediate amplitude and temporal spread. Time is represented in the unit of the time constant τ. (Adapted from Rall W [1967] *J Neurophysiol* 30:1138–1168.)

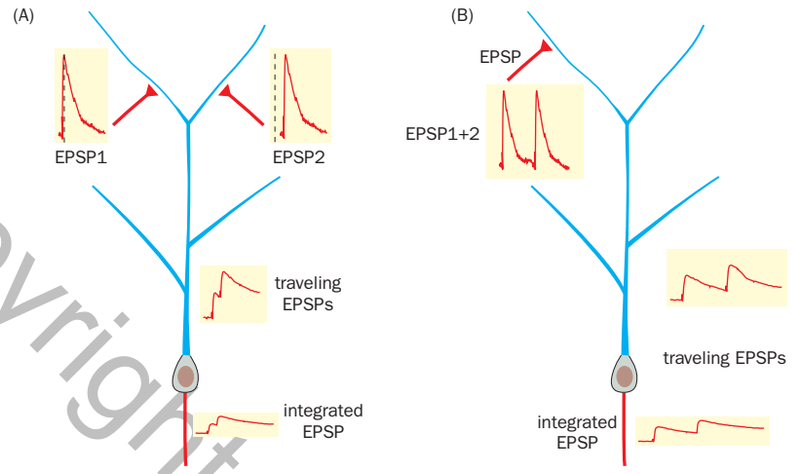

Figure 3-43 Spatial and temporal integration of synaptic inputs. (A) Spatial integration. Two excitatory inputs from two branches of the dendritic tree that arrive shortly after one another (vertical dotted lines in the EPSP traces indicate the same time) summate their signals when they converge, producing depolarization of the membrane potential at the axon initial segment that exceeds the amplitude produced by each alone (compare the heights of the second and first peaks). **(B)** Temporal integration. Two discrete EPSPs produced at the same synapse (top left) become gradually integrated as they travel from distal dendrites toward the soma due to the temporal spread of electrical signals (Figure 3-42B). At the axon initial segment, the integrated EPSP produces a peak potential (the second peak) greater than that produced by a single EPSP (the first peak).

temporal integration, synapses activated within a specific window (including successive activation at the same synapse) sum their postsynaptic currents, producing a larger EPSP (Figure 3-43B).

As we see from the model neuron in Figure 3-42, inputs from proximal synapses contribute more to the firing of the neuron because they are less attenuated. In some mammalian neurons, distal synapses are stronger in order to compensate for such distance-dependent attenuation. Importantly, inputs from distal synapses also have a longer window during which to contribute to temporal integration (Figure 3-43B). Without considering inhibitory inputs, we can already see that individual dendrites are sophisticated integrative devices. At any given moment, a spiking neuron converts analog signals from the many inputs it receives into digital signals (to spike or not to spike).

While the passive properties of neuronal membranes discussed thus far provide a foundation for understanding how synaptic inputs regulate firing of postsynaptic neurons, dendritic integration is more complex and nuanced. Voltage-gated Na^+, Ca^{2+}, and K^+ channels are present on the dendrites of many mammalian CNS neurons. EPSPs can open dendritic voltage-gated Na^+ or Ca^{2+} channels, causing further depolarization and thus signal amplification. Co-activation of nearby excitatory synapses in dendritic branches can produce dendritic spikes that actively propagate across dendritic segments. Although these dendritic spikes are not fully regenerative as are axonal action potentials and may not propagate all the way to the soma (because of the lower density of voltage-gated Na^+ channels in dendrites compared to axons), they nevertheless amplify synaptic input and propagate membrane potential changes across greater distances with smaller attenuation than passive spread. Finally, action potentials generated at the axon initial segment can back-propagate into dendrites via the participation of dendritic voltage-gated Na^+ channels, and these back-propagated action potentials can interact with EPSPs in interesting ways.

As a specific example, we study an experiment in which a cortical pyramidal neuron in an *in vitro* brain slice was subjected to dual patch clamp recording at the soma and at the apical dendrites (**Figure 3-44**A). Electrical stimulation of presynaptic axons produced a subthreshold EPSP at the soma (Figure 3-44B). However, if an action potential was induced in the recorded neuron 5 ms before presynaptic stimulation (by injecting a pulse of depolarizing current through the somatic patch pipette), the back-propagated action potential synergized with the dendritic synaptic potential to reach the threshold of a dendritic spike, which greatly amplified the synaptic potential. This allowed the neuron to produce two additional somatic action potentials (Figure 3-44C). Assuming that under physiological conditions, the pyramidal neuron fires action potentials in response to proximal dendritic inputs, this integration mechanism can enable amplification of near-synchronous input at the proximal and distal dendrites by producing a

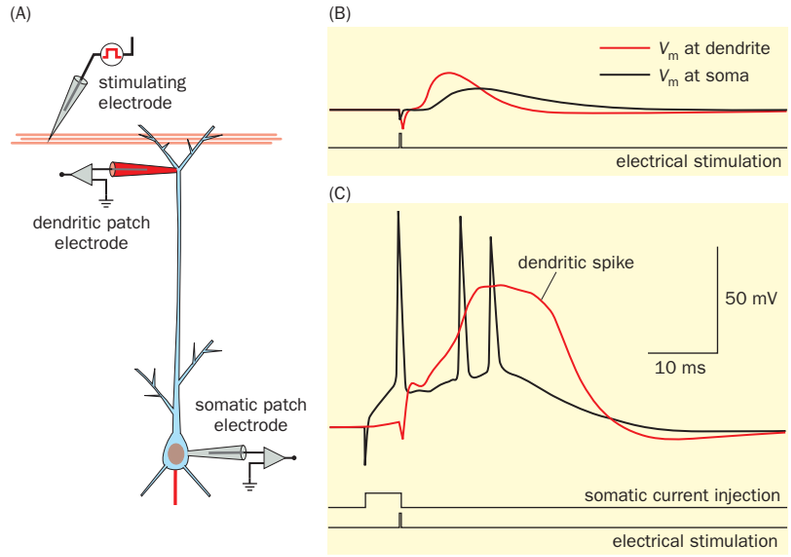

Figure 3-44 Interactions between synaptic input and a back-propagating action potential. **(A)** Experimental setup. A cortical pyramidal neuron in a brain slice is being recorded by patch electrodes at the apical dendrite (red) and soma (gray), both in whole-cell recording mode. A stimulating electrode delivers electrical stimulation to presynaptic axons. **(B)** Electrical stimulation (bottom trace) produces a dendritic EPSP recorded by the dendritic patch electrode (red), and an attenuated somatic EPSP recorded by the somatic patch electrode. The somatic EPSP is below the threshold for firing an action potential. **(C)** A 5-ms depolarizing current pulse injected into the soma before electrical stimulation produces an action potential (the first black spike), which propagates back to the dendrites and integrates with the dendritic EPSP, reaching the threshold for producing a dendritic spike (red trace). The propagation of the dendritic spike to the soma produces two additional somatic action potentials (the second and third black spikes). Thus, the back-propagating action potential synergizes with the dendritic EPSP to produce additional output spikes. (Adapted from Larkum ME, Zhu JJ, & Sakmann B [1999] *Nature* 398:338–341. With permission from Springer Nature.)

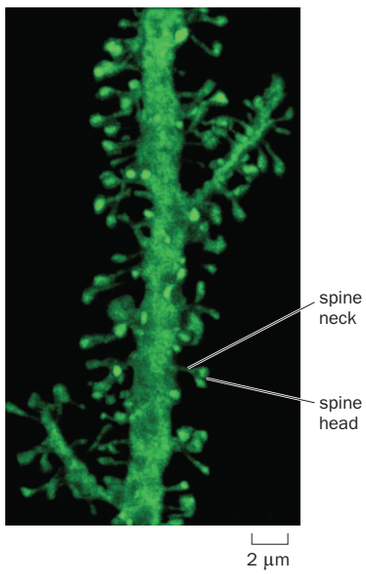

Figure 3-45 Dendritic spines. A dendritic segment of a human cortical pyramidal neuron ~100 µm from the cell body, showing dendritic spines with long necks. Imaged after intracellular injection of a fluorescent dye. (From Yuste R. Dendritic Spines, Cover Image, © 2010 Massachusetts Institute of Technology, by permission of The MIT Press.)

burst of action potentials that could not be generated by either the proximal or distal inputs alone.

Active properties of mammalian CNS neurons can vary in different neuronal types or even in different compartments of the same neuron because of particular distributions and densities of voltage-gated ion channels. We are far from a complete understanding of how synaptic potentials are integrated in light of these active properties; this is an active area of research fundamental to our understanding of neuronal communication and neural circuit function.

3.26 Synapses are strategically placed at specific locations in postsynaptic neurons

In addition to excitatory inputs, each neuron also receives inhibitory and modulatory inputs. How these inputs shape the output of a postsynaptic neuron depends on which subcellular compartments of the postsynaptic neuron these inputs contact.

In general, most excitatory synapses are located on dendritic spines distributed throughout the dendritic tree (**Figure 3-45**). The various presynaptic terminals targeting a given postsynaptic neuron may originate from many different presynaptic partner neurons, but each dendritic spine typically receives synaptic input from a single excitatory presynaptic terminal. The thin spine neck chemically and electrically compartmentalizes each synapse such that it can be modulated semi-independently from neighboring synapses. These semi-independent compartments enable neurons to encode information in the strengths of individual synapses with different input neurons. The strength of each synapse can be

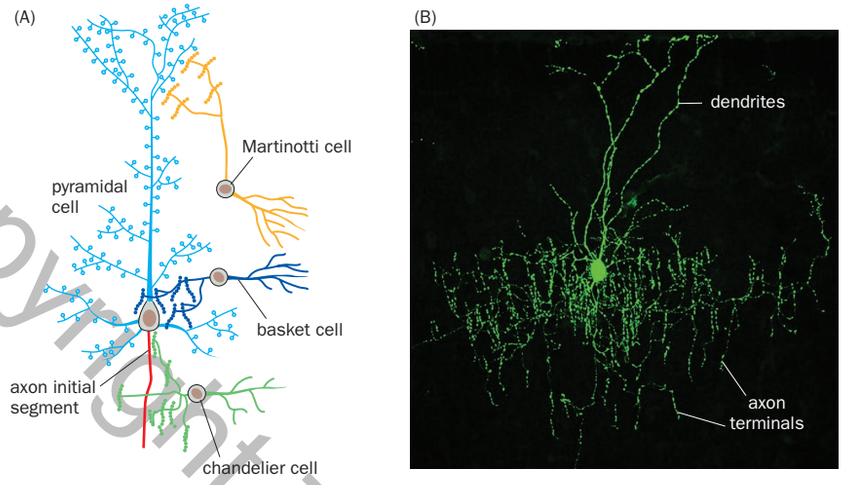

Figure 3-46 Inhibitory inputs onto a cortical pyramidal neuron. (A) Schematic of presynaptic terminals (shown as short strings of beads) from three different types of GABAergic inhibitory neurons onto a cortical pyramidal neuron, whose dendrites are in cyan and axons are in red. The Martinotti (yellow), basket (blue), and chandelier (green) cells form synapses respectively onto the distal dendrites, the cell body and proximal dendrites, and the axon initial segment of the pyramidal neuron (and other pyramidal neurons not shown). **(B)** A chandelier cell in the mouse cerebral cortex. Each group of presynaptic terminals, which looks like a candle on an old-fashioned chandelier, wraps around the initial segment of a pyramidal neuron. Each chandelier cell thus controls the firing of many pyramidal neurons. (B, courtesy of Z. Josh Huang. See also Taniguchi H, Lu J, & Huang ZJ [2013] *Science* 339:70–74.)

modified by prior synaptic activity of that particular synapse, a property crucial for memory as we will discuss in Chapter 11.

In contrast to excitatory synapses, which are most enriched on spines, inhibitory synapses form on dendritic spines, dendritic shafts, the cell body, and the axon initial segment. These distributions allow inhibitory synapses to oppose the action of EPSPs as they pass by (Figure 3-29). Let's use a typical pyramidal neuron in the cerebral cortex to describe inhibitory inputs it receives from three types of GABAergic neurons (**Figure 3-46**A). **Martinotti cells** target the distal dendrites of the pyramidal neuron. Thus, activation of Martinotti cells can inhibit the production or propagation of dendritic spikes. By contrast, **basket cells** target the cell body of the pyramidal neuron and thereby influence the overall integration of synaptic input from all dendritic branches. Last, **chandelier cells** target the axon initial segment of the pyramidal neuron (Figure 3-46B), meaning that chandelier cells have the most direct impact on the production of action potentials. In summary, inhibitory neurons have specialized functions partly because they make synapses onto specialized locations on postsynaptic cells.

A postsynaptic neuron can also receive synaptic input at its own axon terminals, as discussed in Section 3.21. Here, inputs do not control action potential firing but rather the efficacy with which action potentials lead to neurotransmitter release. The presynaptic partners in these cases can be modulatory neurons using transmitters such as acetylcholine and the monoamines. GABAergic and glutamatergic neurons can also affect their target neurons via both ionotropic and metabotropic receptors on their axon terminals (Figure 3-37).

In summary, individual neurons are complex, highly organized integrators. Each neuron receives inputs from numerous presynaptic partners at different parts of its complex dendritic tree, its cell body, its axon initial segment, and its axon terminals (**Figure 3-47**). The interactions of excitatory, inhibitory, and modulatory inputs together shape the neuron's output patterns, which are communicated to its postsynaptic target neurons by the frequency and timing of action potentials and the probability of neurotransmitter release induced by each action potential. Some neurons also receive input (and send output) through electrical synapses

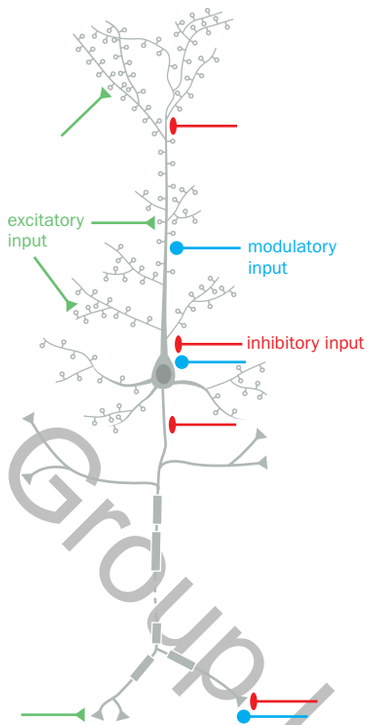

Figure 3-47 Subcellular distribution of synaptic input. In a typical mammalian neuron, excitatory inputs are received mostly at dendritic spines (and along the dendrites for neurons lacking dendritic spines) and presynaptic terminals. Inhibitory inputs are received at the dendritic spines and shaft, cell body, axon initial segment, and presynaptic terminals. Modulatory inputs are received at dendrites, cell bodies, and presynaptic terminals.

(**Box 3-5**). At a higher level, individual neurons are parts of complex neural circuits that perform diverse information-processing functions underlying processes ranging from sensory perception to behavioral control. Having studied the basic concepts and principles of neuronal communication, we are now ready to apply them to fascinating neurobiological processes in the following chapters.

Box 3-5: Electrical synapses

Although chemical synapses are the predominant form of interneuronal communication, electrical synapses are also prevalent in both vertebrate and invertebrate nervous systems. The morphological correlate of the electrical synapse is the **gap junction**, which usually contains hundreds of closely clustered channels that bring the plasma membranes of two neighboring cells together (Figure 1-14B) and allow passage of ions and small molecules between the two cells. In mammalian neurons, electrical synapses usually occur at the somatodendritic compartments of two partner neurons.

In vertebrates, gap junctions are made predominantly by a family of **connexin** proteins, encoded by about 20 genes in the mammalian genome. Each gap junction channel has 12 connexin subunits, with 6 subunits on each apposing plasma membrane forming a hemichannel. Each connexin subunit has four transmembrane domains with an additional N-terminal domain embedded in the membrane. As revealed by the crystal structure of connexin-26 (**Figure 3-48**), extensive interactions between the extracellular loops of the hemichannels bring the two apposing membranes from neighboring cells within 4 nm of each other, and align the two hemichannels, forming a pore with an innermost diameter of 1.4 nm. Invertebrate gap junctions are made by a different family of proteins called **innexins** (invertebrate connexin). A third family of proteins called pannexins may contribute to gap junctions in both vertebrates and invertebrates.

Electrical synapses differ from chemical synapses in several important ways. First, whereas chemical synapses transmit signals with a delay on the order of 1 ms between depolarization in the presynaptic terminal and synaptic potential generation in the postsynaptic cell, electrical synapses transmit electrical signals with virtually no delay. Second, whereas chemical synapses are activated only by presynaptic depolarization (and, in spiking neurons, only suprathreshold signals that produce action potentials), electrical synapses transmit both depolarization and hyperpolarization. Third, whereas chemical synapses are asymmetrical—membrane potential changes in the presynaptic neuron produce membrane potential changes in the postsynaptic neuron, but not vice versa—electrical signals can flow in either direction across electrical synapses. Exceptions exist to this rule, however; some electrical synapses prefer one direction over the opposite direction and are thus called rectifying electrical synapses. Finally, many electrical synapses allow small molecules such as peptides and second messengers to pass through; indeed, the diffusion of small-molecule dye from one cell to another, called **dye coupling**, is often used as a criterion to identify the presence of gap junctions between two cells. The conductance of electrical synapses can be mod-

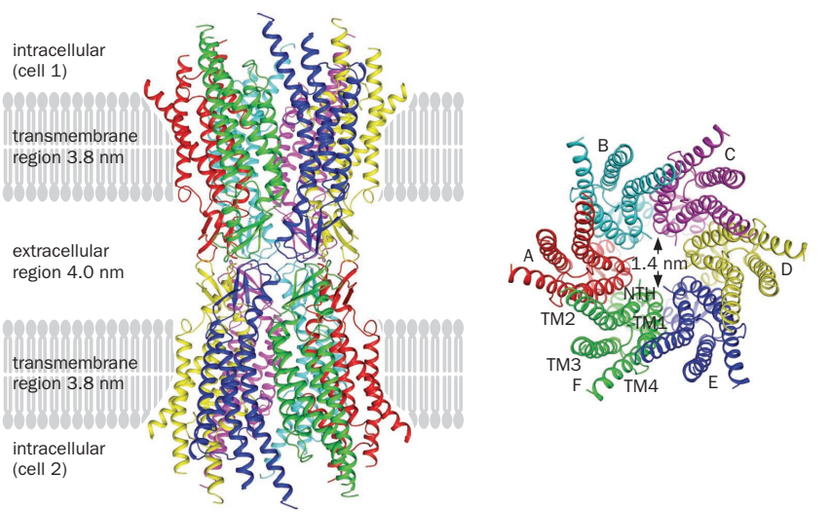

Figure 3-48 Structure of a gap junction channel. Summary of crystal structures of connexin-26. Left, view from the side. Each hemichannel consists of six subunits, which are differentially colored. Each subunit has four transmembrane helices and an N-terminal helix (NTH) embedded in the membrane. Right, surface view, with the transmembrane helices and NTH labeled for subunit F. The central passage allows molecules with a linear dimension smaller than 1.4 nm to pass freely between two cells. (Adapted from Maeda S, Nakagawa S, Suga M, et al. [2009] *Nature* 458:597–602. With permission from Springer Nature.)

Box 3-5: continued

ulated by several factors, such as the membrane potential, the transjunctional voltage (the difference between membrane potentials across the electrical synapse), and other factors such as phosphorylation state, pH, and Ca^{2+} concentration.

The special properties of electrical synapses discussed here are utilized in many circuits in invertebrates and vertebrates. For instance, electrical synapses are found in circuits where rapid transmission is essential, such as in vertebrate retinal circuits that processes motion signals (where analog signals are transmitted between nonspiking neurons), and in predator avoidance escape circuits. Indeed, electrical synapses were first characterized between the giant axon and motor neuron in the crayfish escape circuit in the 1950s. Another use of electrical synapses is to facilitate synchronized firing between electrically coupled neurons (another term for neurons that form electrical synapses with each other). As a specific example, we study electrical synapses in the mammalian cerebral cortex.

Using whole-cell recording techniques (see Box 14-3 and Section 14.21 for details) in a cortical slice preparation, researchers found that when two fast-spiking (FS) inhibitory neurons (corresponding mostly to basket cells in Figure 3-46A) were recorded simultaneously with patch electrodes, current injection into one cell caused nearly synchronous membrane potential changes in both cells; both depolarization and hyperpolarization could result, depending on the sign of the injected current (**Figure 3-49**A), indicating that these two cells formed electrical synapses with each other. Paired recordings of many cell types indicated that electrical synapses form with substantial cell-type specificity. For example, low-threshold-spiking (LTS) inhibitory neurons (corresponding mostly to Martinotti cells in Figure 3-46A) also form electrical synapses with each other at a high probability, but rarely with FS neurons. Excitatory pyramidal neurons, which could be identified as regular-spiking (RS) cells by their electrophysiological properties, did not form any electrical synapses with other pyramidal neurons or with FS or LTS neurons (Figure 3-49B). Furthermore, while injecting subthreshold depolarizing currents into one of the two electrically coupled FS cells did not elicit action potentials, injecting the same subthreshold depolarizing currents into both FS cells elicited synchronous action potentials (Figure 3-49C). This suggested that a network of FS cells can act as detectors for synchronous inputs and their synchronous firing can further strengthen network synchrony. Subsequent work indicated that in addition to FS and LTS cells, other specific types of inhibitory neurons also form type-specific electrical synapse networks, thus providing a rich substrate for coordinating electrical activity in the cerebral cortex.

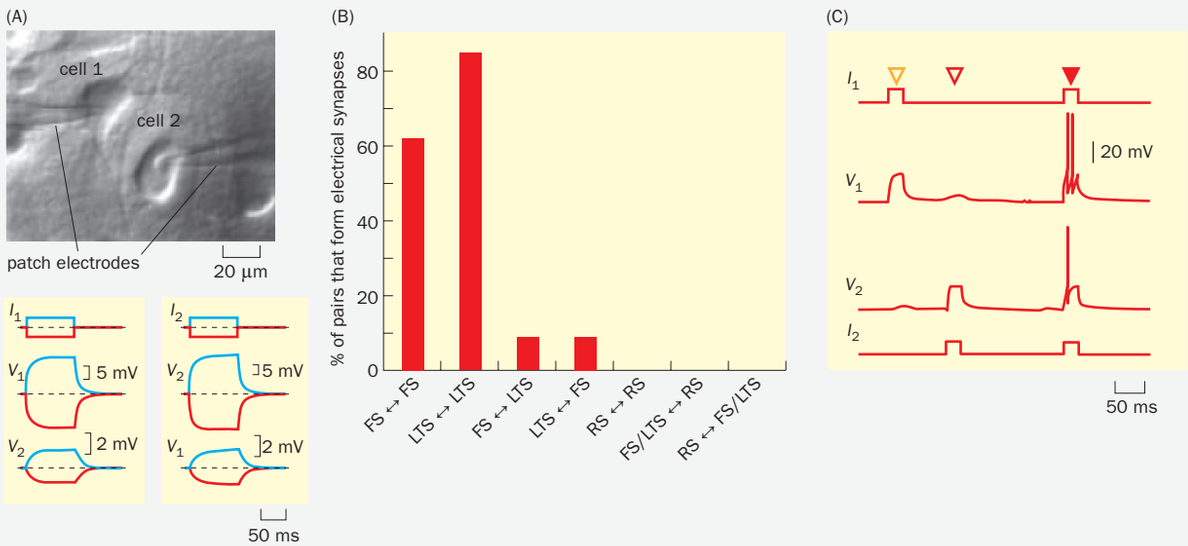

Figure 3-49 Electrical synapses between inhibitory neurons in the rat cerebral cortex. (A) Top, image of a rat cortical slice with two cells and two patch electrodes, taken with differential interference contrast microscopy. Bottom left, when positive (blue) or negative (red) current (I_1) was injected into cell 1, it depolarized or hyperpolarized, respectively, the membrane potential of cell 1 (top or bottom traces of V_1). In addition, cell 2 was correspondingly depolarized or hyperpolarized at the same time (top or bottom traces of V_2). Note the reduced amplitude and slower rising time of V_2 compared to V_1 due to attenuation across the gap junction and the time taken to charge the membrane capacitance of cell 2. Bottom right, positive or negative current injected into cell 2 (I_2) also caused depolarization or hyperpolarization, respectively, of both cells. Thus, these two cells form electrical synapses. **(B)** Quantification of electrical synapses between specific types of cells based on paired recordings in Panel A. Cells were classified based on their firing patterns into fast spiking (FS), low-threshold spiking (LTS), or regular spiking (RS), corresponding roughly to basket, Martinotti, and pyramidal cells, respectively. Arrows indicate the directionality of electrical synapses tested in paired recordings. **(C)** The top and bottom traces show the injection of small depolarizing currents into cell 1 (top) or cell 2 (bottom). Injection into a single cell (open arrowheads) did not cause firing of either cell. Injecting the same current into both cells simultaneously (filled arrowhead) caused both cells to fire action potentials. (Adapted from Galarreta M & Hestrin S [1999] *Nature* 402:72–75. With permission from Springer Nature. See also Gibson JR, Beierlein M, & Connors BW [1999] *Nature* 402:75–79.)

SUMMARY

Neurons communicate with each other through electrical and chemical synapses. Electrical synapses allow rapid and bidirectional transmission of electrical signals between neurons via gap junctions. Although less prevalent than chemical synapses, electrical synapses are widely used in both invertebrates and vertebrates in neural circuits that require rapid information propagation or synchronization. Chemical synapses are unidirectional: electrical signal in the presynaptic neuron is transmitted to the postsynaptic neuron or muscle via the release of a chemical intermediate, the neurotransmitter.

At the presynaptic terminal, neurotransmitter release is mediated by fusion of the synaptic vesicle with the presynaptic plasma membrane. Action potential arrival depolarizes the presynaptic terminal, opening voltage-gated Ca^{2+} channels at the active zone. Ca^{2+} influx, acting through the synaptic vesicle-associated Ca^{2+} sensor synaptotagmin, releases a break on partially assembled SNARE complexes. The full assembly of the SNARE complex provides the force that drives membrane fusion and transmitter release from within the synaptic vesicle to the synaptic cleft. Excess neurotransmitters are rapidly degraded or recycled through reuptake mechanisms. Synaptic vesicles are rapidly recycled and refilled with neurotransmitter, enabling continual synaptic transmission in response to future action potentials.

Nervous systems across the animal kingdom utilize a common set of neurotransmitters. In the vertebrate CNS, glutamate is the main excitatory neurotransmitter, while GABA and glycine are the main inhibitory neurotransmitters. Acetylcholine is the excitatory neurotransmitter at the vertebrate neuromuscular junction, but can also act as a modulatory neurotransmitter in the CNS. Other neuromodulators include monoamines and neuropeptides. The specific actions of neurotransmitters are determined by the properties of their receptors on the postsynaptic neurons.

Neurotransmitter receptors are either ionotropic or metabotropic. Ionotropic receptors are ion channels gated by neurotransmitter binding and act rapidly to produce synaptic potentials within a few milliseconds of presynaptic action potential arrival. Ionotropic acetylcholine and glutamate receptors are nonselective cation channels; upon neurotransmitter binding, these receptors produce depolarization in the form of excitatory postsynaptic potentials. NMDA receptors act as coincidence detectors, because channel opening depends on both presynaptic glutamate release and a depolarized state of the postsynaptic neuron. Ionotropic GABA and glycine receptors are Cl^- channels. Their opening usually produces Cl^- influx, which impedes postsynaptic neurons from reaching the threshold at which they fire action potentials.

All metabotropic receptors are G-protein-coupled receptors. Neurotransmitter binding activates trimeric G proteins associated with the receptors. Gα-GTP and Gβγ each can activate different effectors, depending on G protein variants and cellular contexts. Gβγ can act on K^+ and Ca^{2+} channels directly, whereas Gα usually acts via second messengers such as cAMP and Ca^{2+} to activate protein kinases that phosphorylate ion channels to change the membrane potential and excitability of postsynaptic neurons. Metabotropic receptor activation causes membrane potential changes within tens of milliseconds to seconds. Longer-term changes of postsynaptic neurons in response to neurotransmitter release and neuronal activity involve synapse-to-nucleus signaling and alterations of gene expression.

Chemical synapses are highly organized. At the presynaptic terminal, the active zone protein complexes bring synaptic vesicles to the immediate vicinity of voltage-gated Ca^{2+} channels such that Ca^{2+} influx rapidly triggers neurotransmitter release. Trans-synaptic cell adhesion proteins align presynaptic active zones with postsynaptic high-density neurotransmitter receptor clusters. Postsynaptic density scaffold proteins further link neurotransmitter receptors to their regulators and effectors for efficient synaptic transmission and for regulating synaptic plasticity.

Integration of excitatory, inhibitory, and modulatory inputs at the dendrites, cell bodies, and axon initial segments of postsynaptic neurons collectively deter-

mine their own action potential firing patterns. Synaptic inputs to axon terminals further modulate the efficacy with which postsynaptic action potentials lead to neurotransmitter release. These mechanisms are used extensively by the nervous system in all the processes, from sensation to action, that we will study in the following chapters.

OPEN QUESTIONS

- How is neuropeptide release regulated?
- When a neuron produces multiple neurotransmitters, can it separately regulate the release of each? How?
- Are there more neurotransmitters and receptors to be discovered? How would you discover them?
- How can we build a model of a synapse depicting all of its molecular components, their three-dimensional structures, and their precise localizations in the pre- and postsynaptic compartments and the synaptic cleft?
- How do different GPCR ligands differentially activate different downstream signaling cascades?
- What are the generalizable rules that govern how complex dendrites of mammalian CNS neurons integrate thousands of synaptic inputs?

FURTHER READING

Books and reviews

Cohen S & Greenberg ME (2008). Communication between the synapse and the nucleus in neuronal development, plasticity, and disease. *Annu Rev Cell Dev Biol* 24:183–209.

Hille B (2001). Ion Channels of Excitable Membranes, 3rd ed. Sinauer.

Huang EJ & Reichardt LF (2003). Trk receptors: roles in neuronal signal transduction. *Annu Rev Biochem* 72:609–642.

Katz B (1966). Nerve, Muscle, and Synapse. McGraw-Hill.

Sheng M, Sabatini BL, & Südhof TC (2012). The Synapse. Cold Spring Harbor Laboratory Press.

Südhof TC & Rothman JE (2009). Membrane fusion: grappling with SNARE and SM proteins. *Science* 323:474–477.

Unwin N (2013). Nicotinic acetylcholine receptor and the structural basis of neuromuscular transmission: insights from *Torpedo* postsynaptic membranes. *Q Rev Biophys* 46:283–322.

Presynaptic mechanisms

Augustine GJ, Charlton MP, & Smith SJ (1985). Calcium entry and transmitter release at voltage-clamped nerve terminals of squid. *J Physiol* 367:163–181.

Bennett MK, Calakos N, & Scheller RH (1992). Syntaxin: a synaptic protein implicated in docking of synaptic vesicles at presynaptic active zones. *Science* 257:255–259.

Del Castillo J & Katz B (1954). Quantal components of the end-plate potential. *J Physiol* 124:560–573.

Fernandez-Chacon R, Konigstorfer A, Gerber SH, Garcia J, Matos MF, Stevens CF, Brose N, Rizo J, Rosenmund C, & Südhof TC (2001). Synaptotagmin I functions as a calcium regulator of release probability. *Nature* 410:41–49.

Heuser JE & Reese TS (1981). Structural changes after transmitter release at the frog neuromuscular junction. *J Cell Biol* 88:564–580.

Ichtchenko K, Hata Y, Nguyen T, Ullrich B, Missler M, Moomaw C, & Südhof TC (1995). Neuroligin 1: a splice site-specific ligand for beta-neurexins. *Cell* 81:435–443.

Katz B & Miledi R (1967). The timing of calcium action during neuromuscular transmission. *J Physiol* 189:535–544.

Koenig JH & Ikeda K (1989). Disappearance and reformation of synaptic vesicle membrane upon transmitter release observed under reversible blockage of membrane retrieval. *J Neurosci* 9:3844–3860.

Kuffler SW & Yoshikami D (1975). The number of transmitter molecules in a quantum: an estimate from iontophoretic application of acetylcholine at the neuromuscular synapse. *J Physiol* 251:465–482.

Llinas R, Sugimori M & Silver RB (1992). Microdomains of high calcium concentration in a presynaptic terminal. *Science* 256:677–679.

Sabatini BL & Regehr WG (1996). Timing of neurotransmission at fast synapses in the mammalian brain. *Nature* 384:170–172.

Schiavo G, Benfenati F, Poulain B, Rossetto O, Polverino de Laureto P, DasGupta BR, & Montecucco C (1992). Tetanus and botulinum-B neurotoxins block neurotransmitter release by proteolytic cleavage of synaptobrevin. *Nature* 359:832–835.

Schneggenburger R & Neher E (2000). Intracellular calcium dependence of transmitter release rates at a fast central synapse. *Nature* 406:889–893.

Söllner T, Whiteheart SW, Brunner M, Erdjument-Bromage H, Geromanos S, Tempst P, & Rothman JE (1993). SNAP receptors implicated in vesicle targeting and fusion. *Nature* 362:318–324.

Sutton RB, Fasshauer D, Jahn R, & Brunger AT (1998). Crystal structure of a SNARE complex involved in synaptic exocytosis at 2.4 A resolution. *Nature* 395:347–353.

Takamori S, Holt M, Stenius K, Lemke EA, Gronborg M, Riedel D, Urlaub H, Schenck S, Brugger B, Ringler P, et al. (2006). Molecular anatomy of a trafficking organelle. *Cell* 127:831–846.

Tang AH, Chen H, Li TP, Metzbower SR, MacGillavry HD, & Blanpied TA (2016). A trans-synaptic nanocolumn aligns neurotransmitter release to receptors. *Nature* 536:210–214.

Watanabe S, Mamer LE, Raychaudhuri S, Luvsanjav D, Eisen J, Trimbuch T, Sohl-Kielczynski B, Fenske P, Milosevic I, Rosenmund C, et al. (2018). Synaptojanin and endophilin mediate neck formation during ultrafast endocytosis. *Neuron* 98:1184-1197.

Postsynaptic mechanisms

Chen L, Chetkovich DM, Petralia RS, Sweeney NT, Kawasaki Y, Wenthold RJ, Bredt DS, & Nicoll RA (2000). Stargazin regulates synaptic targeting of AMPA receptors by two distinct mechanisms. *Nature* 408:936–943.

Galarreta M & Hestrin S (1999). A network of fast-spiking cells in the neocortex connected by electrical synapses. *Nature* 402:72–75.

Larkum ME, Zhu JJ, & Sakmann B (1999). A new cellular mechanism for coupling inputs arriving at different cortical layers. *Nature* 398:338–341.

Lipscombe D, Kongsamut S, & Tsien RW (1989). Alpha-adrenergic inhibition of sympathetic neurotransmitter release mediated by modulation of N-type calcium-channel gating. *Nature* 340:639–642.

Lu W, Du J, Goehring A, & Gouaux E (2017). Cryo-EM structures of the triheteromeric NMDA receptor and its allosteric modulation. *Science* 355:eaal3729.

Ma H, Groth RD, Cohen SM, Emery JF, Li B, Hoedt E, Zhang G, Neubert TA, & Tsien RW (2014). GammaCaMKII shuttles $Ca2^{+}$/CaM to the nucleus to trigger CREB phosphorylation and gene expression. *Cell* 159:281–294.

Magee JC & Cook EP (2000). Somatic EPSP amplitude is independent of synapse location in hippocampal pyramidal neurons. *Nat Neurosci* 3:895–903.

Magleby KL & Stevens CF (1972). A quantitative description of end-plate currents. *J Physiol* 223:173–197.

Montminy MR, Sevarino KA, Wagner JA, Mandel G, & Goodman RH (1986). Identification of a cyclic-AMP-responsive element within the rat somatostatin gene. *Proc Natl Acad Sci U S A* 83:6682–6686.

Nowak L, Bregestovski P, Ascher P, Herbet A, & Prochiantz A (1984). Magnesium gates glutamate-activated channels in mouse central neurones. *Nature* 307:462–465.

Rall W (1967). Distinguishing theoretical synaptic potentials computed for different soma-dendritic distributions of synaptic input. *J Neurophysiol* 30:1138–1168.

Rasmussen SG, DeVree BT, Zou Y, Kruse AC, Chung KY, Kobilka TS, Thian FS, Chae PS, Pardon E, Calinski D, et al. (2011). Crystal structure of the beta2 adrenergic receptor-Gs protein complex. *Nature* 477:549–555.

Takeuchi A & Takeuchi N (1960). On the permeability of end-plate membrane during the action of transmitter. *J Physiol* 154:52–67.

Taniguchi H, Lu J & Huang ZJ (2013). The spatial and temporal origin of chandelier cells in mouse neocortex. *Science* 339:70–74.

Twomey EC, Yelshanskaya MV, Grassucci RA, Frank J, & Sobolevsky AI (2017). Channel opening and gating mechanism in AMPA-subtype glutamate receptors. *Nature* 549:60–65.

Walsh RM Jr., Roh SH, Gharpure A, Morales-Perez CL, Teng J, & Hibbs RE (2018). Structural principles of distinct assemblies of the human alpha4beta2 nicotinic receptor. *Nature* 557:261–265.

Wang R, Walker CS, Brockie PJ, Francis MM, Mellem JE, Madsen DM, & Maricq AV (2008). Evolutionary conserved role for TARPs in the gating of glutamate receptors and tuning of synaptic function. *Neuron* 59:997–1008.

Zeng M, Chen X, Guan D, Xu J, Wu H, Tong P, & Zhang M (2018). Reconstituted postsynaptic density as a molecular platform for understanding synapse formation and plasticity. *Cell* 174:1172–1187.